2009

Development and characterization of Sulfur dioxide gas analyzer

Samira Mohamed Saeed Mohamed Baomran

United Arab Emirates University
Deanship of Graduate Studies
M.Sc. Program in Environmental Sciences

Development and Characterization of Sulfur Dioxide Gas Analyzer

By

Samira Mohamed Saeed Mohamed Saeed

A thesis
Submitted to

United Arab Emirates University
In partial fulfillment of the requirements
For the Degree of M.Sc. in Environmental Sciences

2009

United Arab Emirates University
Deanship of Graduate Studies
M.Sc. Program in Environmental Sciences

Development and Characterization of Sulfur Dioxide Gas Analyzer

By

Samira Mohamed Saeed Mohamed Saeed

A thesis
Submitted to

United Arab Emirates University
In partial fulfillment of the requirements
For the Degree of M.Sc. in Environmental Sciences

Supervisors

Dr. Sayed A. M. Marzouk Associate Professor of Analytical Chemistry Department of Chemistry College of Sciences United Arab Emirates University	Dr. Mohamed H. Hassan Al-Marzouqi Associate Professor of Chemical Engineering and Chair of the Department of Chemical and Petroleum Engineering College of Engineering United Arab Emirates University

2009

The Thesis of **Samira Mohamed Saeed Baomran** for the Degree of Master of Science in Environmental is approved.

Examining Committee Member, **Dr. Sayed Marzouk**

Examining Committee Member, **Dr. Fakhr Eldin Suliman**

Examining Committee Member, **Dr. Muftah El-Naas**

Program Director, **Dr. Tarek Youssef**

Acting Dean, College of Science, **Prof. Mohammed N. Anwar**

United Arab Emirates University
2008/2009

"To me research means to see what all people have seen and to think what no body has thought"

Dedicated to my Beloved Parents
And my husband

Acknowledgement

All praises to Allah. All loves for the holy prophet Mohammad "peace be upon him", all devotions to Islam. It is a dept of honour for me to express my deep sense of gratitude to my supervisor Dr. Sayed A. M. Marzouk, Associate Professor of Analytical Chemistry, for providing me inexhaustible inspiration and enthusiastic guidance throughout my research work. I want also to thank him for allotment of this thesis and providing facilities of all kinds.

I offer my heartfelt thanks to Dr. Mohammad Almarzouqi, Chair of the Department of Chemical and Petroleum Engineering for his help and support.

I'm also grateful to Prof. Ben Bennani, Dean of Graduate Studies and Dr.Tarek Youssef, Chair of the Committee of the Environmental Science M.Sc. Program for their helpful attitude and providing me with initial tangible encouragement. I also acknowledge the Department of Chemistry, UAEU, and the Department of Chemical and Petroleum Engineering for their help and providing me with the required facilities.

Also I would like to pay tribute to all my family members, specially my parents and my husband as they have been a constant source of encouragement and inspiration. I thank them for providing me with support, faith, confidence and patience. I would also like to thank my precious sisters and my beloved brothers for their love and devotion.

Finally I have to express my thanks and appreciation to all my friends, specially my best friend Zahara Alyahyaie for her help, understanding and encouragement and being such a real friend.

Abstract

Sulfur dioxide (SO_2) is considered one of the main contaminants in air because of its major contribution to acid rain and due to the major health concerns associated with exposure to high concentrations of SO_2. Hence, there has been a great interest in the determination of SO_2 because of continuous monitoring its impacts on the environment and public health. However, limited reports targeted SO_2 in gas streams.

Therefore, the primary objective of the present work was to develop affordable gas analyzer for continuous monitoring of SO_2 in gas streams. The principle of operation of the described analyzer was based on a gas diffusion scrubber (in the form of hollow fiber membrane module, HFMM) as a prior gas sampling unit which allowed the contact between the gas stream and a selected carrier solution. SO_2, present in the gas stream diffuses to and dissolves in the flowing carrier solution. The concomitant changes of the carrier solution can be measured by means of a suitable flow-through detector placed downstream to produce analytical signal for the quantification of SO_2 in the gas stream.

The selected detectors were limited to electrochemical detectors because of their simplicity and they do not usually require additional reagents or prior derivatization reactions. With regards to the chemical properties of SO_2, pH, conductivity and amperometric detectors were selected as potential detectors for the construction of SO_2 gas analyzers.

The first detector evaluated in the current project was based on potentiometric pH-measurements. The obtained optimum experimental conditions for SO_2 detection were 0.1 M potassium oxalate buffer as carrier solution at flow rate 1.5 mL/min, gas flow rate 250 mL/min, using flat-bottom pH glass electrode and HFMM consisting of 60 PP fibers. Under the optimized conditions, a Nernestian slope up to 10000 ppm with a detection

limit of 1.0 ppm SO_2 was obtained. The response time varied from 20 to 200 seconds whereas the recovery time was 600 seconds when SO_2 concentration decreased from 1000 ppm to zero. The pH-detector showed excellent selectivity. CO_2 up to 500 folds did not exert significant interference and H_2S up to 5 folds greater than that of SO_2 was tolerated.

The second described detector was based on conductivity detection. The obtained optimum experimental conditions for SO_2 detection were 1.0 mM H_2O_2 as carrier solution at flow rate 2.0 mL/min, gas flow rate 200 mL/min, using commercial conductivity probe and HFMM consisting of 60 PP fibers. The favorable performance characteristics of the proposed SO_2 analyzer was successfully applied in monitoring real experiment of removing SO_2 from a gas stream. The optimized detector gave linear range up to 2500 ppm, a detection limit of 16 ppm for SO_2 in nitrogen and 115 to 180 seconds for recovery time. In addition the conductometric detector showed no interference of CO_2 up to 100 folds greater than that of SO_2.

The third detector was based on a novel amperometric detection. The utilized electrode was based on an organic conducting salt (OCS) based on tetrathiafulvalene-tetracyanoquinodimethane [TTF-TCNQ] complex. The TTF-TCNQ was mixed with silicone oil in 1:1.25 ratio. The formed paste was packed in Teflon cavity (12 mm in diameter). The obtained optimum experimental conditions for SO_2 detection were 0.2 M potassium phosphate buffer pH 6.5 as carrier buffer at flow rate 5.0 mL/min, using commercial HFMM mini-module. The TTF-TCNQ electrode was polarized at 0.24 V vs. SCE. The obtained amperometric response was linear up to 500 ppm and can detect as small as 10 ppm of SO_2 and showed no interference at very high levels of CO_2 (3900 folds).

The advantages of the developed SO_2 gas analyzers were manifold which include (i) the obtained performance characteristics of the described SO_2 analyzer can be tuned for

certain application requirements such as high sensitivity, wide linearity range, high selectivity towards a particular interfering gas, etc. (ii) low construction and operational cost, (iii) no special disposal required for the waste carrier, (iv) favorable response characteristics such as fast response, excellent reproducibility and signal stability, (v) the entire analyzer construction can be miniaturized to provide low-cost portable unit for industrial and/or environmental monitoring. This latter advantage presents some potential for commercialization of the described analyzer.

Key words: SO_2, potentiometric detection, conductometric detection, amperometric detection, Tetrathiafulvalene-7,7,8,8-tetracyanoquinodimethane [TTF-TCNQ], electrochemical methods, hollow fiber membrane module HFMM.

Table of Content

List of Figures

List of Abbreviations

ADC	:	Analog to digital converter
CL	:	Chemiluminescence
CLU	:	Central laboratories unit
CME	:	Chemically modified electrodes
DAQ	:	Data acquisition interface
DI water	:	Deionized water
DPP	:	Differential pulse polarography
EMF	:	Electromotive force
FR	:	Flow rate
GC	:	Glassy carbon
HFMM	:	Hollow fiber membrane module
IARC		International Agency for Research on Cancer
IC	:	Ion chromatography
IUPAC	:	International Union of Pure and Applied Chemistry
MLPM	:	mL per minute
µS	:	Microsiemens
OCS	:	Organic conducting salt
OSHA	:	Occupational Safety and Health Administration
PAD	:	Pulsed amperometric detection
PB	:	Prussian blue
PP	:	Polypropylene
R	:	Ratio between the total system volume and the carrier flow rate
SCE	:	Saturated calomel electrode
SEM	:	Scanning electron microscope
TTF-TCNQ	:	Tetrathiafulvalene -7,7,8,8-tetracyanoquinodimethane
UAEU	:	United Arab Emirates University

CHAPTER I

Introduction

Featuring sulfur in the +4 oxidation state, sulfur dioxide as well as sulfurous acid has reducing properties. In rare occasion SO_2 can act as an oxidizing agent, e.g., Calus process, to convert H_2S into elemental sulfur as given in Equation [1.4].

$$SO_2 + 2\ H_2S \rightarrow 3\ S + 2\ H_2O \qquad [1.4]$$

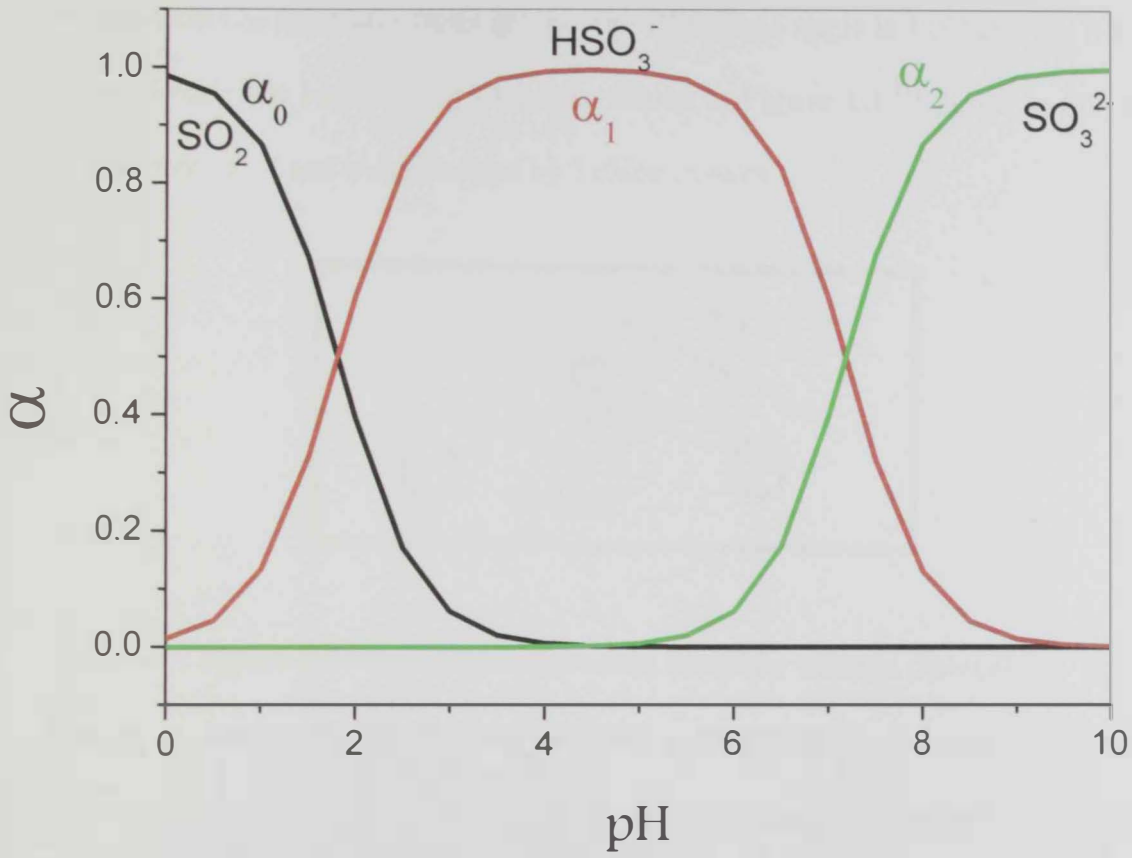

Figure 1.2: Effect of pH on the fraction of sulfurous acid, bisulfite and sulfite species.

1.1 Chemistry of Sulfur dioxide

Sulfur dioxide (SO_2) is a dense colorless gas, which is soluble in water, and has a suffocating and unpleasant smell of burnt matches. It has a melting point of −72.7°C, and a boiling point of −10°C. Sulfur dioxide exists as individual covalent V-shaped planar molecules with C_{2v} symmetry point group. The OSO bond angle is 119° and the S-O bond in sulfur dioxide has length of 143.1 pm as shown in **Figure 1.1**.[1] Sulfur in SO_2 has an oxidation state of +4 and is surrounded by 5 electron pairs.

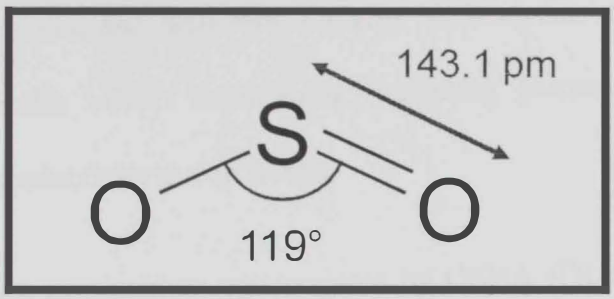

Figure 1.1: The chemical structure for sulfur dioxide molecule.

Due to its bent geometry, SO_2 molecule is a polar (dipole moment of 1.63D) and dissolves appreciably in water (9.4 g/100mL at 25°C) according to equations [1.1] and [1.2]. The resulting acid is the weakly diprotic acid, i.e., sulfurous acid (H_2SO_3) with pK_1 and pK_2 values of 1.81 and 7.18, respectively.

$$SO_2\,(g) \leftrightarrow SO_2\,(aq) \qquad [1.1]$$

$$SO_2\,(aq) + H_2O\,(l) \leftrightarrow H_2SO_3\,(aq) \qquad [1.2]$$

Treatment of basic solutions with sulfur dioxide produces sulfite salts as shown in equation [1.3]:

$$SO_2 + 2\,NaOH \rightarrow Na_2SO_3 + H_2O \qquad [1.3]$$

Figure 1.2 shows the fractions of free SO_2, bisulfite, and sulfite at different pH values. It is clear that at pH values ≥ 4 SO_2 is completely converted into bisulfite and sulfite ions.

1.2 Health and environmental aspects of SO_2

SO_2 is a colorless gas with a strong pungent odor, which is one of the main contaminants in air. It is produced by volcanoes and in various industrial processes involving burning of substances containing sulfur such as coal and fuel oil, during metal smelting, by the paper industry, petroleum refining and by incineration of solid waste.[2] Further oxidation of SO_2 forms H_2SO_4, and thus acid rain.[3] This is one of the causes for concern over the environmental impact of the use of fossil fuels as power sources.[4] SO_2 is a known contributor to smog and acid rain. Ontario Medical Association studies (June 2001) point out the health effects from smog, including premature deaths, hospital admissions and loss of productivity due to illness.

Sulfur Dioxide is not regulated as carcinogenic by OSHA (Occupational Safety and Health Administration). IARC (International Agency for Research on Cancer) has evaluated sulfur dioxide and concluded that there is inadequate evidence for the carcinogenicity in humans of sulfur dioxide.

The major health concerns associated with exposure to high concentrations of SO_2 including effects on breathing, respiratory illness, alterations in the lungs' defenses, and aggravation of existing cardiovascular disease. SO_2 vapors are extremely irritating to throat, mucous membranes and upper respiratory tract. Sulfur dioxide has been shown to lead to an inflammation of the airways as a consequence of neutrophil activation and is directly implicated in the bronchoconstriction and general aggravation of asthmatic conditions.[5-6] While the precise mechanism through which sulfite acts remains contentious, there is a body of evidence that links its presence with neutrophil activation – characterized by the sulfite-induced release of reactive oxygen species (principally H_2O_2) and chemotactic factor (IL-8).[7-8] Moreover, it has been found that elevated sulfite

concentrations are sustained in patients suffering from renal complications; it is unclear as to whether such increases lead to further complications or are simply a result of reduced clearance.[9]

Short exposures to concentrations as low as 1 ppm may produce a reversible decrease in lung function. Concentrations as low as 5 ppm have produced constriction of the bronchiole tubes. Severe overexposure may result in pulmonary edema, permanent lung injury or death. The effects of pulmonary edema which include coughing and shortness of breath may be delayed for hours or days after exposure. Major subgroups of the population that are most sensitive to SO_2 include asthmatics and individuals with cardiovascular disease or chronic lung disease, as well as children and the elderly.[10]

1.3 Uses of SO_2

Sulfur dioxide is sometimes used as a preservative for dried apricots and other dried fruits due to its antimicrobial properties. In winemaking, it serves as an antibiotic and antioxidant, protecting wine from spoilage by bacteria and oxidation. Sulfur dioxide is also a good reductant. In the presence of water, sulfur dioxide is able to decolorize substances. Specifically it is useful reducing bleach for papers and delicate materials such as clothes. Sulfur dioxide is also used to make sulfuric acid, being converted to sulfur trioxide, and then to oleum, which is made into sulfuric acid. Sulfur dioxide for this purpose is made when sulfur combines with oxygen. The method of converting sulfur dioxide to sulfuric acid is called the contact process.[11]

1.4 Emissions of SO_2

Industry, transportation and nature contribute to huge amounts of annual sulfur dioxide emissions. The combustion of coal and petroleum accounts for 90% of the total sulfur emitted by man, the only other large source being the smelting of copper ores.[12] One of the surveys of global data sets considering annual volcanic gas emissions into the atmosphere estimated SO_2 emissions in the range from 1.5 - 50 × 10^{12} g/a.[13] SO_2 emissions per populated area in the United Arab Emirates is estimated to be 1,520 thousand tons.[14] According to the Environmental Protection Agency's (EPA) 2006: Acid Rain Progress Report, the power sector is responsible for 70% of SO_2 emissions and 20% of NO_x emissions. The following amount of sulfur dioxide was released in the U.S. per year, measured in thousands of short tons (a unit of weight equal to 907.18474 Kg):

Table 1.1: Annual SO_2 emissions released in the U.S measured in thousands of tons:

Year	SO_2 emissions per year
1970	31,161
1980	25,905
1990	23,678
1999	18,867

US annual emission of SO_2 was reduced by 32% in the period of 1990 and 2002. According to the US EPA's Acid Rain Program, decreasing in the amount of sulfur dioxide emissions is due to flue gas desulfurization, a technology that enables SO_2 to be chemically bound in power plants burning sulfur-containing coal or oil.

1.5 Analytical methods and techniques available for SO_2 detection

1.5.1 Titrimetric methods

Sulfite can be quantified by different titrimetric methods such as the modified Monier-Williams method,[15] iodometric method,[16-18] and Ripper method.[19] In the first method the sample is distilled under acidic conditions and then titrated with standardized hydroxide.[15] In the second method the sample is reacted with excess iodine and back titrated with sodium thiosulfate.[17] In the third method the sample is directly titrated with standard iodine. However, each of the methods have some limitations, e.g. the modified Monier-Williams method is not suitable for routine analysis and is not readily applicable to the determination of low sulfite concentrations. While the iodometric method suffers from interference from other oxidizable materials, such as sulfide, thiosulfate, and Fe (II) ions, thus can cause apparently high results for sulfite. Also some metal ions, such as Cu (II), may catalyze the oxidation of sulfite to sulfate when the sample is exposed to air, thus leading to low results. On the other hand, the Ripper method for free and total SO_2 suffers from several deficiencies: (1) volatilization and loss of SO_2 during titration; (2) other reducing agents present in the air, such as hydrogen sulfide and some iodide is oxidized to iodine by the air bubbling through the solution or by oxidants that may be present in the atmosphere; (3) analysis cannot be accurately performed in juices or wines that contain ascorbic acid; (4) difficulty of the end point detection in red wines.

1.5.2 Spectrochemical methods

1.5.2.1 Spectrophotometric methods

West–Gaeke method [20] is one of the general standard reference methods used for the determination of sulfite/sulfur dioxide, which is based on the Schiff's reaction. Schiff's reaction was reported for the first time in 1866 in which the color was regenerated in an SO_2-blended fuchsin solution upon the addition of aldehyde. Since then, this important reaction has been studied continuously for extensive applications, and was applied for identification and determination of sulfite/sulfur dioxide. There are many other reagents studied in the literature such as pararosaniline,[20-25] malachite green solution,[26] bromine and methyl red dye,[27] 5,5-dithiobis(2-nitrobenzoic acid) (DTNB) or Ellman's reagent,[25,28] dichromate solution in acidic medium followed by diphenylcarbazide,[29] and mercury (II) ion.[30]

Sulfur dioxide gas can be separated from the sample matrix by means of gas diffusion cells,[31] microdistillation,[32] or by pervaporation.[33] On the other hand it can be sampled into a flow through system by flow injection analysis (FIA),[31,34,35] or sequential injection analysis (SIA).[24,36]

Spectrophotometric techniques revealed number of limitations such as (i) difficulty of establishing reliable calibration graph when dyes from different sources are used (ii) requirement of sample pre-derivatization process and (iii) long time (a minimum period of 15 min) is essential for full color development.

1.5.2.2 Luminescence methods

Several methods based on fluorescence,[4,37,38] phosphorescence,[39] and chemiluminescence[40-41] techniques were also reported for the determination of sulfite and sulfur dioxide. Some of the sensors operate on the basis of luminescence (either fluorescence or phosphorescence) detection,[4,41] while some of them operates on the basis of luminescence quenching.[37,39] Dynamic quenching is measured and related to analyte concentration through the well-known Stern-Volmer relationship.

1.5.3 Chromatographic methods

Ion chromatography (IC) is a suitable analytical technique for the simultaneous determinations of low concentration of anions and cations. Several ion chromatographic methods for the determination of sulfite have been reported using ion detectors based on amperometric,[42] and conductometric detection.[43] Gaseous SO_2 is sampled either by hollow cylindrical absorption bottle containing 5% triethanolamine (TEA)-absorbing solution,[43] or diffusion scrubber.[44]

In general these techniques require elaborate technical specification and user expertise and, as such, require substantial running costs.[9]

1.5.4 Electrochemical methods

1.5.4.1 Potentiometric methods

Potentiometry is an electrochemical technique which measures the electrode potential and utilizes the galvanic cell concept.[45] In this technique, a pair of electrode is immersed and the potential, or voltage, of one of the electrodes is measured relatively to the other. Examples include pH meters,[46] ion-selective electrode measurement,[47-50] and potentiometric titrations.[51] Nernest equation can be applied in this technique since it states that a potential is proportional to ion concentration. The Nernest equation is normally used to describe the ideal response of such a detector:

$$\mathrm{EMF} = K + R\,T / z\,F \ln a_I \qquad [1.5]$$

where EMF is the electromotive force (the observed potential at zero current), K is a constant potential contribution that often includes the liquid-junction potential at the reference electrode, a_I is the sample activity for the ion I with charge z, and R, T, and F are the gas constant, absolute temperature, and Faraday constant, respectively.

1.5.4.2 Conductometric methods

Conductometry continues to be an important tool in the analysis of sulfite or sulfur dioxide. This method is popular because of its high sensitivity, fast response, minimal maintenance and simple operation. Conductometric analysis measures the increase in conductivity as sulfur dioxide is absorbed into either hydrogen peroxide,[52-53] or de-ionised water.[54-55]

1.5.4.3 Differential Pulse Polarographic method

Differential Pulse Polarography (DPP) is a polarographic technique that uses a series of discrete potential steps rather than a linear potential ramp to obtain the experimental polarogram. DPP technique can be used for sulfite determination in petroleum and its distillates,[56] in atmosphere,[57] and in food analysis.[58]

1.5.4.4 Coulometric method

Coulometric method is an electrochemical technique that determines the amount of matter transformed during an electrolysis reaction by measuring the amount of electricity consumed or produced. Chen et al. developed a coulometric detector based on carbon felt as a working electrode.[59] Although the sensitivity of coulometric detectors is higher than that of amperometric detector. However, in practice, there are some special problems in the design of coulometric detectors. It is difficult to satisfy the condition of a 100% current efficiency and to complete electrolysis in the cell. Therefore, coulometric detectors are not as popular as the amperometric ones.

1.5.4.5 Amperometric methods

Amperometric detection is based on oxidation or reduction of an analyte at a working electrode held at a potential that is high enough to initiate the oxidation or reduction process. The electric current resulting from this electrochemical reaction serves as the analytical signal and is directly proportional to the concentration of the electrochemically active analyte.

Sulfite oxidation has been studied at a range of bare electrodes, including gold,[60] platinum,[61-62] palladium,[63] copper,[64] glassy carbon,[65] boron-doped diamond,[66] and various forms of carbon.[42] The detection limits achievable at bare, unmodified electrodes, irrespective of substrate material, tend to be in the low micro-molar range, which is

normally sufficient for monitoring both endogenous and exogenous sulfite. One of the problems associated with such processes is the potential fouling of the electrode, which leads to a cumulative loss in sensitivity and compromises the reproducibility of the method.[67] This can be as a consequence of either sample components or the products of the oxidation process itself adsorbing onto the electrode. Pulsed amperometric detection (PAD) has been employed in an effort to minimize the loss in electrode performance through imposing multi-step waveforms that serve to clean the electrode in situ.[67] On the other hand, attempts to counter the lack of selectivity obtained at bare electrodes has therefore taken a number of other, more elaborate routes that involve either sample pre-treatment (principally the gas-diffusion model) or electrode modification through the incorporation of catalysts (chemical or biological).

According to the International Union of Pure and Applied Chemistry (IUPAC) the chemically modified electrode (CME) is an electrode made of a conducting or semiconducting material that is coated with a selected monomolecular, multimolecular, ionic, or polymeric film of a chemical modifier and that by means of faradaic (charge-transfer) reactions or interfacial potential differences (no net charge transfer) exhibits chemical, electrochemical, and/or optical properties of the film.[68] The principal goal of modifying electrodes is to reduce the potential required to initiate the oxidation of sulfite, thereby minimizing the opportunity for unwanted electrode processes to contribute to the analytical signal.

In the case of sulfite, electrode modification was achieved either by using metal complexes or biological agents. The first one was more common and variety of complexes has been assessed such as PVP/Pd/IrO_2 modified platinum electrode,[10] Poly[Ni-(protoporphyrin IX)] (NiPPIX) film modified glassy carbon electrode,[69] cobalt pentacyanonitrosylferrate film modified glassy carbon electrode,[70] polymeric film of Fe-

tetra-4-Aminophenylporphyrin modified glassy carbon electrode,[71] nikel pentacyanonitrosylferrate (NiPCNF) film modified aluminum electrode,[72] ferrocene derivative-modified carbon paste electrode,[73] and copper hexacyanoferrate modified graphite electrode.[74] Although the modifying metal complexes were initially used as solution-based mediators,[75] they are now more commonly immobilised on the electrode as mono or multilayer films or incorporated within the body of composite electrode materials, such as sol gels.[76-77] The complexes can significantly enhance the current response to sulfite and often succeed in shifting the over-potential for sulfite oxidation to less positive potentials such that the oxidation of interfering agents could be avoided.

The second approach for modification of the electrodes was the use of enzyme, i.e., sulfite oxidase.[78-84] In general, the bio component can be coupled to conventional electrode substrates and the analytical signal derived from monitoring peroxide oxidation,[78,79,81] oxygen reduction,[83] or the regeneration of electron-transfer mediators.[82,83] The basic reaction schemes are summarized in **Figure 1.3**. The oxidation of the peroxide by-product (Figure 1.3A) is often regarded as the simplest approach but, like direct sulfite oxidation, suffers from the need for large overpotentials. The peroxide by-product can also be reduced (Figure 1.3B), with the cathodic potentials avoiding the unwanted oxidation of ascorbate and polyphenols. The enzymatic process consumes oxygen, and this can be monitored through the electrochemical reduction of oxygen (Figure 1.3C) and is the predominant methodology employed when using microbial agents. The dependence on molecular oxygen is removed by using electron-transfer mediators (Figure 1.3D), which also remove the peroxide by-product and can allow operating potentials significantly less than those required to oxidise either peroxide or sulfite.

However, a lack of enzyme stability is the major draw back of such biosensors.

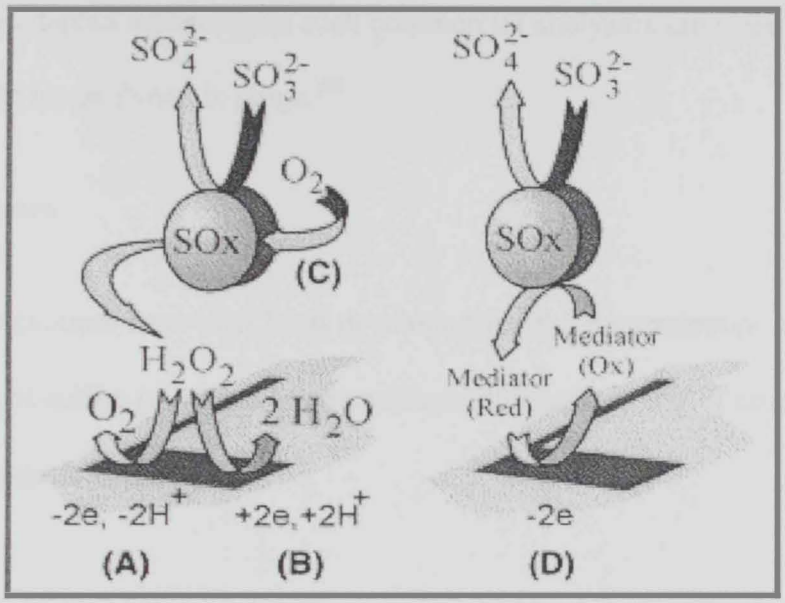

Figure 1.3: Reaction schematics highlighting the possible modes through which a sulfite-oxidase enzyme can be integrated within conventional electrode systems.

1.5.5 SO_2 analyzers

Different technologies have been utilized so far in the construction of the commercial SO_2 analyzers. These include UV fluorescent sulfur dioxide analyzer (Environment S. A.),[85] Nondispersive infrared absorption method (VIG Industries),[86] SO_2 pulsed fluorescence detector (PFD) (Thermmo Scientific),[87] and surface acoustic wave (SAW). Regardless of the adapted technologies such commercial analyzers are usually of high cost and exhibit limited linear dynamic range.[88]

1.5.6 SO_2 biosensors

Biological procedures have also been developed for the determination of sulfite. The redox conversion of sulfite to sulfate can be achieved through the use of enzymes [78,89] and biological microorganisms.[90-91].

1.6 Objectives of the present work

In the present work, attempts were made to develop analyzers for continuous monitoring of SO_2 in gas streams based on polymeric diffusion scrubbers coupled with electrochemical detectors including potentiometric, conductometric and amperometric detectors in flow arrangements.

The specific objectives set at the beginning of the present work included:

i. Evaluation of different hollow fiber membrane contactors for the construction of SO_2 gas analyzer.

ii. Evaluation and comparison between different potential detectors.

iii. Evaluation of different carrier/stripping solutions.

iv. Full analytical characterization of the recommended analyzer.

v. Application of the developed analyzer in monitoring real experiment of removing SO_2 from a gas stream.

Since pH, conductivity and amperometric detectors were used in the present work, it is appropriate to provide a brief theoretical background about potentiometry, conductometry and amperometry as electroanalytical techniques in the following sections.

1.7 Background of potentiometric measurements

Potentiometry can be simply described as the measurement of a potential in an electrochemical cell. It is the only electrochemical technique that directly measures a thermodynamic equilibrium potential and in which essentially no net current flows. Two electrodes are used in measuring cell potentials; a reference and an indicator (working) electrode. One of the unique features of potentiometry is the ability to monitor the activity of an ion in the sample rather than the concentration. For direct potentiometric measurements, the potential of a cell can be expressed as a sum of an indicator electrode potential, a reference electrode potential, and a junction potential.[92]:

$$E_{cell} = E_{ind} - E_{ref} + E_j \qquad [1.6]$$

All direct potentiometric methods are based upon equation [1.7] or [1.8], for cations:

$$E_{cell} = K + 0.0592/n \text{ pX} \qquad [1.7]$$

and for anions

$$E_{cell} = K - 0.0592/n \text{ pA} \qquad [1.8]$$

Potentiometric analysis involves the measuring the potential difference, E_{cell}, between a working and a reference electrode, which depends on the membrane potential, E_m.

$$E_{cell} = K + E_m \qquad [1.9]$$

Where, K refers to the all contributing potentials in the cell like the internal reference potential of the working electrode, potential of the reference electrode and the junction potential. There are two commonly used instruments for making potential measurements. One is the potentiometer and the other is the pH meter. The potentiometer can be used for measurements of low resistance circuits. The pH meter is a voltage measuring device designed for use with high-resistance glass electrodes and can be used with both low and high-resistance circuits.

One of the most common and earliest applications of potentiometry is pH determination. The heart of the pH electrode is the glass membrane, typically about 50 μm thick, which ideally only allows H_3O^+ ions to become incorporated in its inner and outer layer. The inside is filled with saturated AgCl solution that has a fixed concentration of H_3O^+ and hence fixed internal potential. The outside of the membrane is exposed to our solution. If there is much more H_3O^+ in the solution compared to the internal solution, the outer layer of the glass membrane will build up a positive charge relative to the inside. This difference in electrical charge across the glass membrane is the membrane potential that depends only on the concentration of H_3O^+ in the outer solution. The electrical potential across that membrane is the signal that must be measured.[93] pH measurement has some advantages over other electrodes like: its potential is not affected by the presence of oxidizing or reducing agents, operates over a wide pH range and responds quickly to pH changes and functions well in physiological systems.

1.8 Background of conductometric measurements

The conductance of a solution is a physical property that can give important quantitative information regarding the composition of the solution. Conductance is a measure of the ability of a solution to carry current and depends on the concentration, mobility, charge of ions in the solution, and on temperature. For a solution to conduct electricity ions must be present; which are produced by the dissociation of electrolytes into cations and anions. The limiting ionic equivalent conductivities are known for many ions, i.e., H_3O^+ and OH^- ions have an extremely high equivalent ionic conductance (λ_+ = 349.81 and 198.3 S cm^2 $equiv.^{-1}$, respectively) in comparison to other cations, which can provide very sensitive conductivity detection.

From Ohm's law ($E = IR$) it is apparent that the electric current (I) is inversely proportional to the resistance (R), where E represents potential difference. The inverse of the resistance is the conductance ($G = 1/R$).

The great features of routine conductance measurements are ease, robustness, and nondistructiveness. The mean weakness is that the conductance measurement by itself gives no molecular information and cannot identify the species that carry the current.[93]

1.9 Background of amperometric measurements

Amperometry is an electroanalytical technique that is widely used to quantify electroactive species. Amperometric detection is based on oxidation or reduction of an analyte at a working electrode held at a fixed potential that is high enough to initiate the oxidation or reduction process. The electrode acts as an oxidizing or reducing agent of variable power. The electric current resulting from this electrochemical reaction serves as the analytical signal and is directly proportional to the concentration of the electroactive analyte as long as the transport of material to the electrode is constant. The current response is most often measured as a function of time.

The potential applied to the electrochemical cell between the reference and working electrode serves as the driving force for the detection redox reaction to occur. All amperometric determinations ultimately depend on Faraday's law:[93]

$$Q = nFN \qquad [1.10]$$

Where Q is the number of coulombs used in converting N moles of material, n is the number of electron equivalents lost or gained in the transfer process per mole of material, and F is Faraday's constant (96,500 C equiv^{-1}). Differentiation of equation 1.10 with respect to time *(t)* yields current *(I)*, which is the measure of the rate at which material is converted:

$$dQ/dt = I = nFA\ dN/dt \qquad [1.11]$$

When a sufficient potential is applied the electrochemically active material comes into contact with the electrode being converted to a product. Under this condition, current depends on mass transport. The rate of mass transport (mol cm^{-2} s^{-1}) is given by:

$$dN/dt = -D(dc_{x,}/d_x)_{x=o} \qquad [1.12]$$

Or in terms of the current response

$$I = -nFAD\,(dc/dx)_{x=0} \qquad [1.13]$$

Under constant flow or controlled hydrodynamic conditions, the concentration gradient is constant because the diffusion layer, δ, is nonvarying:

$$I = nFAD\,c^*_o/\delta \qquad [1.5]$$

Where I is the current, D diffusion coefficient, c_o is the unperturbed concentration of the reactant and δ is the length of diffusion layer.

Amperometry has an advantage over most analytical detection techniques in that it involves a direct conversion of chemical information to an electrical signal without the use of optical or magnetic carriers.

Under steady-state conditions, the current measured is contributed from three sources: the background electrolyte, the electrode material itself, and the analyte. The medium and the electrode are chosen so that the contributions of the first two sources are as small as possible and the small residual current from these two sources is electronically removed before quantitation of the analyte. Hydrodynamic voltammetry, a steady-state technique from which amperometry is derived, is used to select the operating potential. Electrode kinetics, which depends on a number of factors (electrode material, electrolyte type etc.) plays a significant role in practice.

The simplicity of the technique leads to many applications such as development of biosensors, environmental analysis and endpoint indicator for titrations.[93].

Pulsed amperometric detection (PAD): The potential applied to the working electrode may be constant during the time of separation or it may be applied in a pulsed mode.[94] Triple-pulse (**Figure 1.4**) and related waveforms are often applied when the electrode surface gets deactivated by products of the electrochemical reaction. In this case, the successive application of a measuring potential, a cleaning potential and a conditioning potential in a repetitive way (typical frequency 1 to 2 Hz) can lead to a stable response.

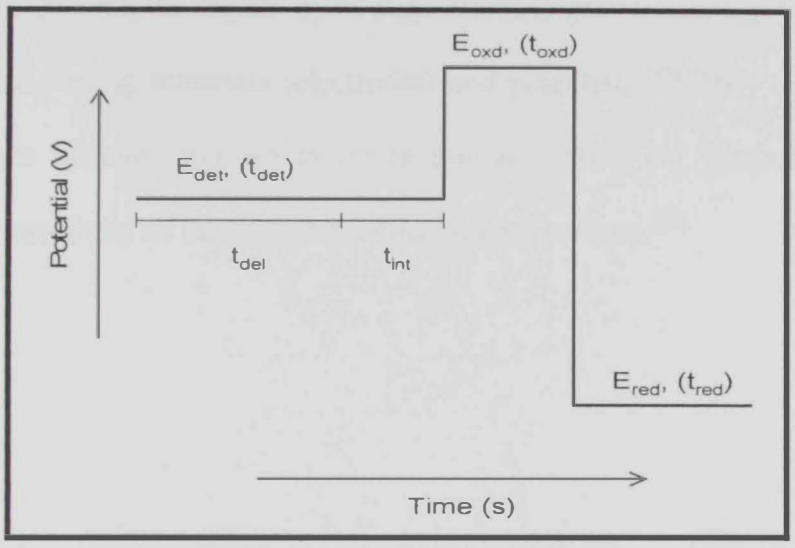

Figure1.4: PAD waveform.

The detection potential in the potential-time wave form is chosen to be appropriate for the desired surface-catalyzed reaction, and the electrode current is sampled during a short time period (t_{int}) after a delay of t_{del}. The delay time is necessary to overcome the double-layer charging currents, which would dramatically affect S/N ratio. The combination of t_{del} and t_{int} constitutes the detection period (t_{det}). Following the detection process, adsorbed carbonaceous species are oxidatively desorbed simultaneously with anodic formation of surface oxide following a positive-potential step to the value E_{oxd} for duration of t_{oxd}. The activity of the "clean", but inert, electrode surface is then regenerated by a subsequent

negative-potential step to E_{red} for duration of t_{red} to achieve cathodic dissolution of the oxide film prior to the next cycle of the wave form.[94]

Among electrochemical sensors, those based on amperometric detection, which employs chemically modified electrodes, are probably the most popular [2] because they are fast, sensitive and convenient.[3] Amperometric gas sensors have an advantage of linear responses versus the concentrations of sensing targets to result in a high precision characteristic. In general, the selectivity of amperometric gas sensors can be increased by a proper choice of sensing materials (electrodes) and potentials.[95] They usually contain a liquid electrolyte solution and are therefore not as robust, but generally have higher selectivity and sensitivity as the resistive semiconductor sensors.[96]

CHAPTER II

Materials and Methods

2.1 Materials and Reagents

Nitrogen (99.99%), carbon dioxide (99.99%), sulfur dioxide standard (1%, i.e., 10,000 ppm in N_2) and hydrogen sulfide (5% in N_2) were received from Air products, UAE. Polyester membranes (6 μm thick) with pore sizes of 1.0, 2.0 and 3.0 microns were received from Osmonics Inc. Microporous polypropylene (PP) loose fibers (OD 300 μm and ID 220 μm) and hollow fiber membrane contactor (model G591) based on the same PP fibers were received from Membrana (USA). Hollow fiber membrane modules based on silicone rubber (model M300) were received from Nagayanagi (Japan). Teflon AF-2400® single fiber (OD 0.82 mm and ID of 0.62) mm (wall thickness = 0.10 mm) was received from Biogeneral (USA). Tetrathiafulvalene (TTF), 7,7,8,8-tetracyanoquinodimethane 98% (TCNQ) and silicone oil were purchased from Aldrich (USA). Sperctroscopic grade graphite rods (6.25 mm dia) were purchased from Alfa Aesar (USA). Potassium Oxalate-1-hydrate (184.23 g/mol) was received from Riedel-deHaen. Hydrogen peroxide (30% w/v) was received from Panreac (Barcelona). All chemicals were used without further purification and other chemicals were of the highest available purity. All solutions were prepared using deionized water.

2.2 Apparatus

A 4-Ch, computer controlled gas mixer (Sabel Systems, USA) Model MFC-4 was used to control four Mass flow controllers (Sierra Instruments, Inc. USA) to prepare variable concentrations of SO_2 in the gas stream for calibration and characterization purposes. The MFC-4 utility software (Sabel Systems) was used to run a given preset program of SO_2 concentration steps. The flow range of the mass flow controllers were 0-

10, 0-100, 0-1000 and 0-1000 mL per minute (MLPM), respectively. These flow ranges allowed the use of SO_2 standard concentrations as low as 10 ppm in gas stream of 1000 MLPM. The low-flow mass flow controllers (i.e., 0-10 and 0-100 MLPM) were used to control the flow of the standard 1% SO_2 gas and/or the tested interference gases. Whereas the high-flow mass flow controllers (i.e., 0-1000 MLPM) were used for the nitrogen gas diluent unless otherwise stated.

The potentiometric pH-detector was based on a commercial acrylic flow cell (Sensorex, model FC47C, 50 μL internal volume) and a flat-bottom combination glass electrode (Sensorex, model S450C). A custom made high-input (10^{15} Ω) impedance differential amplifier was used for pH measurements. The output of the amplifier was measured using a 16 bit-analog to digital converter (ADC) interface (Pico Technology, model ADC 16) connected to a PC installed with PicoLog software (Pico Tech.) for data display and storage.

The conductometric detector was based on a commercial Microflow-through conductivity probe (Lazar Lab, model COND-158BL) with conductivity range of 0 to 100,000 μS/cm (1 μS/cm resolution). The equivalent analog output voltage (0 to 2,000 mV) of the probe was measured using the ADC 16 interface card as described above and used as the analytical signal.

The developed amperometric detector (discussed below in section 2.4) was controlled by a potentiostat (CH Instruments, USA) Model 842B connected to a PC was used in all amperometric measurements. All batch experiments were carried out using three-electrode electrochemical cell configuration. A calomel (Cole Parmer) and platinum wire were used as reference and counter electrodes, respectively. pH measurements were made using a combination glass-Ag/AgCl reference electrode and a pH/mV meter (Thermo-

Orion, Model 420). All measurements in the present work were carried out in air conditioned lab at 22±1 °C.

2.3 SO_2 Gas Analyzer

The proposed SO_2 analyzer in this work is designed for continuous monitoring of SO_2 in gas streams. The analyzer consists of two main components, i.e., the gas sampling unit and the detector. The gas sampling unit is based on a diffusion scrubber in the form of hollow fiber membrane module (HFMM) which allows efficient contact between two flowing fluids without physical mixing. The construction and the principle of operation of such HFMM are shown in **Figure 2.1**. An appropriately selected carrier solution is pumped through the tube side of the module (and the gas stream is flown through the shell side - counter current) using a peristaltic pump (Masterflex, Model 7519-20). SO_2 gas molecules diffuse through the porous wall of the fibers and dissolve in (and possibly react with) the carrier solution which results in a chemical change in the carrier solution to be detected by a flow-through detector located downstream. The complete experimental setup used in testing and evaluation of different parameters for SO_2 detection is shown in **Figure 2.2**.

2.4 Fabrication of amperometric detector for SO_2 determination

Unlike the commercial pH and conductivity detectors, a novel amperometric detector was developed in the present work for the detection of sulfite/SO_2. The electrode was based on an organic conducting salt (OCS) based on tetrathiafulvalene-tetracyanoquinodimethane (TTF-TCNQ) complex. The OCS was prepared according to the literature method.[97] In brief, the TTF-TCNQ was formed by slow mixing of equimolar (~0.05 M) solutions of neutral TTF and TCNQ in hot acetonitrile (HPLC

grade). A black complex immediately precipitated as a microcrystalline powder. The precipitate was filtered through a filter paper and washed with cold acetonitrile and diethyl ether, and finally dried under vacuum.

The amperometric electrodes were prepared using either pure TTF-TCNQ complex or in the form of paste with silicone oil. The pure TTF-TCNQ powder was packed into a graphite cavity (4 mm in diameter and 2 mm in depth) and smoothed against a weighing paper and secured in place using a microporous polyester membrane (pore size of 3 μm, Osmonics Inc., USA) and a Teflon O-ring as shown in **Figure 2.3**.

A three-electrode flow cell was designed for the amperometric determination of sulfite ions and constructed from a Teflon rod (40 mm in diameter and 30 mm height) as shown in **Figure 2.4**. The working electrode was made by inserting a stainless steel rod (12 mm in dia) snugly in a Teflon tube (ID 11.5 mm, 20 mm OD) to create a cavity of ~1 mm deep. The cavity was packed with TTF-TCNQ-silicone oil paste (1:1.25) and smoothed against a glass slide. The inlet stainless steel tube served also as counter electrode. The reference electrode was placed in a parallel compartment as shown in **Figure 2.4**. The space between the counter and the working electrode was about 1 mm.

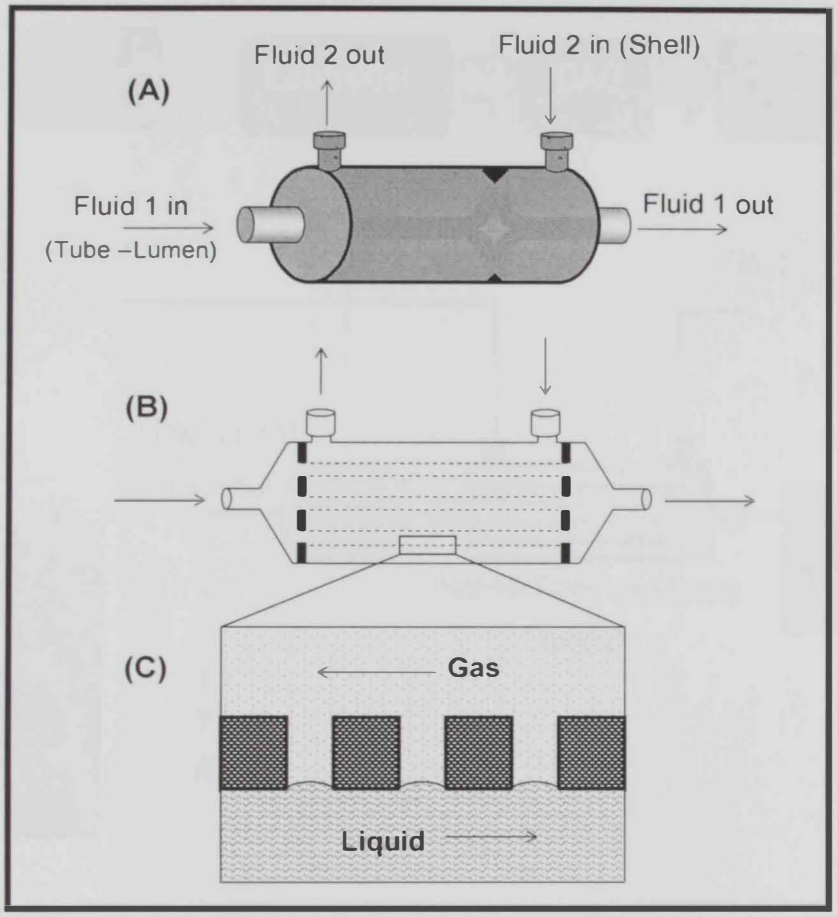

Figure 2.1: Physical arrangement of the contacting fluids in a HFMM (A). Lumen (tube) and shell compartments created by the hollow fibers (B). Liquid-gas interface at the pore mouth of the membrane (C).

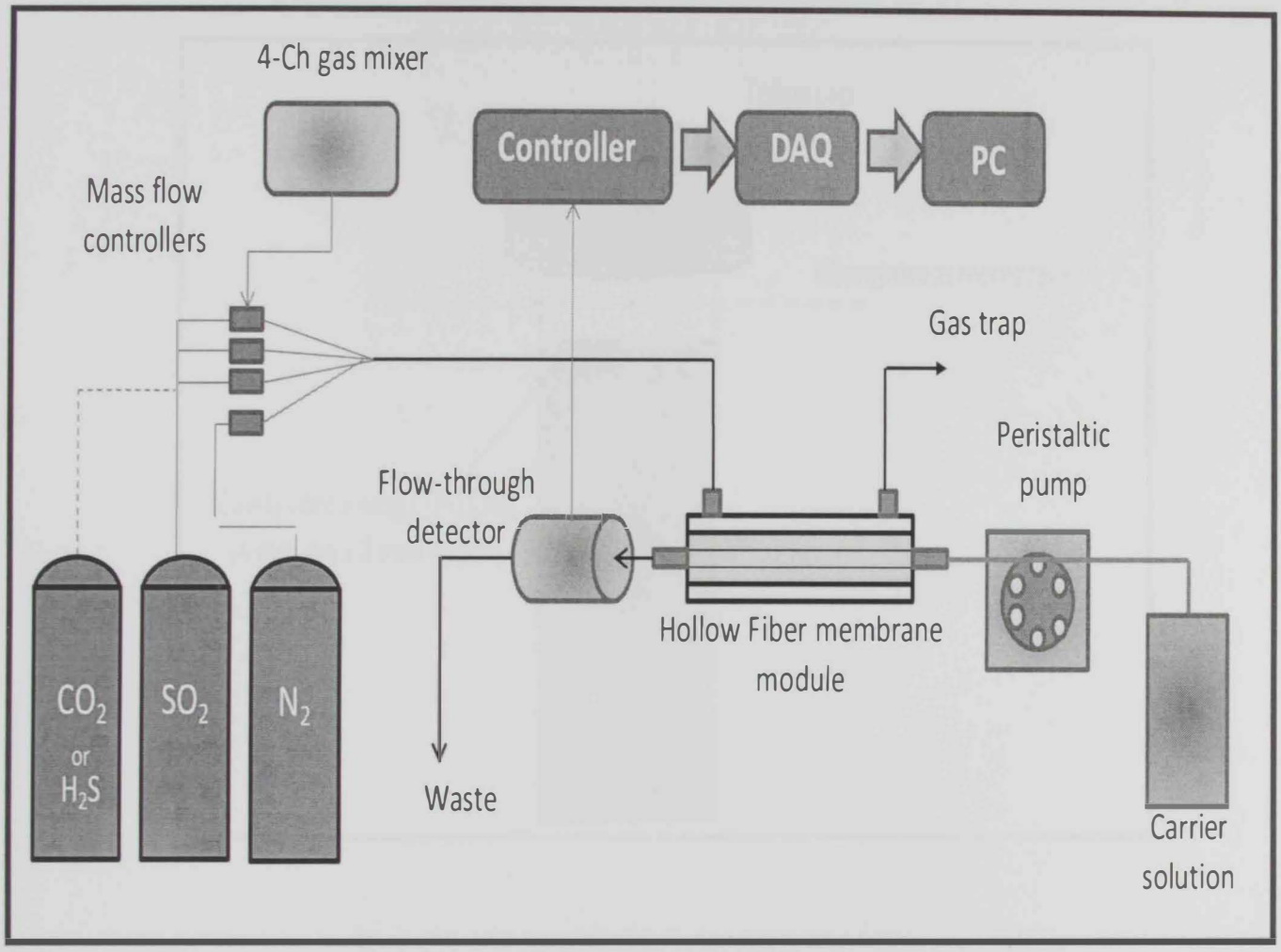

Figure 2.2: Experimental setup used in the development and evaluation of different SO_2 gas analyzers.

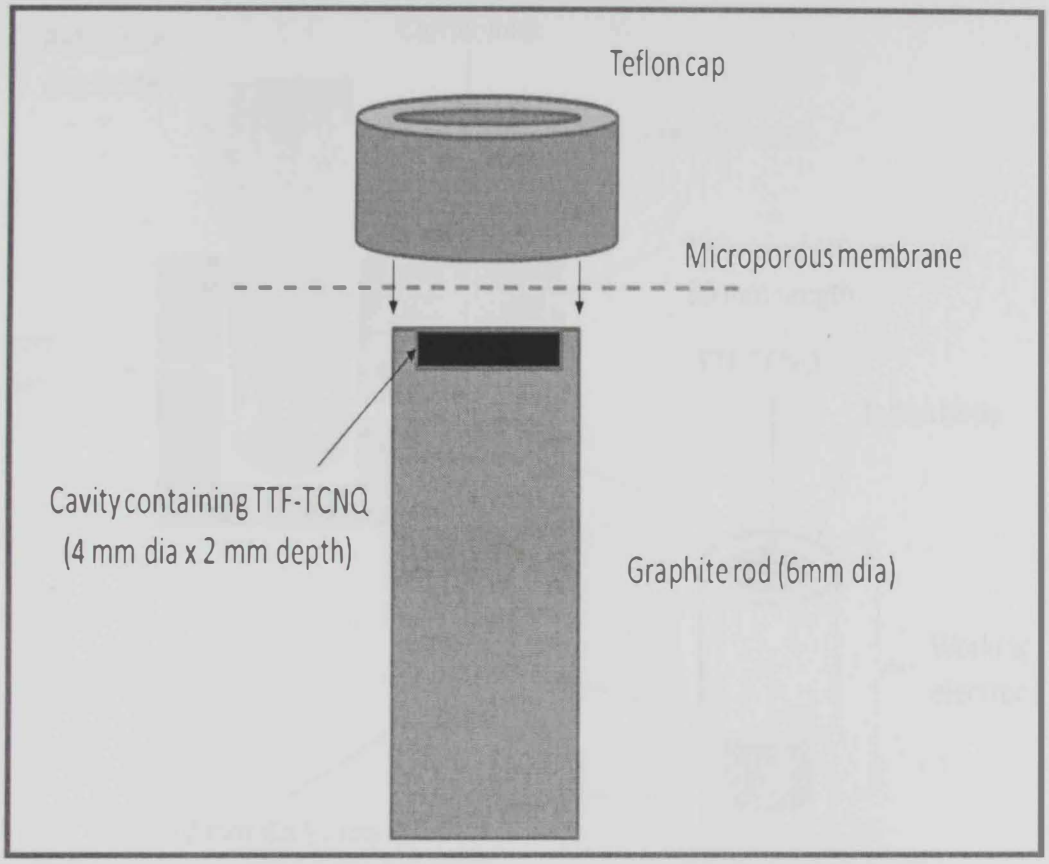

Figure 2.3: Construction of the TTF-TCNQ electrode for the amperometric detection of sulfite ions.

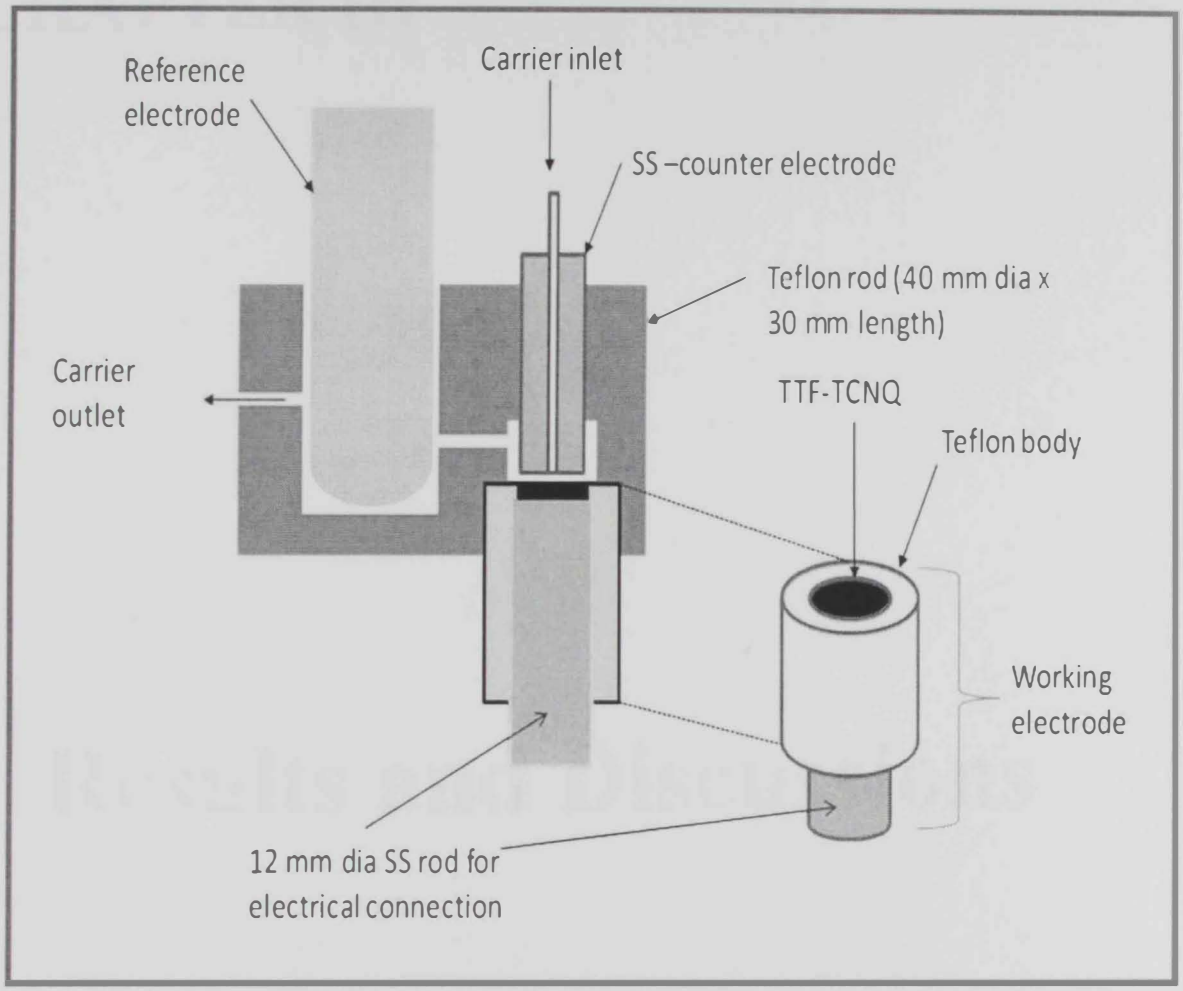

Figure 2.4: The flow-through amperometric detector based on a TTF-TCNQ amperometric electrode for sulfite ions.

CHAPTER III

Results and Discussions

3.1. Principle of operation of the developed SO_2 gas analyzer

Gas analyzers aim to continuously monitor/determine certain species in gas streams can be built on different principles such as radiation absorption measurements,[20] or conductometric measurements in thin solid layers.[52] Such analyzers usually offer the advantage of standalone operation, i.e., does not require consumption of reagents. However, such analyzers are usually available at high cost. Alternatively, gas monitoring in gas streams can be achieved by employing a prior step in which the analyte gas is stripped in an appropriate carrier solution. The concomitant changes in the solution as a result of gas absorption can be measured in a subsequent step to produce analytical signal proportional to the concentration of the analyte gas.[98,99] This latter approach, although requires carrier solution as a consumable reagent and a sort of liquid pumping, it offers the advantages of low cost, simple construction and operation, versatile detection schemes, tunable selectivity and sensitivity.

Owing to the attractive advantages offered by the second approach it was adapted in the present work to develop gas analyzer for continuous monitoring of SO_2 in gas streams. Moreover, a set of favorable intrinsic physical and chemical properties of SO_2 such as its high solubility in water, high acidity and its reducing properties suggested that a number of potential simple detectors in combination with simple aqueous solutions can be used to construct sensitive and selective SO_2 analyzer.

3.2 SO_2 gas analyzer based on potentiometric pH-detection

The use of potentiometric pH detectors to construct electrodes for gaseous species such as CO_2,[98] NH_3,[100] NO_x,[101] hydrazoic acid,[102] has been well known in literature. The common Severinghaus type sensing probe,[103] is based on a pH glass electrode entrapped behind a gas permeable membrane through which the gas diffuses as shown in **Figure 3.1**. Unlike CO_2, NH_3 and NO_x, commercially successful probes for SO_2 based on Severinghaus type are not available due to the instability of hydrogen sulfite internal solution.

In the present work, a pH detection was proposed because the significantly acidic SO_2 gas ($pK1$ = 1.81) was anticipated to produce appreciable pH changes in the flowing carrier solution shown in the experimental setup (**Figure 2.2**). The additional potential advantages offered by the proposed SO_2 analyzer compared to Severinghaus type setup include (i) the response time can be controlled by both the carrier flow rate and the total system (HFMM and the detector) internal volume. Whereas, in Severinghaus type the response time is mainly determined by the gas diffusion to and from the internal electrolyte layer (ii) the proposed analyzer is more suitable for continuous monitoring of the analyte gas streams than Severinghaus gas probes. Because the latter is based on a thin electrolyte layer, entrapped behind the gas permeable membrane, which is susceptible for evaporation when used in dry gas streams for prolonged time and (iii) The proposed setup offers the advantage to possibly separate the gas sampling step (which takes place in the HFMM) and the detection step downstream. Such remote placement of the detector could be of exceptional importance if the gas stream conditions (e.g., high temperature) do not suit the Severinghaus type gas probes.

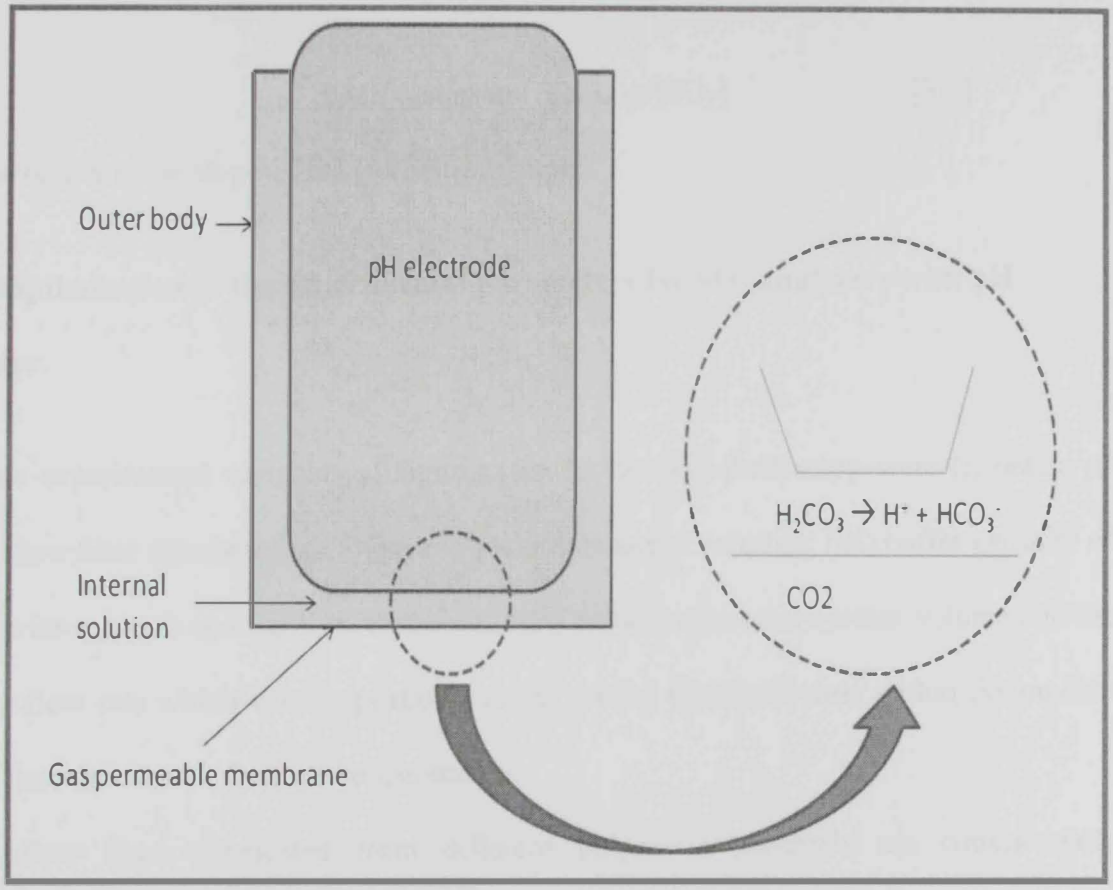

Figure 3.1: Construction of Severinghaus gas sensing probe, illustrated for CO_2.

Part of SO_2 from the gas stream permeates through the hollow fiber membrane walls and dissolves in the carrier solution which experiences pH drop to an extent determined by the partial pressure of SO_2 (P_{SO2}) in the gas stream. The electromotive force (EMF) of the pH electrode cell can be shown to relate linearly to the logarithmic SO_2 concentration using a treatment similar to that used with other acidic gases [102,103] as shown in Equation 3.1

$$EMF = \text{constant} + S \text{ Log } [SO_2] \qquad [3.1]$$

Where S is the slope of the calibration graph.

3.2.1 Optimization of the experimental parameters for SO_2 analyzers with pH detector.

The experimental variables of significance to the described setup were (i) nature of the hollow fiber membrane; (ii) type and pH of the carrier solution; (iii) buffer capacity of the carrier solution and finally (iv) the ratio (R) between the total system volume and the carrier flow rate which was proportional to the carrier residence time within the module and hence the contact time of the gas stream.

Hollow fibers fabricated from different polymeric materials are commercially available in different dimensions (i.e., ID, OD and wall thickness). The fibers are either microporous (e.g., polypropylene) or non-porous (e.g., silicone ruber and Teflon AF). Gas permeation in the latter type is based on dissolution-evaporation mechanism (pervaporation).[104,105] Microporous fibers provide the advantage of the higher gas flux but the non-porous fibers can provide some selective permeation for different gases. The interfacial membrane area and hence the efficiency of gas absorption and detection sensitivity are enhanced with smaller fiber dimensions. Hydrophobic polypropylene (PP) fibers (microporous) are selected in the present work of evaluating the pH detector owing

to its high permeability to SO_2 which would enhance the sensitivity. The reduction in linear response is not relevant with the glass pH detector which is known for its linear dynamic range.

The buffer capacity of the carrier solution should be a tradeoff between baseline stability (achieved with increased buffer capacity) and signal sensitivity which should be enhanced at lower buffer capacity. Otherwise, strongly buffered carrier solution would exhibit little pH change upon SO_2 absorption.

The resultant sensitivity and linearity of the analyzer will be due to combination of the SO_2 gas permeability in the HFMM, carrier buffer capacity as well as the ratio (R) which determine the extent of the gas pre-concentration and, in turn, the observed pH change. The ratio (R) also participates to the overall response and recovery times of the analyzer.

Higher gas flux should provide more sensitive detection. To maximize the sensitivity, all fibers should be accessible to the gas stream. Moreover, the buffer capacity of the carrier solution should be carefully selected. On the other hand, to decrease the response and recovery times the total tube volume and the connection between the module and the flow cell should be kept to minimum.

Given the above consideration, the response of the analyzer shown in **Figure 2.2** equipped with pH flow-through detector was evaluated using a custom made HFMM containing 60 PP fibers (25cm in length) sealed in glass tube (8 mm OD, 5 mm ID) using epoxy (Araldite). Gas inlet and outlet were made using stainless tubes (3 cm in length and 1/8" OD). The module tube volume was measured as 0.8 mL.

The glass electrode potentiometric response to SO_2 concentrations in gas stream was tested with several carrier solutions and the obtained results were shown in **Figure 3.2** and **3.3.** Dilute carrier solutions ($\leq$ 0.05 M), i.e., with low buffer capacities, exhibited a potential jump (characteristic to acid-base titration) at certain SO_2 concentration as shown

in **Figure 3.2**. More linear responses were obtained with more concentrated buffers as shown in **Figure 3.3**. Such behavior was predicted because Equation 3.1 was obtained by assuming that the acceptor solution has a fixed concentration of the conjugate base which predicted in the derivation of Equation 3.1.[102] Although bisulfate and sulfite solutions showed acceptable linear responses they were excluded as potential carrier because of their intrinsic instability in aqueous solutions. Potassium phosphate and sodium citrate showed slightly less linear and less sensitive responses than that obtained with 0.1M potassium oxalate as carrier solution. Therefore, 0.1M potassium oxalate solution was used as carrier throughout the remaining characterization.

A real time recording of the potentiometric response of the combination glass electrode for step increase in SO_2 concentrations in range of 40 to 10,000 ppm was shown in **Figure 3.4**. The potentiometric glass electrode detector could provided wide dynamic range up to 10,000 ppm with adequate limit of detection estimated as 1.0 ppm (S/N ratio = 3).

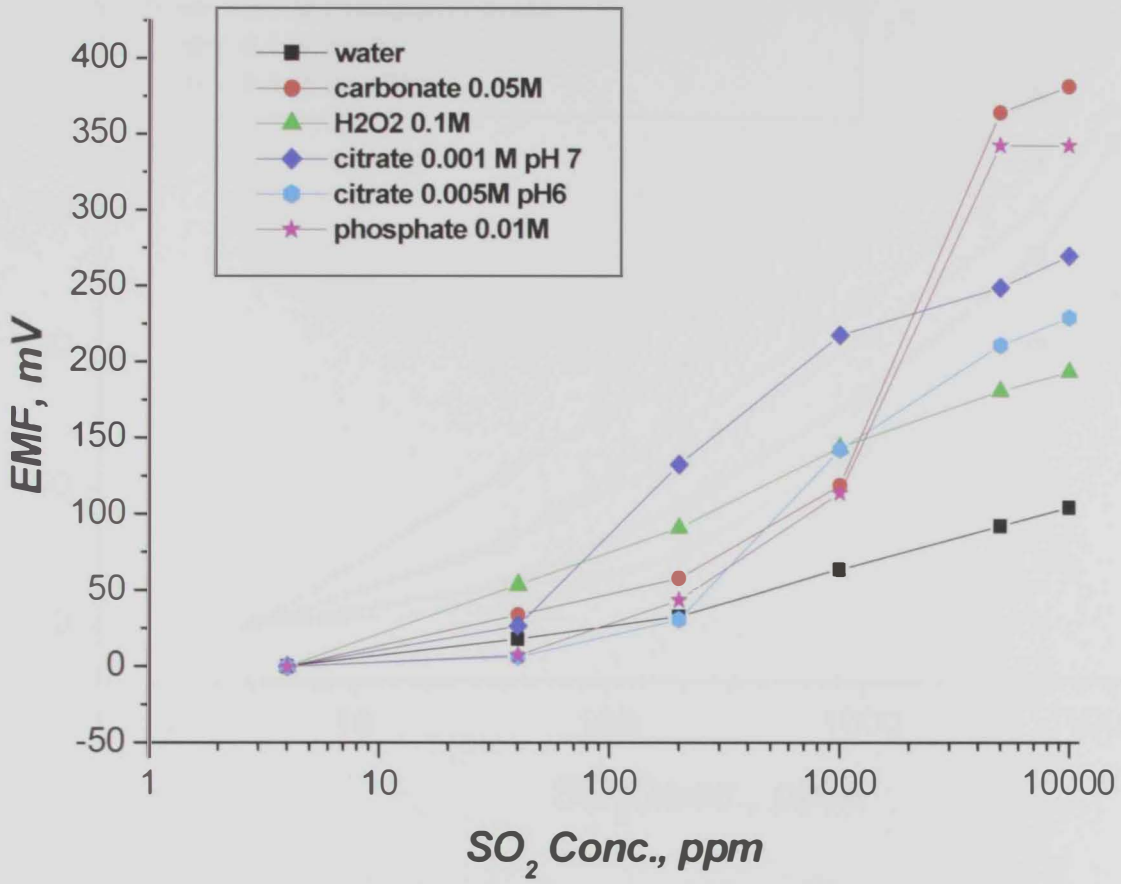

Figure 3.2: Potentiometric response to SO_2 concentration using dilute buffers. SO_2 was diluted with N_2, gas flow rate = 250 mL/min and the carrier solution flow rate = 1.5 mL/min, using custom HFMM based on 60 PP fibers.

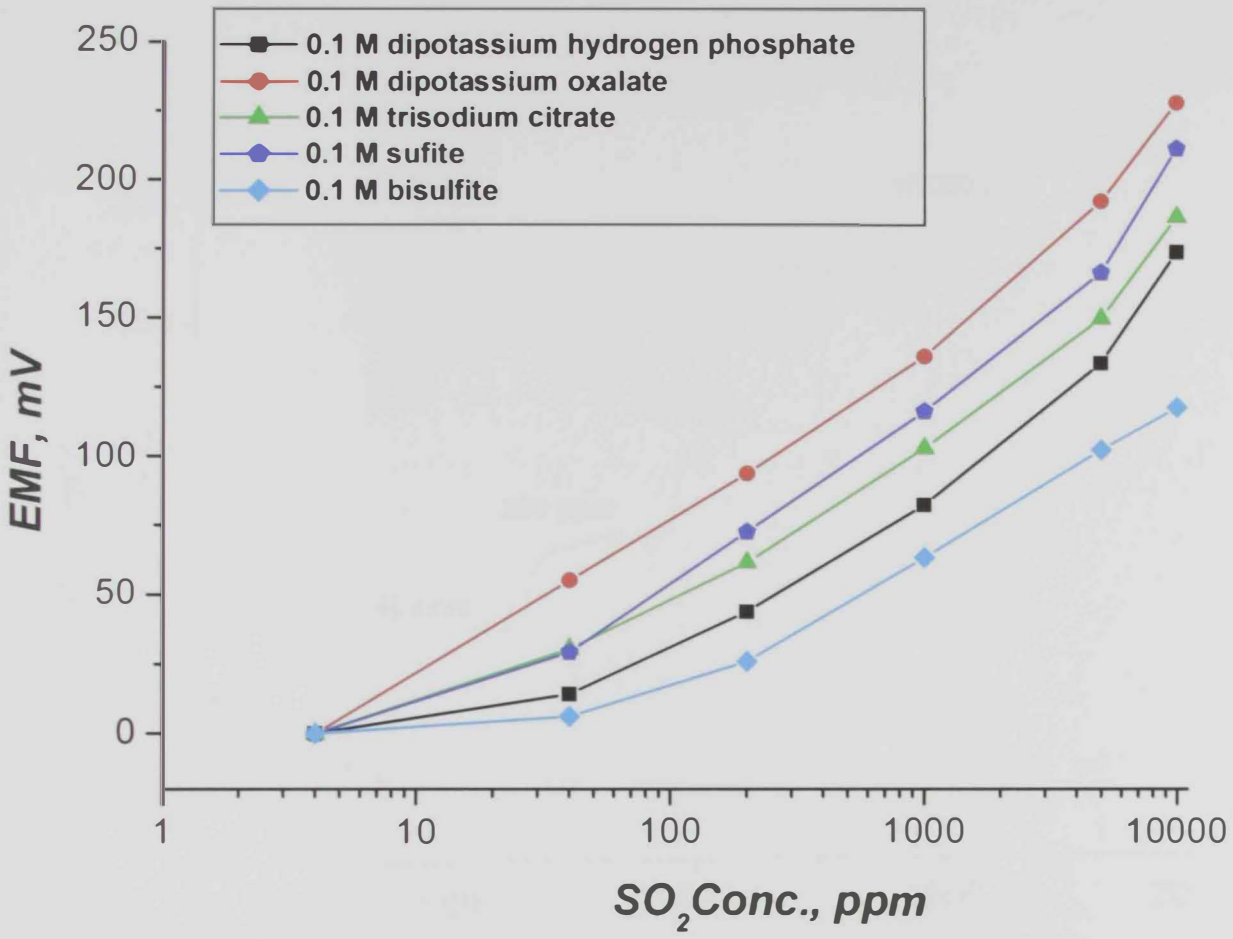

Figure 3.3: Potentiometric response to SO_2 concentration using more concentrated buffers. The rest of conditions were similar to those in Figure 3.2

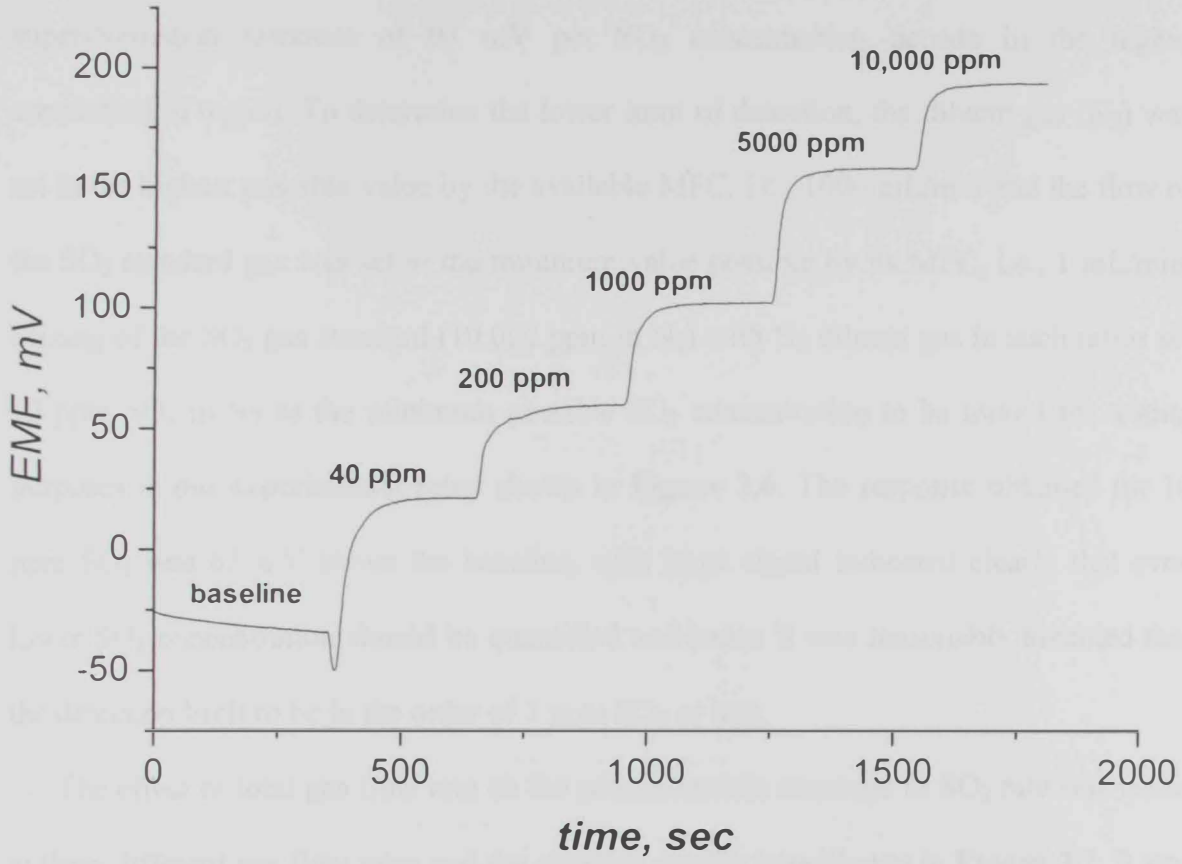

Figure 3.4: Real time potentiometric response obtained for step changes in SO_2 concentration in nitrogen. gas flow rate = 250 mL/min and the carrier solution flow rate = 1.5 mL/min, using custom HFMM based on 60 PP fibers.

3.2.2 Characterization of the SO_2 analyzer based on pH detector

The real time recording and the corresponding calibration curve based on multi-step increments in SO_2 concentration were shown in **Figure 3.5**. The calibration graph exhibited Nernstian slope of 61 mV per SO_2 concentration decade up to 1000 ppm and a super-Nernstian response of 95 mV per SO_2 concentration decade in the higher concentration region. To determine the lower limit of detection, the diluent gas (N_2) was set to the highest possible value by the available MFC, i.e., 1000 mL/min and the flow of the SO_2 standard gas was set to the minimum value possible by its MFC, i.e., 1 mL/min. Mixing of the SO_2 gas standard (10,000 ppm in N_2) with N_2 diluent gas in such ratios set 10 ppm SO_2 in N_2 as the minimum possible SO_2 concentration to be mixed for testing purposes in our experimental setup shown in **Figure 3.6**. The response obtained for 10 ppm SO_2 was 65 mV above the baseline, such large signal indicated clearly that even lower SO_2 concentration should be quantified and hence it was reasonably assumed that the detection limit to be in the order of 1 ppm SO_2 or less.

The effect of total gas flow rate on the potentiometric response to SO_2 rate was tested at three different gas flow rates and the obtained results were shown in **Figure 3.7**. It was evident that the limit of detection enhanced at higher gas flow rate which could be attributed to the higher SO_2 flux. However, the rest of characterization was conducted using gas flow rate 250 mL/min.

The repeatability of the analyzer response was evaluated by series of step changes between pure N_2 and 1000 ppm SO_2 at the same flow rate. The response to SO_2 was reproducible as shown in **Figure 3.8** and the between-peak variations were less than 0.4% at the tested concentration level.

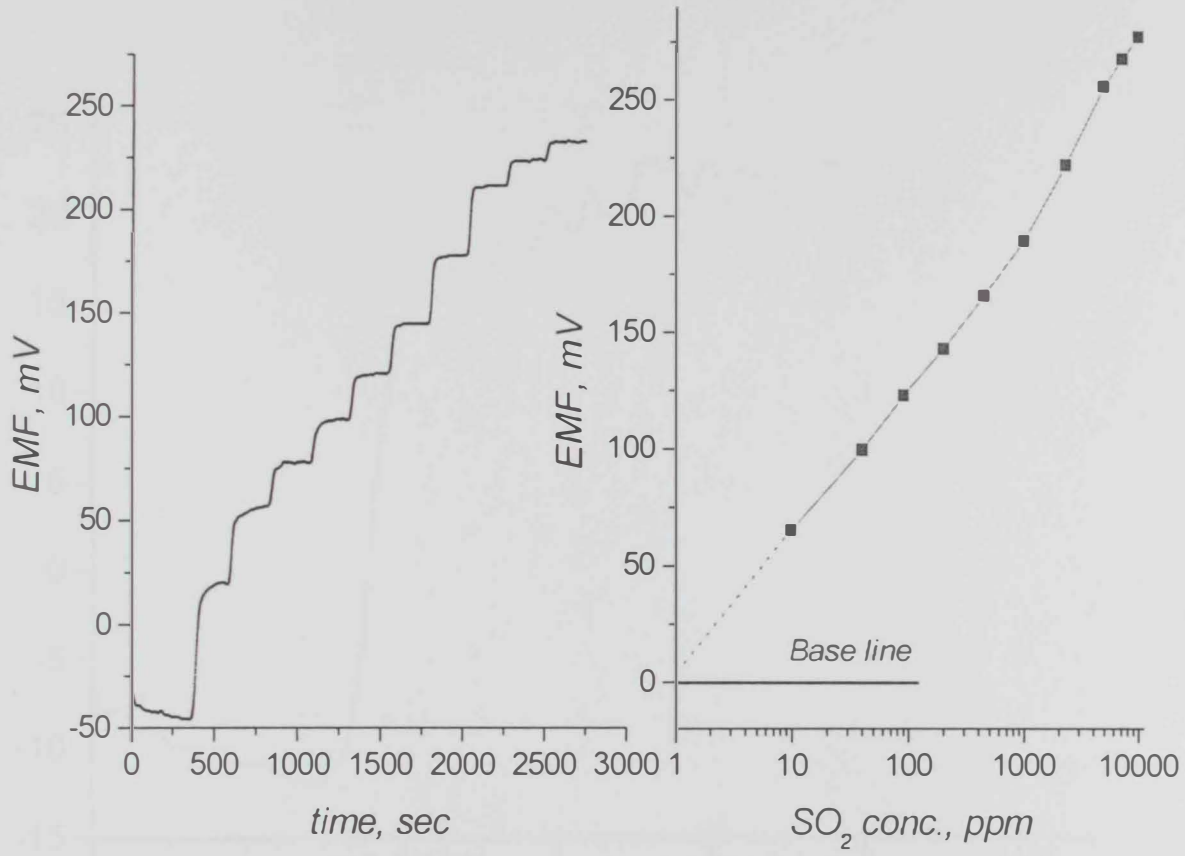

Figure 3.5: Real time potentiometric response obtained for step changes in SO_2 concentration in nitrogen and its calibration curve at total flow rate 1000mL/min, using 0.1 M oxalate as buffer solution at flow rate 1.5 mL/min, using HFMM. (PP fibers)

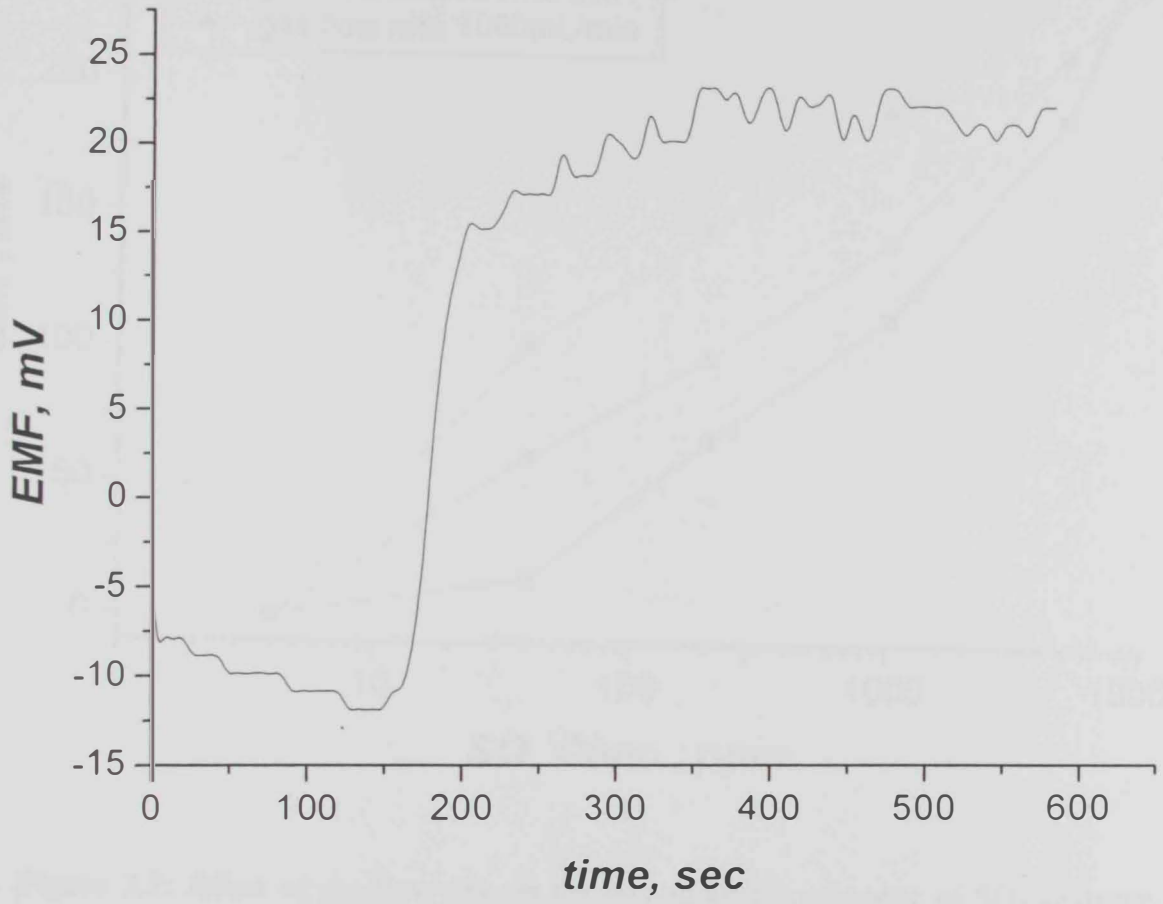

Figure 3.6: Real time response shows the minimum possible SO_2 concentration (10 ppm) to be mixed for testing purposes in our experimental setup, using 0.1 M oxalate as buffer solution at flow rate 1.5 mL/min, using HFMM. (PP fibers)

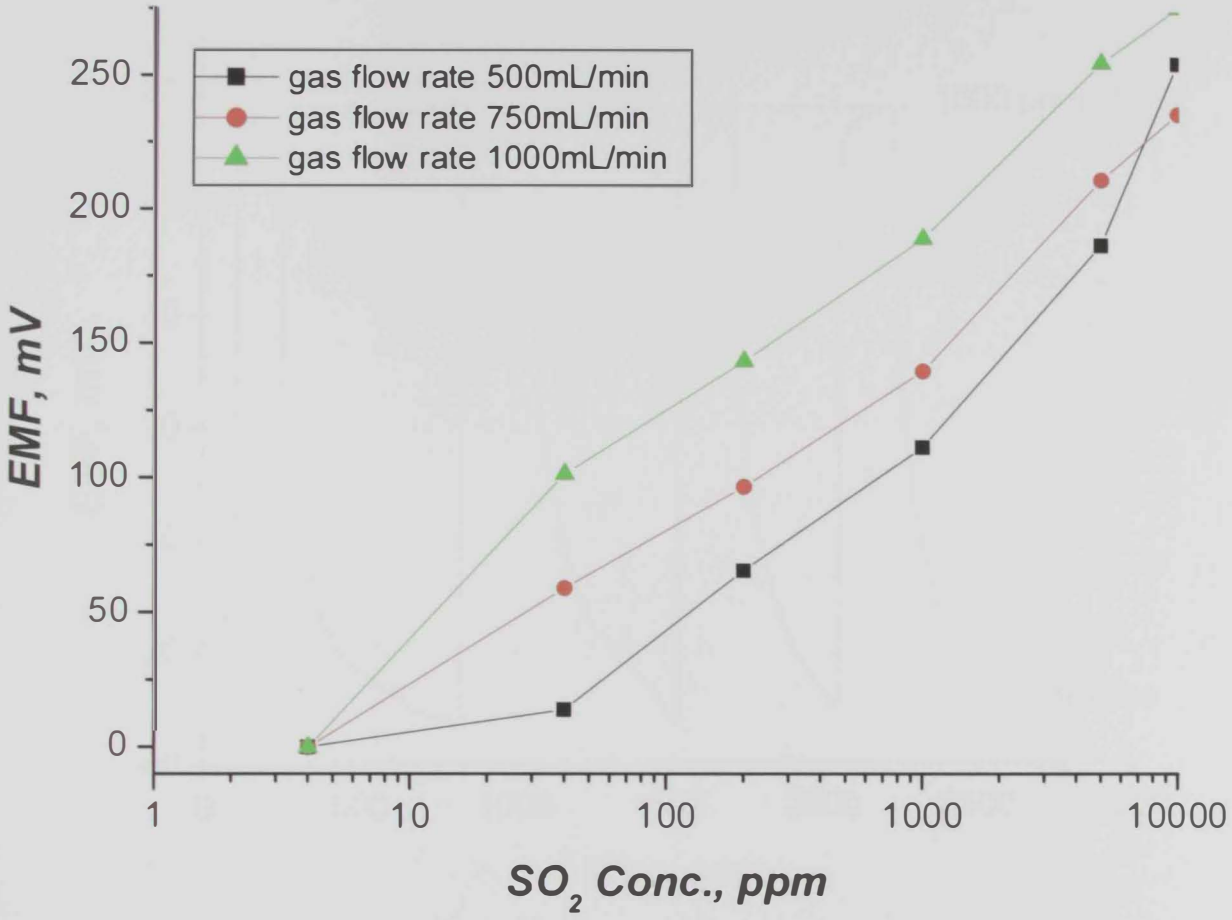

Figure 3.7: Effect of gas flow rate on the potentiometric response of SO_2 analyzer. Using 0.1M oxalate buffer at flow rate 2 mL/min and using HFMM. (PP fibers).

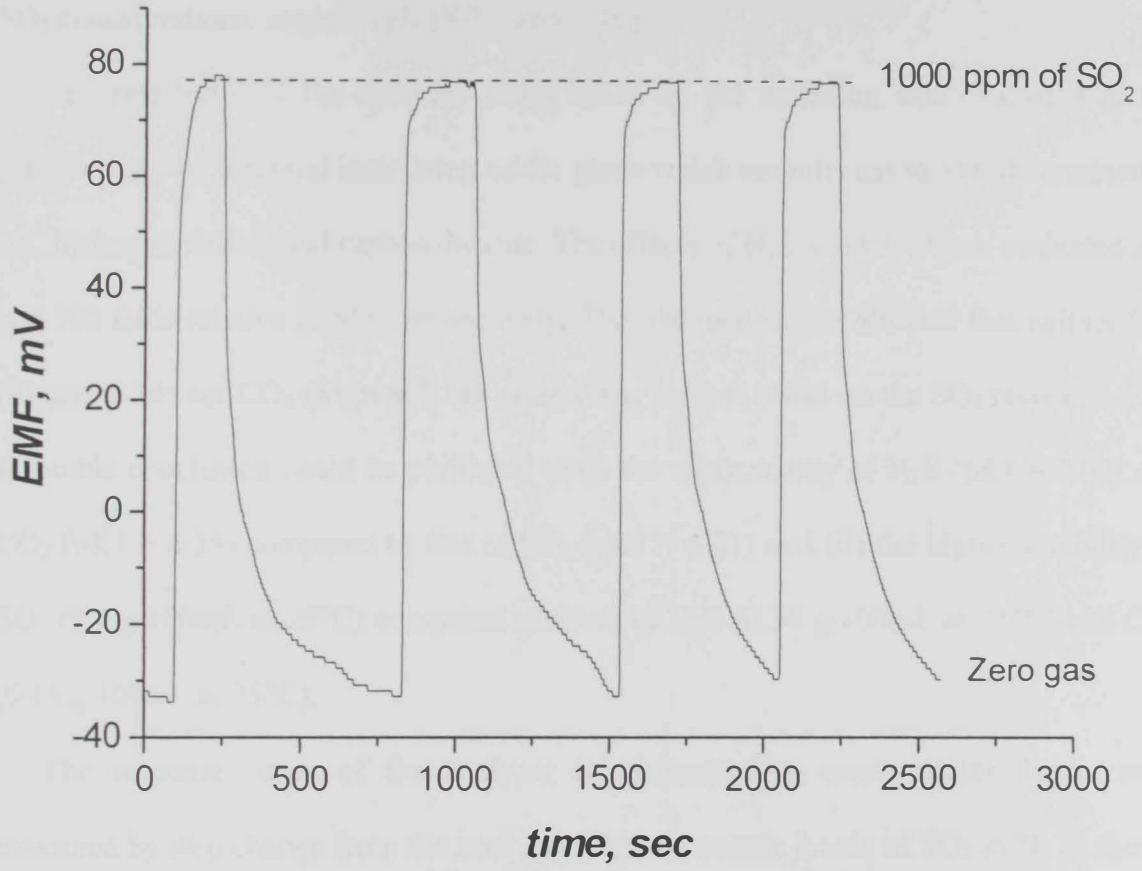

Figure 3.8: Repeatability of the SO_2 analyzer response using 0.1 M oxalate carrier at 1.5 mL/min, gas flow rate 250 mL/min using custom HFMM based on 60 PP fibbers.

The reliability of the developed analyzer setup to continuously detect small changes at relatively large concentrations of SO_2 in gas streams, as a measure of sensitivity, was assessed by several step changes in SO_2 between 1000 and 960 ppm. The obtained results (**Figure 3.9**) showed stable and well distinguished signal levels corresponding to the two SO_2 concentrations, respectively (S/N ratio = 10).

The selectivity of the analyzer setup based on pH detection was evaluated in the presence of two potential interfering acidic gases which are relevant to SO_2 determination, i.e., hydrogen sulfide and carbon dioxide. The effects of H_2S and CO_2 were evaluated at 5 and 500 folds relative to SO_2, respectively. The obtained results showed that neither H_2S (**Figure 3.10**) nor CO_2 (**Figure 3.11**) exerted any serious effect on the SO_2 response. This favorable conclusion could be attributed to (i) the weak acidity of H_2S ($pK1$ = 7.02) and CO_2 (pK1 = 6.35) compared to that of SO_2 ($pK1$ = 1.81) and (ii) the higher solubility of SO_2 (9.4 g/100mL at 25°C) compared to those of H_2S (0.34 g/100mL at 25°C) and CO_2 (0.15 g/100mL at 25°C).

The response times of the analyzer to different SO_2 concentration levels were measured by step change from the zero gas (N_2) to a certain levels of SO_2 in N_2 as shown in **Figure 3.12**. The observed response times ($t_{0.95}$) were 204, 47, 48, and 23 sec for 100, 1000, 5000 and 10000 ppm, respectively. Such fast response times were due to combination of several optimization factors including the selection of microporous hollow fibers, carrier flow rate, the flow detector with small dead volume (50 μL) and the intrinsic fast response of the glass electrode. The fast response of the developed analyzer suggests its suitability for continuous real time monitoring of SO_2 in gas streams. The recovery times were also measured as shown in **Figure 3.13** which revealed also fast recovery of the analyzer response when the SO_2 concentration was stepped from different levels to zero gas. The recovery time was in the range of 600 seconds. However, shorter

recovery times were obtained for smaller concentration changes. For example, recovery time for step concentration from 1000 ppm to 960 ppm was 30 seconds as shown in **Figure 3.9.**

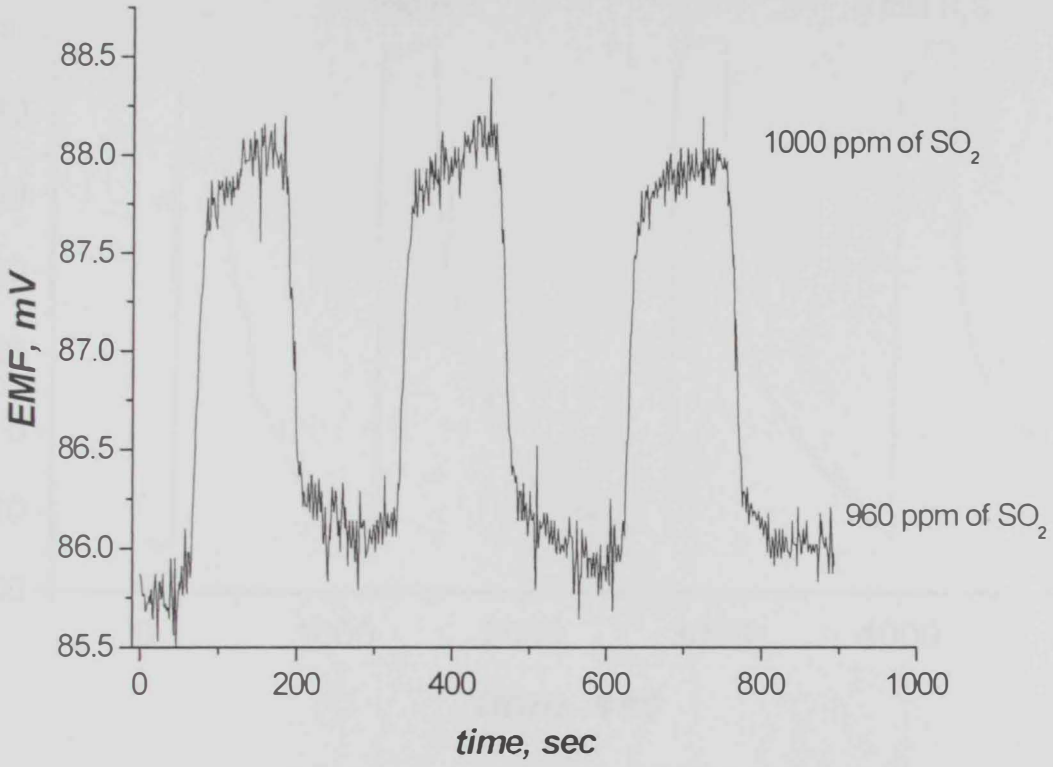

Figure 3.9: Sensitivity test for the SO_2 analyzer towards two close concentrations of SO_2, carrier flow rate 2 ml/min, gas flow rate 250 mL/min using custom HFMM based on 60 PP fibbers.

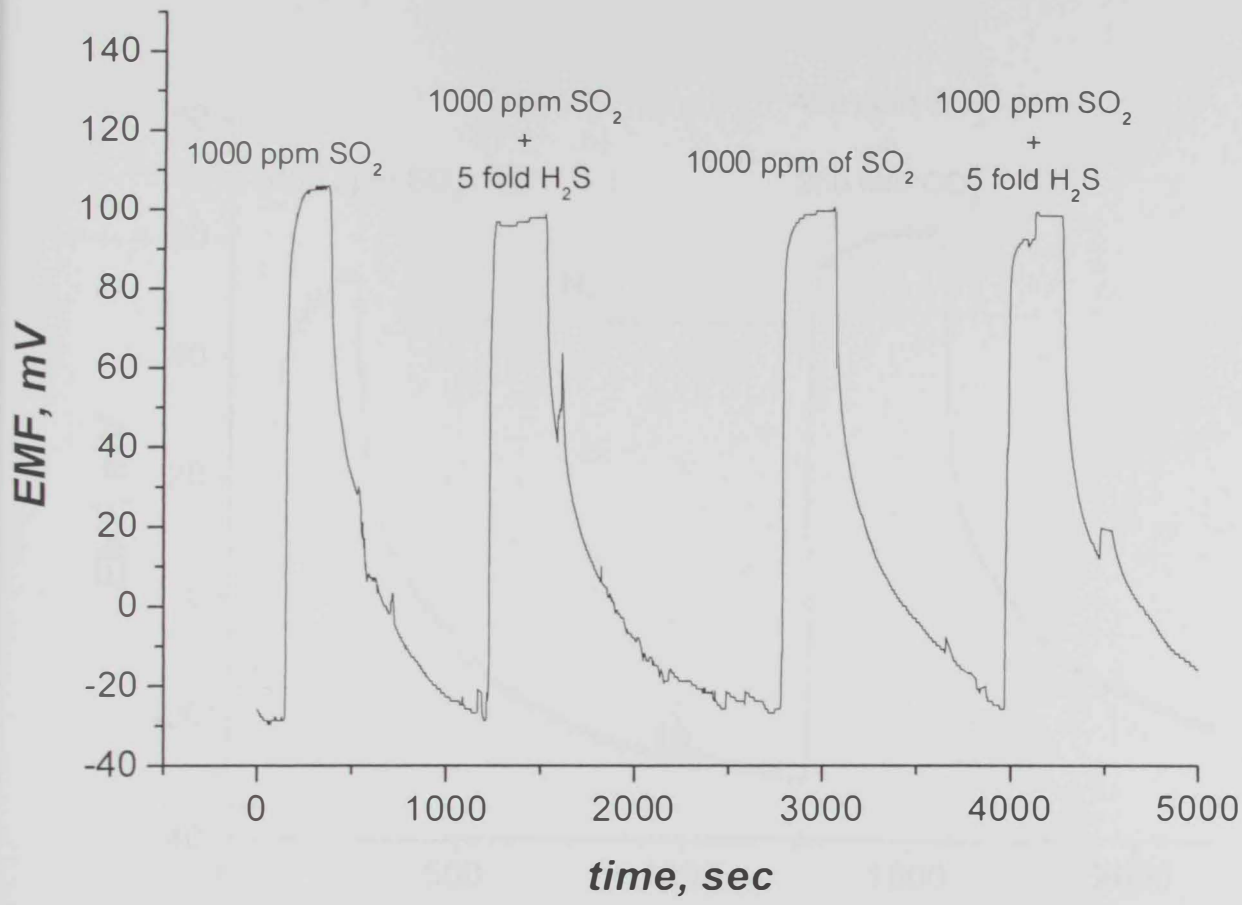

Figure 3.10: Interference effect of H_2S gas on the proposed SO_2 analyzer, gas flow rate 250 mL/min using custom HFMM based on 60 PP fibbers.

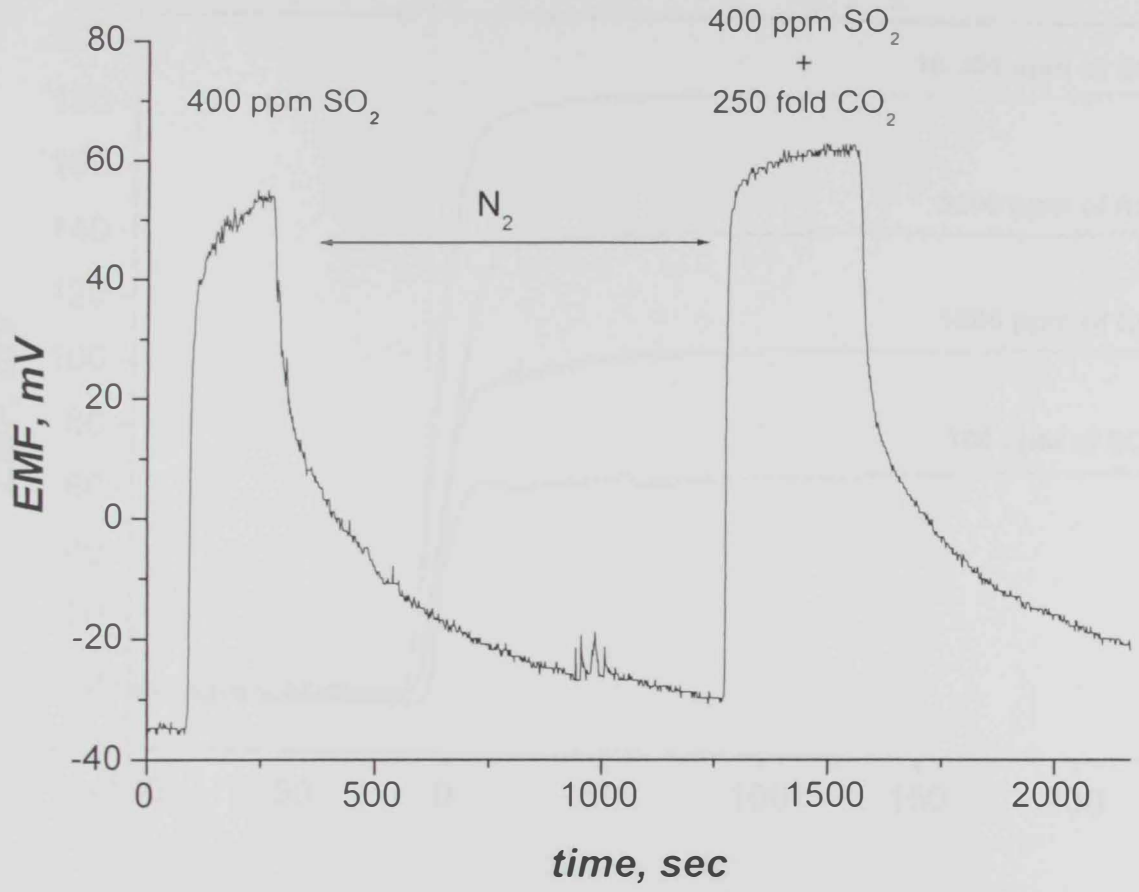

Figure 3.11: Interference effect of CO_2 on the proposed SO_2 analyzer, carrier flow rate 2mL/min, gas flow rate 250 mL/min using custom HFMM based on 60 PP fibbers.

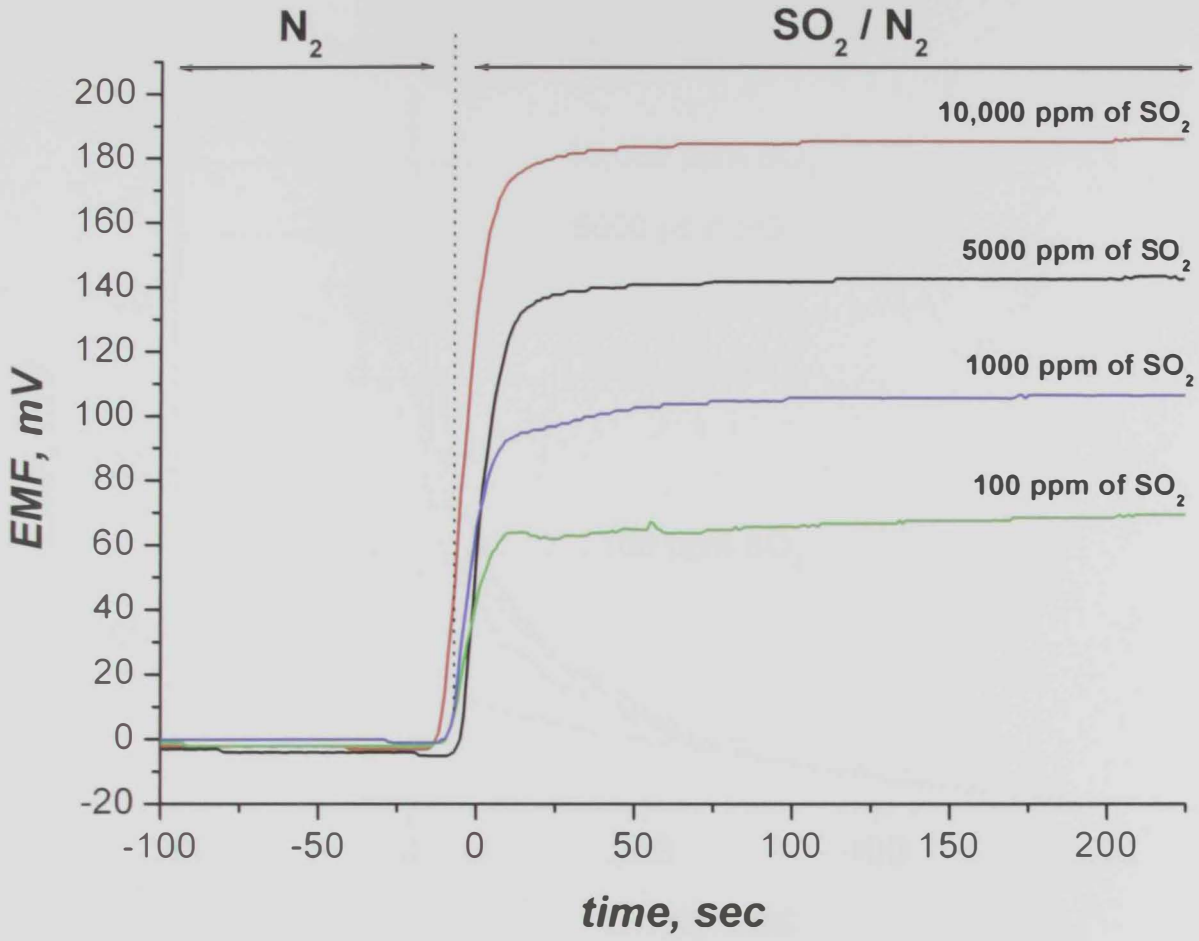

Figure 3.12: The response times of the analyzer to different SO_2 concentration levels, gas flow rate 250 mL/min using custom HFMM based on 60 PP fibbers.

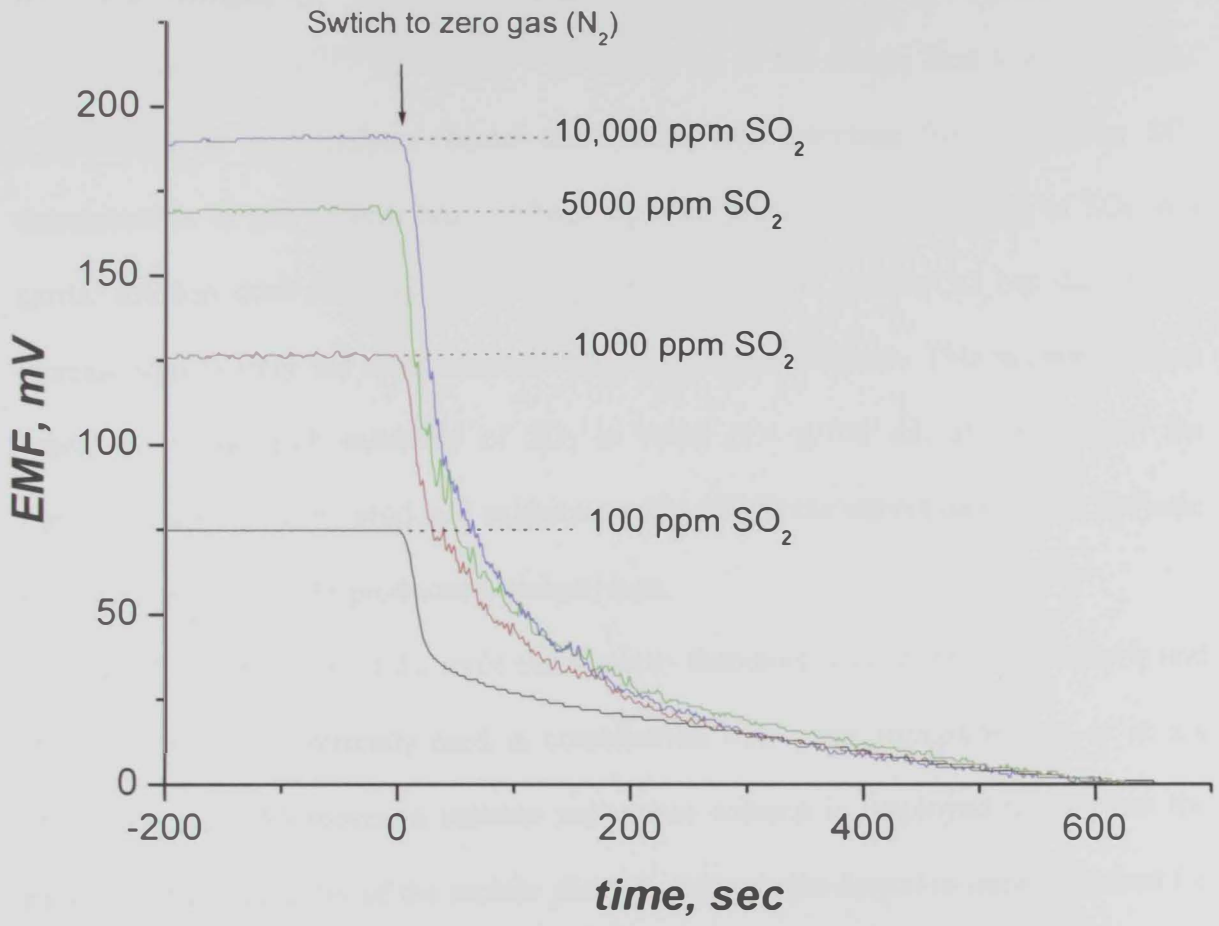

Figure 3.13: The recovery times of the analyzer to different SO_2 concentration levels, gas flow rate 250 mL/min using custom HFMM based on 60 PP fibbers.

3.3 SO_2 gas analyzer based on conductivity detector

Conductivity detectors have been reliably used in several analytical systems such as liquid chromatography.[106] Moreover, gas detection based on conductivity detectors was also reported for CO_2[107] and SO_2.[55] However, up to the author best knowledge that construction of gas analyzer based on conductivity detection for continuous SO_2 determination in gas streams has not been reported previously. Absorption of SO_2 in a carrier solution does not only lower the pH as described in section 3.2 but also should increase significantly the ionic conductivity of the carrier solution. This assumption was based on (i) the high solubility of SO_2 in water (9.4 g/100 mL at 25 °C), (ii) the significant acidity of the produced sulfurous acid and (iii) the exceptionally high intrinsic ionic conductivity of the produced hydrogen ions.

The major limitation of the ionic conductivity detectors is their lack of selectivity and therefore they are commonly used in combination with prior separation step as in ion chromatography. Moreover, a suitable suppressor column is employed to suppress the background conductivity of the mobile phase to enhance the detection limits obtained for the determined ions. Therefore, in the present work buffer aqueous carrier solutions tested in the pH detection described in section 3.2 were not attempted because of their high ionic conductivity. Instead, deionized (DI) water was first tested as carrier liquid with the conductivity detector to obtain baseline with very low background conductivity.

3.3.1 Optimization of the experimental parameters for the SO_2 analyzers with conductivity detector

The commercial conductivity probe used in the present work has wide dynamic range up to 2000 μSiemens. Hence, the limitation of signal saturation is not expected with this detector (similar to the glass electrode in section 3.2). Therefore, the same HFMM with high gas absorption efficiency based on microporous PP fibers used in pH detection was also used with the conductivity detection.

The obtained voltage signal proportional to the carrier solution conductivity was shown in **Figure 3.14** in the concentration range between 50 and 250 ppm SO_2. The response was fast (80 sec) and linear over the tested concentration range.

To further enhance the sensitivity of conductivity detection, hydrogen peroxide was suggested to convert (*in line*) sulfurous acid to the stronger sulfuric acid which should lead to higher ionic conductivity. It is worth mentioning here that hydrogen peroxide when added to the deionized (DI) water, carrier did not increase the background conductivity to any appreciable level. Different concentrations of hydrogen peroxide in DI water were tested and the obtained results were shown in **Figure 3.15**. The highest sensitivity (indicated by the slope of the calibration graph) was obtained using 1.0 mM H_2O_2 in DI water. It was not fully understood why the sensitivity decreased at higher concentrations of H_2O_2 but this test was repeated several times and it was proved reproducible. Comparison between real time recording of the analyzer response to same concentration levels of SO_2 using DI water and 1.0 mM H_2O_2 in DI water was given in **Figure 3.16**.

The effect of carrier solution flow rate was tested at three different values and the obtained results (shown in **Figure 3.17**) indicated that the sensitivity of SO_2 detection was

enhanced at lower flow rates. This was explained on the basis of longer contact time between the carrier solution and the gas stream inside the module which allowed more preconcentration of SO_2 gas in the carrier solution.

A

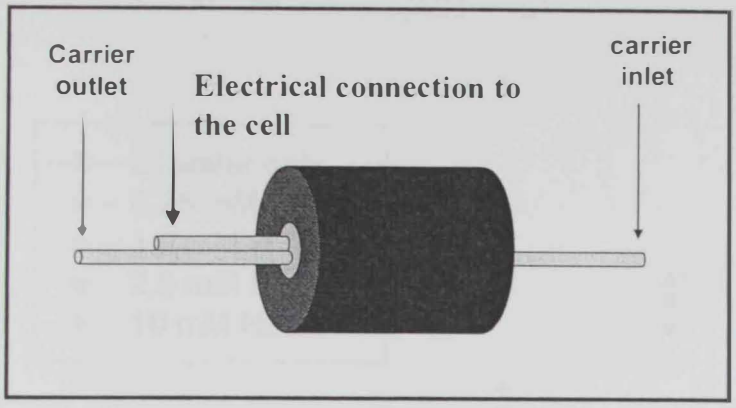

B

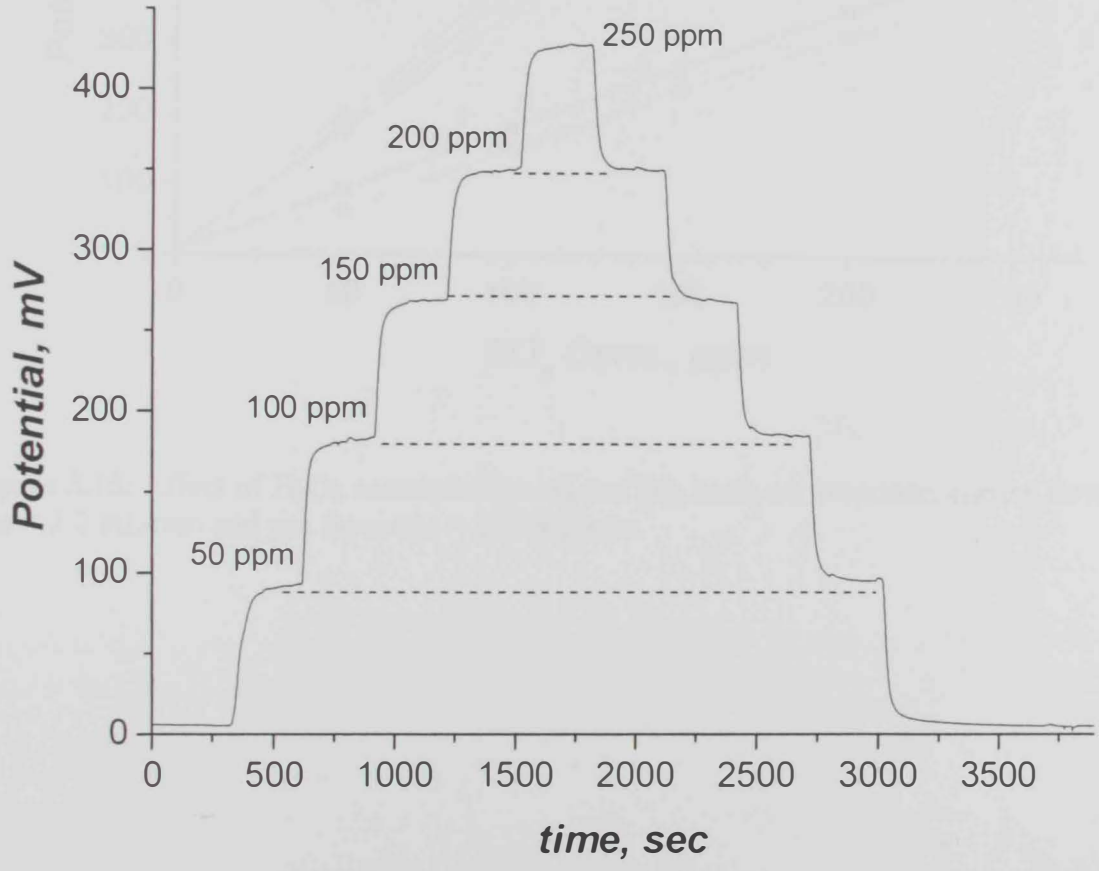

Figure 3.14: A: Construction of commercial conductometric probe. B: The obtained voltage signal for different SO_2 concentrations, using HFMM (PP fibers), with DI water as carrier solution at flow rate 2.0 mL/min and gas flow rate 200 mL/min.

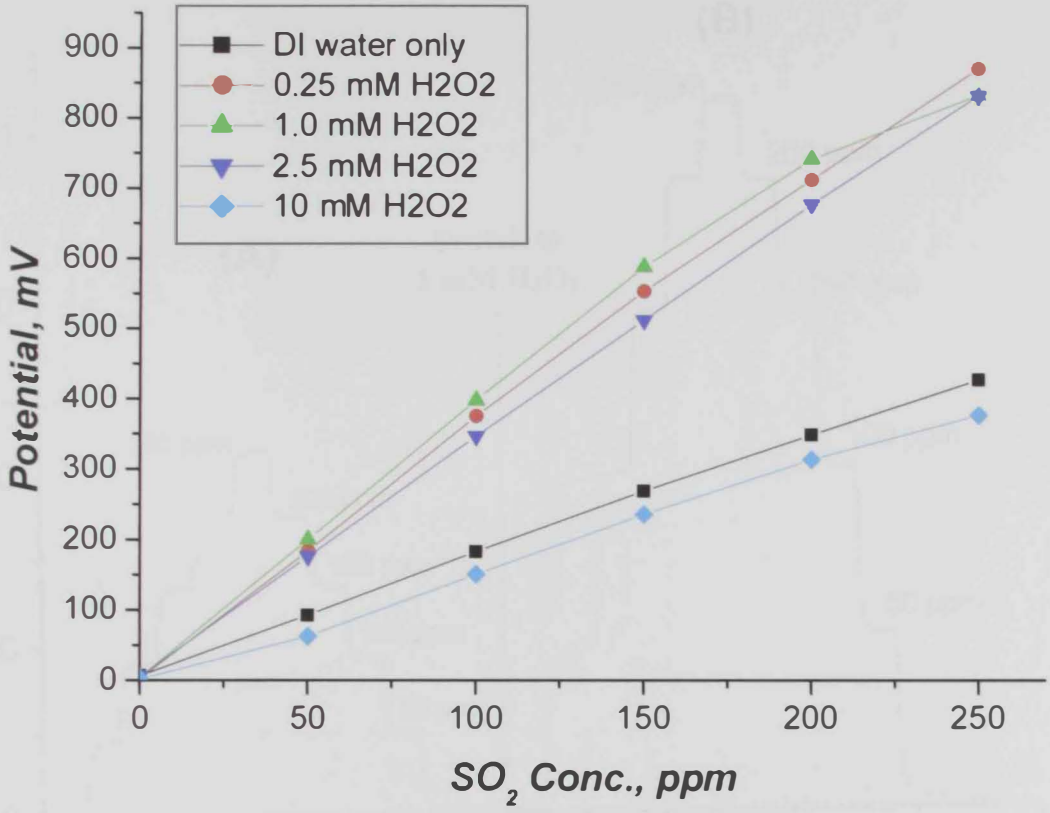

Figure 3.15: Effect of H_2O_2 concentration on the SO_2 analyzer response, carrier flow rate = 2.0 mL/min and gas flow rate = 200 mL/min.

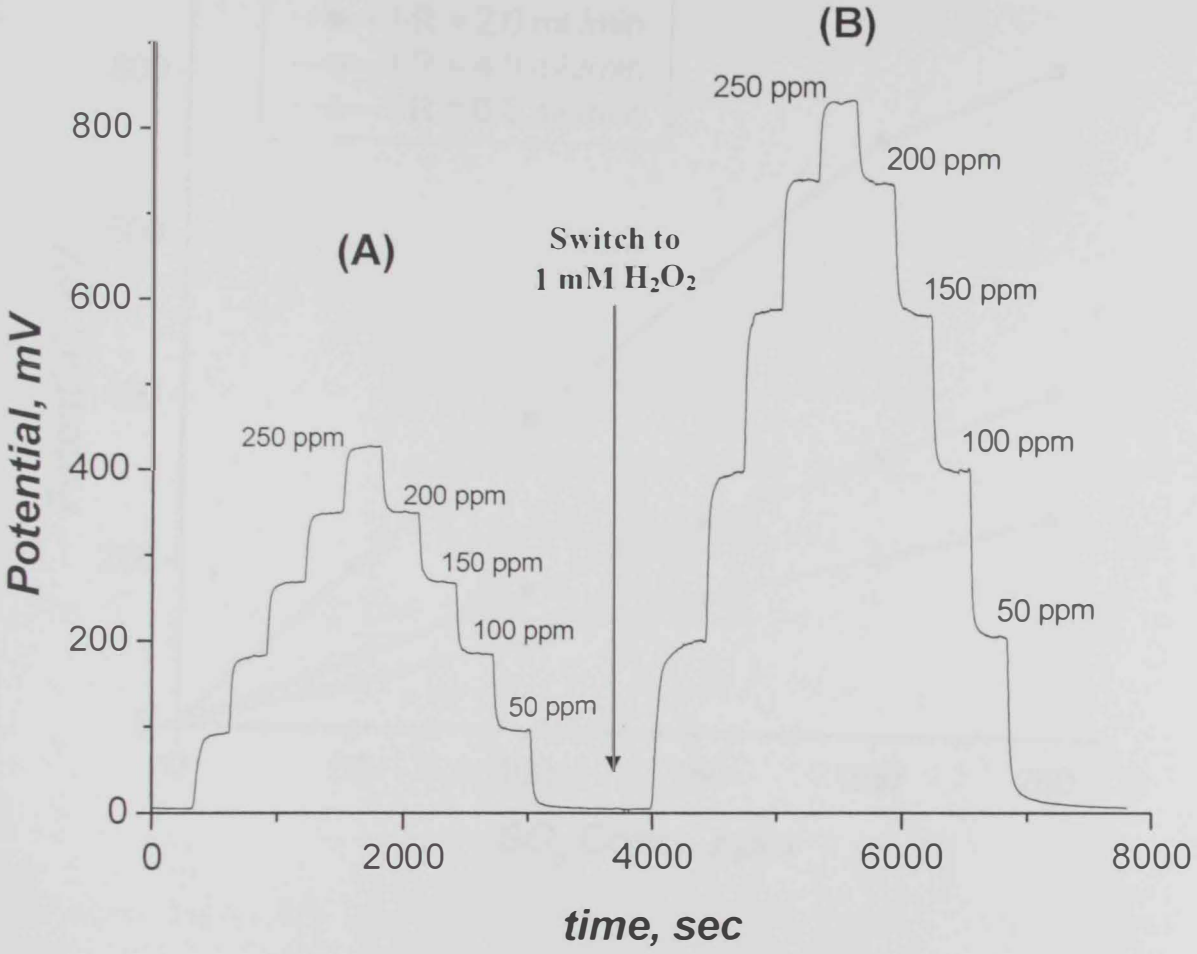

Figure 3.16: Comparison between the sensitivity of the SO_2 detection using DI water (A) and 1.0 mM H_2O_2 (B), carrier flow rate = 2.0 mL/min and gas flow rate = 200 mL/min.

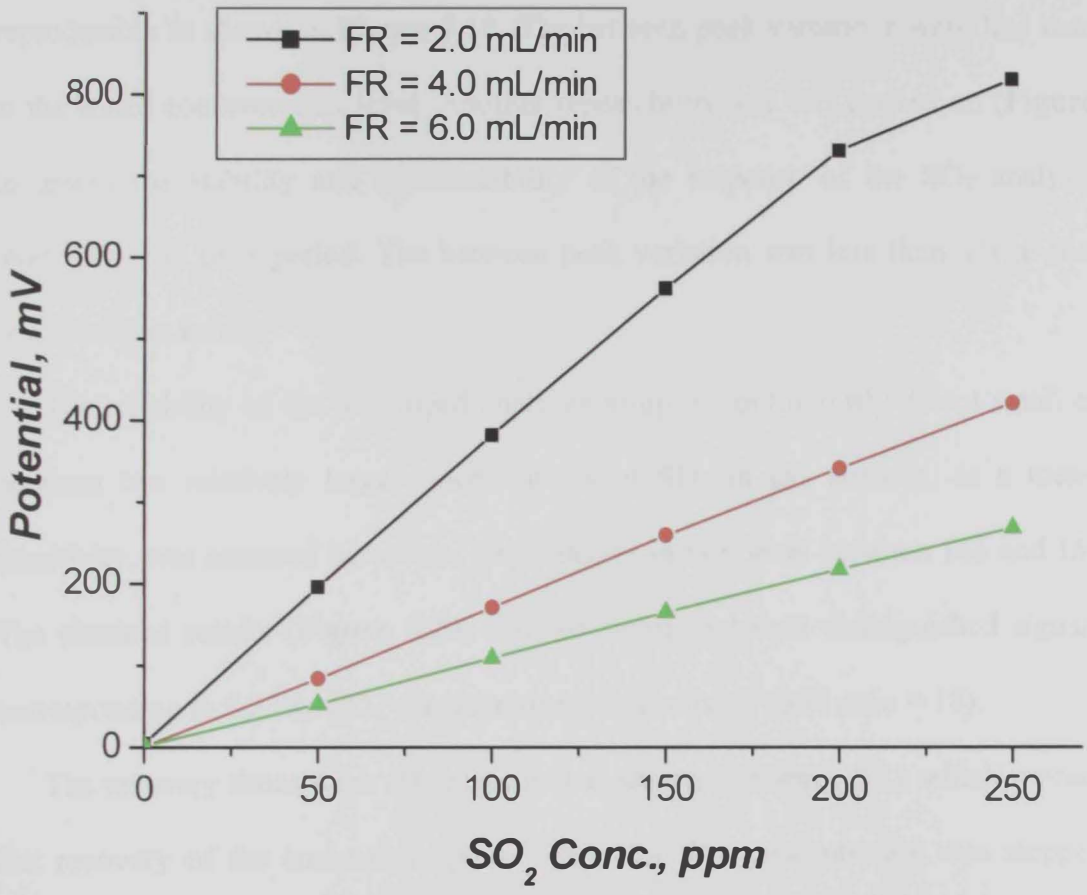

Figure 3.17: Effect of different carrier flow rates using 1.0 mM H_2O_2, carrier flow rate = 2.0 mL/min and gas flow rate = 200 mL/min.

3.3.2 Characterization of the SO_2 analyzer based on the conductivity detector

The repeatability of the analyzer response was evaluated by series of step changes between pure N_2 and 250 ppm SO_2 at the same flow rate. The response to SO_2 was reproducible as shown in **Figure 3.18**. The between peak variations were less than 1.6% at the tested concentration level. Another repeatability test was carried on (**Figure 3.19**) to assess the stability and reproducibility of the response of the SO_2 analyzer over relatively long time period. The between peak variation was less than 4% at the tested concentration levels.

The reliability of the developed analyzer setup to continuously detect small changes between two relatively large concentrations of SO_2 in gas streams, as a measure of sensitivity, was assessed by several step changes in SO_2 level between 166 and 150 ppm. The obtained results (**Figure 3.20**) showed stable and well distinguished signal levels corresponding to the two SO_2 concentrations, respectively (S/N ratio = 18).

The recovery times were also measured as shown in **Figure 3.21** which revealed also fast recovery of the analyzer response when the SO_2 concentration was stepped from different levels to zero gas. The recovery time was in the range of 115 to 180 seconds. Compared with pH-detector ($t_{0.95}$ = 600 sec) the conductivity detector exhibited faster recovery time. This was mainly attributed to the slow response of the glass electrode in the vicinity of the neutral pH.

The selectivity of the analyzer based on the conductivity detection was evaluated in the presence of CO_2 which is a potentially interfering acidic gas and usually relevant to SO_2 determination. The effect of CO_2 was evaluated at concentration level which was 100 folds greater than that of SO_2. Although CO_2 did not cause any appreciable effect in SO_2 determination (*cf.* **Figure 3.10**) using the pH detector, it exerted a significant positive

interference with the conductivity detector (**Figure 3.22**). This difference is attributed to the nature of the response of the detector. The weak effect of carbonic acid on the pH changes caused by sulfurous acid was substantially smaller than the effect of the bicarbonate/carbonate ions on the conductivity detector.

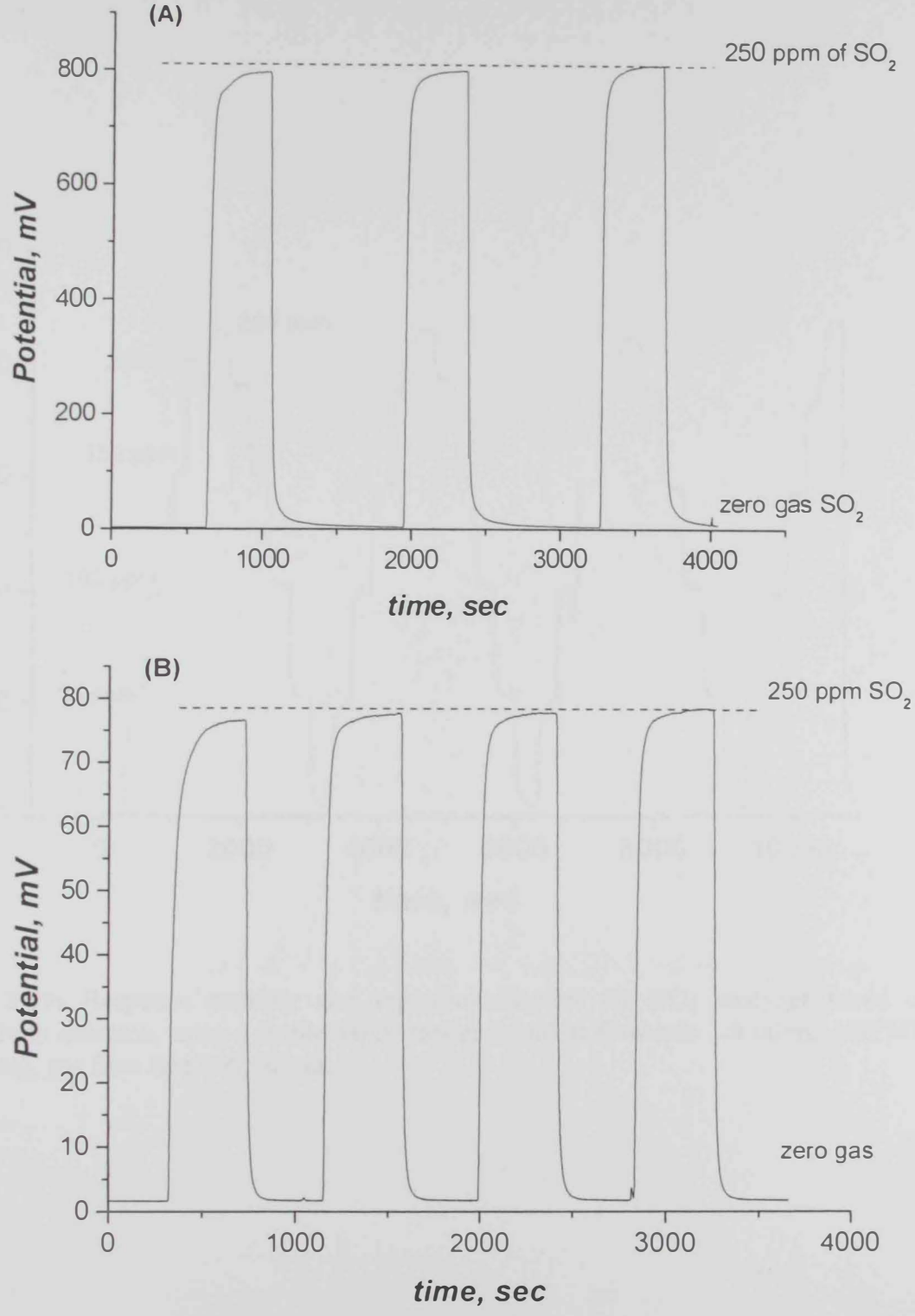

Figure 3.18: Repeatability test of the SO_2 analyzer to 250 ppm of SO_2 using 1.0 mM H_2O_2 carrier liquid at flow rate 2.0 ml/min, HFMM (PP fibers), gas flow rate 200 ml/min. (A): run on scale 100x, while (B): run on scale 10x.

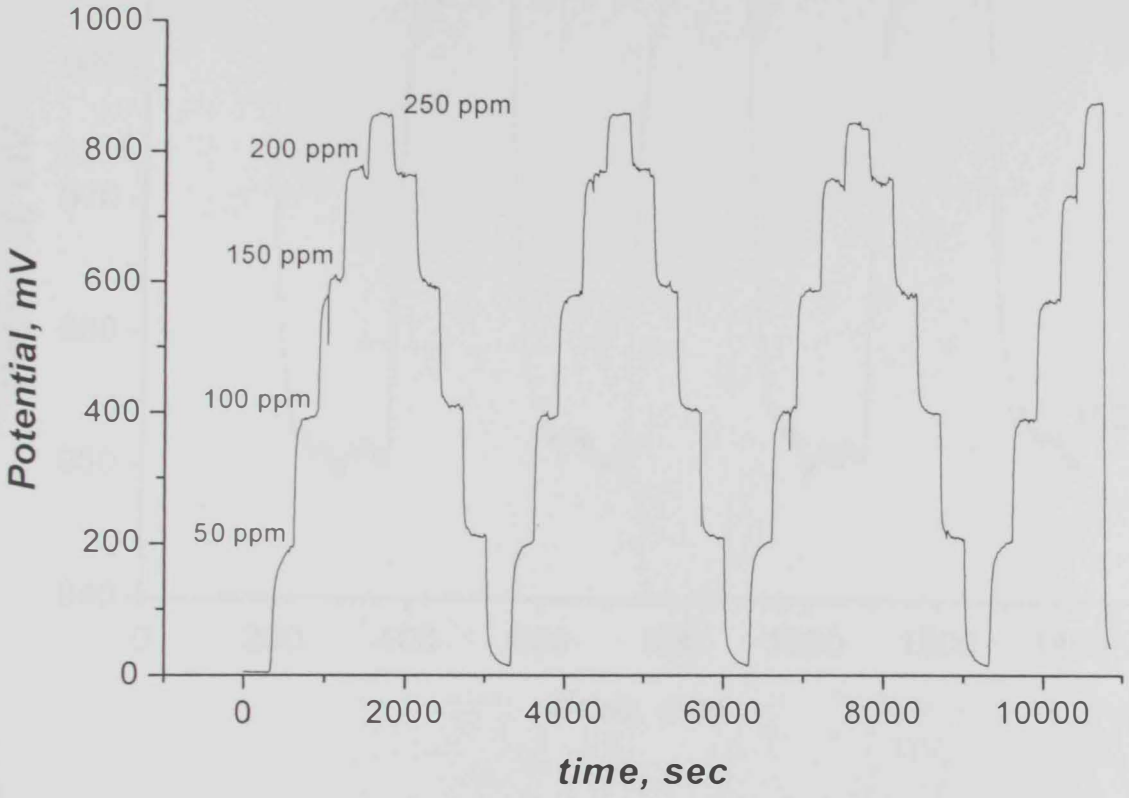

Figure 3.19: Response stability and reproducibility of the SO_2 analyzer based on conductivity detector, using 1.0 mM H_2O_2 carrier liquid at flow rate 2.0 ml/min, HFMM (PP fibers), gas flow rate 200 ml/min.

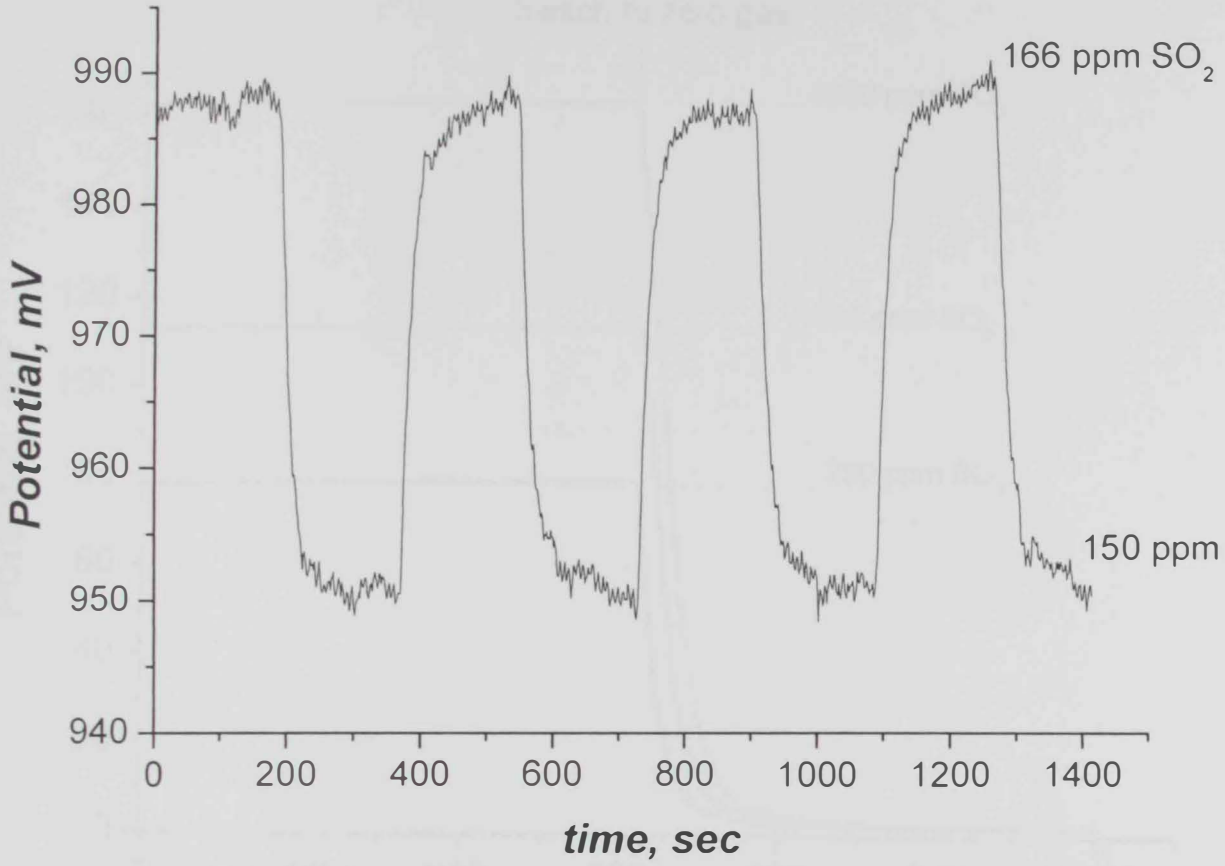

Figure 3.20: Real time recording of the analyzer response based on the conductivity detector to series of small step changes in SO_2 concentration between 150 and 166 ppm levels; carrier flow rate: 6 mL/min and gas flow rate 600 mL/min using HFMM (PP fibers).

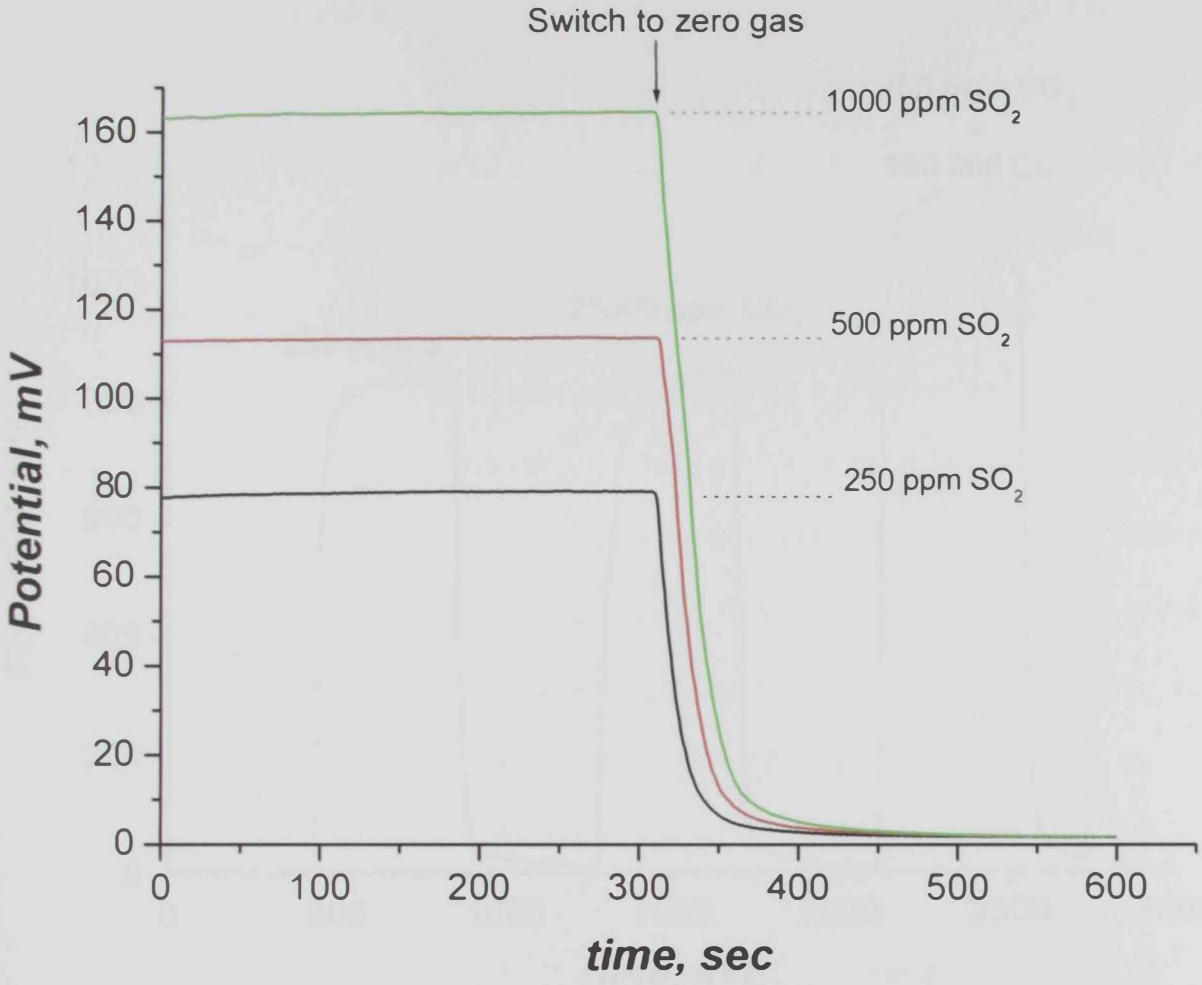

Figure 3.21: Recovery time obtained for the signal response at different SO_2 concentrations, using 1.0 mM H_2O_2 carrier liquid at flow rate 2.0 ml/min, HFMM (PP fibers), gas flow rate 200 ml/min.

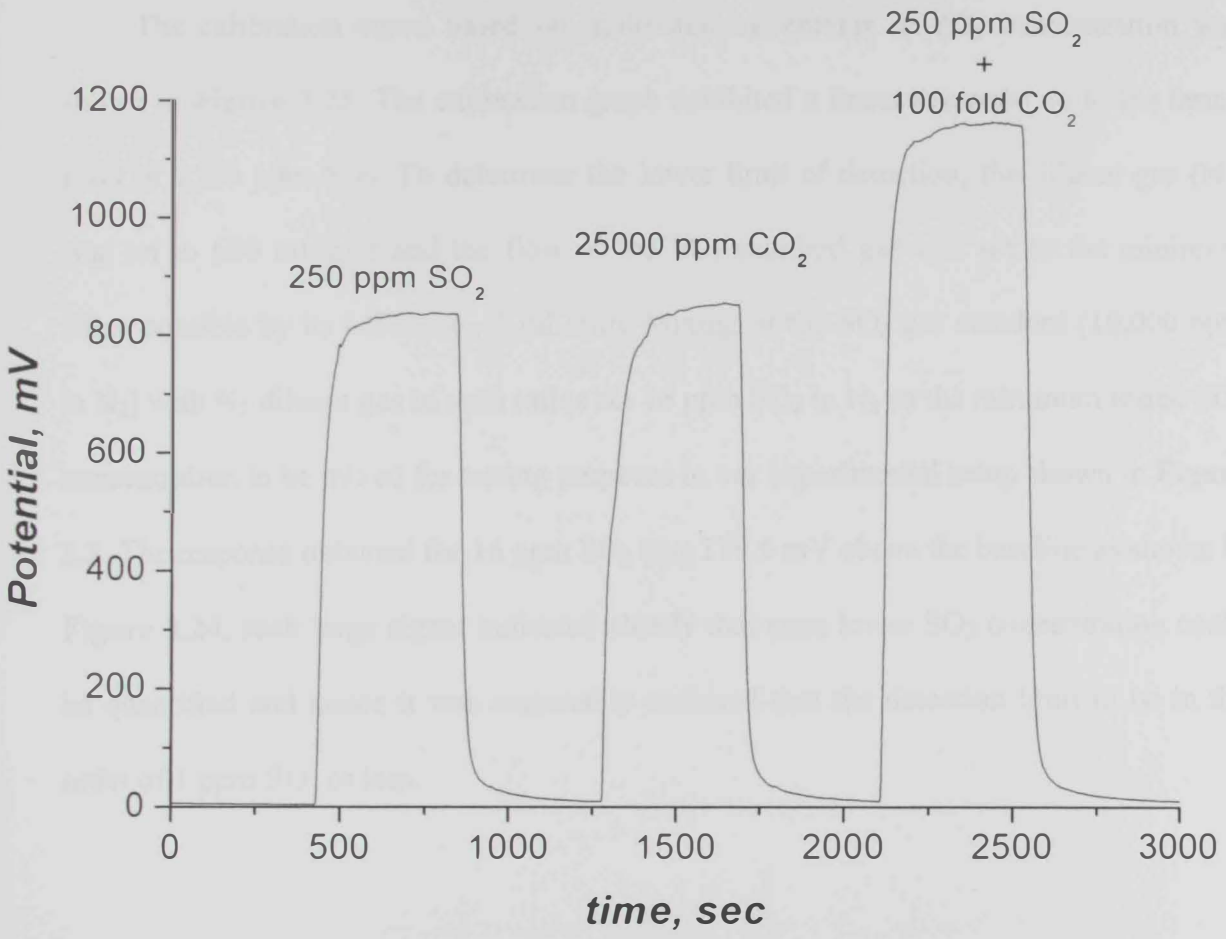

Figure 3.22: Effect of CO_2 on SO_2 analyzer response, where the first peak shows the response of SO_2 gas in N_2, the second peak shows the response of CO_2 gas in N_2 and the third peak shows the response of SO_2 when mixed with 100 fold CO_2 gas in N_2, using 1.0 mM H_2O_2 carrier liquid at flow rate 2.0 ml/min, HFMM (PP fibers), gas flow rate 200 ml/min.

The evaluation of the interfering effect of H_2S, a relevant gas in SO_2 determination, was not attempted because of the deleterious effect of sulfide ions on the platinum electrodes of the conductivity probe. Unfortunately, this will limit the utility of the conductivity detector to monitor SO_2 in gas streams containing H_2S at appreciable levels.

The calibration curve based on multi-step increments in SO_2 concentration was shown in **Figure 3.23**. The calibration graph exhibited a linear response up to the tested level of 2500 ppm SO_2. To determine the lower limit of detection, the diluent gas (N_2) was set to 600 mL/min and the flow of the SO_2 standard gas was set to the minimum value possible by its MFC, i.e., 1 mL/min. Mixing of the SO_2 gas standard (10,000 ppm in N_2) with N_2 diluent gas in such ratios set 16 ppm SO_2 in N_2 as the minimum tested SO_2 concentration to be mixed for testing purposes in our experimental setup shown in **Figure 2.2**. The response obtained for 16 ppm SO_2 was 178.5 mV above the baseline as shown in **Figure 3.24**, such large signal indicated clearly that even lower SO_2 concentration could be quantified and hence it was reasonably assumed that the detection limit to be in the order of 1 ppm SO_2 or less.

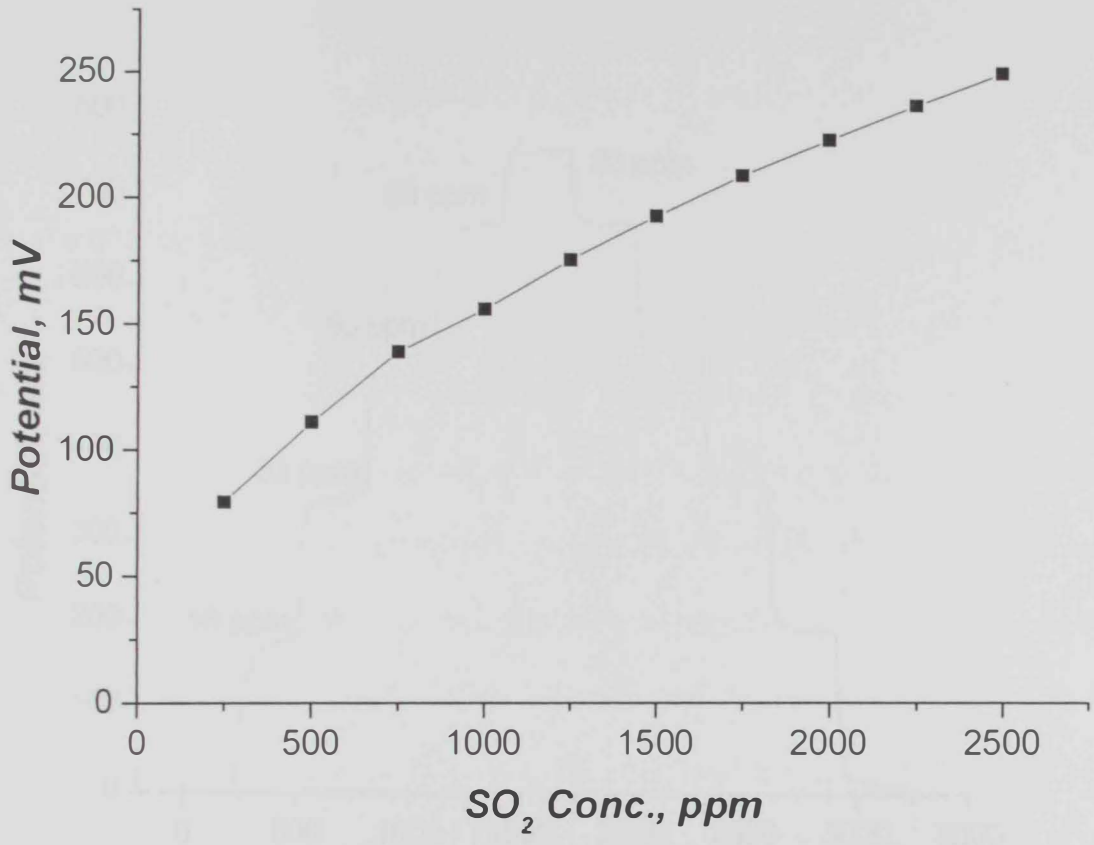

Figure 3.23: The linear response of the SO_2 analyzer at high concentration levels of SO_2. The conductometer was set on scale 100x using 1.0 mM H_2O_2 carrier liquid at flow rate 2.0 ml/min, HFMM (PP fibers), gas flow rate 200 ml/min.

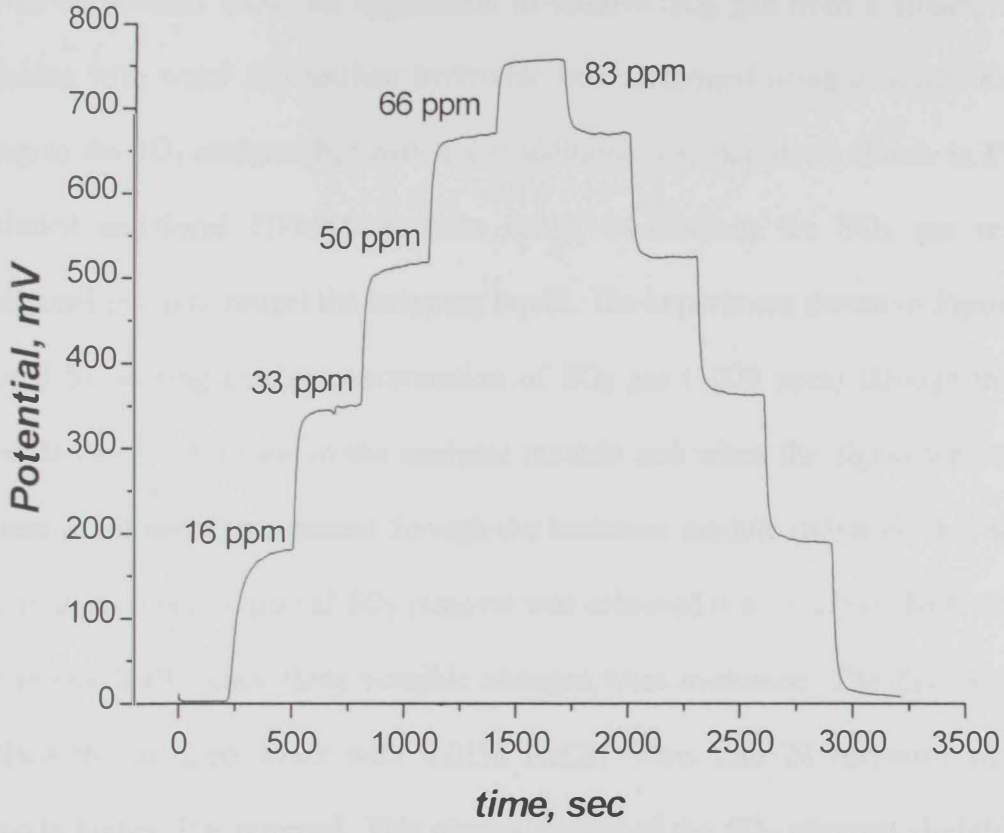

Figure 3.24: SO_2 analyzer response based on the conductivity response to low SO_2 concentration levels with gas flow rate 600 mL/min using 1.0 mM H_2O_2 carrier liquid at flow rate 2.0 ml/min, HFMM (PP fibers).

The effect of total gas flow rate on the analyzer response to SO_2 was tested at four different gas flow rates and the obtained results were shown in **Figure 3.25**. It was evident that the limit of detection was enhanced at higher gas flow rates which could be attributed to the larger quantities of SO_2 transferred through the HFMM and hence absorbed in the carrier solution per unit time.

In the present work, an application to remove SO_2 gas from a stream of gases by washing with water and sodium hydroxide was performed using a similar experimental setup to the SO_2 analyzer but with some additional compartments shown in **Figure 3.26**, included additional HFMM (module G591, Membrana) for SO_2 gas removal and additional pump to propel the stripping liquid. The experiment shown in **Figure 3.27** was started by passing certain concentration of SO_2 gas (1000 ppm) through the treatment module (shell side) then to the analyzer module and when the signal was stabilized, a stream of DI water was passed through the treatment module (tubes side) at flow rate 20 mL/min. As a result, partial SO_2 removal was achieved (i.e., ~ 25%). To further enhance the removal efficiency three possible changes were evaluated. The first option was to replace the distilled water with 0.01M NaOH (flow rate 20 mL/min) which should provide higher SO_2 removal. This change enhanced the SO_2 removal slightly, i.e., from 25 to 35% compared to distilled water as shown in **Figure 3.27**. Such low SO_2 removal was unexpected given the high solubility of SO_2 in water and NaOH. At this point the analyzer response was suspected and the gas stream was switched to the zero gas as shown in **Figure 3.27**. The analyzer responded quickly to such change and the signal returned to the background level. Therefore, it was confirmed that the unexpectedly low SO_2 removal data was accurate.

To further understand the reason behind the low SO_2 removal, the flow rate of water and the NaOH (0.01M) solution were increased up to 50 mL/min and the concentration of

NaOH was increased up to 0.05 M but apparently complete removal of SO_2 from gas stream was not achieved as shown in **Figure 3.28.** Only 65% of SO_2 was removed using 0.05 M NaOH at flow rate of 50 mL/min.

The third change which extremely enhanced the removal is the switching the gas stream to the tube rather than the shell side of the treatment module and the treatment carrier solution to the shell-side in the treatment module. Using such configuration, SO_2 was totally removed by 0.05M NaOH (flow rate 50 mL/min) as shown in **Figure 3.29**. The efficiency of the gas in tube configuration was further evaluated by using DI water as treatment liquid. The obtained data was presented in **Figure 3.30** and showed complete removal of SO_2 using just DI water at flow rate 50 mL/min. The dramatic enhancement of the removal efficiency was attributed to efficient contact between the gas flowing inside the tube side of the fibers and the surrounding liquid in the shell side. When the water flow was turned off, the SO_2 removal was gradually reduced (as indicated by the rise in the SO_2 level). This was explained by the saturation of the stagnant interfacial water layer with SO_2 and hence was not able to dissolve more SO_2 as shown in the last step in **Figure 3.30.**

This conclusion indicated the usefulness and reliability of the described gas analyzer to monitor and optimize SO_2 gas removal setup by real time monitoring of SO_2 in gas stream.

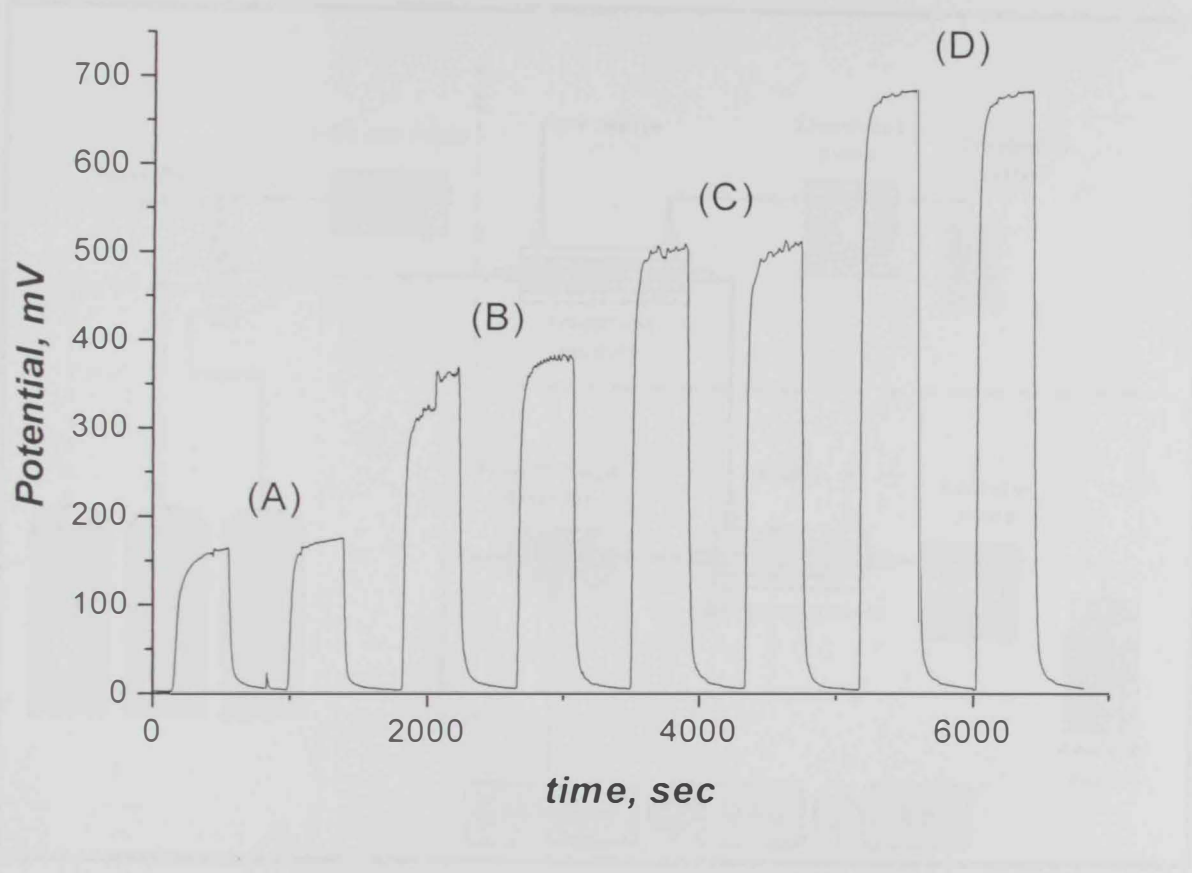

Figure 3.25: Effect of gas flow rate at (A): 200 mL/min, (B): 400 mL/min, (C): 600 mL/min, (D): 1000 mL/min on the analyzer response towards 50 ppm SO_2. For each gas flow rate, the SO_2 conc. was alternately changed between 50 ppm and zero gas twice, using 1.0 mM H_2O_2 carrier liquid at flow rate 2.0 ml/min, HFMM (PP fibers).

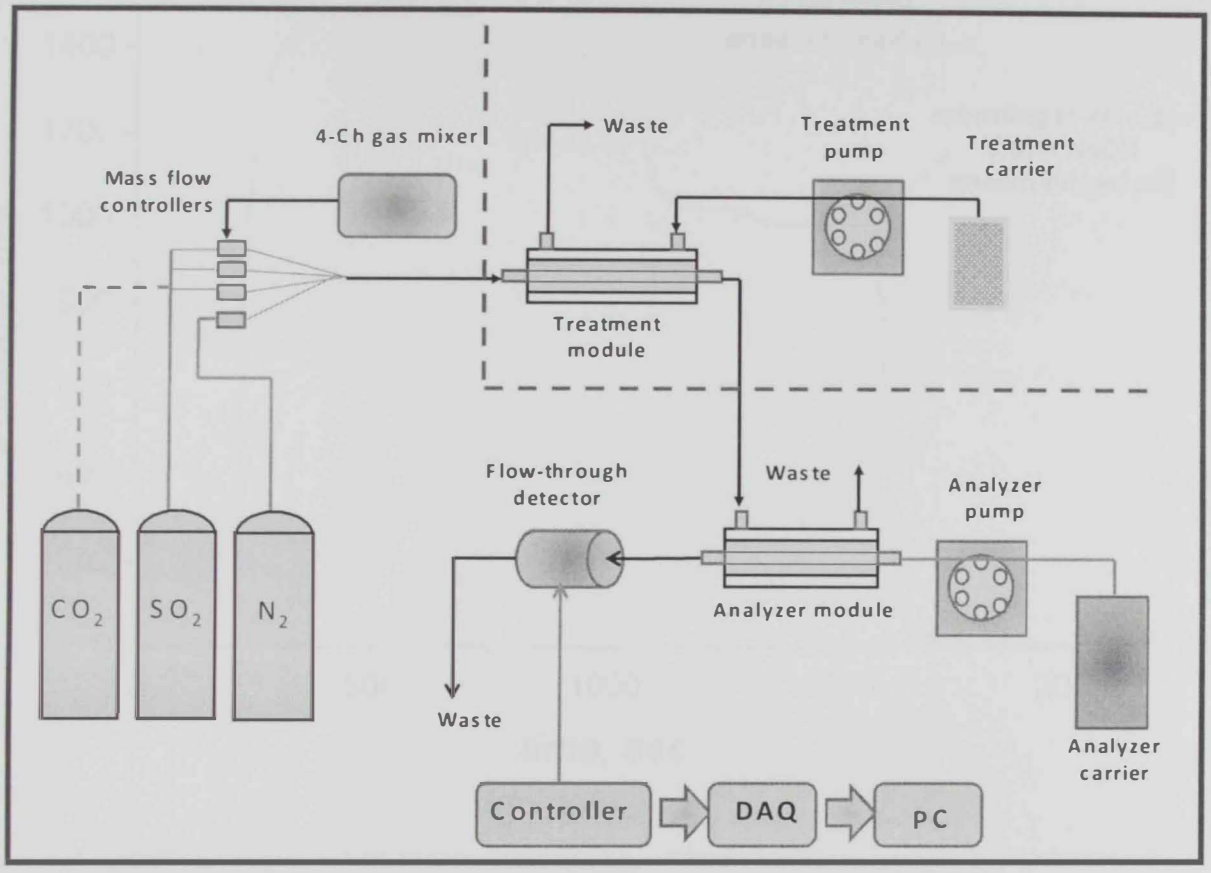

Figure 3.26: Experimental setup used for SO_2 gas treatment in a stream of gases.

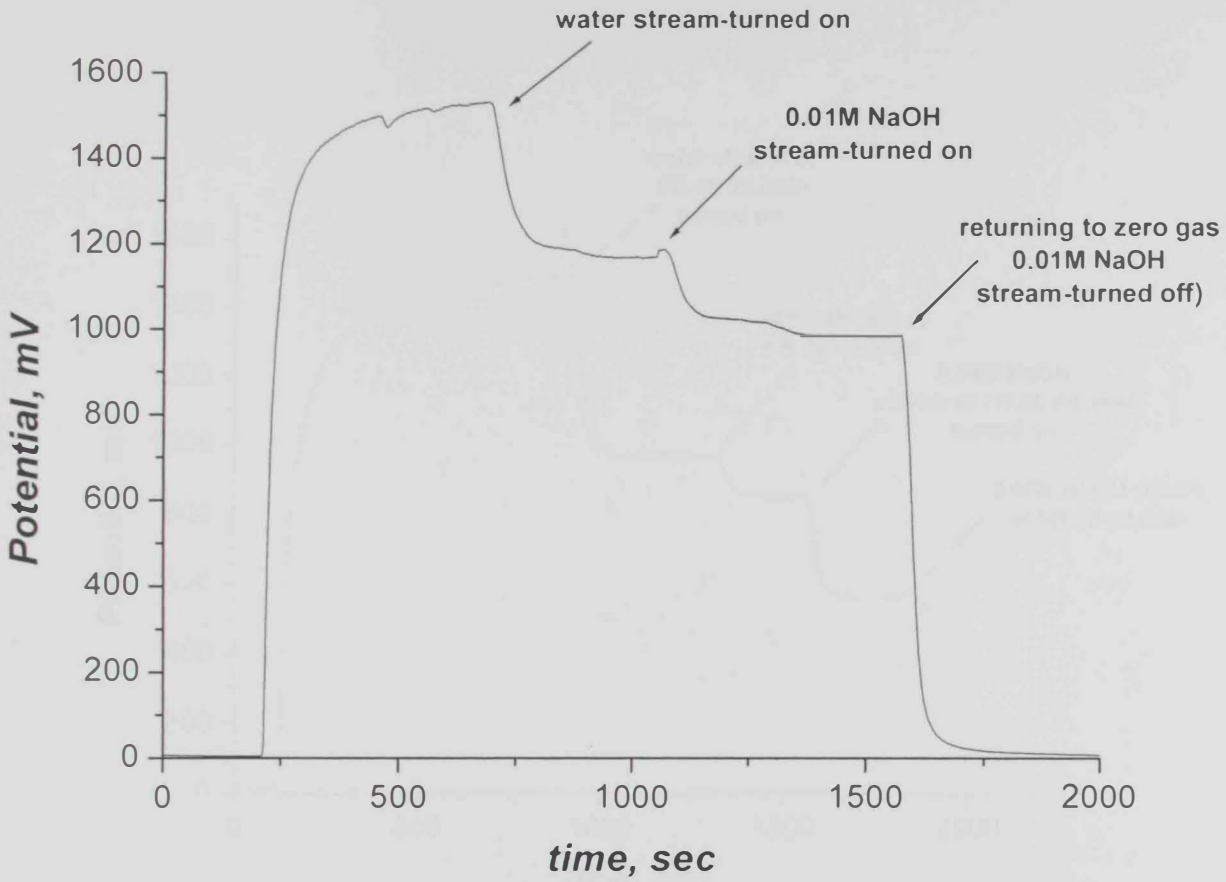

Figure 3.27: Application shows the removal of SO_2 gas (1000 ppm) from a stream of gases by water (FR: 20ml/min) and 0.01M NaOH (FR: 20ml/min), 1mM H_2O_2 was used as analyzer carrier solution, flow rate 2 mL/min, gas passes through shell-side / water passes through tube-side.

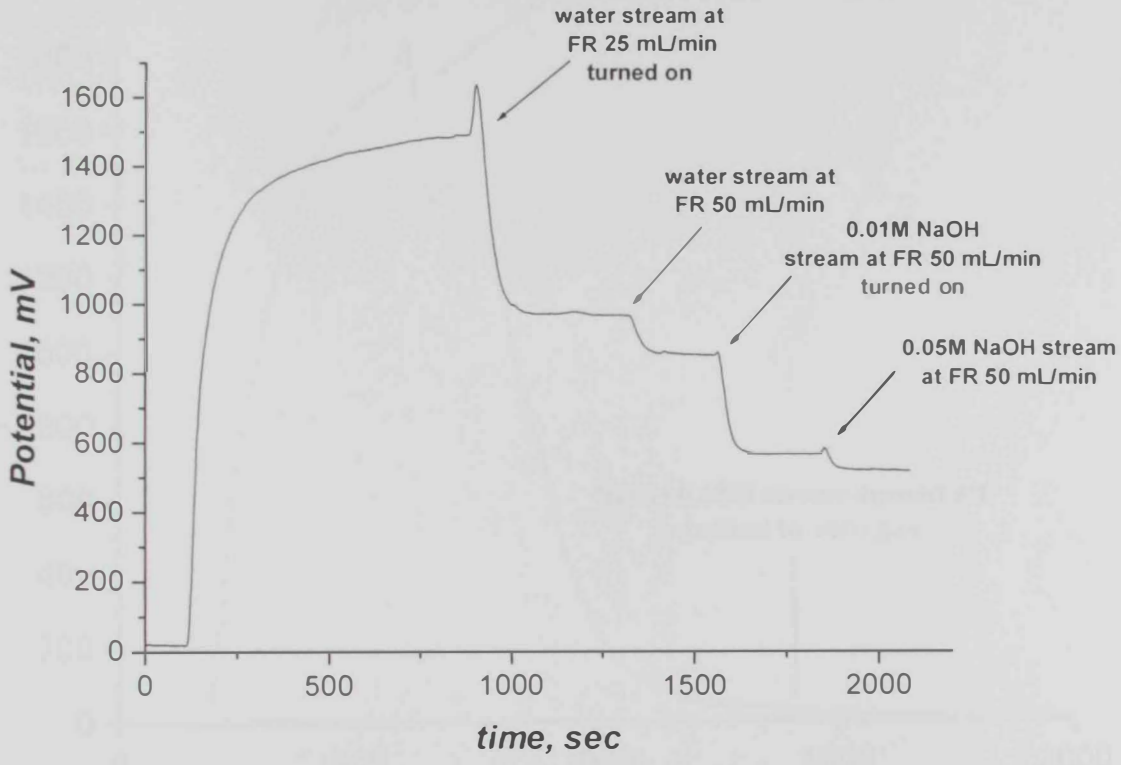

Figure 3.28: Application shows the removal of SO_2 gas (2000 ppm) from a stream of gases by water, 0.01M NaOH and 0.05M NaOH at higher flow rates. 1mM H_2O_2 was used as analyzer carrier solution, flow rate 2 mL/min, gas passes through shell-side / water passes through tube-side.

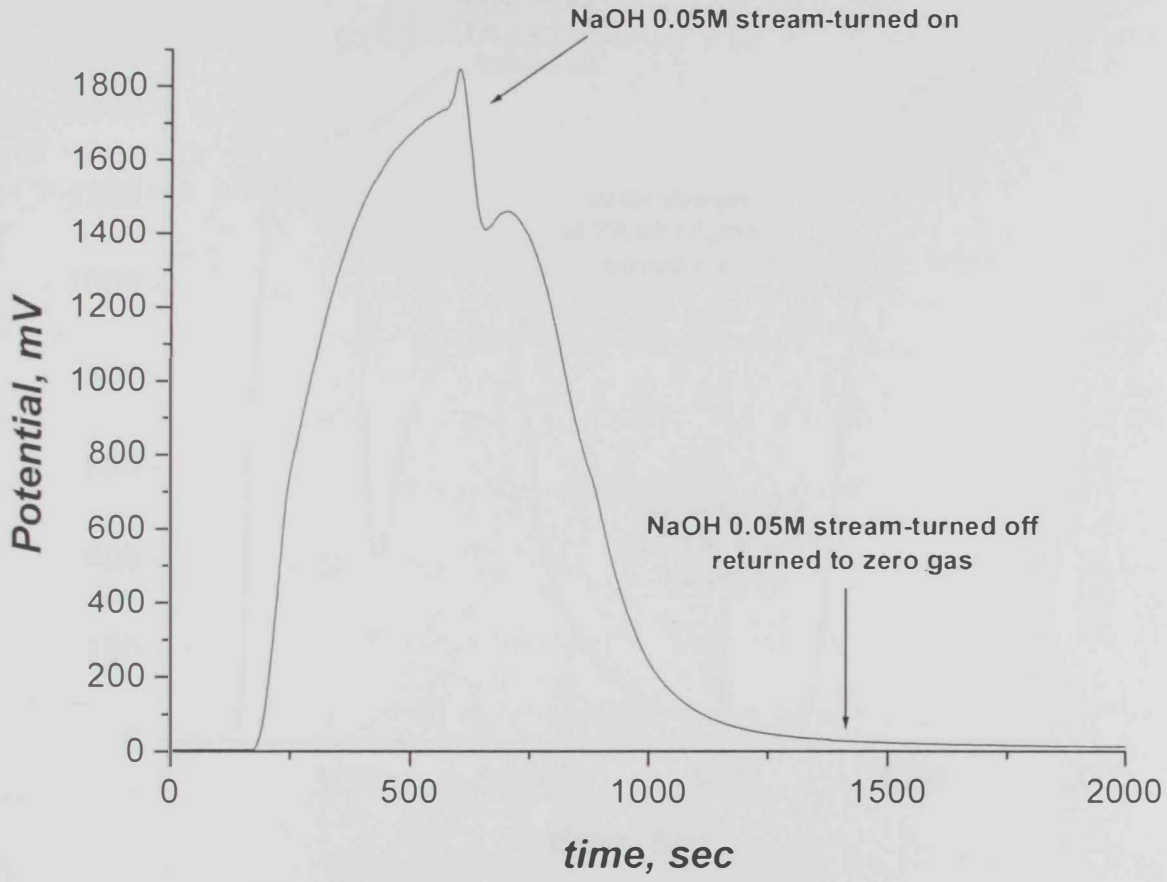

Figure 3.29: Successful complete removal of SO_2 (1000 ppm) by NaOH 0.05M (FR 50 mL/min), 1mM H_2O_2 was used as analyzer carrier solution, flow rate 2 mL/min, gas passes through tube-side / NaOH passes through shell-side.

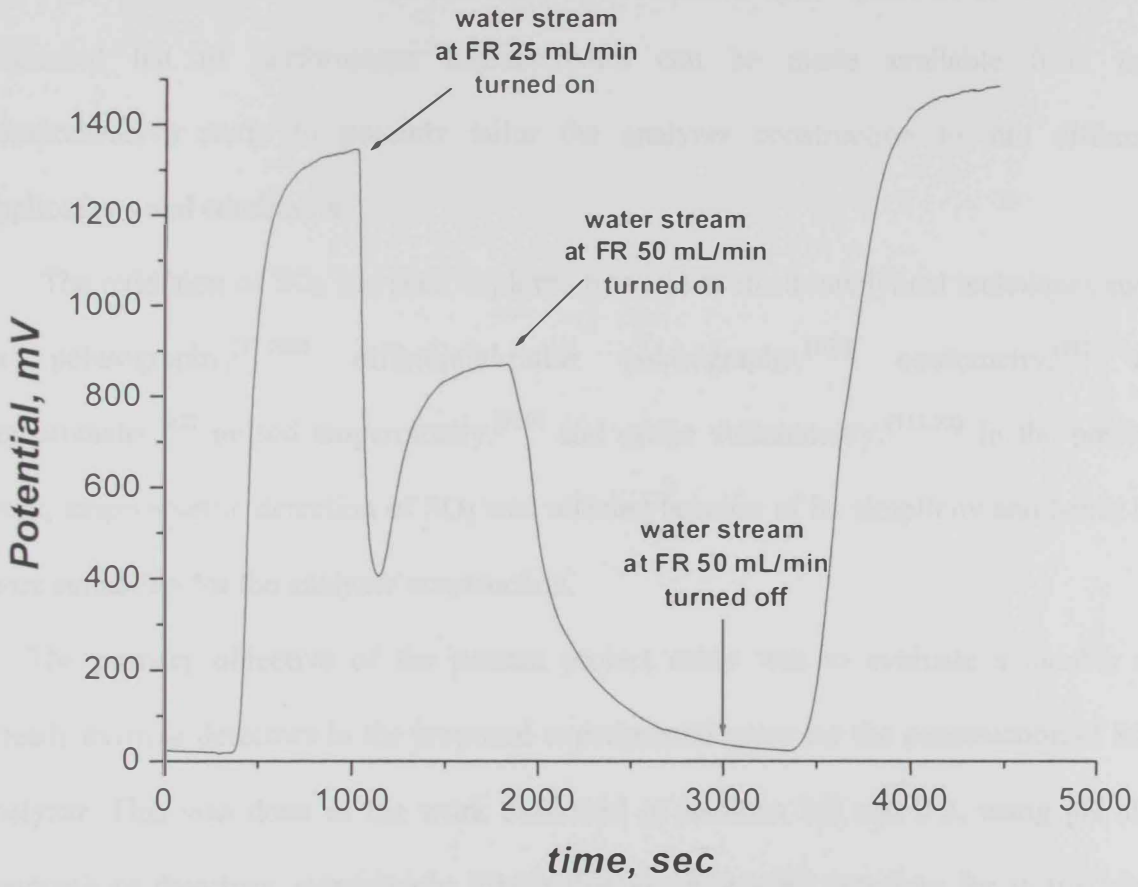

Figure 3.30: Successful complete removal of SO_2 gas (1000 ppm) by water only (FR 50 mL/min), 1mM H_2O_2 was used as analyzer carrier solution, flow rate 2 mL/min, gas passes through tube-side / water passes shell-side.

3.4 SO_2 gas analyzer based on amperometric detection

The third possible way for detecting the dissolved SO_2 in carrier solution (*cf.* **Figure 2.2**) was based on its reducing property. Monitoring such property could provide partially or completely different characteristics for the obtained SO_2 analyzer. In such away, an expanded list of performance characteristics can be made available from this comprehensive study to possibly tailor the analyzer construction to suit different applications and conditions.

The oxidation of SO_2 has been explored by various electroanalytical techniques such as polarography,[57,108] differential-pulse polarography,[109] coulometry,[59] dc amperometry,[62] pulsed amperometry,[110] and cyclic voltammetry.[111,72] In the present work, amperometric detection of SO_2 was selected because of its simplicity and hence its more suitability for the analyzer construction.

The primary objective of the present project study was to evaluate a number of already existing detectors in the proposed experimental setup for the construction of SO_2 analyzer. This was done in the work described in sections 3.2 and 3.3, using pH and conductivity detectors, respectively. Given that amperometric detectors for sulfite were not commercially available; a decision was made to select and reproduce a suitable electrode from the available literature methods. Careful literature search for amperometric methods revealed that SO_2 oxidation could mainly be achieved either at bare solid electrodes (i.e, platinum, gold and glassy carbon) or at modified electrodes. All the reported modifications for various electrode surfaces implied added complexity, to different extents, to the process of electrode construction.

Therefore, in an attempt to retain the major advantage of simple analyzer construction a decision was made to evaluate the solid bare Pt, Au and GC electrodes as working

electrodes in the anodic amperometric detection of sulfite. The best obtained current-time (*i-t*) response curves were still far from being satisfactory (**Figures 3.31, 3.32 and 3.33**) although of the large number of trials in which key experimental parameters were varied and evaluated. The investigated parameters included the nature of the supporting electrolyte, pH, and the applied potential. The obtained amperometric current responses were unstable with time and irreproducible and showed unfavorable signal to noise ratio. These observations were in agreement with the literature reports using solid bare electrode.[65] It was reported that such unsatisfactory response commonly obtained at bare solid electrodes for sulfur containing compounds would be attributed to the strong adsorption of reactants, stable intermediates and/or reaction products on the electrode surface which leads to fouling of the catalytic sites, with subsequent gradual decrease of the electrode response.[42,65] Moreover, the involved mechanism of the oxidation process of sulfite in particular could play a role in such observed behavior.[112]

Pulsed amperometric detection (PAD) and electrochemical pretreatment schemes were suggested to solve the problem of gradual loss of the solid electrode sensitivity in sulfite detection.[42,110,65] The reported results indicated partial stabilization of the amperometric signal. However, the use of the electrodes with such detection schemes was limited in all reports to the flow injection analysis systems only in which the electrode comes into contact with the sulfite ions at relatively long time intervals (i.e., 3 min) to provide enough time for surface regeneration by desorption of any species adsorbed during the oxidation process. Such requirement for intermittent electrode exposure to sulfite solution does not suit the expected operation of the gas analyzer in which the detector might come into contact with sulfite solutions with variable concentrations for extended periods of time. Also, the PAD feature significantly increases the cost of the required potentiostat and hence the overall cost of the SO_2 analyzer. Actually, such

instrument was available in the lab but the primary goal was to construct simple and reliable SO_2 analyzer at low cost discouraged the utilization of such feature in further development of amperometric detector and all the subsequent attempts were limited to dc amperometry available in the simplest potentiostat.

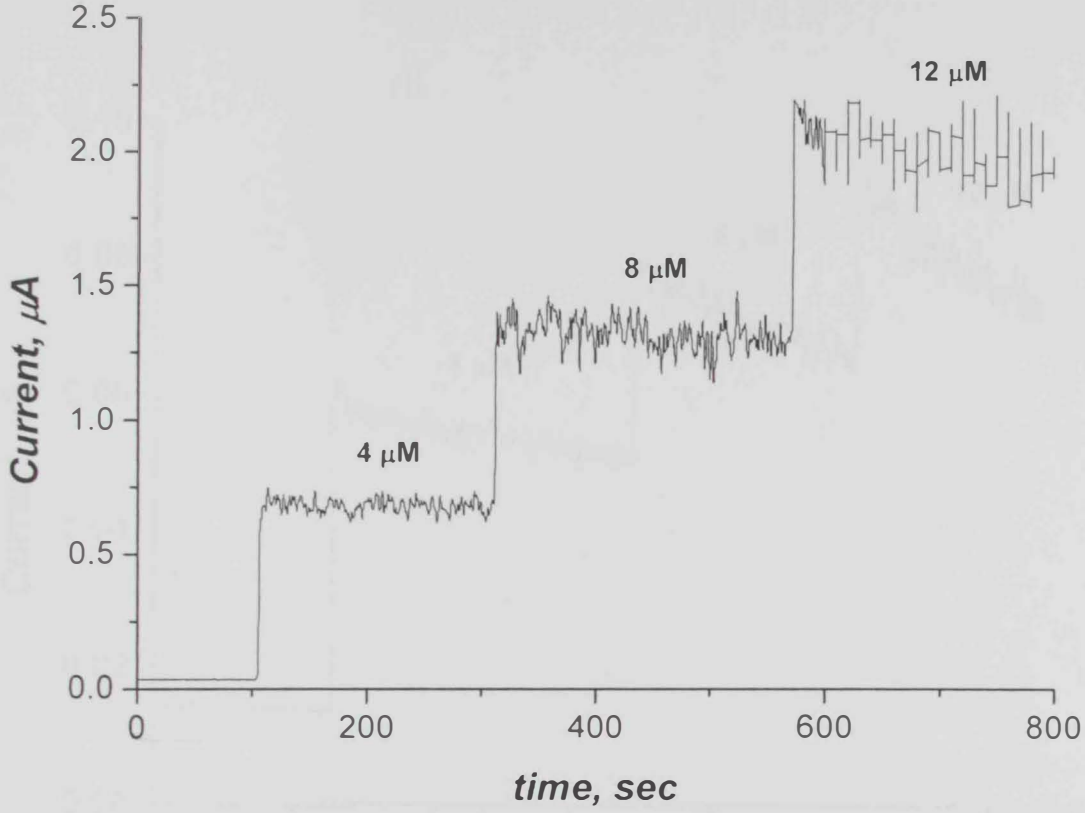

Figure 3.31: Amperometric response of sulfite at bare gold electrode (2 mm diameter) 0.1M acetate buffer pH 4.0, Applied potential 0.6 V (vs SCE).

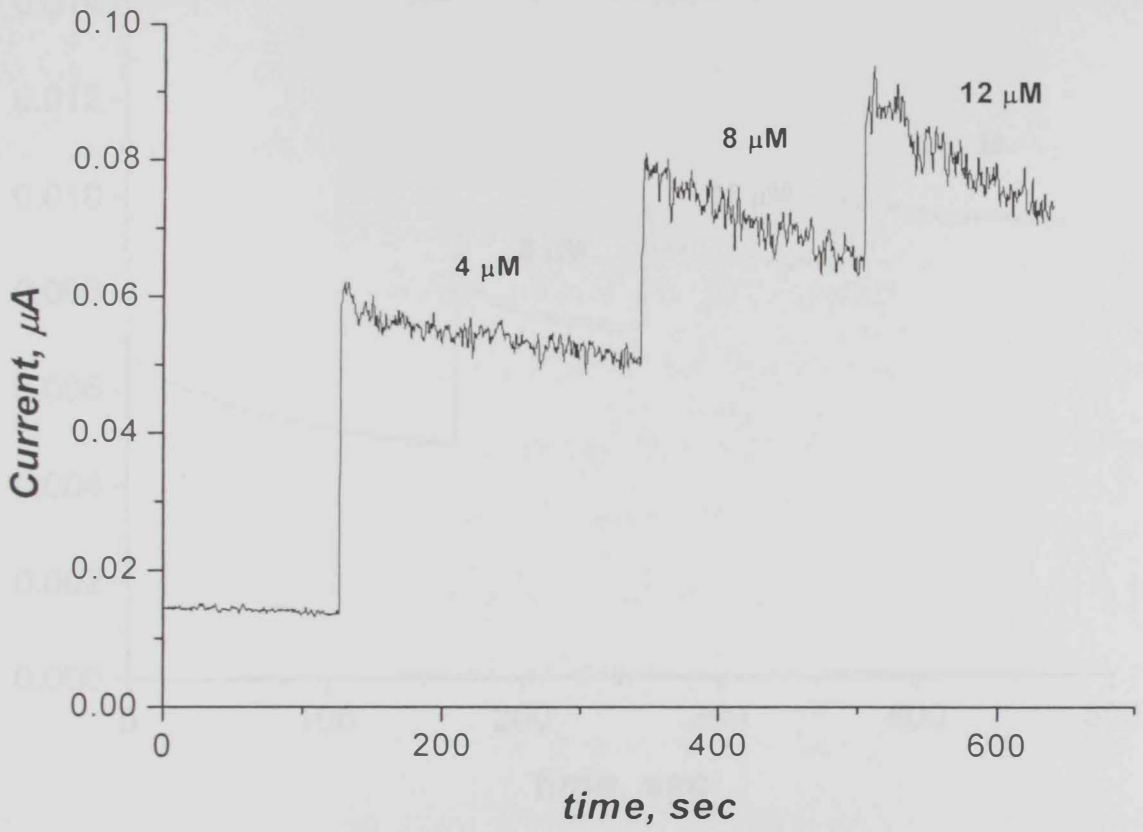

Figure 3.32: Amperometric response of sulfite at bare platinum electrode (2 mm diameter) 0.05 M borax buffer pH 8.0, Applied potential 0.5 V (vs SCE).

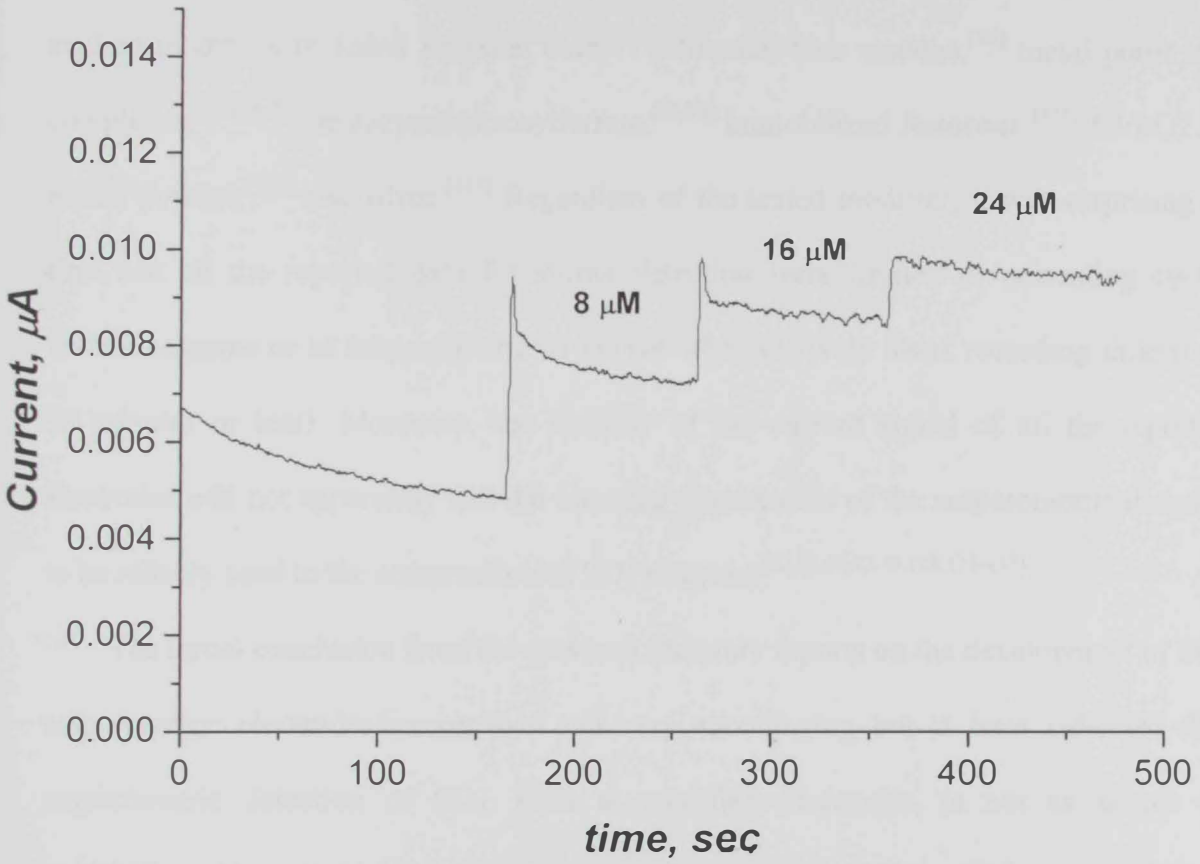

Figure 3.33: Amperometric response of sulfite at bare glassy carbon electrode (2 mm diameter) 0.1 M acetate buffer pH 4.0, Applied potential 0.6 V (vs SCE).

3.4.1 Chemically modified electrodes as amperometric detectors for sulfite

Unlike bare solid electrode, the development of chemically modified electrodes for amperometric detection of sulfite ions in various samples attracted much interest in the past two decades. Several electrode modifiers were previously tested for this purpose. The studied modifiers included Prussian blue,[113] Prussian blue analogs,[74] metal porphyrin complexes,[114,69,71] pentacyanonitrosylferrate,[72,70] immobilized ferrocene,[115] Pd/IrO2,[10] nickel powder,[116] and silver.[117] Regardless of the tested modifier, it was surprising to find that all the reported data for sulfite detection were limited to presenting cyclic voltammograms or to amperometric *i-t* curves with relatively short recording time (i.e., 10 minutes or less). Moreover, the stability of the current signal of all the reported electrodes will not apparently suit the intended requirement of the amperometric detector to be reliably used in the construction of SO_2 analyzer.[82,72,69,77,70,113,115-117]

The initial conclusion from the previous literature reports on the development of SO_2 amperometric electrodes/sensors was not very encouraging but at least indicated that amperometric detection of SO_2, even at modified electrodes, is not as simple or straightforward task as one might predict for SO_2 given its well known reducing properties. The only available option was to continue the attempts to develop SO_2 amperometric detector based on some common electronic mediators as electrode modifiers. A sample of the obtained results will be presented only briefly because (i) the limited success achieved in this direction (ii) the large no. of trials which might distract the reader from the original objective set at the beginning to develop SO_2 analyzer, and finally (iii) to focus more on presenting, in the following section, the more successful findings on developing amperometric detectors for sulfite.

Figure 3.34 shows the response obtained with glassy carbon electrode (5 mm in diameter) modified with a thin layer of Prussian blue (PB) prepared in situ by electrodeposition according to the literature method.[118] The response exhibited high signal to noise ratio but the current response was decreasing with time. Moreover, the deposited layer tended to peel of the electrode surface after short time. To avoid such a problem, Prussian blue was prepare by precipitation using stoichiometric amounts of 0.1 M $FeCl_3$ and 0.1 M $K_4[Fe(CN)_6]$ solutions in 0.1 M HCl. The obtained PB crystals were used to prepare bulk modified electrodes.[119] The tested electrodes were based on mixing graphite powder and PB in variable ratios. The graphite-PB mixture was fixed inside the electrode cavity by means of a polyester membrane and Teflon O-ring. The electrode was then installed in a flow cell similar to that shown in **Figure 2.4** and the response to changing SO_2 level in gas streams was shown in **Figure 3.35**. The response was relatively slow and irreproducible. To simplify the construction of the flow cell, the protecting polyester membrane was eliminated and a certain percent of silicone oil (as binder) was added to provide the electrode self-sustained consistency. A sample response of such electrodes was shown in **Figure 3.36**. As one might expect, the current level was decreased when oil was added but the main response problems were not resolved. Hence, ferrocene[115,120] was tested as another potential electronic mediator. Electrodes based on bulk modification with ferrocene showed unstable baseline and signal instability as shown in **Figure 3.37**.

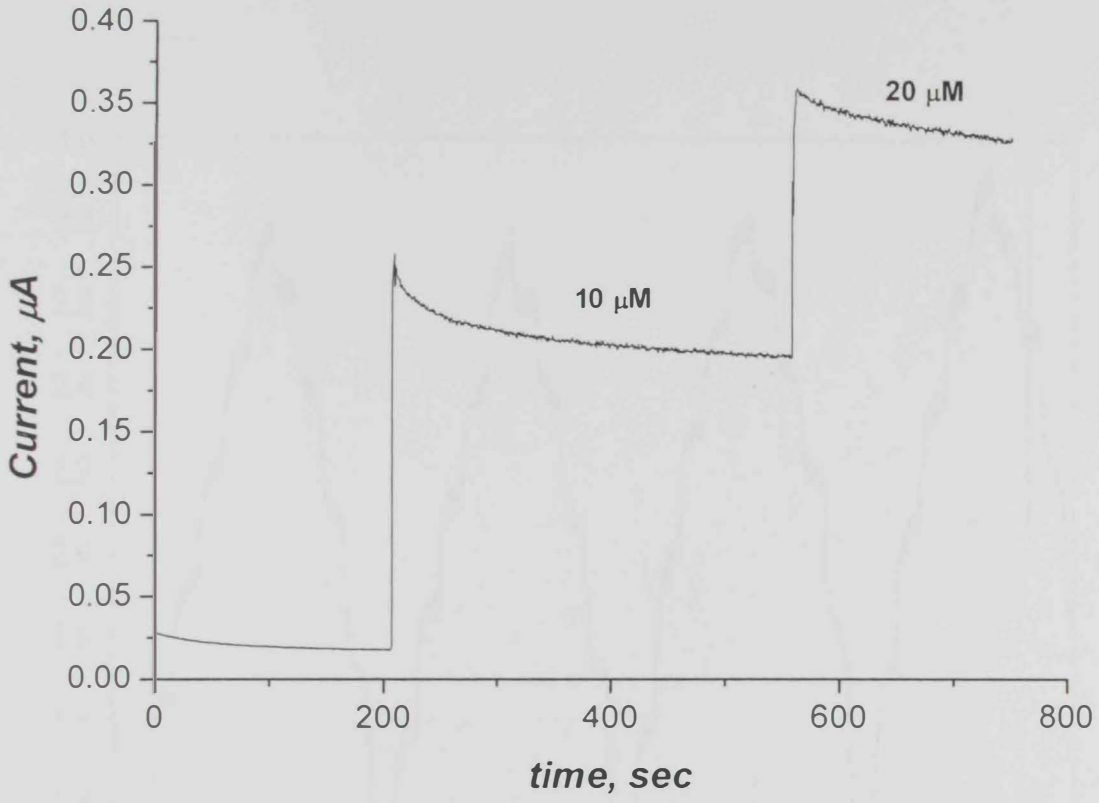

Figure 3.34: Amperometric response of sulfite at Prussian blue surface (electrochemically deposited on GC electrode, 2 mm diameter), 0.1 M acetate buffer pH 4.0, Applied potential 0.6v (vs SCE).

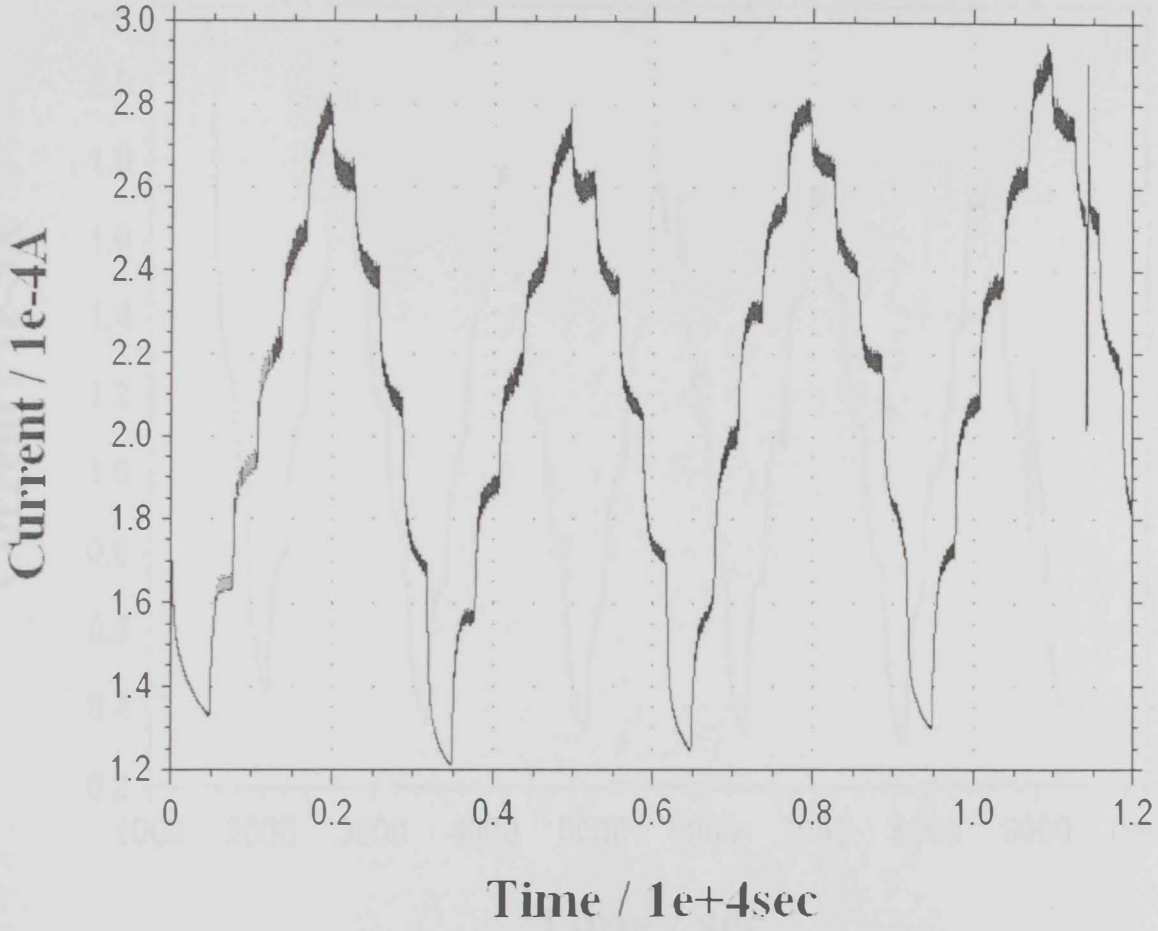

Figure 3.35: Amperometric response of the bulk modified PB electrode (50%graphite - 50% PB) covered with a polyester membrane (2 μm pore size). Each step corresponds to 500 ppm SO_2 in N_2 (200 mL/min). Carrier solution 0.05M NaH_2PO_4. E = 0.8V (vs. SCE).

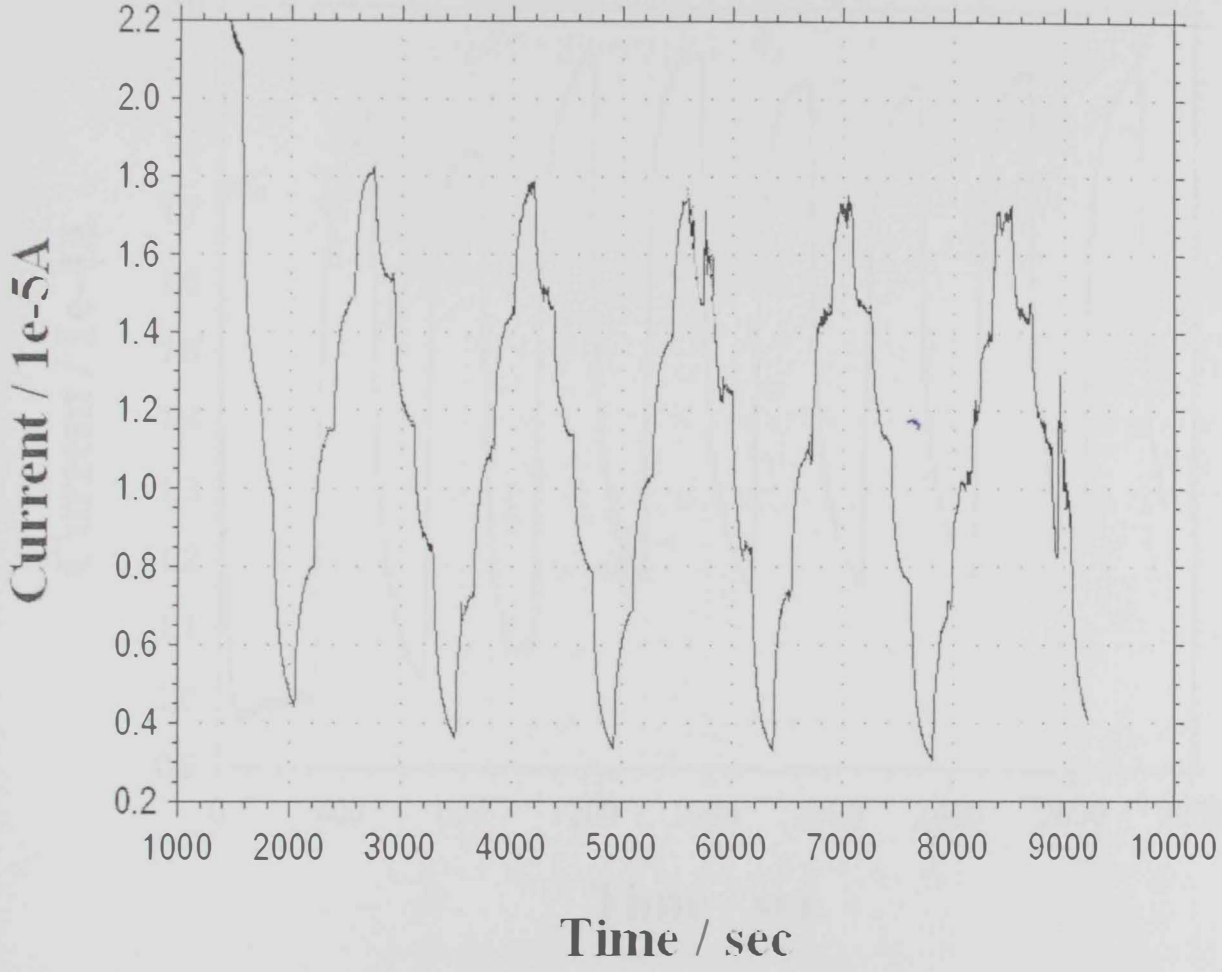

Figure 3.36: Amperometric response of the bulk modified PB electrode (90% graphite - 10% PB - 10% Silicone oil) covered with a polyester membrane (2 μm pore size). Each step corresponds to 250 ppm SO_2 in N_2 (200 mL/min). Carrier solution 0.05M NaH_2PO_4. E = 0.9V (vs. SCE).

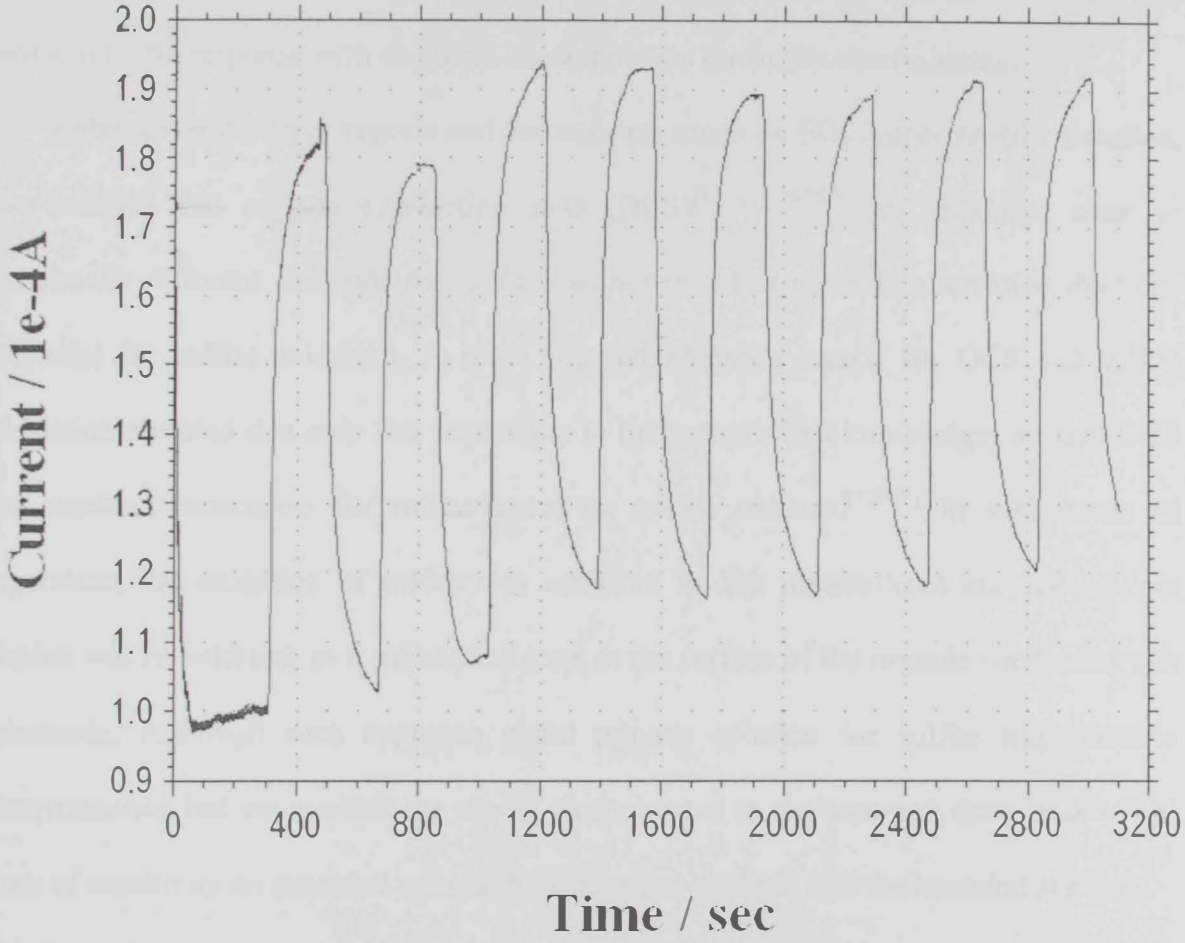

Figure 3.37: Amperometric response of the bulk modified ferrocene electrode. Each peak corresponds to 2500 ppm SO_2 in N_2 (200 mL/min). Carrier solution 0.05 M NaH_2PO_4. E = 0.6V (vs. SCE).

The response of electrodes based on glassy carbon powder and graphite powder were shown in **Figure 3.38** to **Figure 3.40**. It was evident that the common problems of signal instability and slow response and recovery were persistent.

At this stage, it was clear that common electrodes, either bar or modified - based on literature reading or our own experience, carried limited potential to provide amperometric response with desirable characteristics for sulfite determination.

Although of the large reports and the attempts made on SO_2 amperometric detection, we noticed that organic conducting salts (OCS)[97,121-124,78,9] an important class of essentially different electrode materials, was not tested as possible alternative electrode material for sulfite oxidation. A more focused literature search for OCS and sulfite detection revealed that only two papers (up to the author's best knowledge) utilized OCS to construct biosensors for sulfite based on sulfite oxidase.[125,78] In such mode of operation, the oxidation of sulfite was achieved by the immobilized enzyme catalyst which was re-oxidized, in a subsequent step, at the surface of the organic conducting salt electrode. Although such approach could provide solution for sulfite amperometric determination but we avoided the use of enzymes due to the common draw back of the loss of sensitivity on extended operation times which will not suit the intended analyzer.

Instead we attempted to evaluate the direct oxidation of sulfite at organic conducting salt electrode based on tetrathiafulvalene-tetracyanoquinodimethane (TTF-TCNQ), which was not attempted before.

Therefore, such relatively uncommon and fundamentally different material (i.e., non metallic and non carbon) was tested as potential electrode for amperometric sulfite determination. The details will be discussed in the following section.

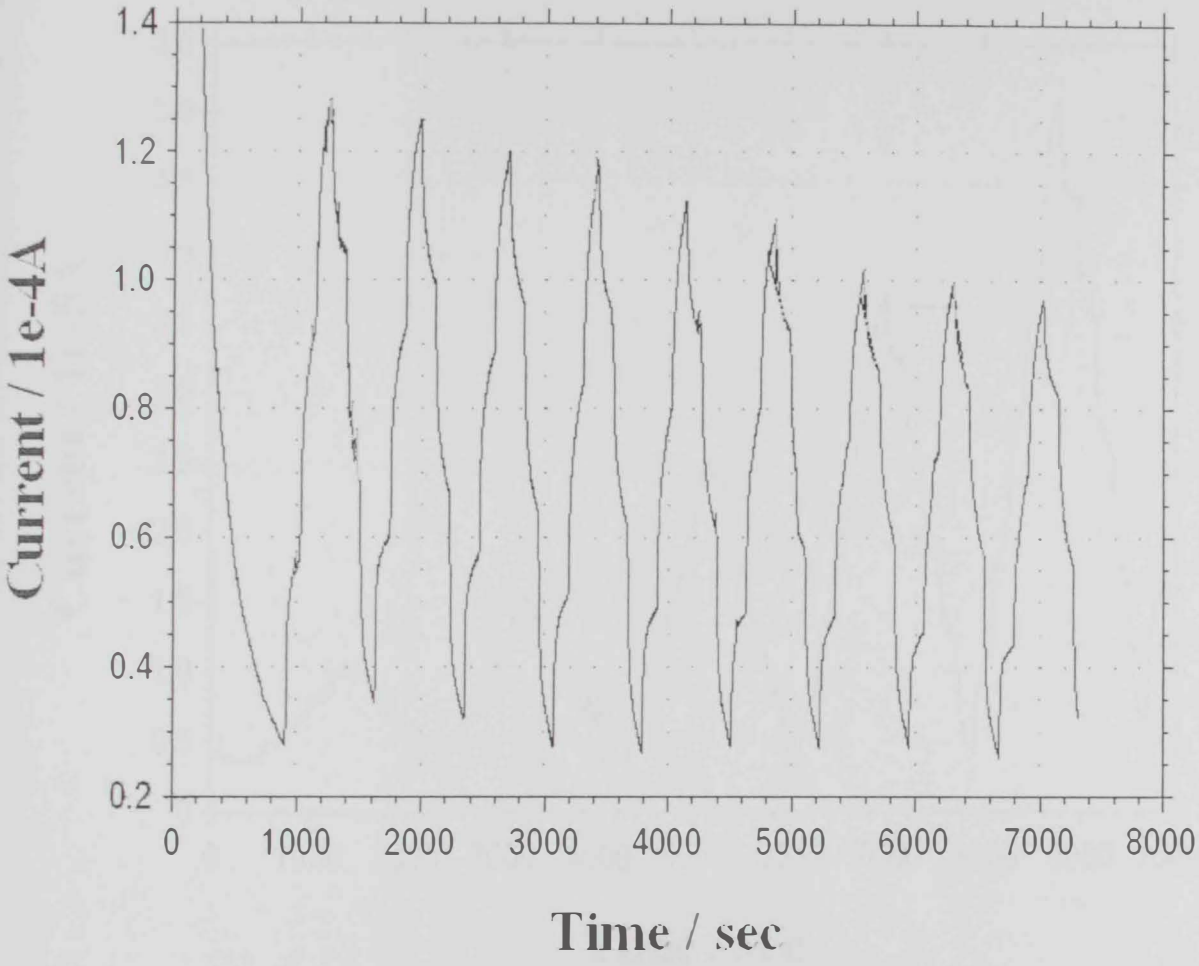

Figure 3.38: Amperometric response of GC powder electrode, covered with a polyester membrane (2 μm pore size). Each step corresponds to 500 ppm SO_2 in N_2 (200 mL/min). E = 0.6V (vs SCE)

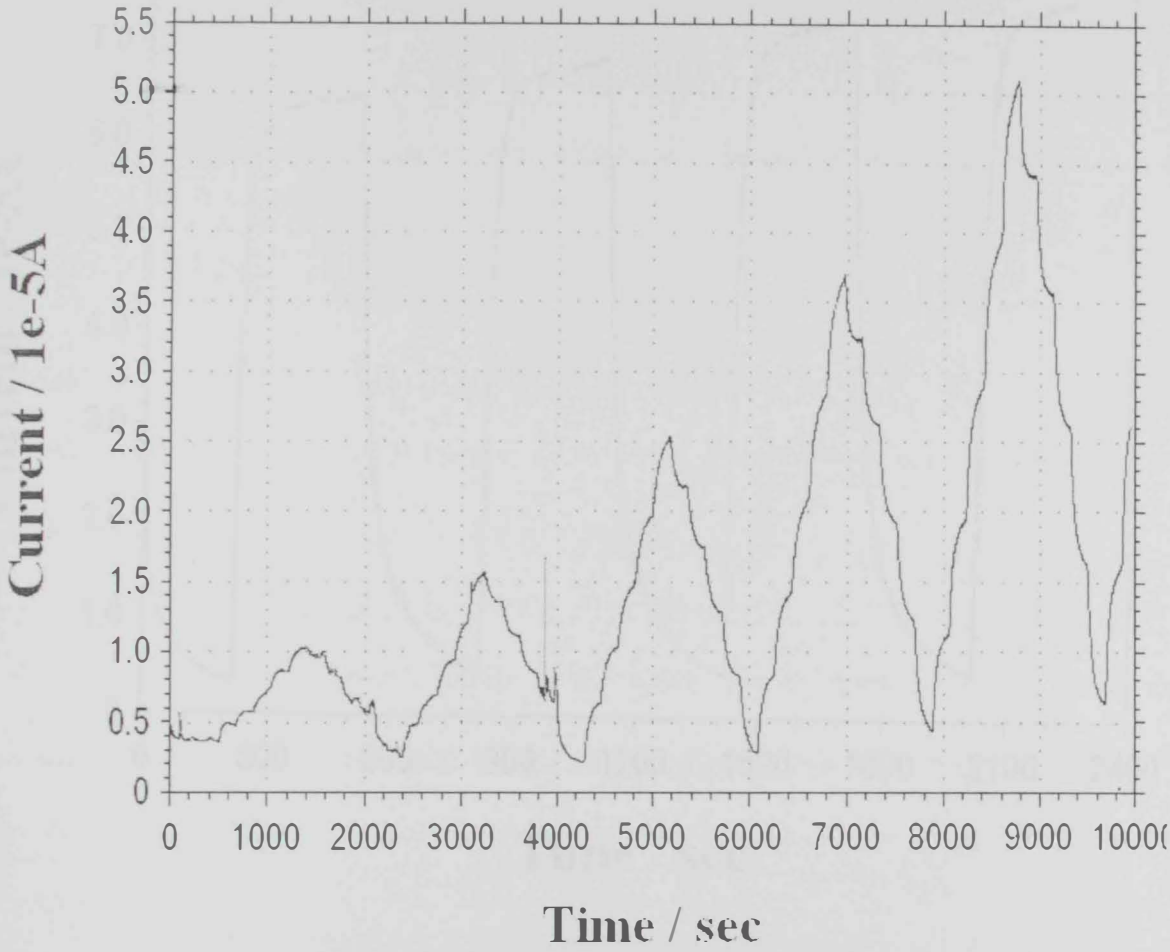

Figure 3.39: Amperometric response of sulfite at graphite powder electrode covered with a polyester membrane (2 μm pore size). Each step corresponds to 500 ppm SO_2 in N_2 (200 mL/min). 0.1 M phosphate buffer pH 7.0. E = 0.6V (vs. SCE).

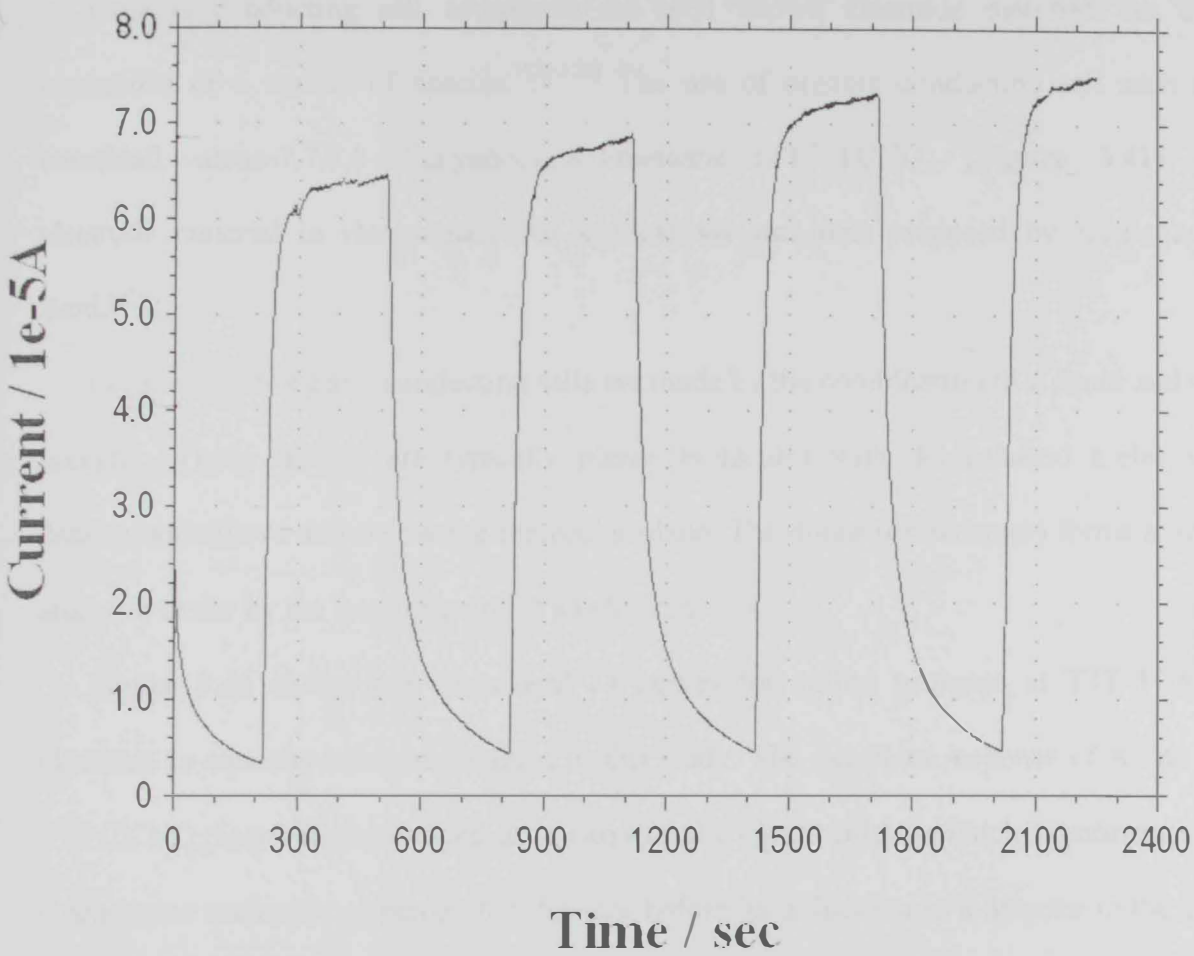

Figure 3.40: Amperometric response of the graphite powder electrode, covered with a polyester membrane (2 μm pore size). Each peak corresponds to 2500 ppm SO_2 in N_2 (200 mL/min). 0.1 M phosphate buffer pH 7.0. E = 0.6V (vs. SCE)

3.4.2 Organic conducting salt (OCS) as electrode for amperometric detection of sulfite

Organic conducting salt complexes are well known electrode materials for the oxidations of a variety of species.[127-130] The use of organic conducting salt such as tetrathiafulvalene-7,7,8,8-tetracyanoquinodimethane (TTF-TCNQ) (**Figure 3.41**) as electrode material in electoranalytical applications was first proposed by Jaeger and Bard.[97]

In general the organic conducting salts are made by the combination of a donor and an acceptor. These species are typically planar molecules with delocalaized π-electron density both above and below the molecular plane. The donor (or acceptor) forms a new aromatic sexlet by the loss (or gain) of an electron.

Figure 3.42 shows one of several *i-t* curves for sulfite response at TTF-TCNQ electrode in aqueous solution obtained in this study. The excellent response of sulfite at TTF-TCNQ electrode encouraged us to carry on the optimization in batch experiments to characterize such new amperometric detector before its utilization as a detector in the gas analyzer setup.

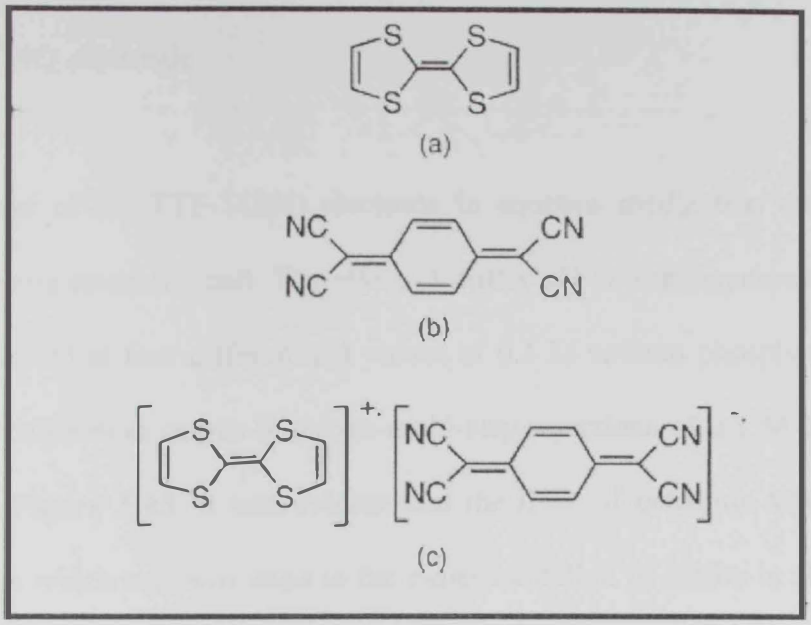

Figure 3.41: Structure of (a) Tetrathiafulvalene (TTF) - donor; (b) tetracyanoquinodimethane (TCNQ) - acceptor; (c) TTF–TCNQ complex.

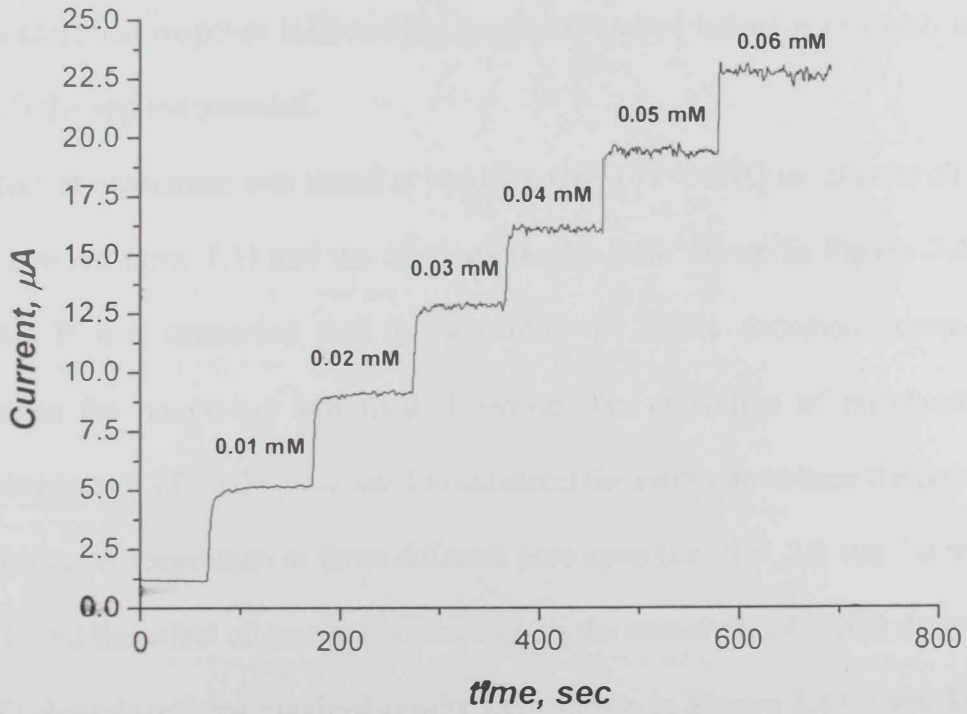

Figure 3.42: i-t curve shows sulfite oxidation at the surface of TTF-TCNQ in 0.1 M phosphate buffer medium pH 7.0, applied potential 0.3 V (vs. SCE).

3.4.3 Optimization of the experimental parameters for determination of sulfite by TTF-TCNQ electrode

The response of the TTF-TCNQ electrode in aqueous media was evaluated using three electrode amperometric cell. The effect of buffer pH on the amperometric response to sulfite was tested at four different pH values of 0.1 M sodium phosphate buffer. The corresponding calibration curves based on multi-step injections of 0.1 M sodium sulfite was shown in **Figure 3.43**. It was evident that the limit of detection was enhanced at higher pH value which was attributed to the easier oxidation of sulfite in alkaline media. Moreover, the TTF-TCNQ electrode response was proportional to the applied potential (**Figure 3.44**) within the stable potential region of TTF-TCNQ.[97] Such results indicated that the oxidation of sulfite is kinetically controlled within the investigated potential region.This electrical response followed the predicted logical behavior in which current increase with the applied potential.

The effect of membrane was tested at two different TTF-TCNQ to silicone oil ratios (i.e., 1:0.5 and the other 1:1) and the obtained results were shown in **Figure 3.45** and **Figure 3.46**. It was concluded that the sensitivity of sulfite detection became less sensitive when the membrane was used. However, the utilization of membrane was essential when pure TTF-TCNQ was used to construct the electrode to keep the powder in the cavity.Polyester membrane of three different pore sizes (i.e., 1.0, 2.0 and 3.0 micron) were used to test the effect of membrane pore size on the sensitivity of sulfite detection at TTF-TCNQ eletrode and the obtained results were shown in **Figure 3.47**. Unluckily the results showed reversed order of sensitivity for the polyester membrane of pore size 1.0 and 2.0 micron, respectively over repeated trials. To investigate this issue we send samples of the used membranes for SEM imaging at the CLU-UAEU. The outcomes of

the SEM images (**Figure 3.48**) revealed that the number of pores in a specific area of polyester membrane-2.0 micron was less than the number of pores in the polyester membrane-1.0 micron. Hence the total available permeation area in the-1.0 μm membrane was larger than that in 2.0 μm membrane. This might resulted in higher fluxes of SO_3^{2-} ions reaching the electrode surface protected with membranes of 2.0 μm pore diameter.

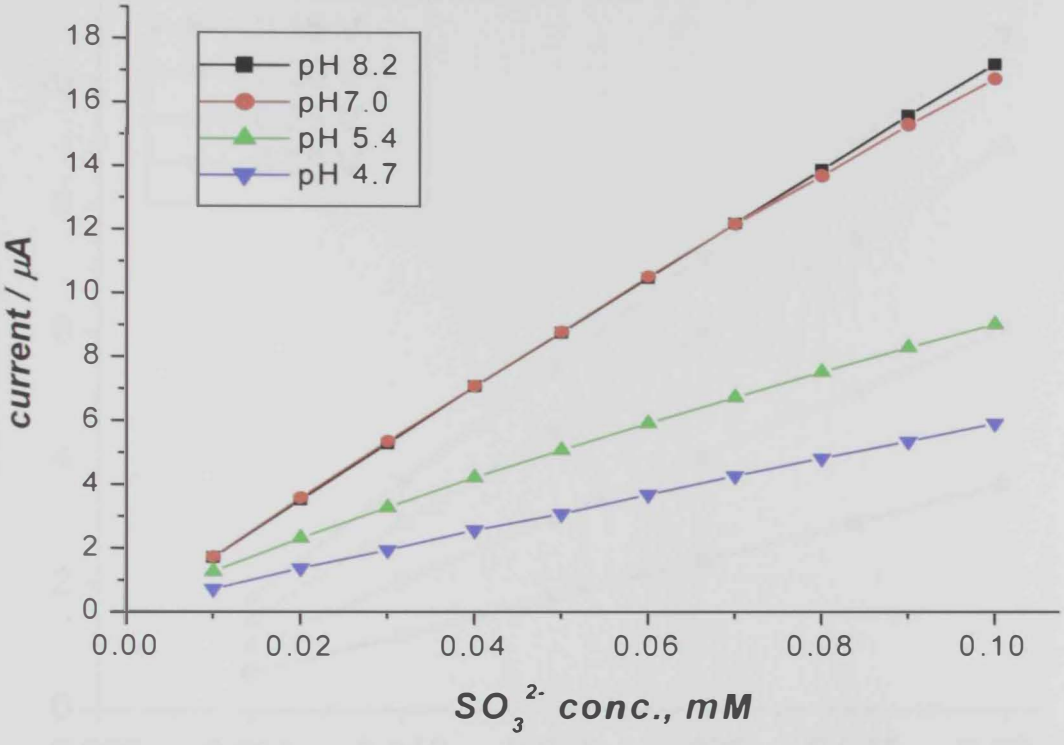

Figure 3.43: Effect of buffer pH vale on the oxidation of sulfite at TTF-TCNQ electrode, in 0.1 M phosphate buffer, applied potential 0.2V (vs. SCE).

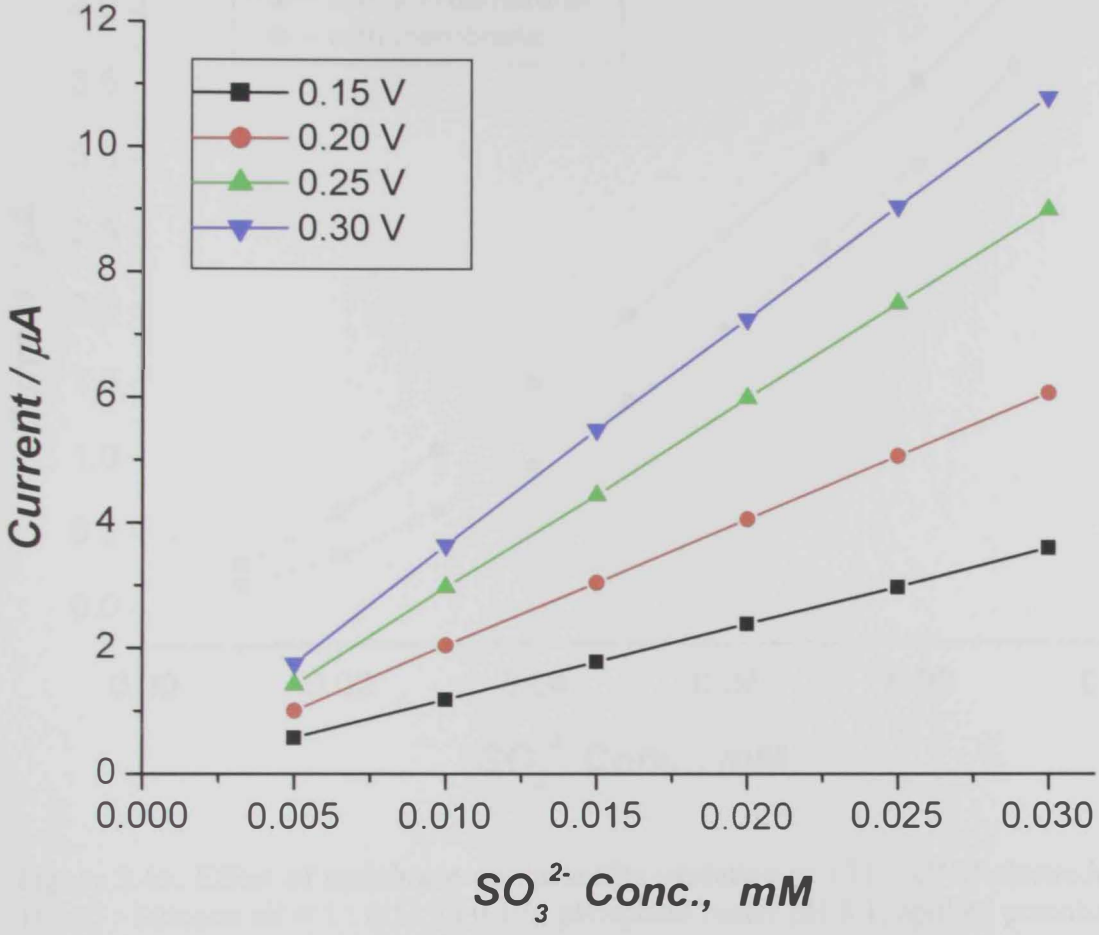

Figure 3.44: Effect of potential on the sulfite oxidation at TTF-TCNQ electrode, in 0.1 M phosphate buffer pH 8.1, (vs. SCE).

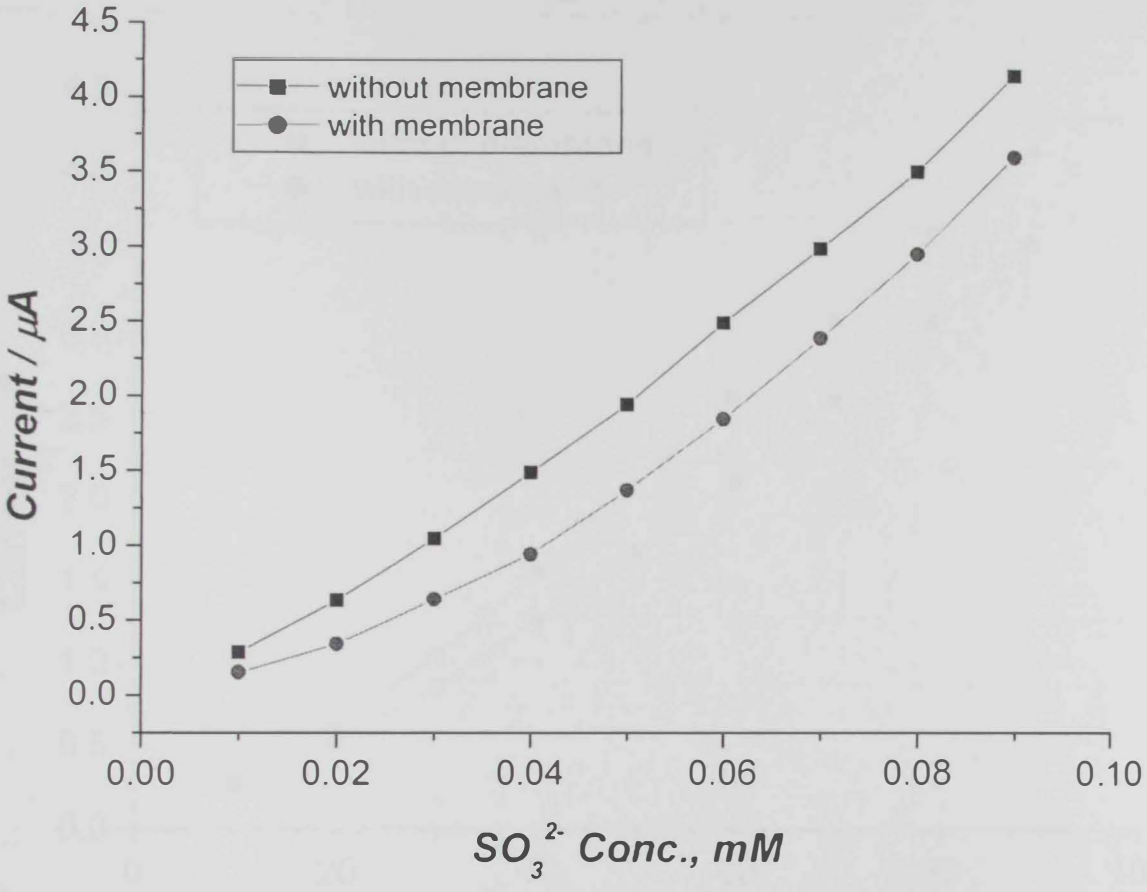

Figure 3.45: Effect of membrane on the sulfite oxidation at TTF-TCNQ electrode (TTF-TCNQ : Silicone oil = 1 : 0.5), in 0.1 M phosphate buffer pH 8.1, applied potential 0.3 V (vs. SCE).

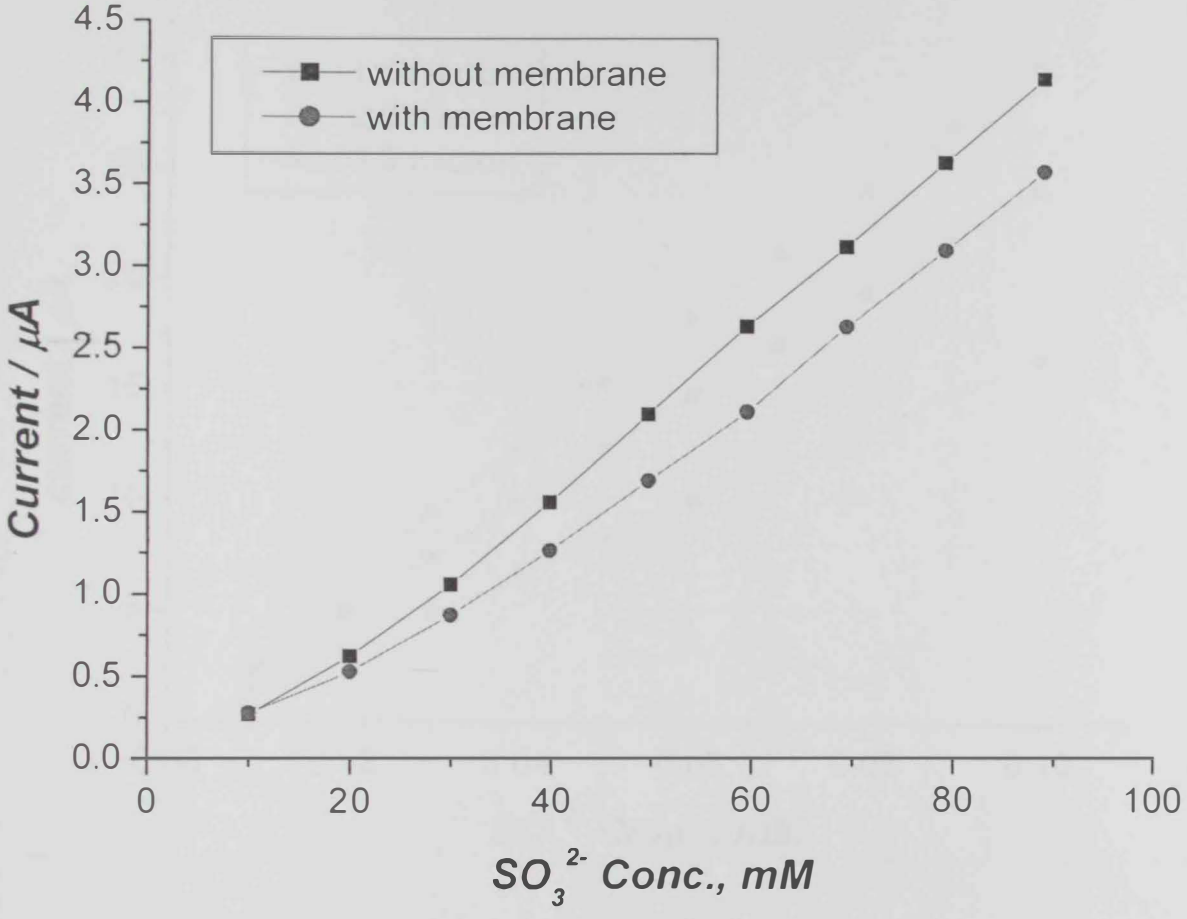

Figure 3.46: Effect of membrane on the sulfite oxidation at TTF-TCNQ electrode (TTF-TCNQ : Silicone oil = 1 : 1), in 0.1 M phosphate buffer pH 8.1, applied potential 0.3 V (vs. SCE).

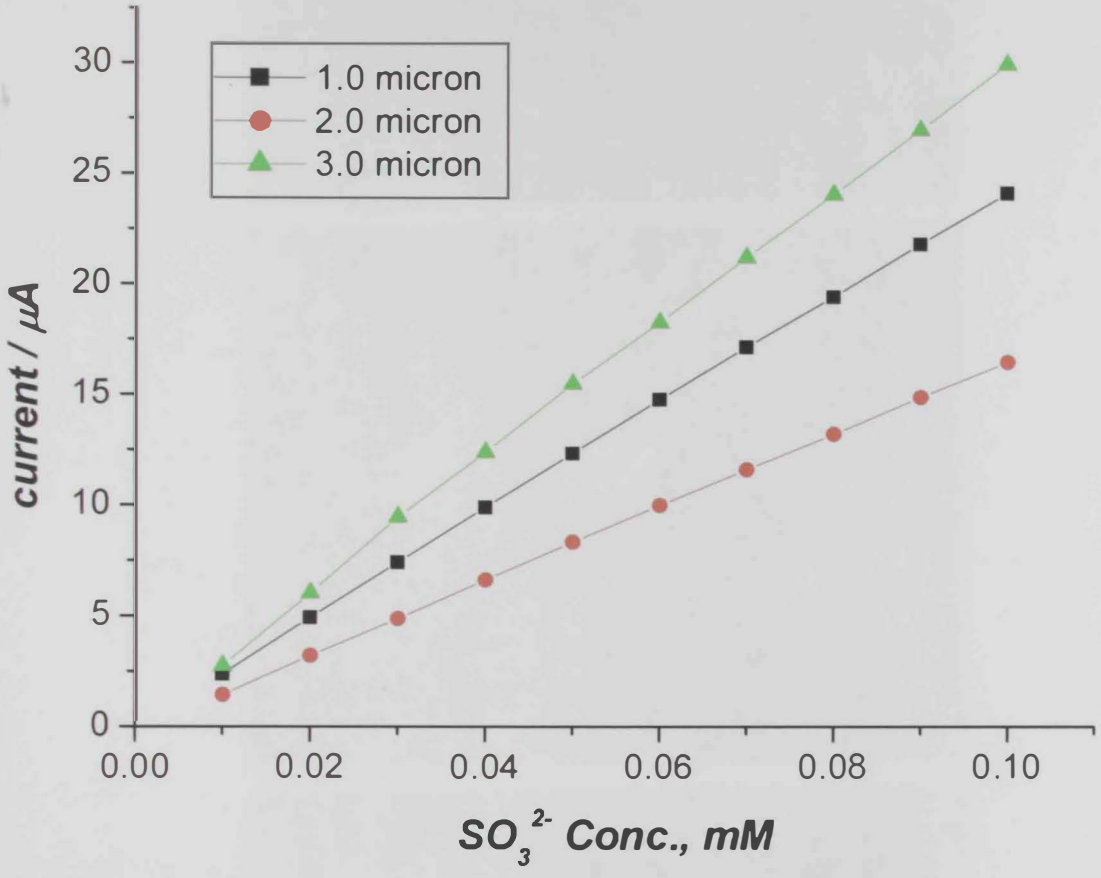

Figure 3.47: Effect of membrane (polyester) pore size on the sulfite oxidation at TTF-TCNQ electrode, in 0.1 M phosphate buffer pH 8.1, applied potential 0.3 V (vs. SCE).

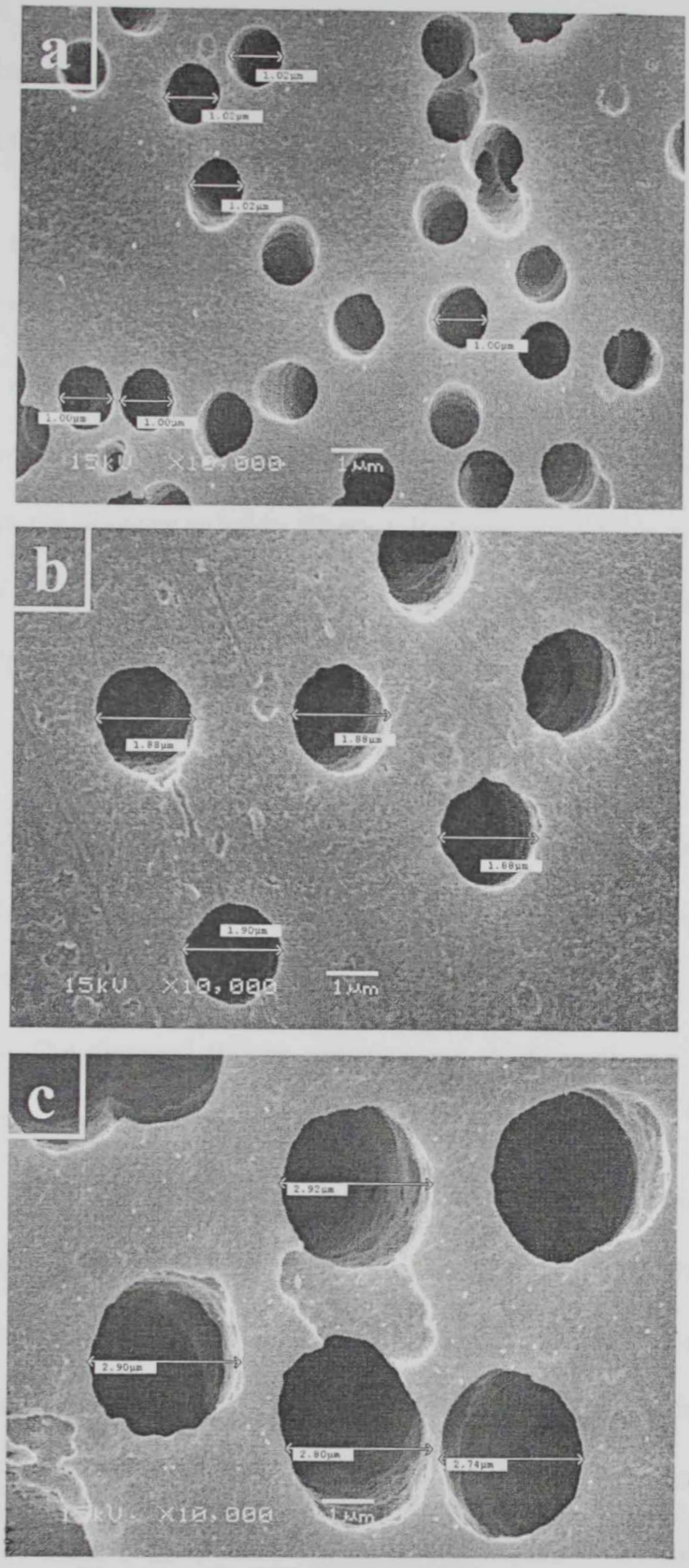

Figure 3.48: SEM show the surface of polyester membrane with (a): 1.0, (b): 2.0 and (c): 3.0 micron pore size.

3.4.4 Characterization of the experimental parameters for determination of sulfite by TTF-TCNQ electrode

The real time recording and the corresponding calibration curve based on multi-step increments in sulfite concentration was shown in **Figure 3.49**. The calibration graph exhibited a linear response up to the tested level of 0.8 mM sulfite in batch experiment. **Figure 3.50** shows the sulfite calibration at the low concentration range at the TTF-TCNQ electrode in the aqueous solution. These minute concentrations were obtained by injecting 40 μL of 0.01 M sodium sulfite solution into 20 mL of 0.1 M phosphate buffer pH 8.1. Such results indicated that sulfite can be easily measured in the micromolar range with excellent S/N ratio.

The repeatability test of the electrode response in the aqueous solution was evaluated by injecting 20 μL of 0.1 M sulfite solution in 20 mL 0.1 M phosphate buffer and the equilibrium amperometric current response was recorded at one hour intervals for a period of 12 hours. The obtained current response was stable as shown in **Figure 3.51** under such conditions injections were repeated.

The selectivity of the TTF-TCNQ electrode in the aqueous medium was tested in the presence of hydrogen peroxide, sodium nitrite and thiosulfite which are common interfering oxidizable species. The obtained results (**Figures 3.52, 3.53** and **3.54**) showed negligible responses for the tested species (i.e., hydrogen peroxide, sodium nitrite and thiosulfite) at the TTF-TCNQ electrode. This indicated that there is no interfering effect of such species on the proposed electrode response. Unlike the above mentioned species, sulfide showed high response at the proposed electrode. However, sulfide interference can be avoided by adding copper powder to the reaction medium (**Figure 3.55**).

The obtained favorable performance characteristics of the proposed TTF-TCNQ electrode leaded to the second phase of the work, i.e., the construction and optimaztion of SO_2 analyzer based on such new amperometric detector.

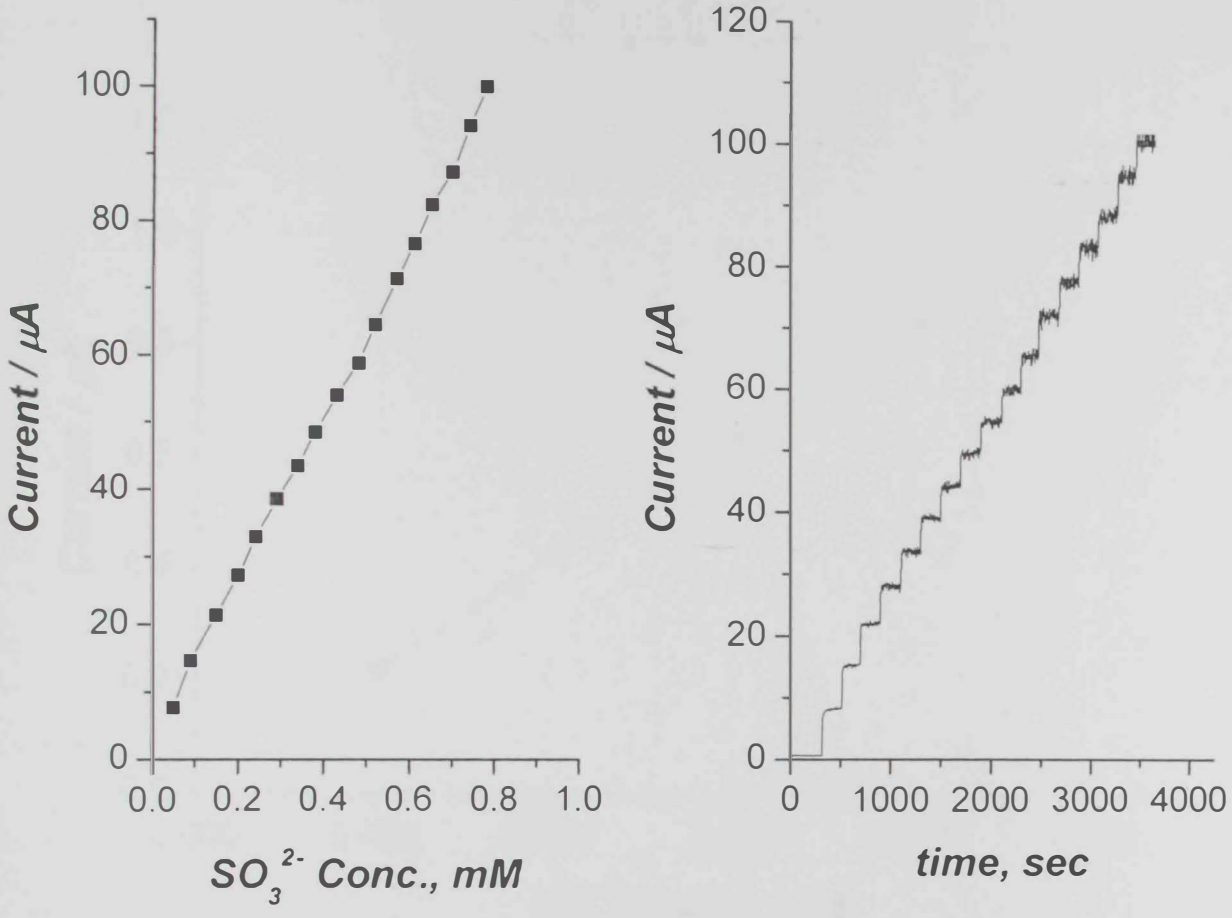

Figure 3.49: The linear response and the corresponding calibration curve for sulfite oxidation at the TTF-TCNQ electrode (pure TTF-TCNQ powder installed in a graphite cavity and protected with membrane), in 0.1 M phosphate buffer pH 8.1, applied potential 0.3 V (vs. SCE).

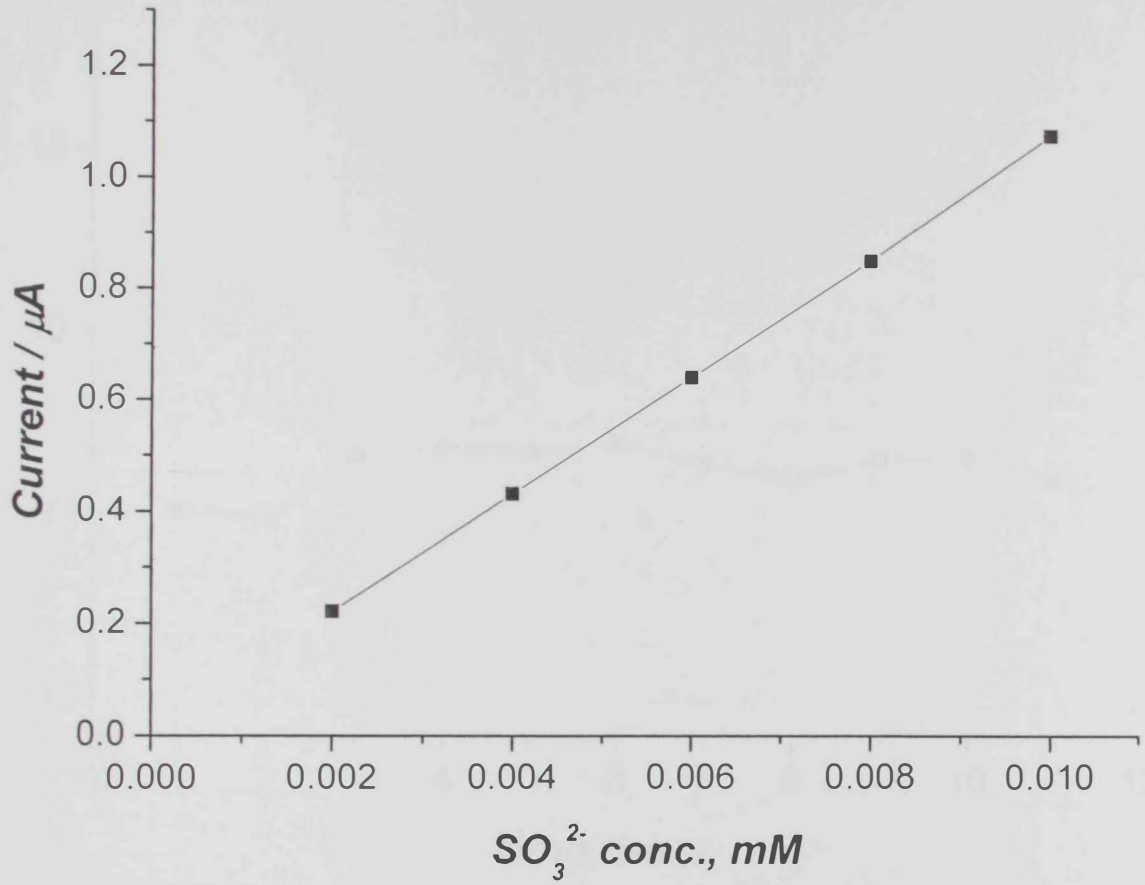

Figure 3.50: Calibration curve shows small concentrations of sulfite can be detected at the TTF-TCNQ electrode, using 0.1 M phosphate buffer pH 8.1, applied potential 0.3 V (vs. SCE).

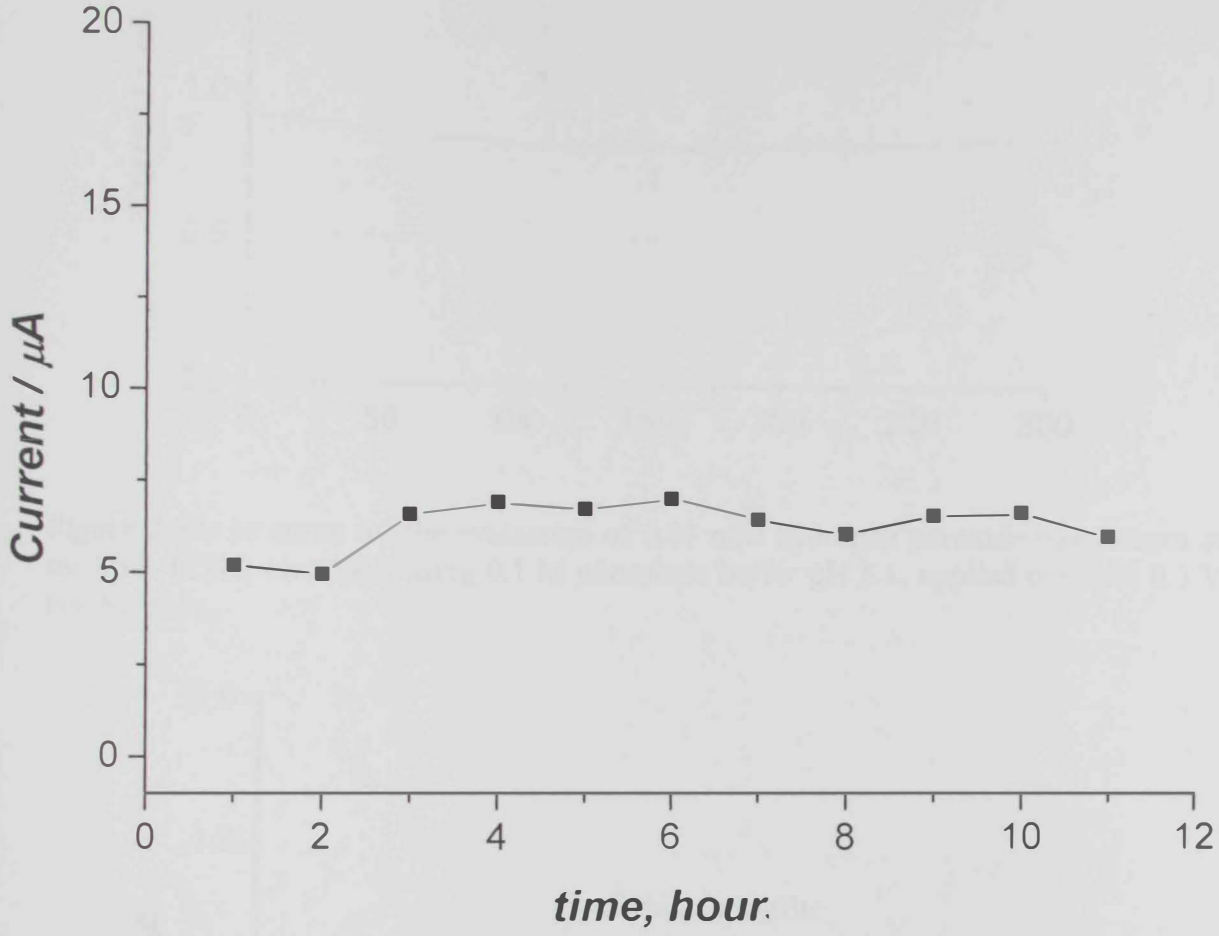

Figure 3.51: Amperometric response for the TTF-TCNQ electrode to 0.01mM of sodium sulfite obtained at one hour intervals, using 0.1 M phosphate buffer pH 8.1, applied potential 0.3 V (vs. SCE).

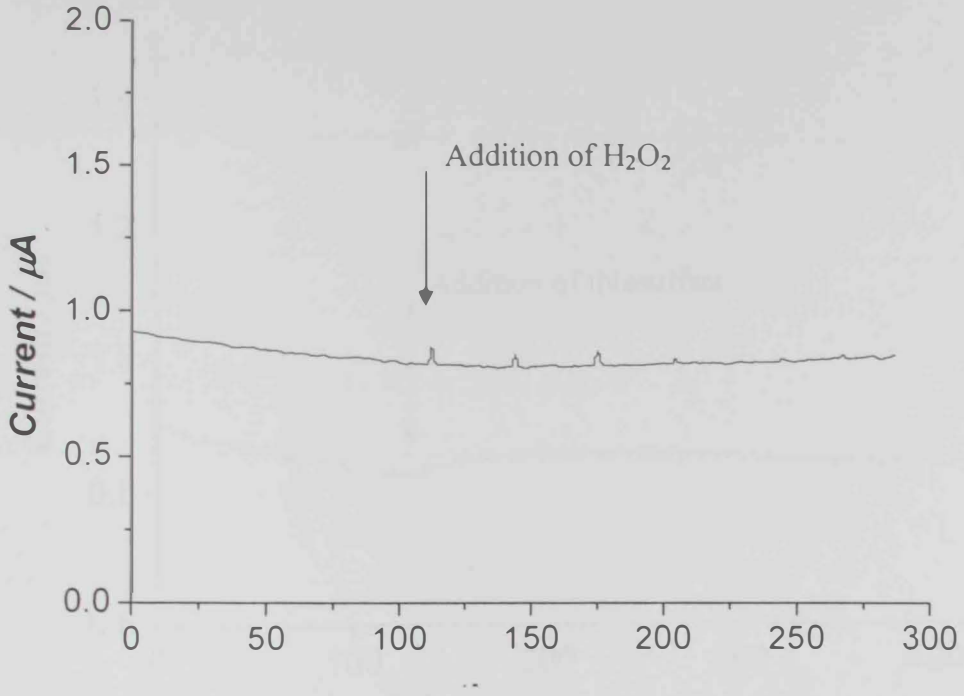

Figure 3.52: *i-t* curve for the evaluation of 0.01 mM hydrogen peroxide interference at the TTF-TCNQ electrode, using 0.1 M phosphate buffer pH 8.1, applied potential 0.3 V (vs. SCE).

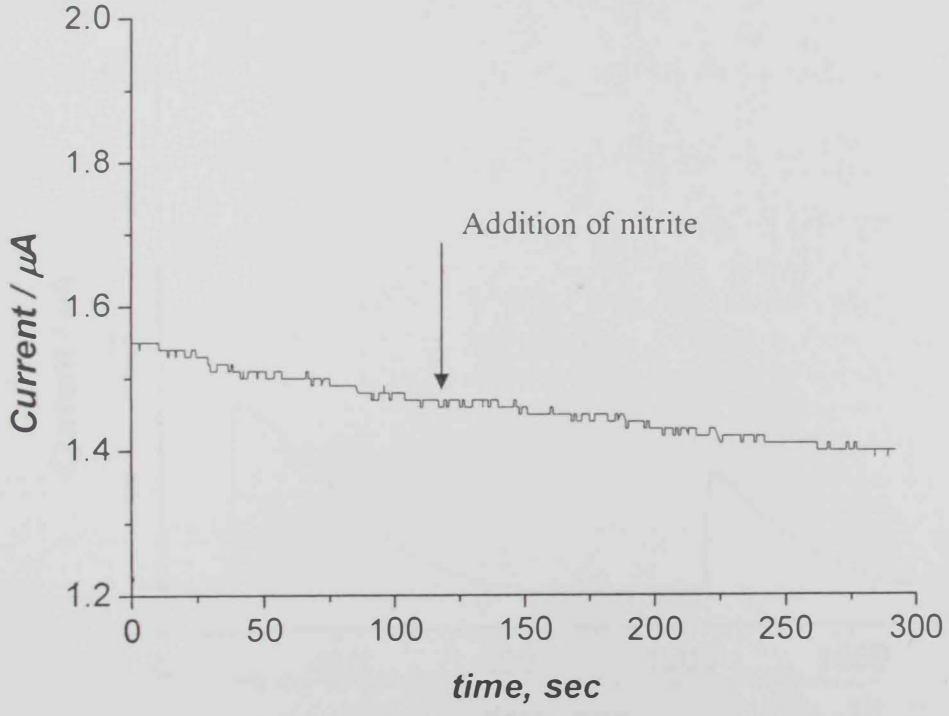

Figure 3.53: *i-t* curve for the evaluation of 0.01 mM sodium nitrite at the TTF-TCNQ electrode in the aqueous solution, using 0.1 M phosphate buffer pH 8.1, applied potential 0.3 V (vs. SCE).

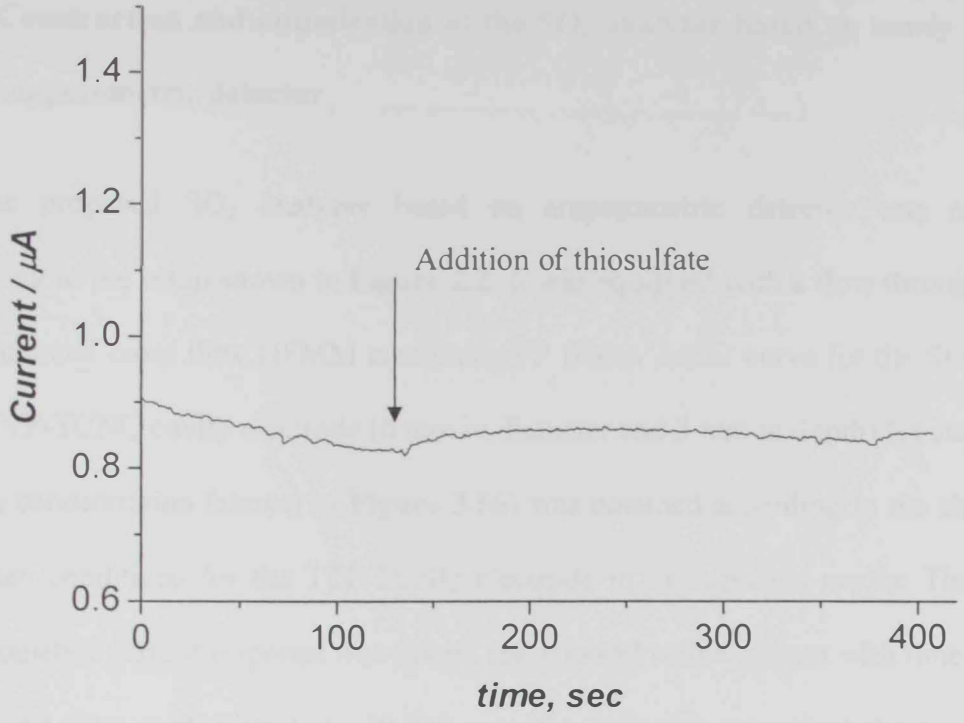

Figure 3.54: *i-t* curve for the evaluation of 0.01 mM thiosulfate at the TTF-TCNQ electrode in the aqueous solution, in 0.1 M phosphate buffer pH 8.1, applied potential 0.3 V (vs. SCE).

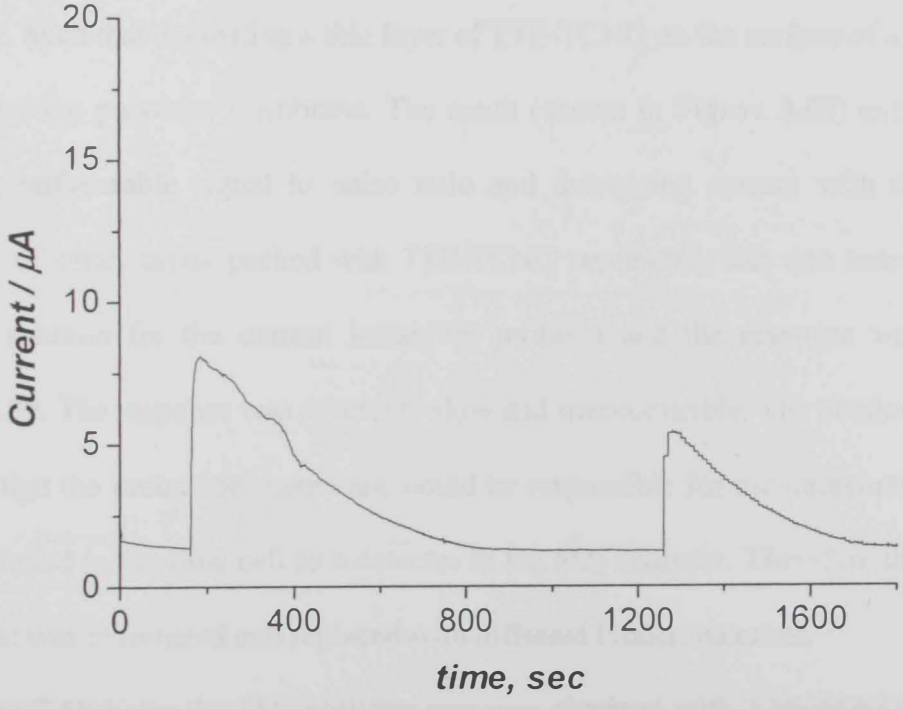

Figure 3.55: *i-t* curve shows the effect of copper powder (masking agent) on the response of 0.01 mM sulfide at the TTF-TCNQ electrode in Aqueous medium.

3.4.5 Construction and optimization of the SO_2 analyzer based on newly described amperometric detector

The proposed SO_2 analyzer based on amperometric detector was constructed according to the setup shown in **Figure 2.2**. It was equipped with a flow through detector a commercial cross flow HFMM containing PP fibers. An *i-t* curve for the SO_2 analyzer with TTF-TCNQ cavity electrode (6 mm in diameter and 3 mm in depth) for step increase in SO_2 concentration (shown in **Figure 3.56**) was obtained according to the above given optimum conditions for the TTF-TCNQ electrode in the aqueous media. The obtained amperometric current response was decent and showed stable current with time. However, upon long time evaluation (i.e., 30,000 sec of continuous operation) the response was unstable and irreproducible (**Figure 3.57**).

To avoid this problem several solutions were attempted to improve the electrode geometry. Such that depositing a thin layer of TTF-TCNQ on the surface of a graphite rod with protecting polyester membrane. The result (shown in **Figure 3.58**) exhibited lower response, unfavorable signal to noise ratio and decreasing current with time. Hence, geometry of small cavity packed with TTF-TCNQ conducting salt was tested as another possible solution for the current instability problem and the response was shown in **Figure 3.59.** The response was relatively slow and irreproducible. The obtained responses revealed that the protection membrane could be responsible for the unfavorable response when installed in the flow cell as a detector in the SO_2 analyzer. Therefore the protection membrane was eliminated and replaced with different binder materials.

Figure 3.60 shows the SO_2 analyzer response obtained with TTF-TCNQ mixed with certain percent of epoxy (as binder) for two concentration levels for SO_2. Unluckily the result did not satisfy the desired stable response. Therefore, another solution was tested

for the same problem; **Figure 3.61** shows the response of the SO_2 analyzer based on TTF-TCNQ electrode (TTF-TCNQ powder deposited on a layer of graphite and silicone oil paste).

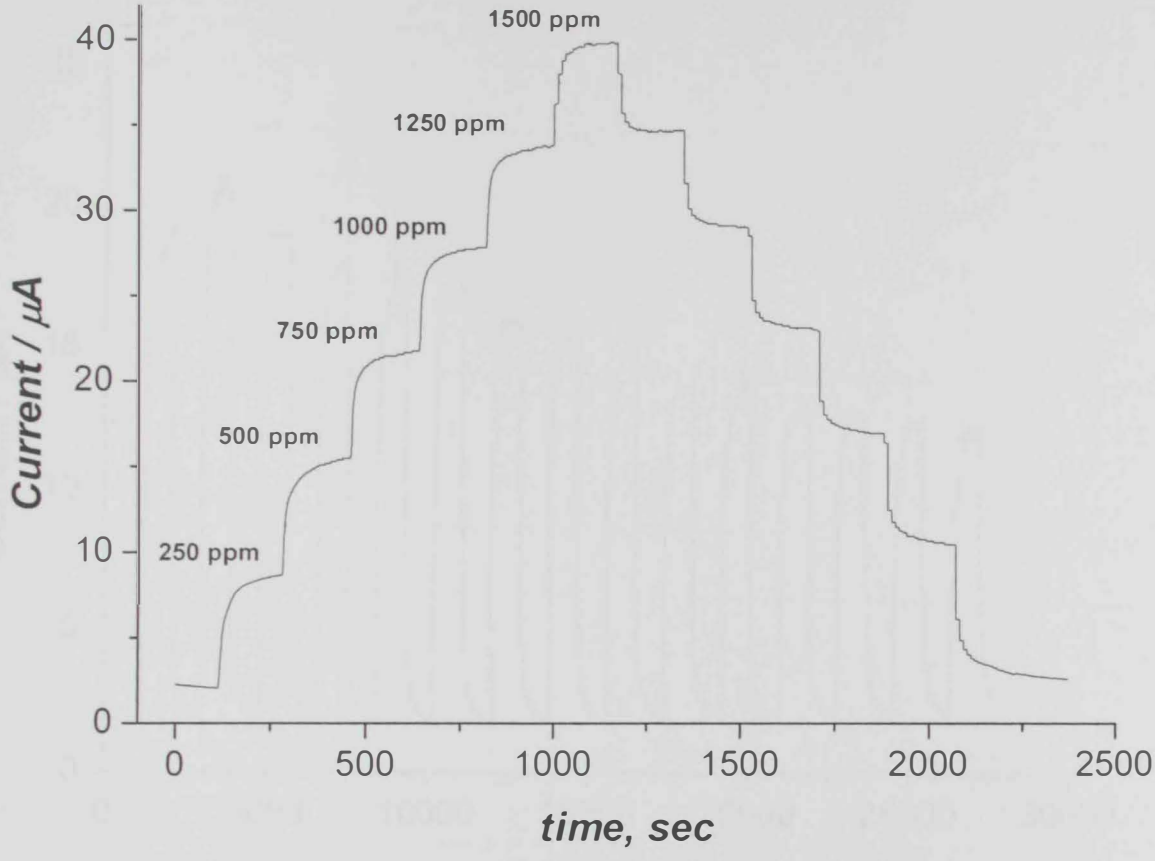

Figure 3.56: Real time response for the proposed SO_2 analyzer, using TTF-TCNQ electrode (pure TTF-TCNQ powder installed in a deep graphite cavity and protected with membrane), 0.1 M phosphate buffer pH 8.1, carrier flow rate: 6 mL/min, applied potential 0.3V (vs. SCE).

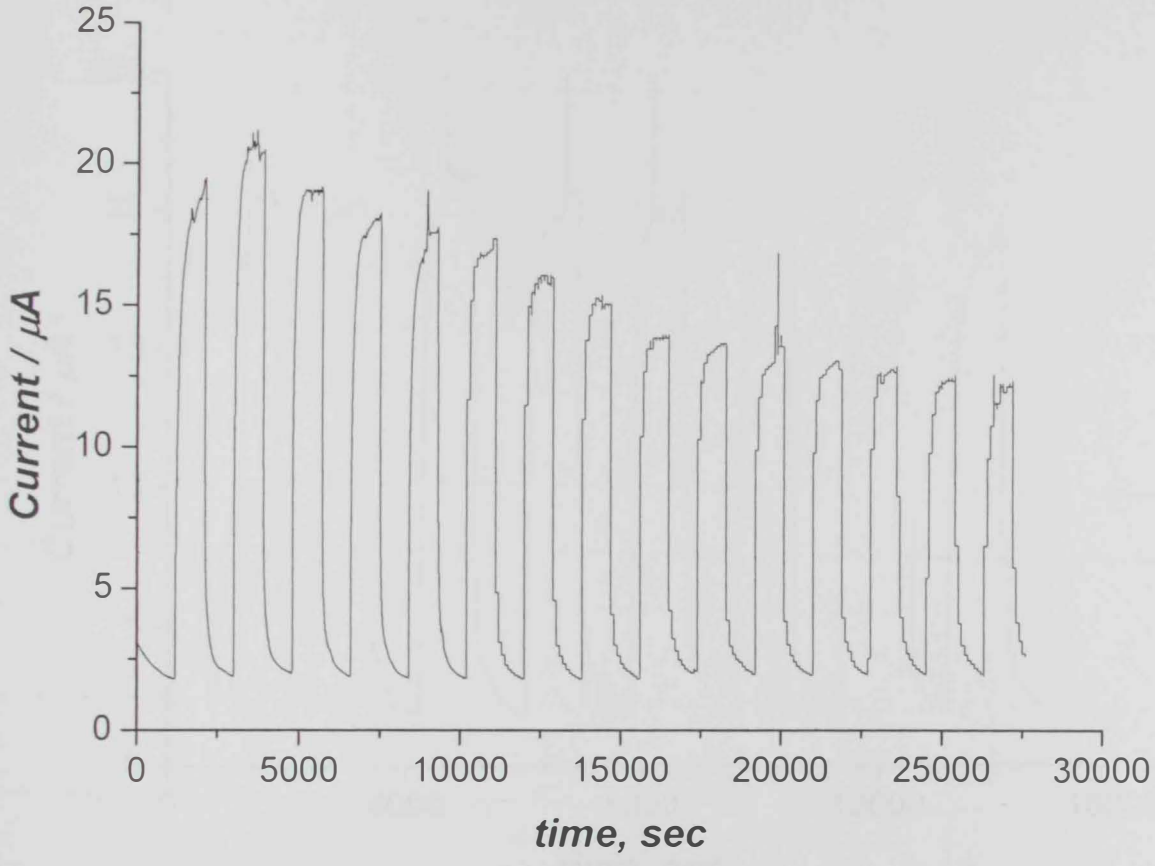

Figure 3.57: Real time response shows the stability test for the SO_2 analyzer (1000 ppm of SO_2) over long duration (more than seven hours), 0.1 M phosphate buffer pH 8.1, carrier flow rate: 6 mL/min, applied potential 0.3 V (vs. SCE).

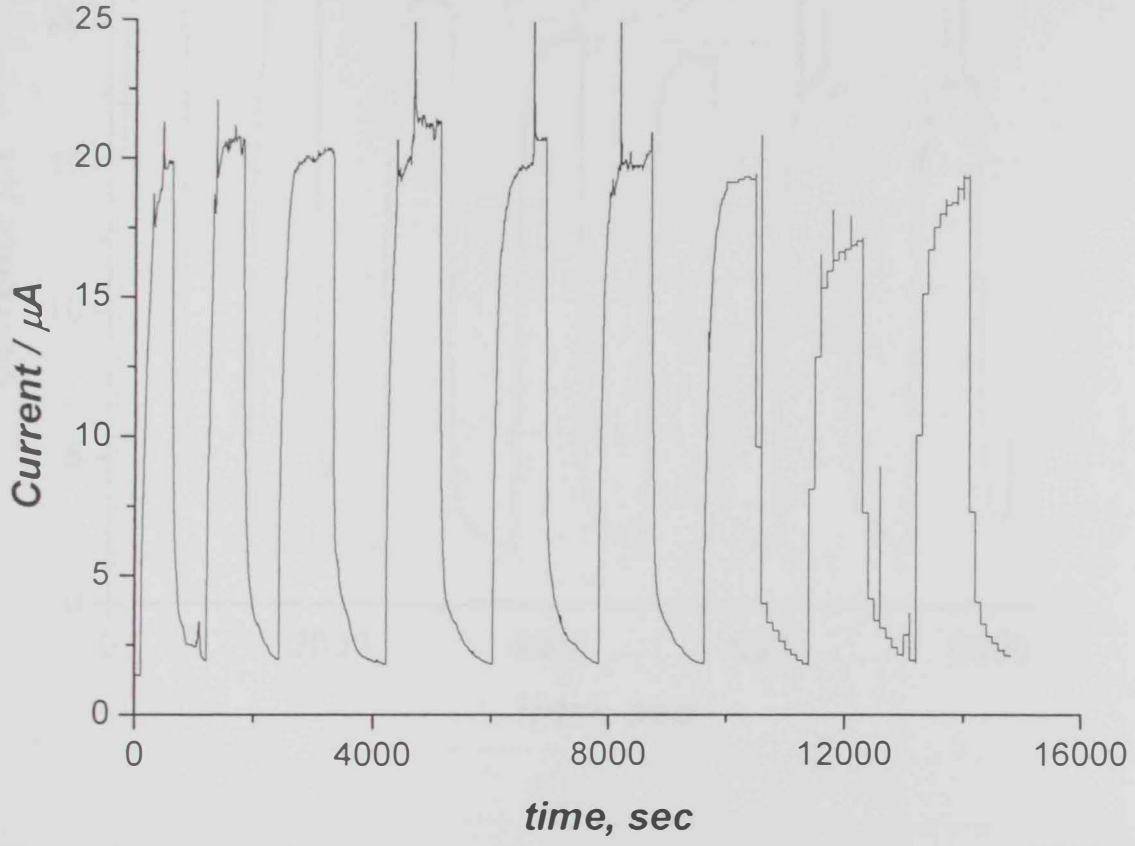

Figure 3.58: Real time response for the proposed SO_2 analyzer with a thin layer of TTF-TCNQ deposited on the surface of a graphite rod and protected with membrane, each peak presents 250 ppm of SO_2, using 0.1 M phosphate buffer pH 8.1, carrier flow rate: 6 mL/min, applied potential 0.3 V (vs. SCE)

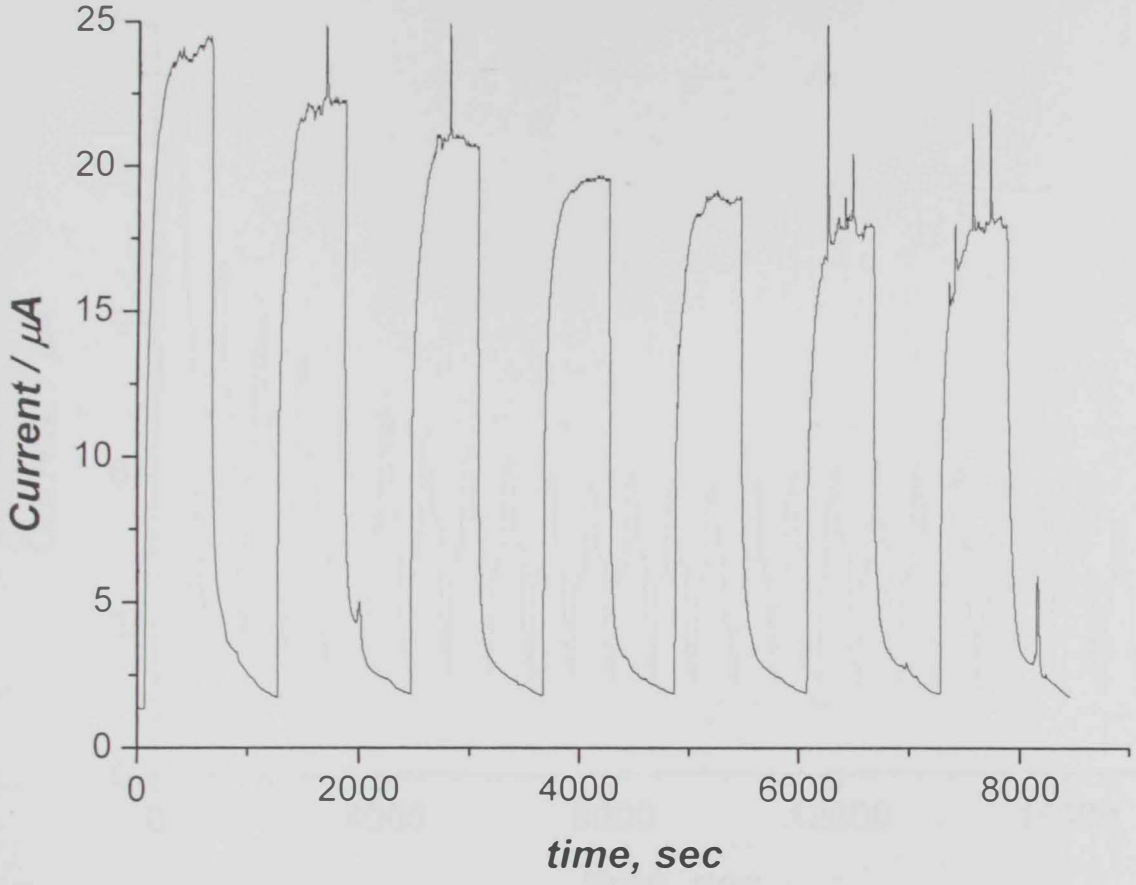

Figure 3.59: Real time response for the proposed SO_2 analyzer with TTF-TCNQ electrode (pure TTF-TCNQ powder installed in a small graphite cavity and protected with membrane), each peak presents 250 ppm of SO_2, using 0.1 M phosphate buffer pH 8.1, carrier flow rate: 6 mL/min, applied potential 0.3 V (vs. SCE).

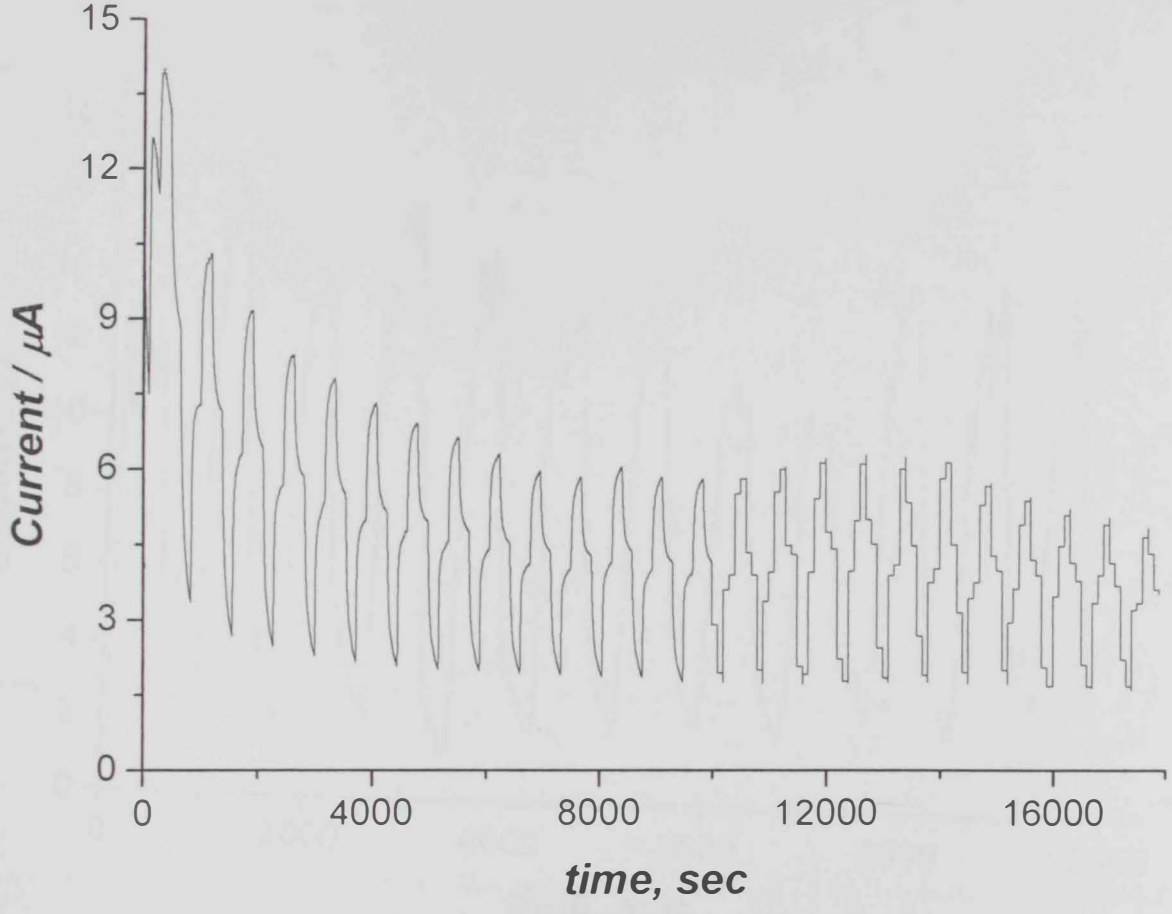

Figure 3.60: Real response time of the SO_2 analyzer based on a mixture of TTF-TCNQ and epoxy, 0.1 M phosphate buffer pH 8.1, carrier flow rate: 3.2 mL/min, applied potential 0.2 V (vs. SCE).each step represents 500 ppm of SO_2 in N_2.

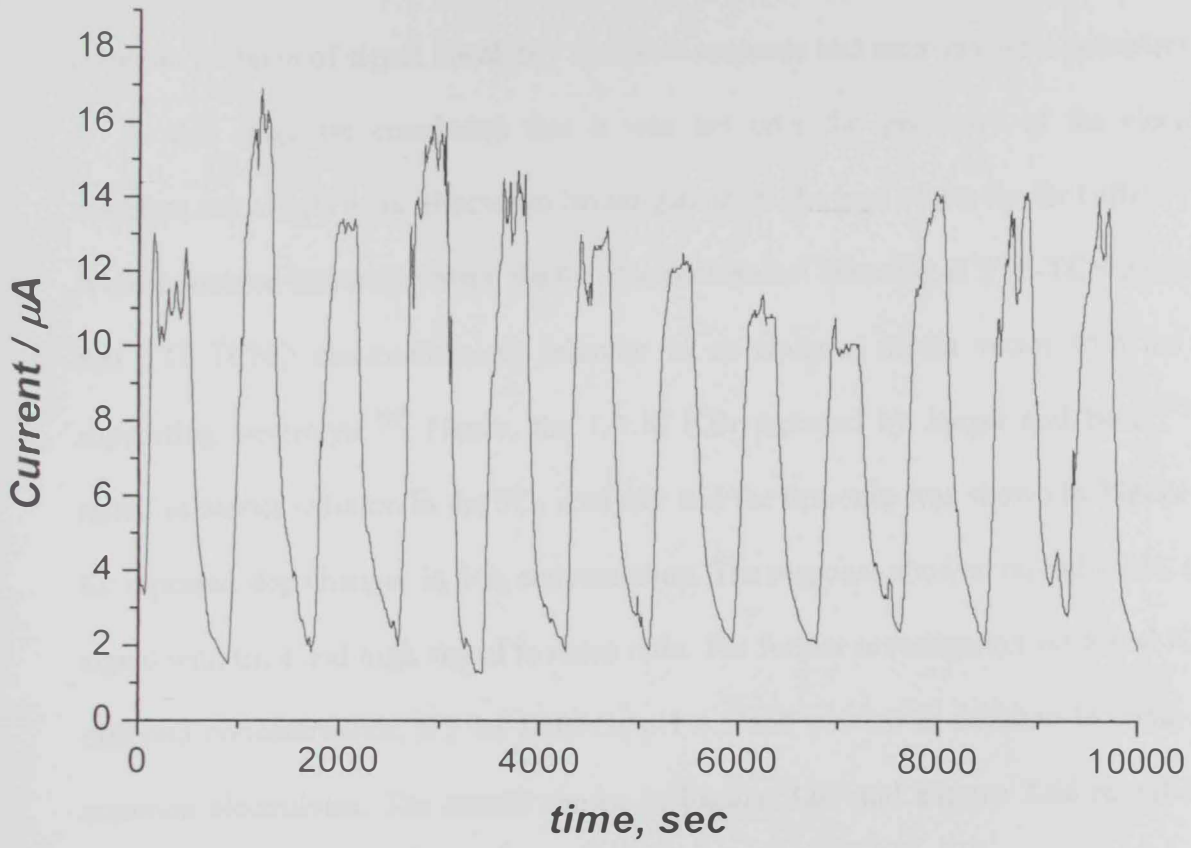

Figure 3.61: Real time response for 1000 ppm of SO_2 using TTF-TCNQ electrode, TTF-TCNQ powder deposited over a base of graphite and silicone oil paste, applied potential at 0.2 V (vs. SCE), 0.1 M phosphate buffer pH 8.1, carrier flow rate: 6 mL/min, applied potential 0.3 V (vs. SCE).

The result showed increasing current with time, which was contributed to the slow conditioning process for the newly prepared electrode or the swelling of the graphite cavity used for such electrodes. The response of electrodes based on TTF-TCNQ and graphite powder were shown in **Figure 3.62** and **Figure 3.63** Even after long time of continuously running experiments under constant conditions, it was evident that the common problem of signal instability and slow response and recovery were persistent.

At this stage we concluded that it was not only the geometry of the electrode, therefore our efforts were directed to investigate more the type of the carrier buffer.
A more focused literature search for the electrochemical behavior of TTF-TCNQ revealed that TTF-TCNQ electrochemical behavior in an aqueous media varies with the type supporting electrolyte.[97] Hence, the 1.0 M KBr reported by Jaeger and Bard,[97] was tested as carrier solution in the SO_2 analyzer and the response was shown in **Figure 3.64** for repeated step changes in SO_2 concentration. The response showed reproducible, stable signal with time and high signal to noise ratio. For further investigation we tested KBr of different concentrations, 0.1 M KH_2PO_4 pH 4.5 and pH 7.0 in addition to some other common electrolytes. The results shown in **Figure 3.65** and **Figure 3.66** revealed that KBr, of any concentration, provides the most stable amperometric response with TTF-TCNQ electrode.

In this work, the long term stability parameter was evaluated (shown in **Figure 3.67**) for the SO_2 analyzer based on TTF-TCNQ paste electrode. Such extremely long runs (i.e., 25,000 sec) were performed to definitely satisfy the desirable characteristics for sulfite determination by amperometric detector. Referring to the reported literature, one can note that all carried experiments were of very short time durations (up to the author best knowledge), maximum of 2000 seconds.[82,117,66]

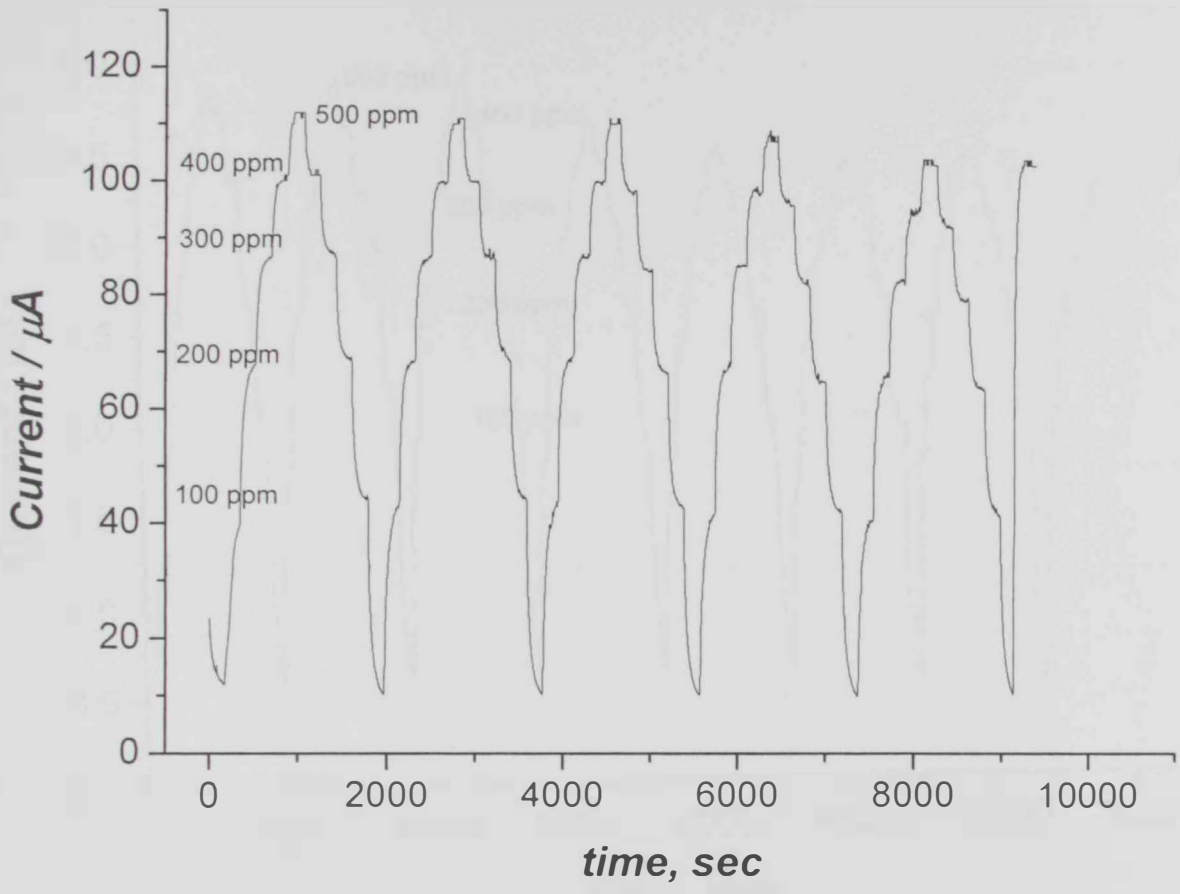

Figure 3.62: Real time response of the SO_2 analyzer (40% TTF-TCNQ mixed with 40% graphite powder and 20%Silicone oil), 0.1 M phosphate buffer, carrier flow rate: 4.5mL/min, applied potential 0.4V (vs. SCE),

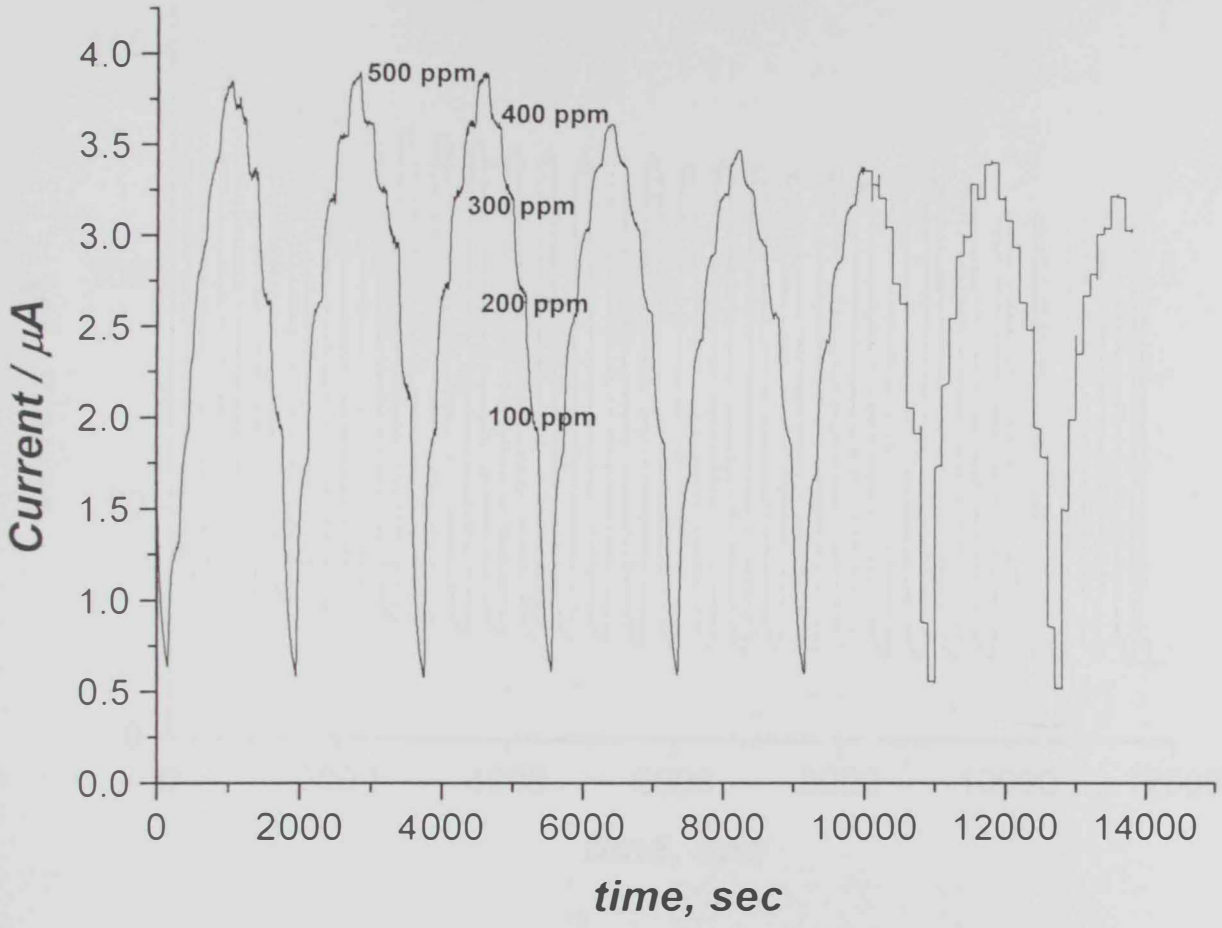

Figure 3.63: Real time response of the SO_2 analyzer (50%TTF-TCNQ mixed with 50%graphite powder), 0.1 M phosphate buffer, carrier flow rate: 4.5 mL/min, applied potential 0.25 V (vs. SCE).

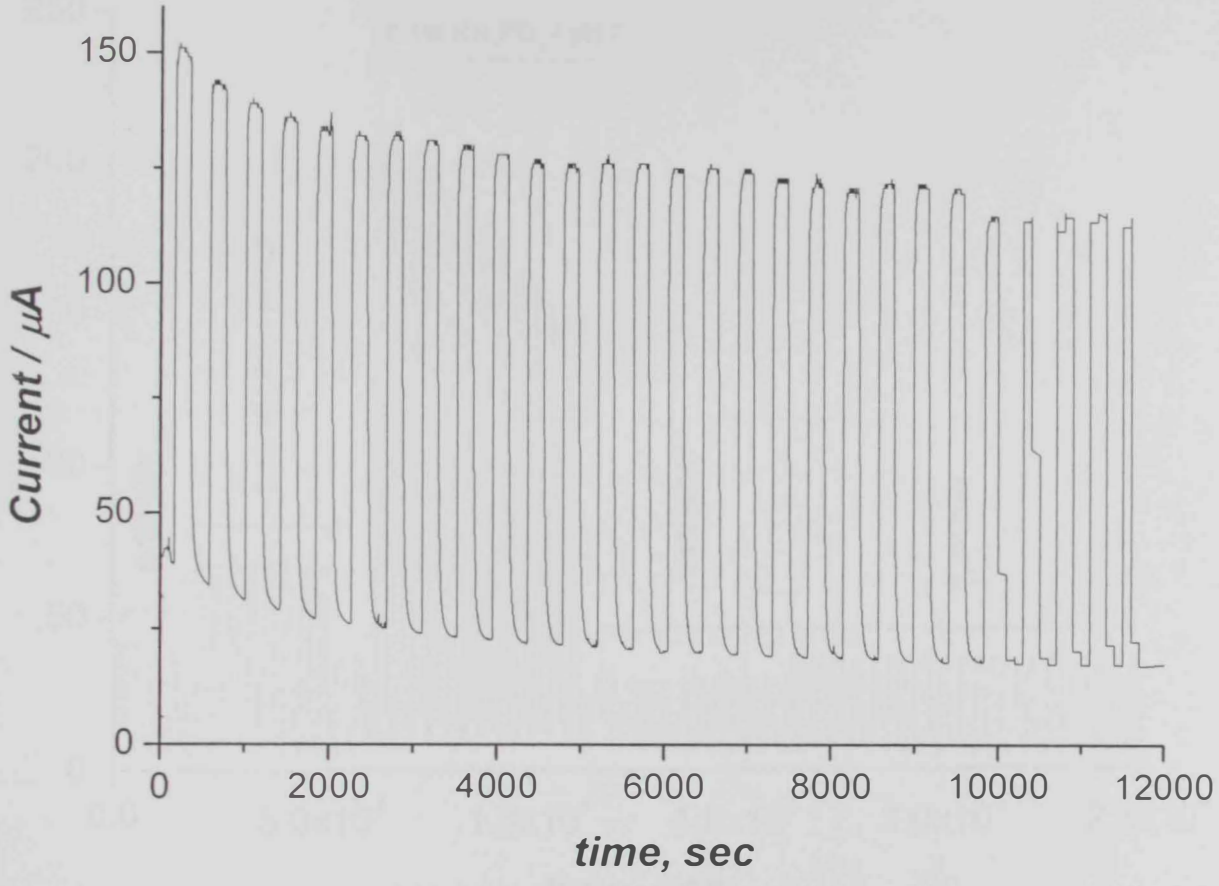

Figure 3.64: Real time response shows the long term stability of the SO_2 analyzer (80% TTF-TCNQ - 20% Silicone oil) with 1.0 M KBr, carrier flow rate 5.0 mL/min, applied potential 0.4 V (vs. SCE), each peak represents 500 ppm SO_2 in N_2.

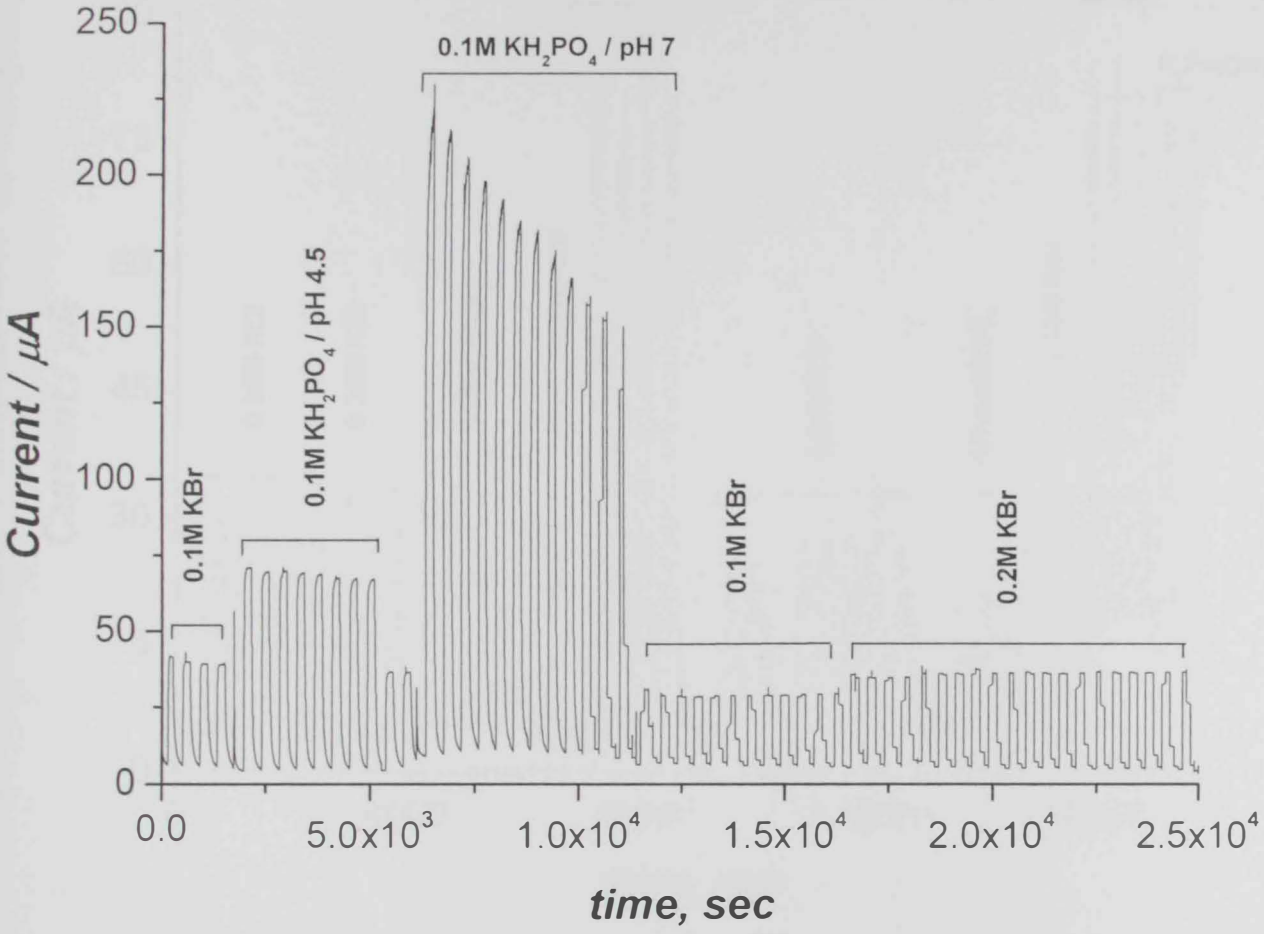

Figure 3.65: Screening for SO_2 analyzer response (80% TTF-TCNQ - 20 % Silicone oil) with different carrier solutions. Carrier flow rate: 4.5 mL/min, applied potential 0.4 V (vs. SCE), each peak represents 500 ppm SO_2 in N_2.

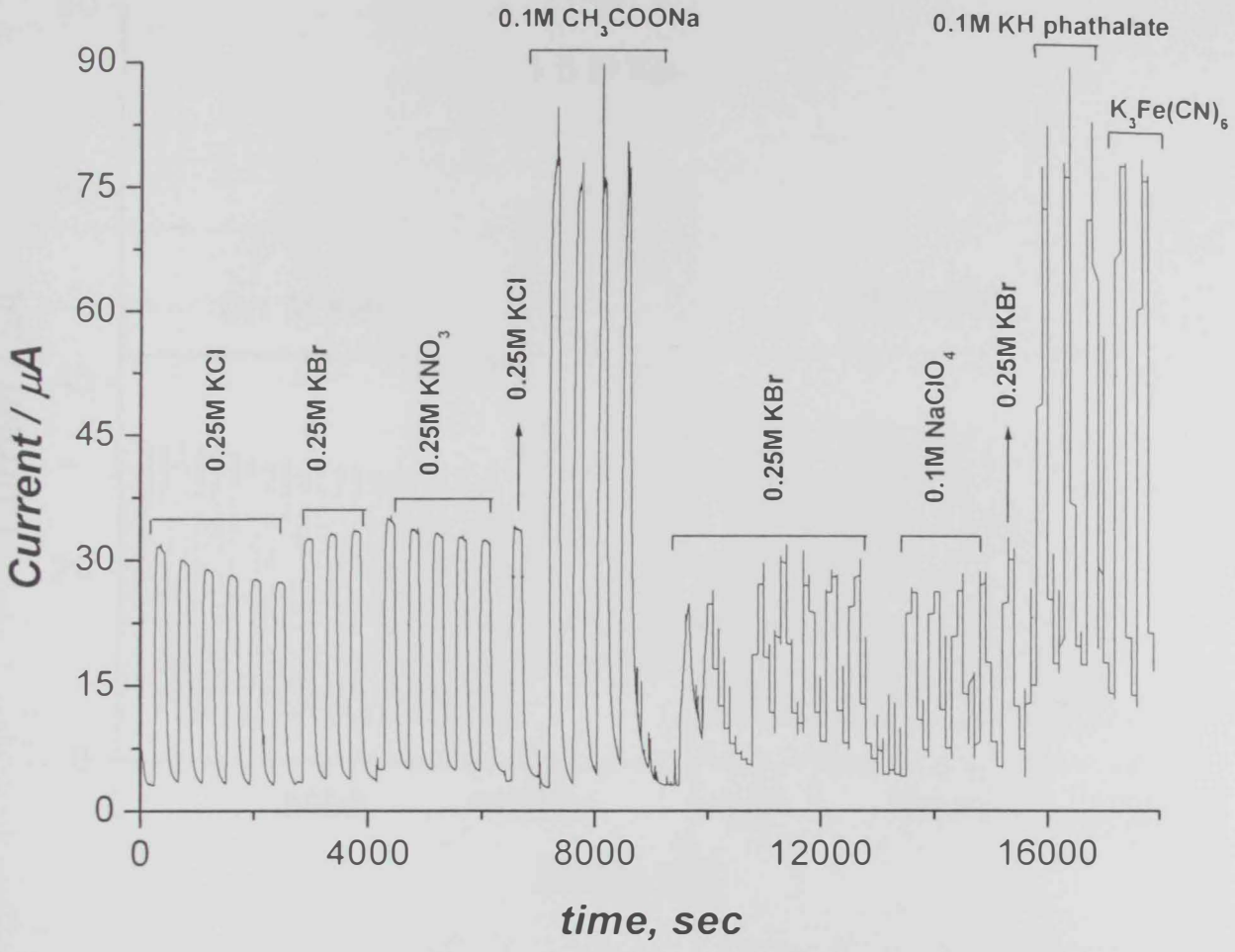

Figure 3.66: Wider screening range for SO_2 analyzer response (80% TTF-TCNQ - 20 % Silicone oil) with various carrier solutions. Carrier flow rate: 4.5 mL/min, applied potential 0.4 V (vs. SCE), each peak represents 500 ppm SO_2 in N_2.

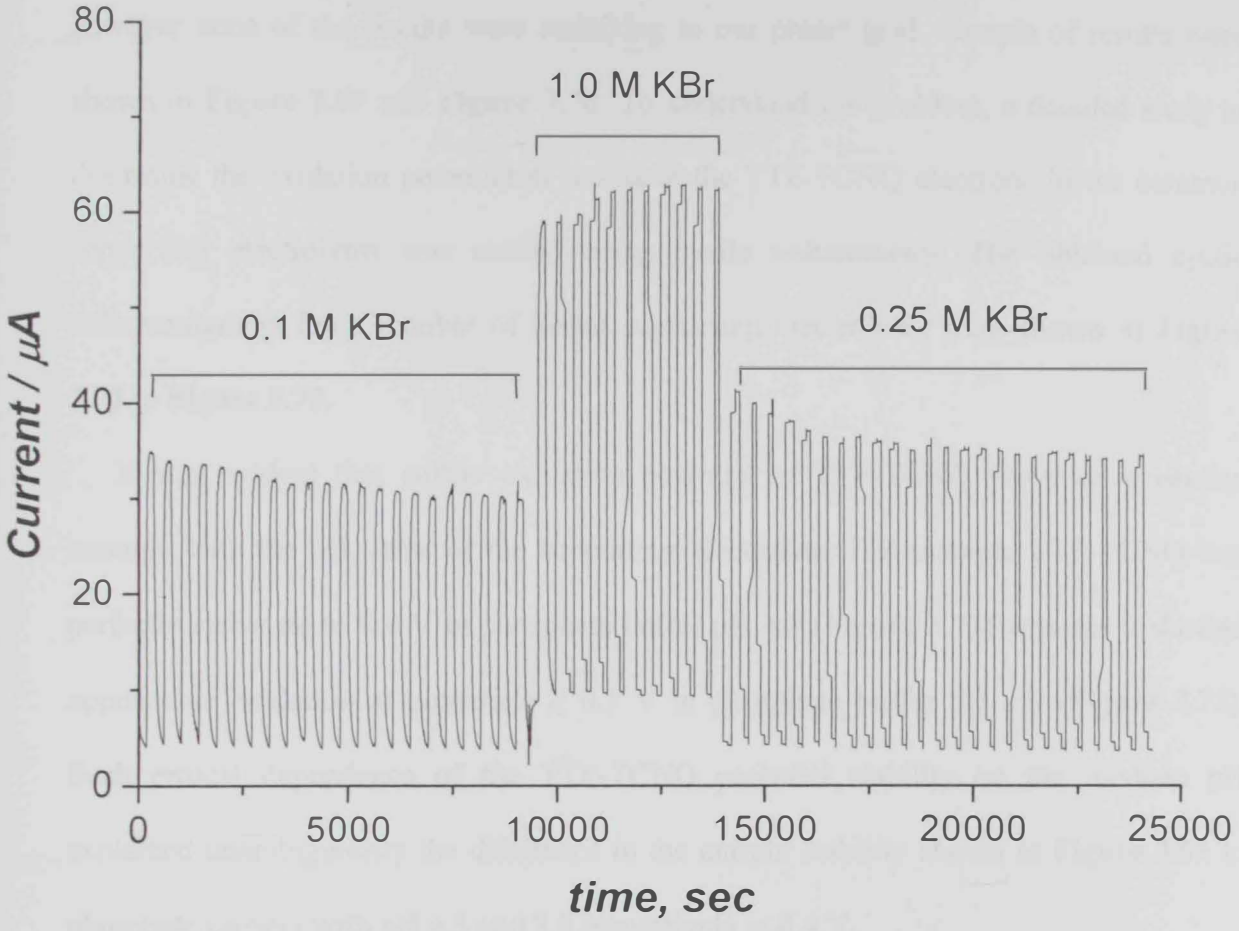

Figure 3.67: long term stability test of the SO_2 analyzer in three different concentrations of carrier buffer-KBr, carrier flow rate 5.0 mL/min, E= 0.4 V, SO_2 concentration 500 ppm, 80% TTF-TCNQ to 20% Silicone oil.

Although the results showed very high reproducibility and stability response for the SO_2 analyzer using KBr as carrier solution, the linearity was very poor (shown in **Figure 3.68**). The linearity was evaluated over a broad range of pH values (from pH 4 to pH 10); however none of the results were satisfying to our preset goal. Sample of results were shown in **Figure 3.69** and **Figure 3.70**. To understand the problem, a detailed study to determine the oxidation potential of sulfite at the TTF-TCNQ electrode in the common supporting electrolytes was carried using cyclic voltammetry. The obtained cyclic voltammograms for a number of tested supporting electrolytes were shown in **Figure 3.71** to **Figure 3.75**.

It was evident that sulfite oxidation potential at TTF-TCNQ electrode depended strongly with the pH value of the supporting electrolyte. For example TTF-TCNQ was perfectly stable up to 0.4 V in phosphate buffer pH 4.3 (**Figure 3.73**) whereas it showed appreciable oxidation at potentials $\geq$ 0.3 V in phosphate buffer pH 7.0 (**Figure 3.73**). Such critical dependence of the TTF-TCNQ potential stability on the medium pH explained unambiguously the difference in the current stability shown in **Figure 3.65** in phosphate carriers with pH 4.5 and 7.0 respectively at 0.4 V.

Thus, critical selection of the TTF-TCNQ electrode potential was made by considering the carrier solution pH in such away that the TTF-TCNQ did not show any self oxidation at the selected potential. Thus we decided to re-evaluate the effect of the carrier buffer pH with new potential values, according to the information we get from the cyclic voltammograms.

Figure 3.76 shows the response of the analyzer using 0.2 M K-phosphate buffer pH 8.0. The response showed stable signal (for ~ 600 sec. long) for 500 ppm SO_2 but the linearity was somehow limited. Therefore the response in carrier solution with lower pH, i.e., pH 5.5 at relatively higher potential, i.e., 0.325 V was tested as shown in **Figure 3.77**.

In spite of the signal stability the linearity was poor. Subsequently, pH as low as pH 4.4 was also tested (**Figure 3.78**), this time the response exhibited very high signal stability but the linearity was worse than pH 5.5. Such behavior could be attributed to the more difficult oxidation of sulfite in acidic media.

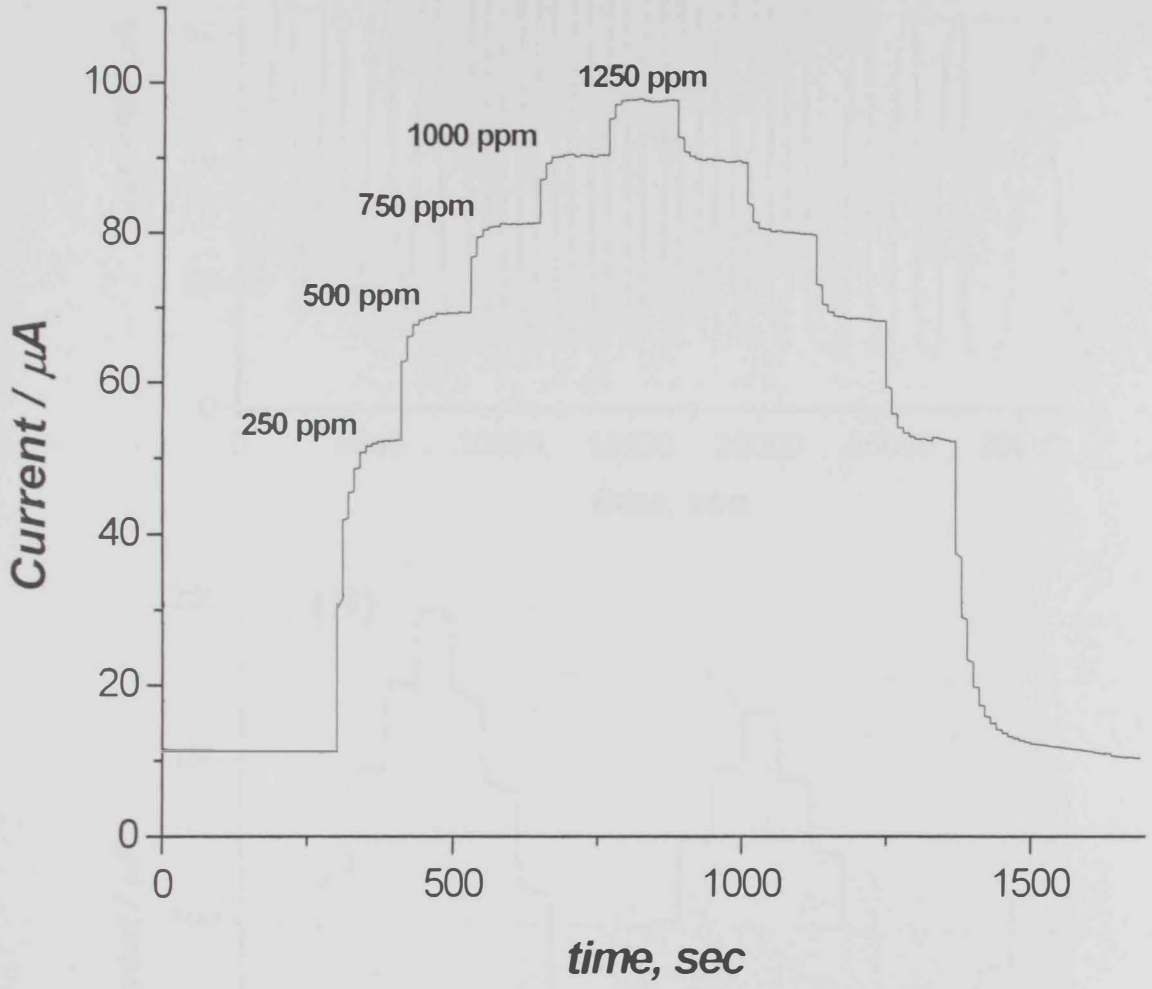

Figure 3.68: *i-t* curve shows the calibration of the SO2 analyzer (80% TTF-TCNQ to 20% Silicone oil) 1.0M KBr, carrier flow rate: 4.5 mL/min, applied potential 0.4 V (vs. SCE).

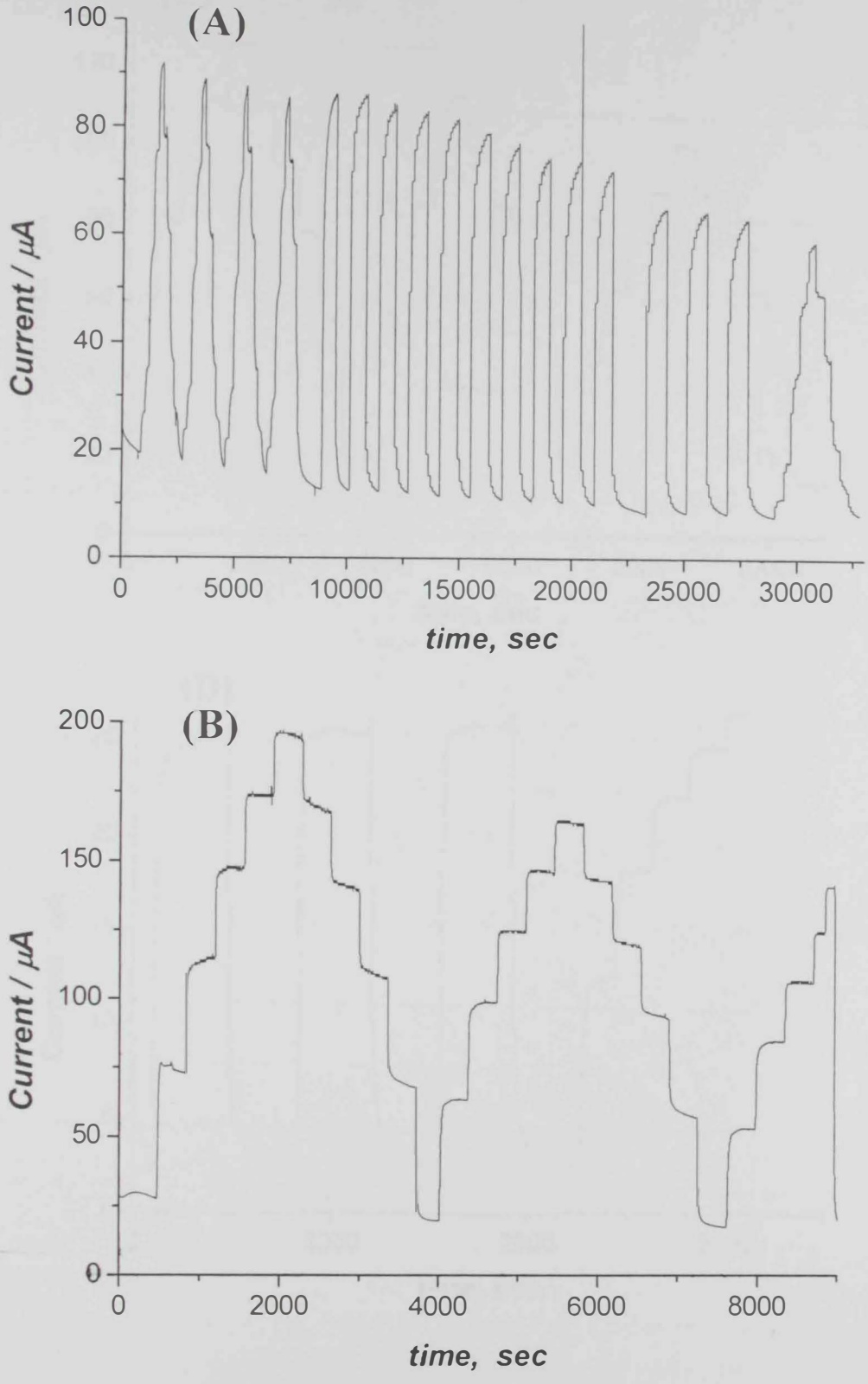

Figure 3.69: Real time response shows linearity of the SO_2 analyzer associated with 0.2 M KBr pH 10.0 (A) and pH 8.0 (B), using TTF-TCNQ mixed with silicone oil (at ratio of 66% to 34%), applied potential 0.45 V (vs. SCE) Increments corresponds to 100 ppm of SO_2.

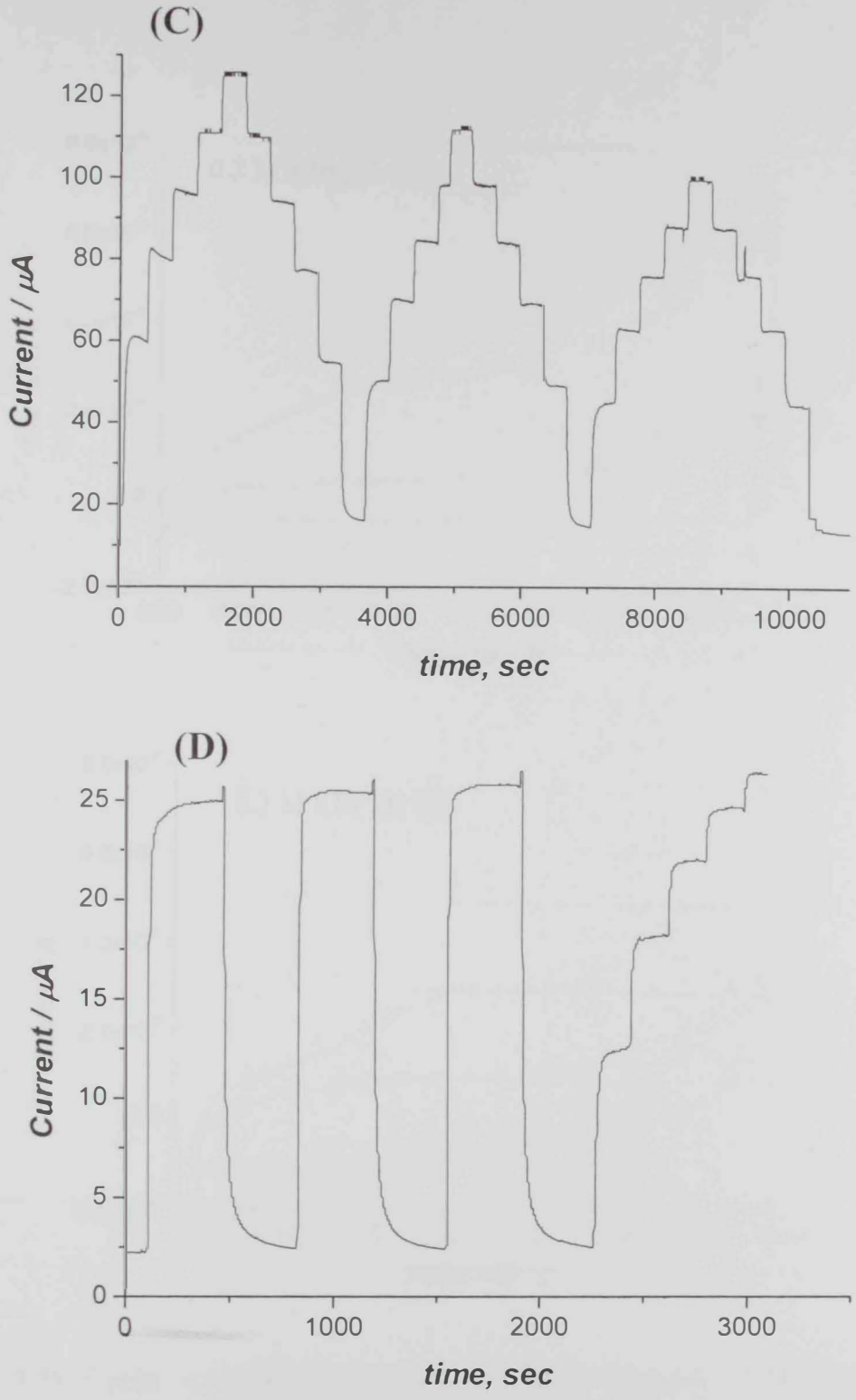

Figure 3.70: Real time response shows linearity of the SO_2 analyzer associated with 0.2 M KBr pH 6.0 (C) and pH 4.0 (D). Using TTF-TCNQ mixed with silicone oil (at ratio of 66% to 34%), applied potential 0.45 V (vs. SCE) Increments corresponds to 100 ppm of SO_2.

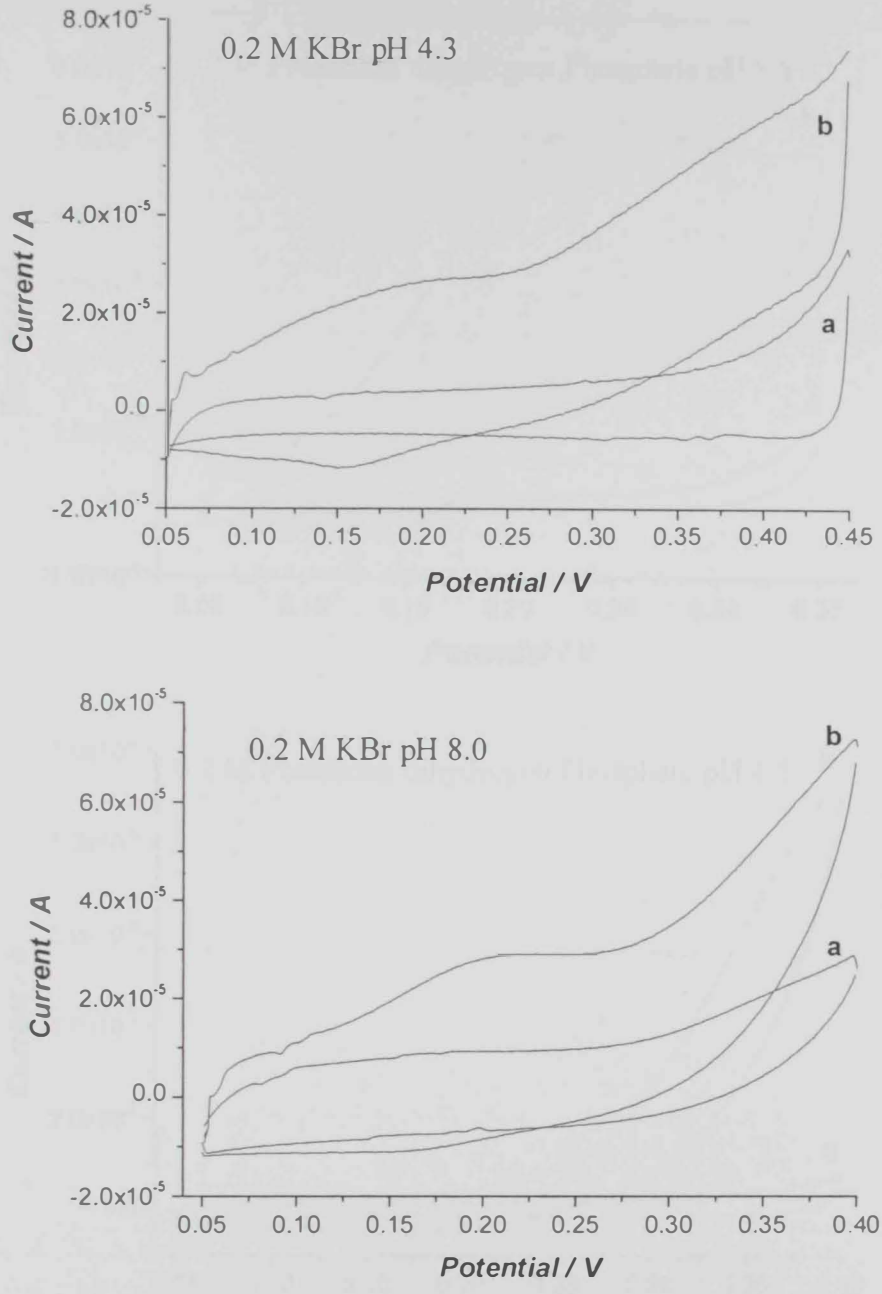

Figure 3.71: Cyclic voltammogram of the TTF-TCNQ electrode (TTF-TCNQ:oil 1:1), (curve a) in the absence and (curve b) in the presence of 10 mM sulfite. Potential scan rate: 5mV s^{-1}

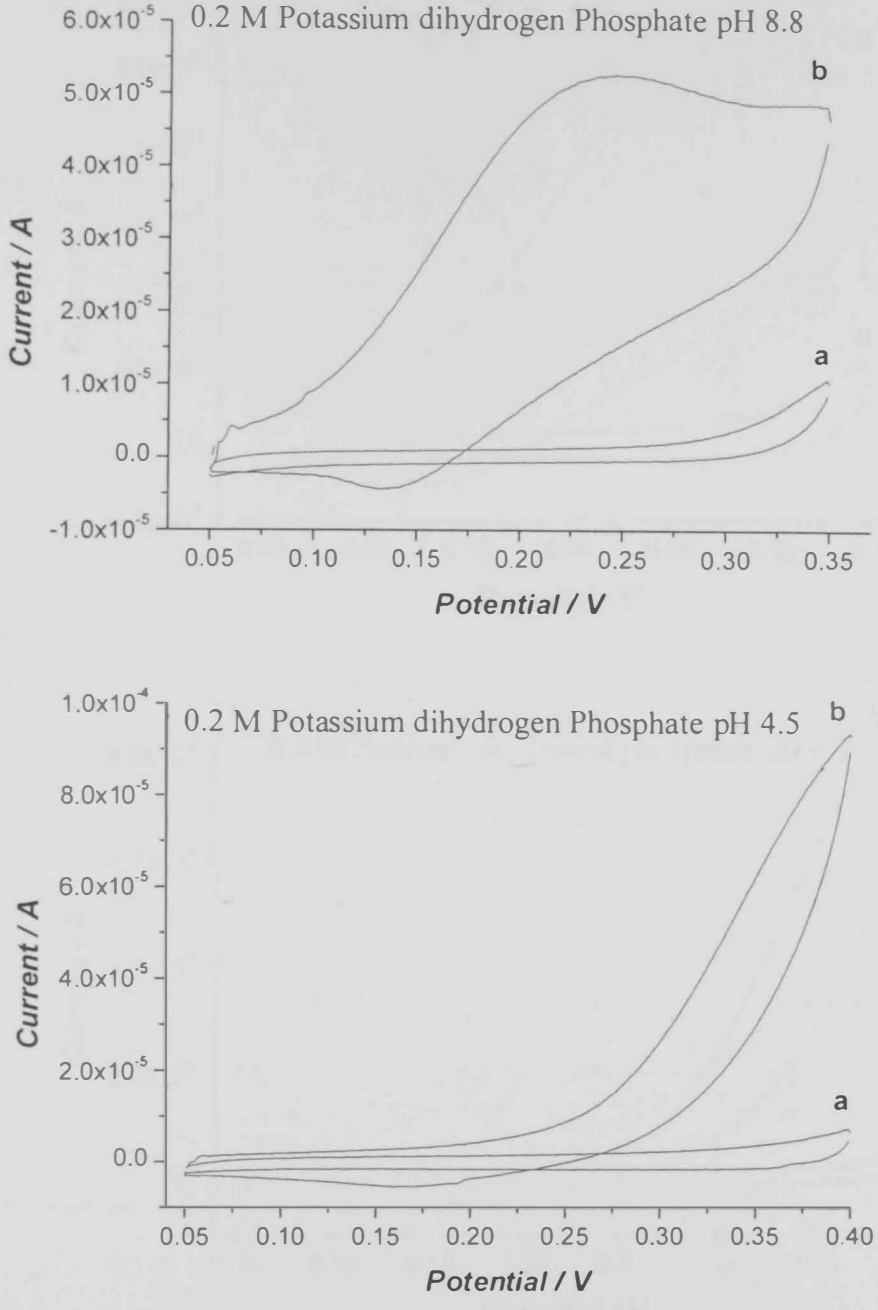

Figure 3.72: Cyclic voltammogram of the TTF-TCNQ electrode (TTF-TCNQ:oil 1:1), (curve a) in the absence and (curve b) in the presence of 10 mM sulfite. Potential scan rate: 5 mV s^{-1}

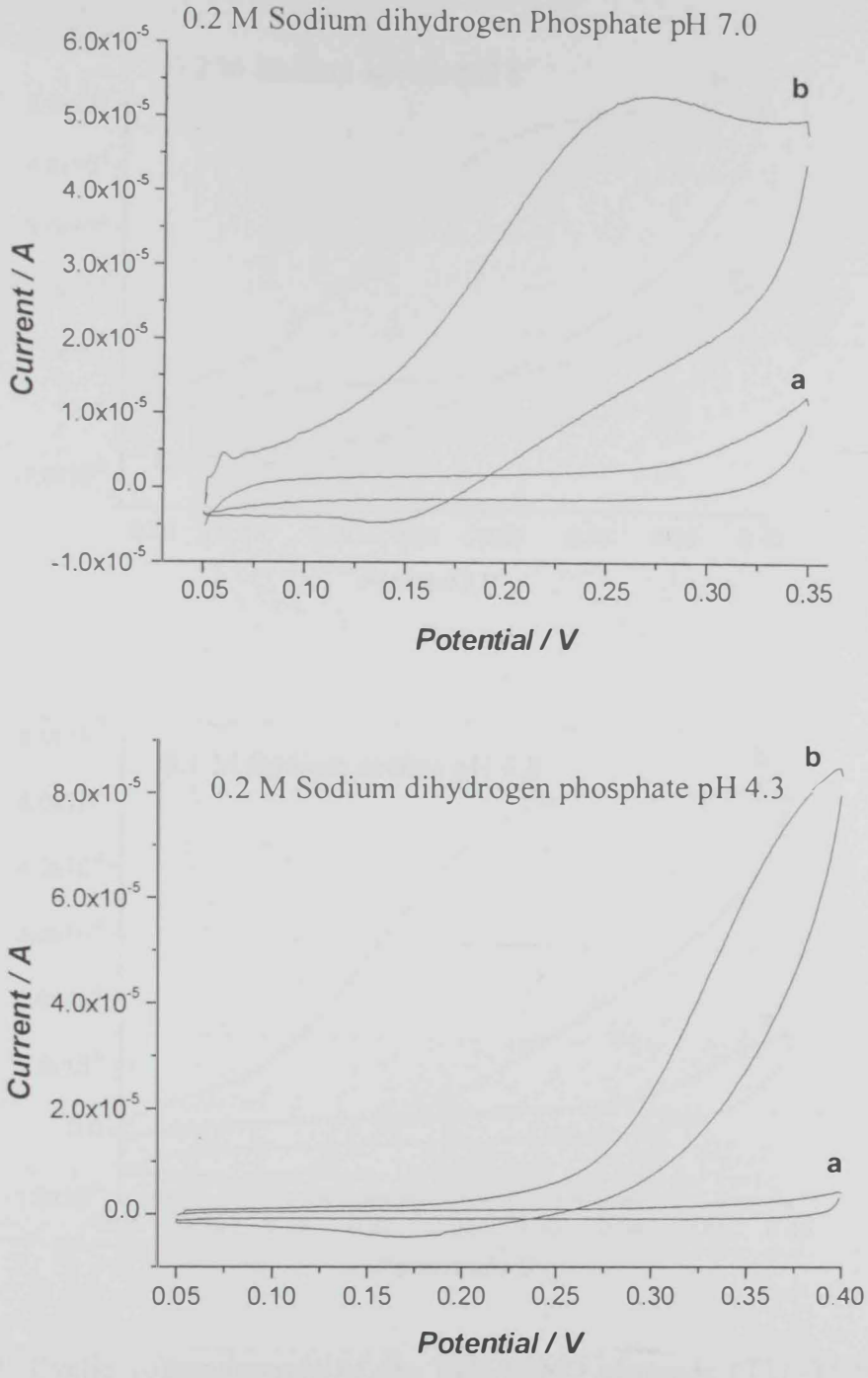

Figure 3.73: Cyclic voltammogram of the TTF-TCNQ electrode (TTF-TCNQ:oil 1:1), (curve a) in the absence and (curve b) in the presence of 10 mM sulfite. Potential scan rate: 5 mV s^{-1}

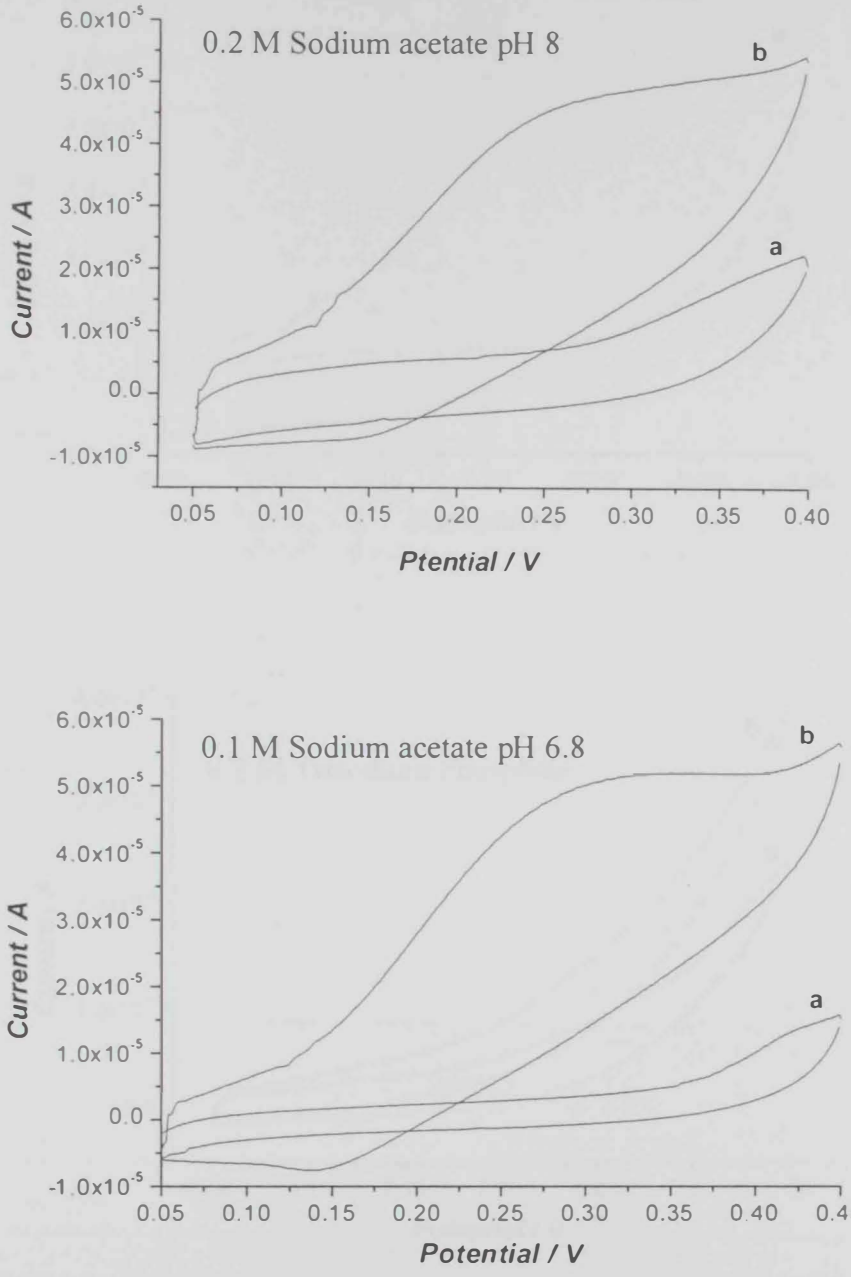

Figure 3.74: Cyclic voltammogram of the TTF-TCNQ electrode (TTF-TCNQ:oil 1:1), (curve a) in the absence and (curve b) in the presence of 10 mM sulfite. Potential scan rate: 5 mV s^{-1}

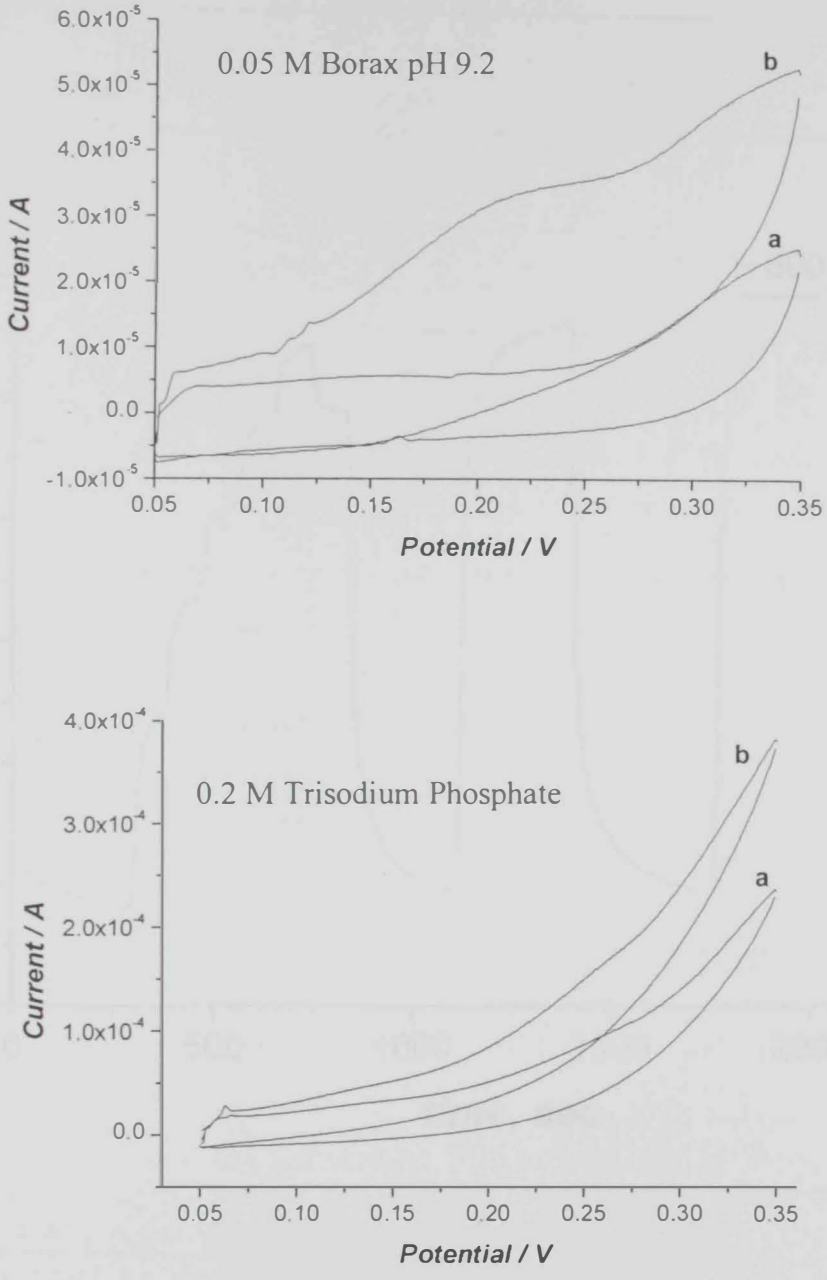

Figure 3.75: Cyclic voltammogram of the TTF-TCNQ electrode (TTF-TCNQ:oil 1:1), (curve a) in the absence and (curve b) in the presence of 10 mM sulfite. Potential scan rate: 5 mV s^{-1}

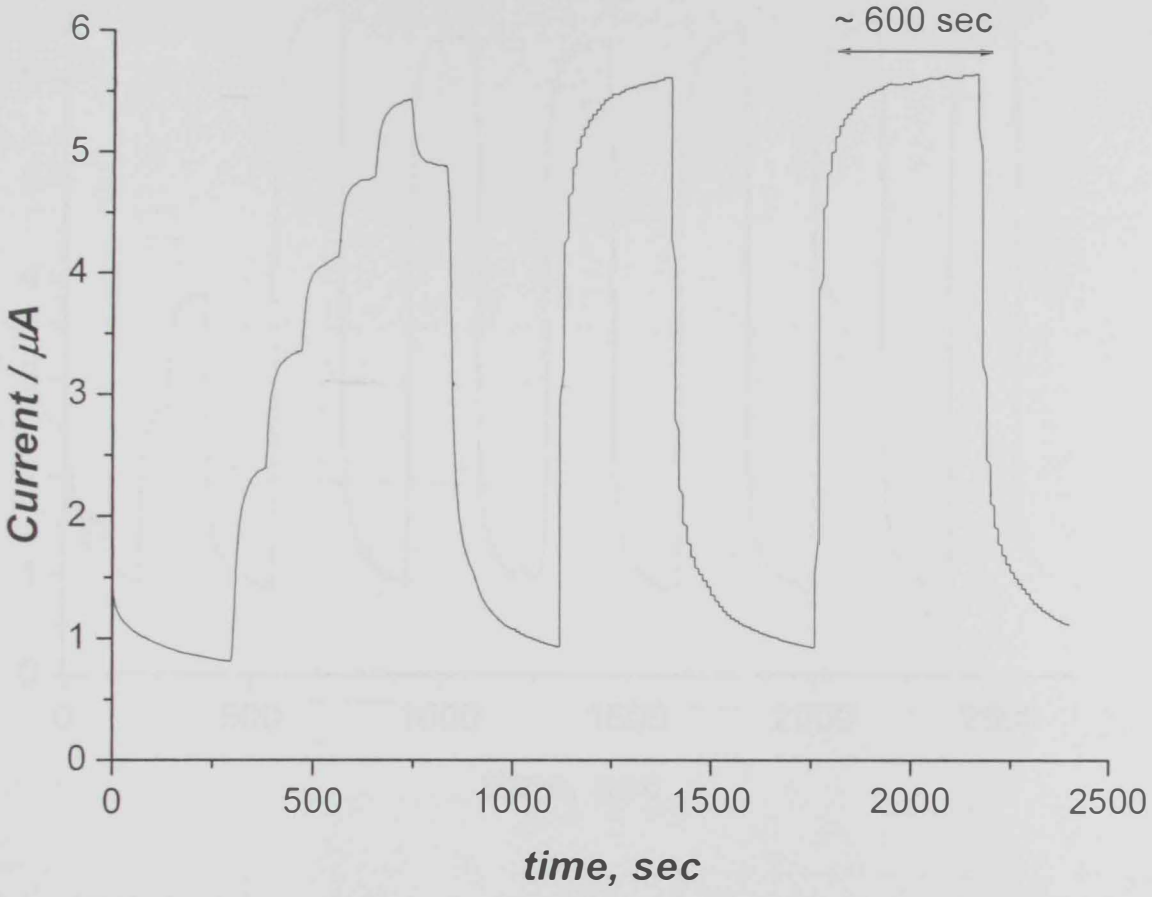

Figure 3.76: Real response time for the SO_2 analyzer, 0.2 M K-phosphate pH 8.0, at TTF-TCNQ/silicone oil ratio of 1:1.6. Each SO_2 increment represents 100 ppm in N_2, applied potential 0.275 V (vs. SCE).

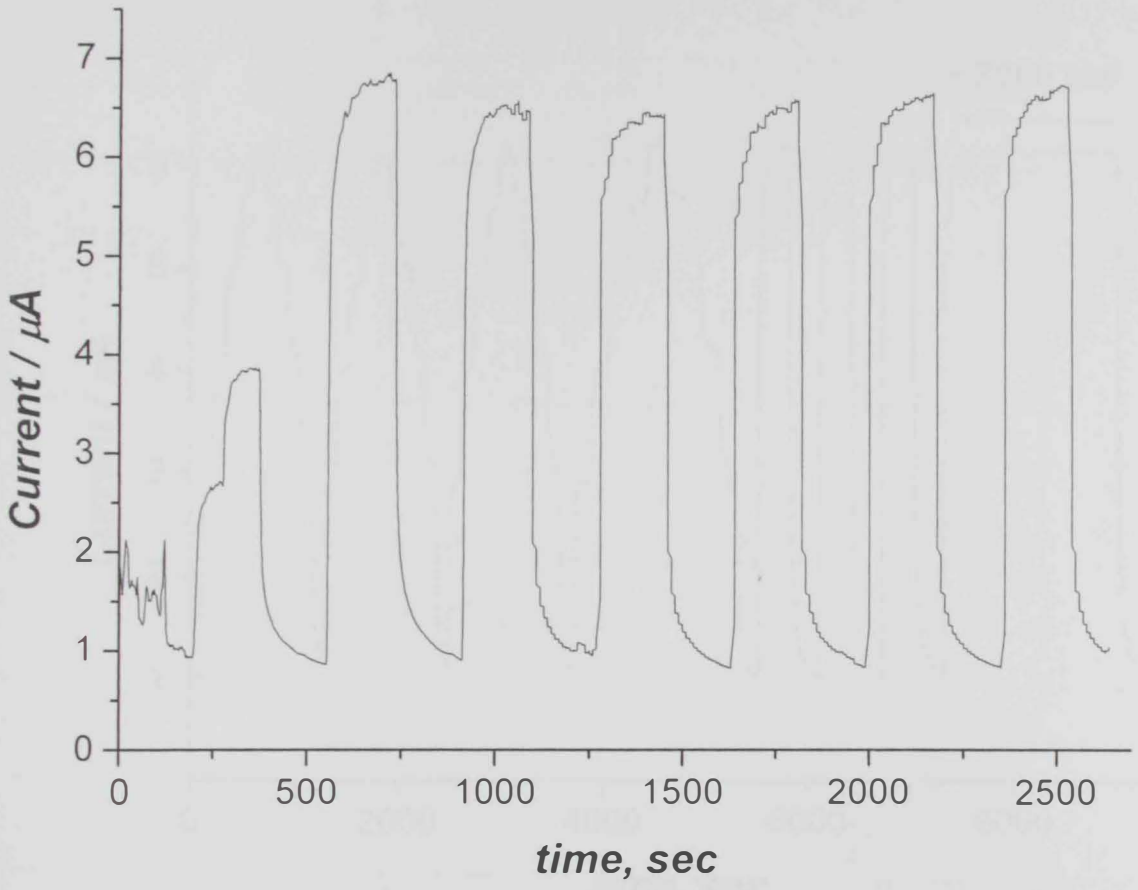

Figure 3.77: Real response time for the SO_2 analyzer, 0.2 M K-phosphate pH 5.5, at TTF-TCNQ/silicone oil ratio of 1:1.25. Each SO_2 increment represents 100 ppm in N_2, applied potential 0.325 V (vs. SCE).

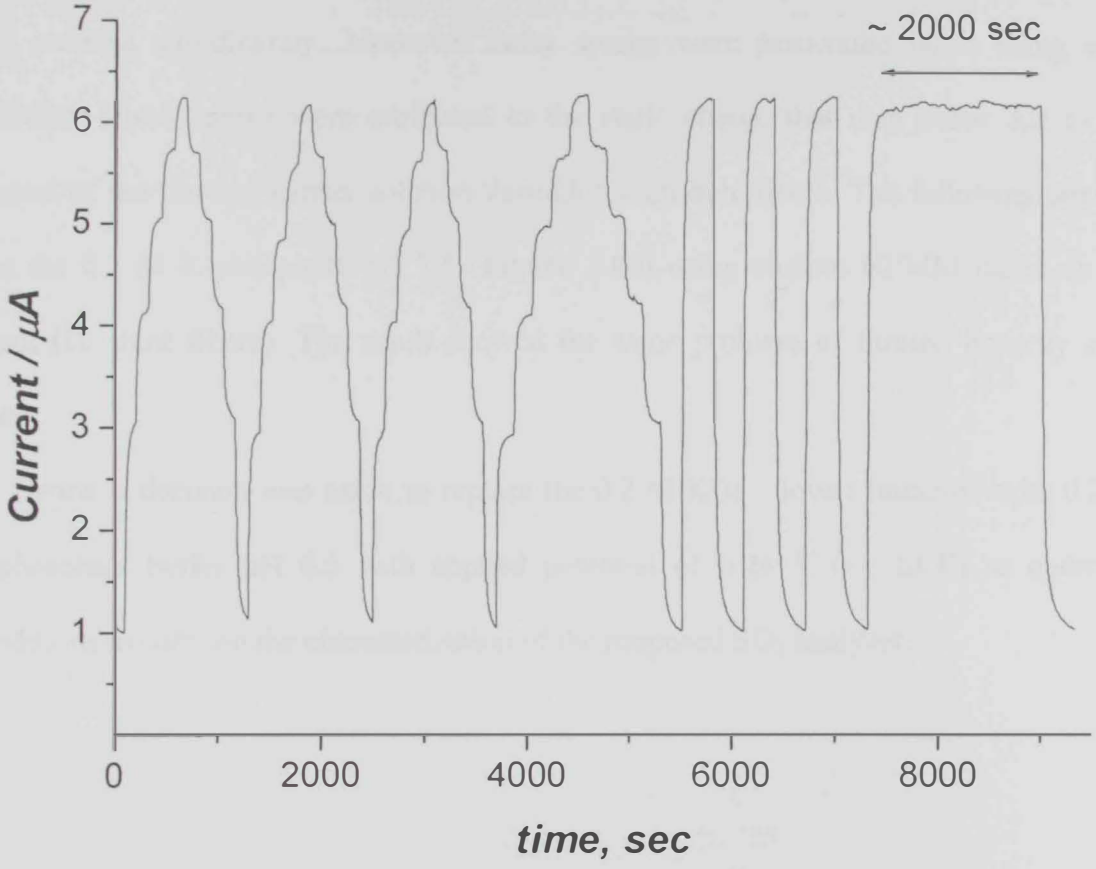

Figure 3.78: Real response time for the SO_2 analyzer, 0.2 M K-phosphate pH 4.4, at TTF-TCNQ/silicone oil ratio of 1:1.25. Each SO_2 increment represents 100 ppm in N_2, applied potential 0.325 V (vs. SCE).

After that 0.2 M K-phosphate pH 6.5 was tested, result was shown in **Figure 3.79**. It showed reasonable stability and enhanced linearity. For further evaluation many linearity tests were done at 0.2 M K-phosphate pH 6.5 using different HFMM based on non-porous fibers which might reduce the flux of SO_2 and hence could improve the linearity. But unfortunately such modules dramatically reduced the sensitivity and hence the S/N ratio was reduced significantly. Moreover noisy sparks were associated when using such modules. These sparks were attributed to the static charge that may occur due to the contact of the flowing carrier solution through the module fibers. The following attempt was the 0.2 M K-phosphate pH 7.5 (**Figure 3.80**) using custom HFMM based on PP fibers (10 short fibers). The result showed the same problem of limited linearity once more.

Hence, a decision was made to replace the 0.2 M KBr – lower linearity- with 0.2 M K-phosphate buffer pH 6.5 with applied potential of 0.24 V (vs. SCE) as optimum conditions to carry on the characterization of the proposed SO_2 analyzer.

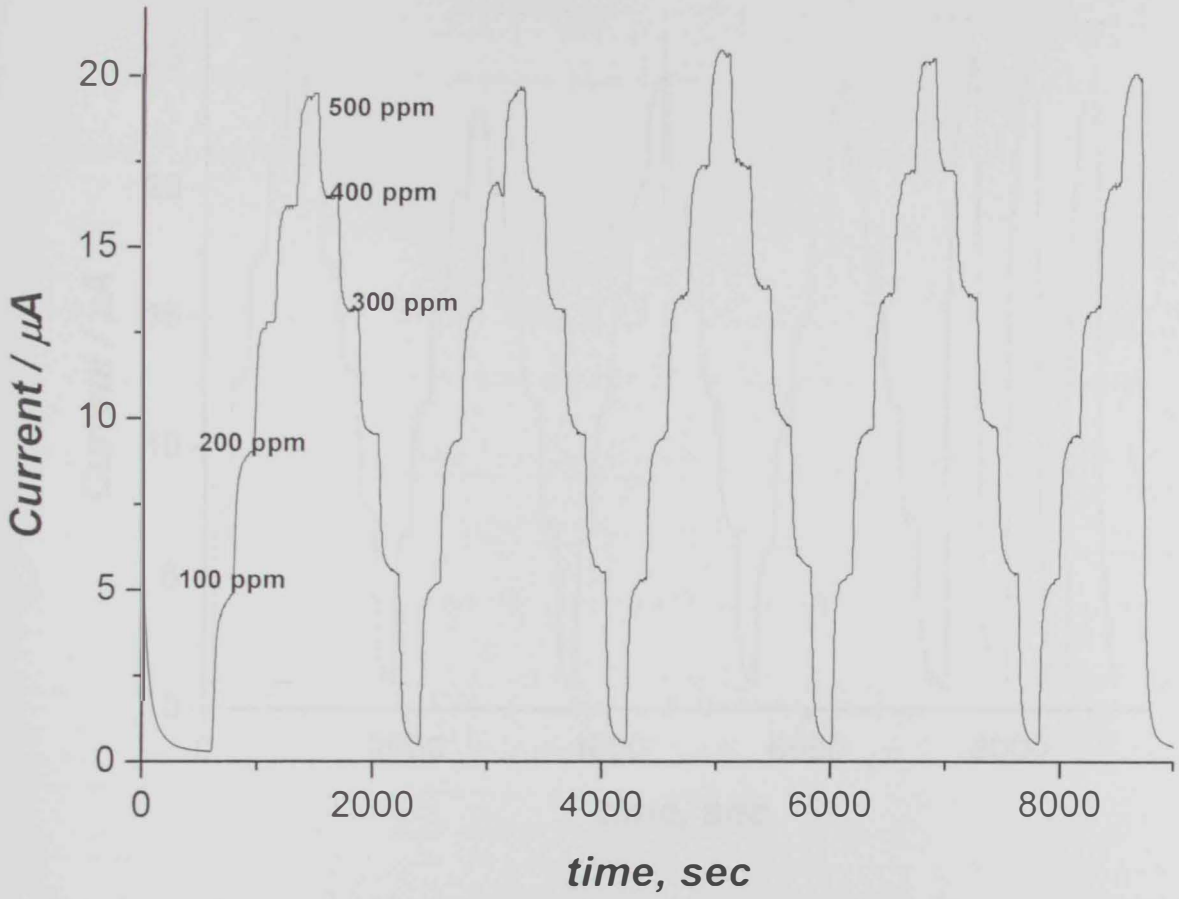

Figure 3.79: Real time response shows the linearity and calibration of the analyzer to different SO_2 level concentration (TTF-TCNQ : Silicone oil = 1:1.25 – 12 mm dia.), 0.2 M K-phosphate buffer pH 6.5, carrier flow rate: 3.7 mL/min, applied potential 0.24 V (vs. SCE).

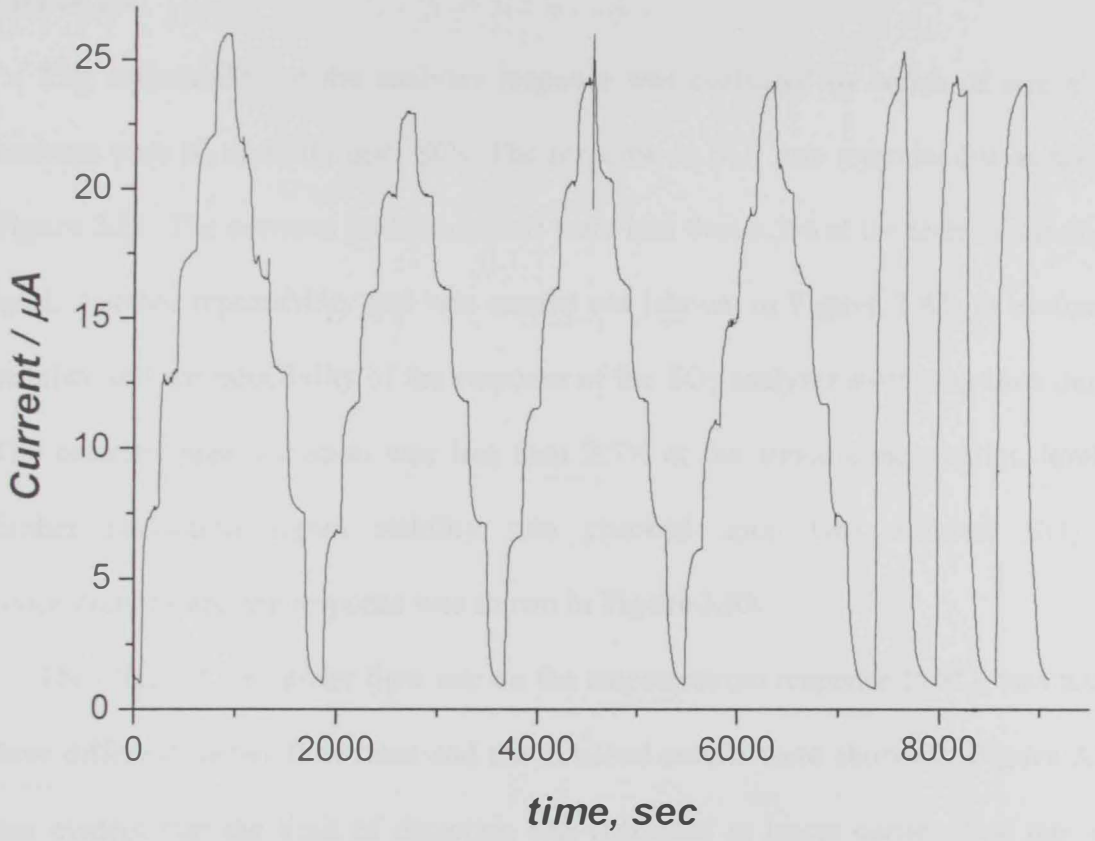

Figure 3.80: Real response time for the SO_2 analyzer, 0.2 M K-phosphate pH 7.5, at TTF-TCNQ/silicone oil ratio of 1:1.25. Using custom HFMM based on PP fibers. Each SO_2 increment represents 100 ppm in N_2, applied potential 0.24 V (vs. SCE).

3.4.6. Characterization of the SO_2 analyzer based on amperometric detector

According to the findings of the previous section the SO_2 analyzer was constructed as shown in Figure 2.2. It was equipped with a commercial cross flow HFMM containing 2500 PP fibers. The electrode (12 mm dia) was based on TTF-TCNQ with silicone oil paste at the ratio of (1:1.25, respectively) and installed in a flow through cell as shown in **Figure 2.4**.

The repeatability of the analyzer response was evaluated by series of step changes between pure N_2 and 500 ppm SO_2. The response to SO_2 was reproducible as shown in **Figure 3.81**. The between peak variations were less than 6.3% at the tested concentration level. Another repeatability test was carried out (shown in **Figure 3.82**) to evaluate the stability and reproducibility of the response of the SO_2 analyzer over long time duration. The between peak variation was less than 2.5% at the tested concentration level. For further evaluation signal stability was checked upon two different SO_2 level concentrations and the response was shown in **Figure 3.83.**

The effect of the carrier flow rate on the amperometric response to SO_2 was tested at three different carrier flow rates and the obtained results were shown in **Figure 3.84**. It was evident that the limit of detection was enhanced at lower carrier flow rate which could be attributed to the slower carrier flow passing through the HFMM and hence absorbing larger amount of SO_2.

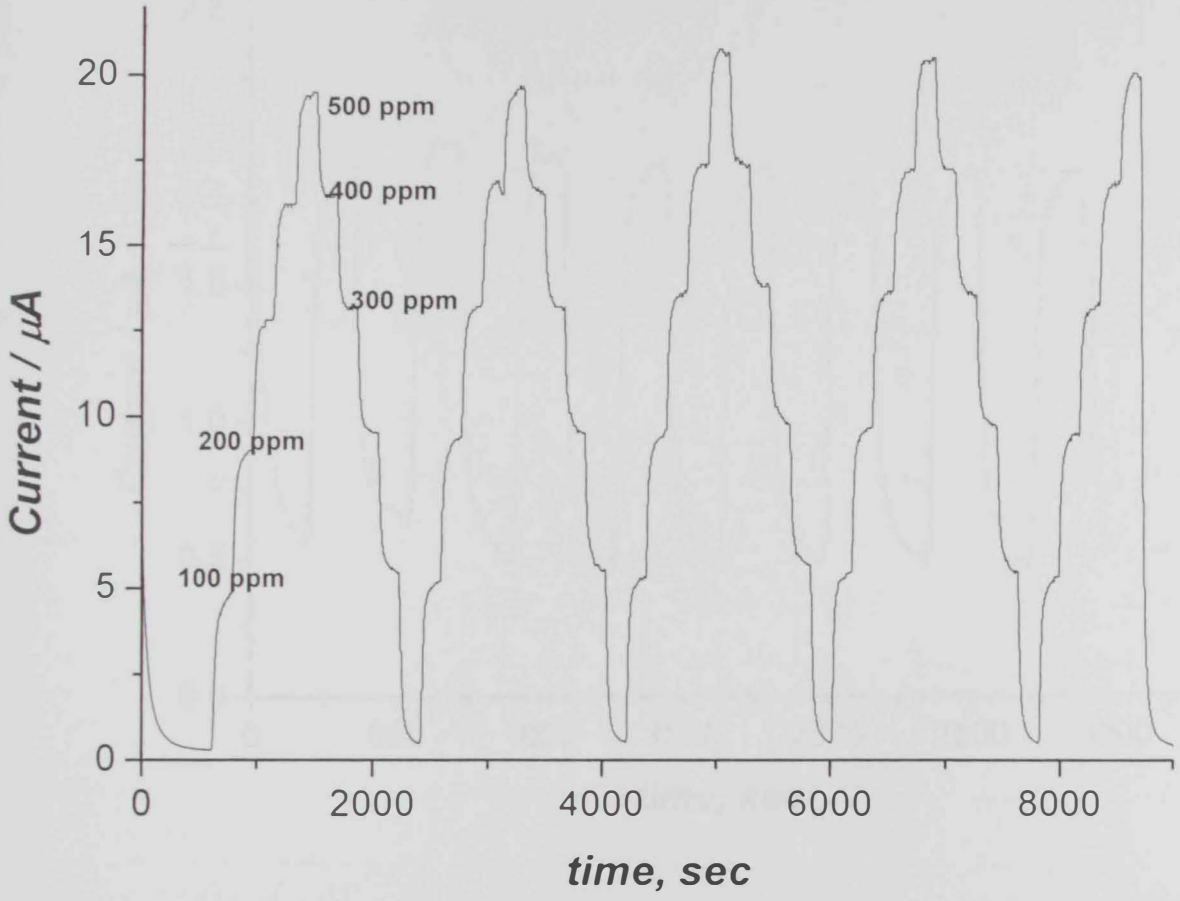

Figure 3.81: Real time response shows the linearity and reproducibility of the analyzer to different SO_2 level concentration (TTF-TCNQ:Silicone oil = 1:1.25 – 12 mm dia.), 0.2 M K-phosphate buffer pH 6.5, carrier flow rate: 3.7 mL/min, applied potential 0.24 V (vs. SCE).

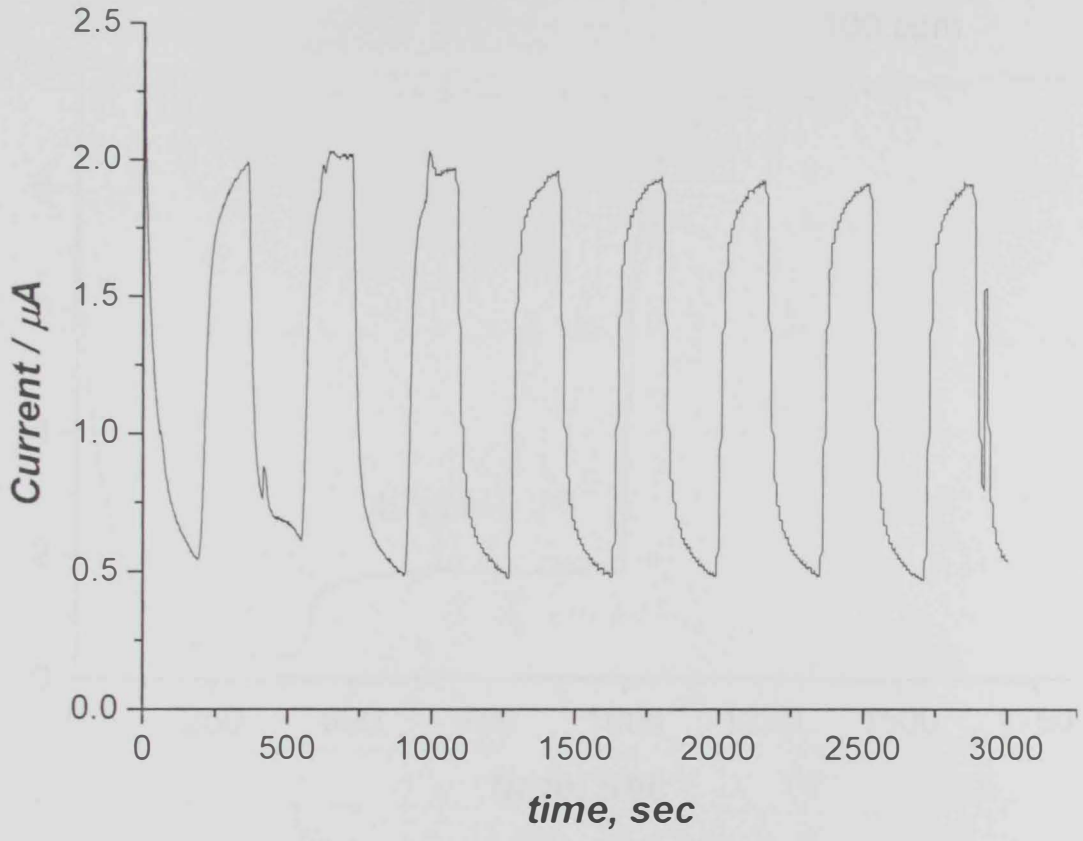

Figure 3.82: Reproducibility test for the SO_2 analyzer, at concentration level of 10 ppm of SO_2, carrier flow rate: 1.0 mL/min, (TTF-TCNQ:Silicone oil = 1:1.25 – 12 mm dia.), 0.2 M K-phosphate buffer pH 6.5, applied potential 0.24 V (vs. SCE).

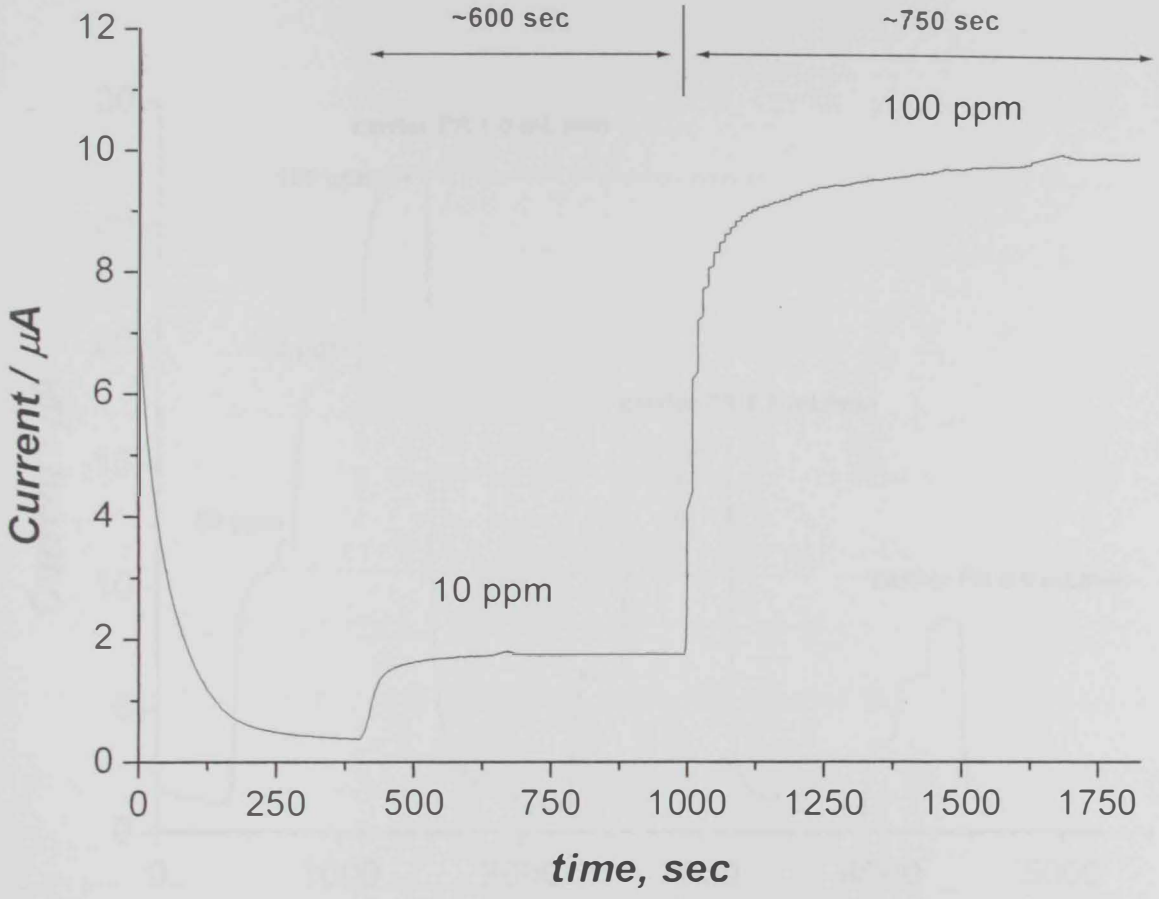

Figure 3.83: Signal stability test, carrier flow rate: 5 mL/min, using the cross flow module, (TTF-TCNQ:Silicone oil = 1:1.25 – 12 mm dia.), 0.2 M K-phosphate buffer pH 6.5, applied potential 0.24 V (vs. SCE).

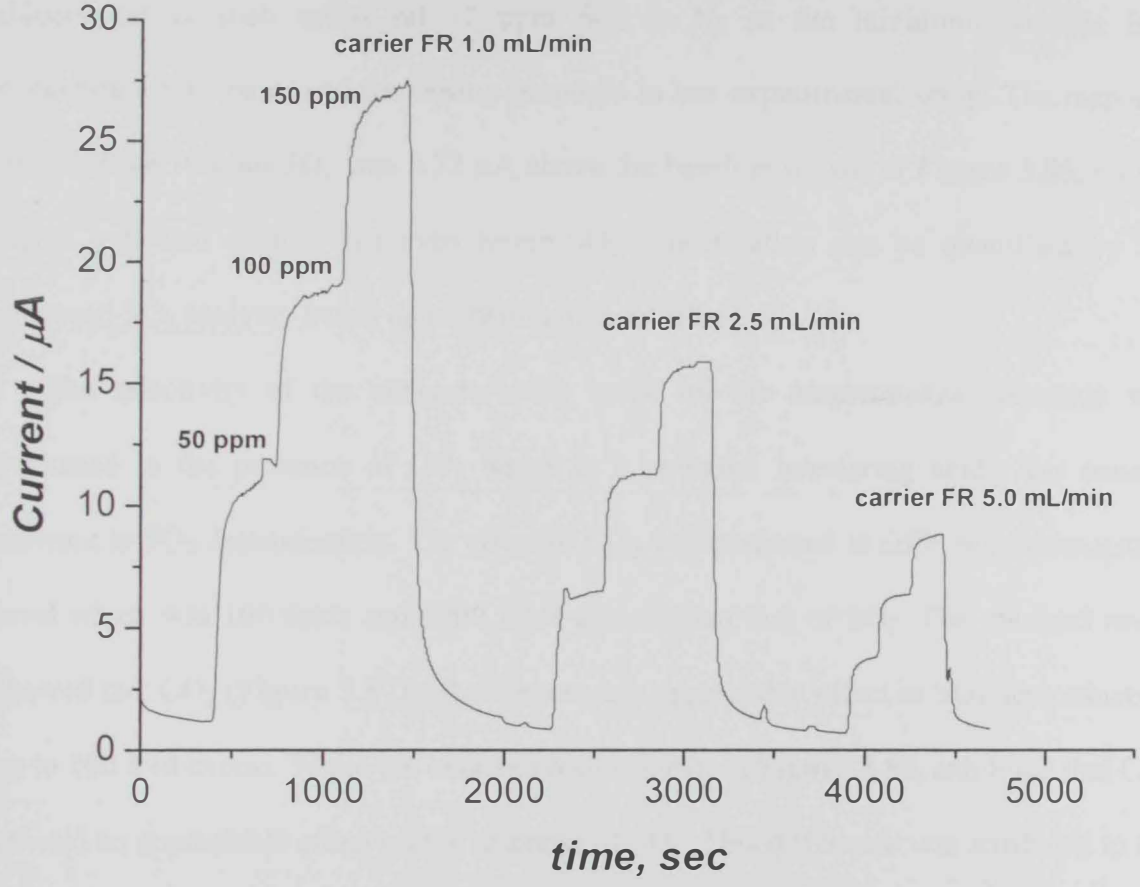

Figure 3.84: Effect of carrier flow rate on the proposed SO_2 analyzer, (TTF-TCNQ:Silicone oil = 1:1.25 – 12 mm dia.), 0.2 M K-phosphate buffer pH 6.5, applied potential 0.24 V (vs. SCE).

The calibration curve based on multi-step increments in SO_2 concentration was shown in **Figure 3.85**. The calibration graph exhibited a linear response up to the tested level of 500 ppm SO_2. To determine the lower limit of detection the diluent gas (N_2) was set to 1000 mL/min and the flow of the SO_2 standard gas was set to the minimum value possible by its MFC, i.e., 1 mL/min. Mixing of the SO_2 gas standard (10,000 ppm in N_2) with N_2 diluent gas in such ratios set 10 ppm SO_2 in N_2 as the minimum possible SO_2 concentration to be mixed for testing purposes in our experimental setup. The response obtained for 10 ppm SO_2 was 5.72 μA above the baseline shown in **Figure 3.86**, such a signal indicated clearly that even lower SO_2 concentration can be quantified by the proposed SO_2 analyzer based on amperometric detection.

The selectivity of the analyzer setup based on the amperometric detection was evaluated in the presence of CO_2 which is a potential interfering acidic gas usually relevant to SO_2 determination. The effect of CO_2 was evaluated at different concentration level which was 100 folds and 3900 folds greater than that of SO_2. The obtained result showed that CO_2 (**Figure 3.87**) did not cause any appreciable effect in SO_2 determination up to 100 fold excess. While the obtained result shown in **Figure 3.88**, exhibited that CO_2 exerted an appreciable effect on the response of SO_2. This difference was attributed to the slight change in the acidity of the carrier solution caused by the large concentration of CO_2 (975,000 ppm) passes through the module per unit time and hence decreases the oxidizability of the sulfite at TTF-TCNQ electrode at the fixed applied potential selected for carrier of pH 6.5.

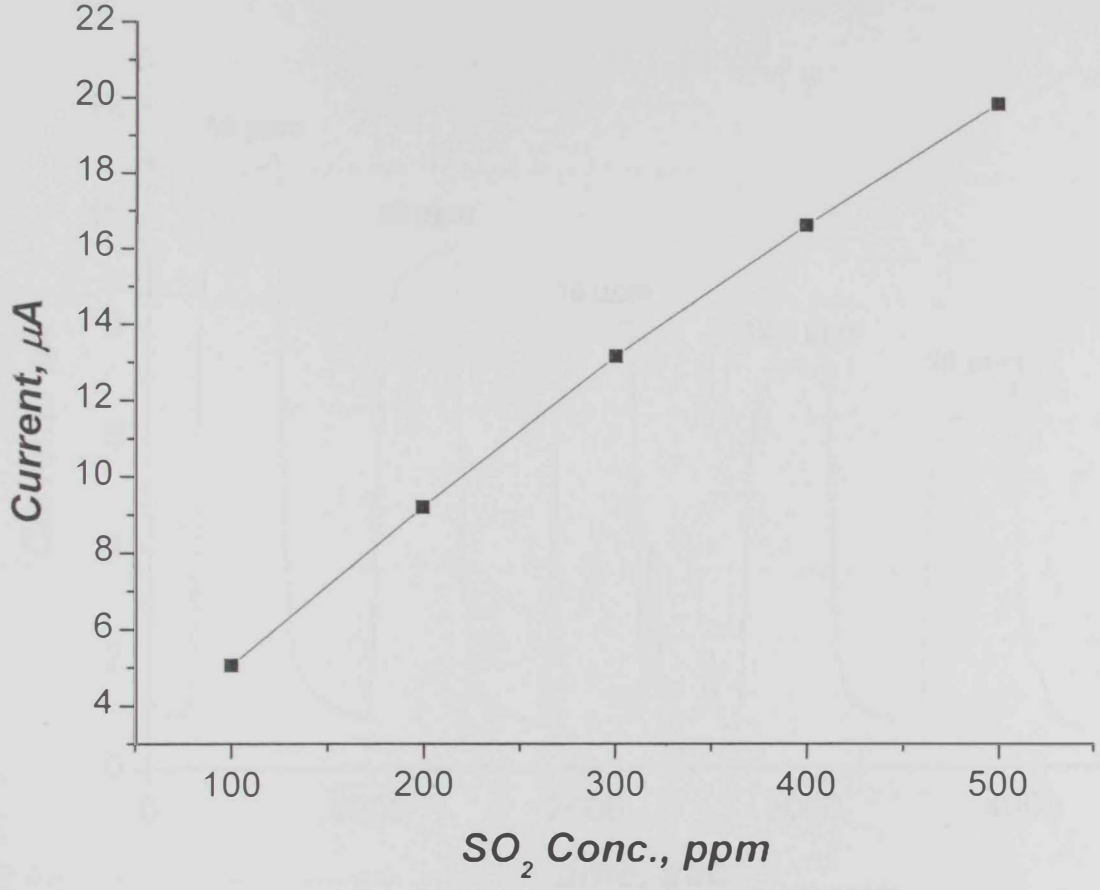

Figure 3.85: Calibration curve based on multi-step increments in SO_2 concentrations, (TTF-TCNQ:Silicone oil = 1:1.25 – 12 mm dia.), 0.2 M K-phosphate buffer pH 6.5, carrier flow rate: 3.7 mL/min, applied potential 0.24 V (vs. SCE).

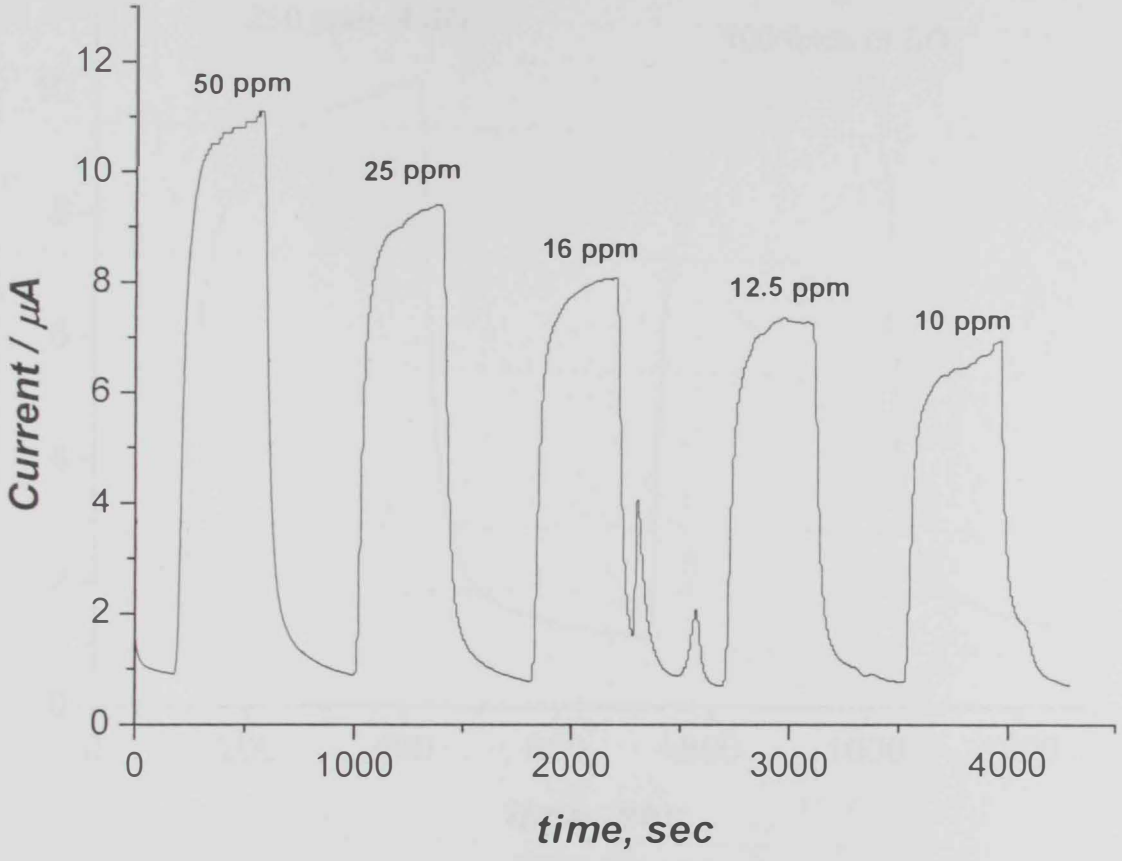

Figure 3.86: Sensitivity test for different SO_2 level concentrations, using the cross flow module. (TTF-TCNQ:Silicone oil = 1:1.25 – 12 mm dia.), 0.2 M K-phosphate buffer pH 6.5, carrier flow rate: 1.0 mL/min, applied potential 0.24 V (vs. SCE).

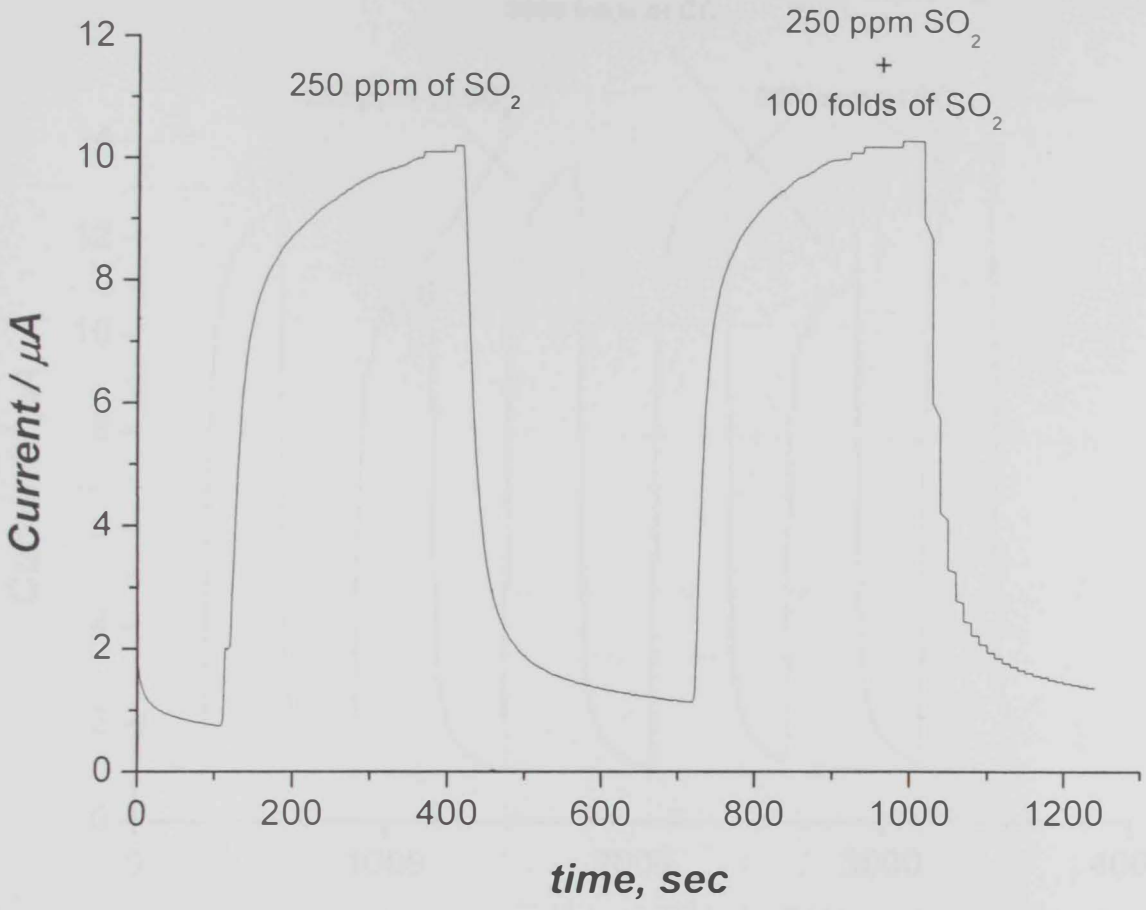

Figure 3.87: Real time response shows the selectivity of the proposed SO_2 analyzer in the presence of CO_2, (TTF-TCNQ:Silicone oil = 1:1.25 – 12 mm dia.), 0.2 M K-phosphate buffer pH 6.5, carrier flow rate: 5 mL/min, applied potential 0.24 V (vs. SCE).

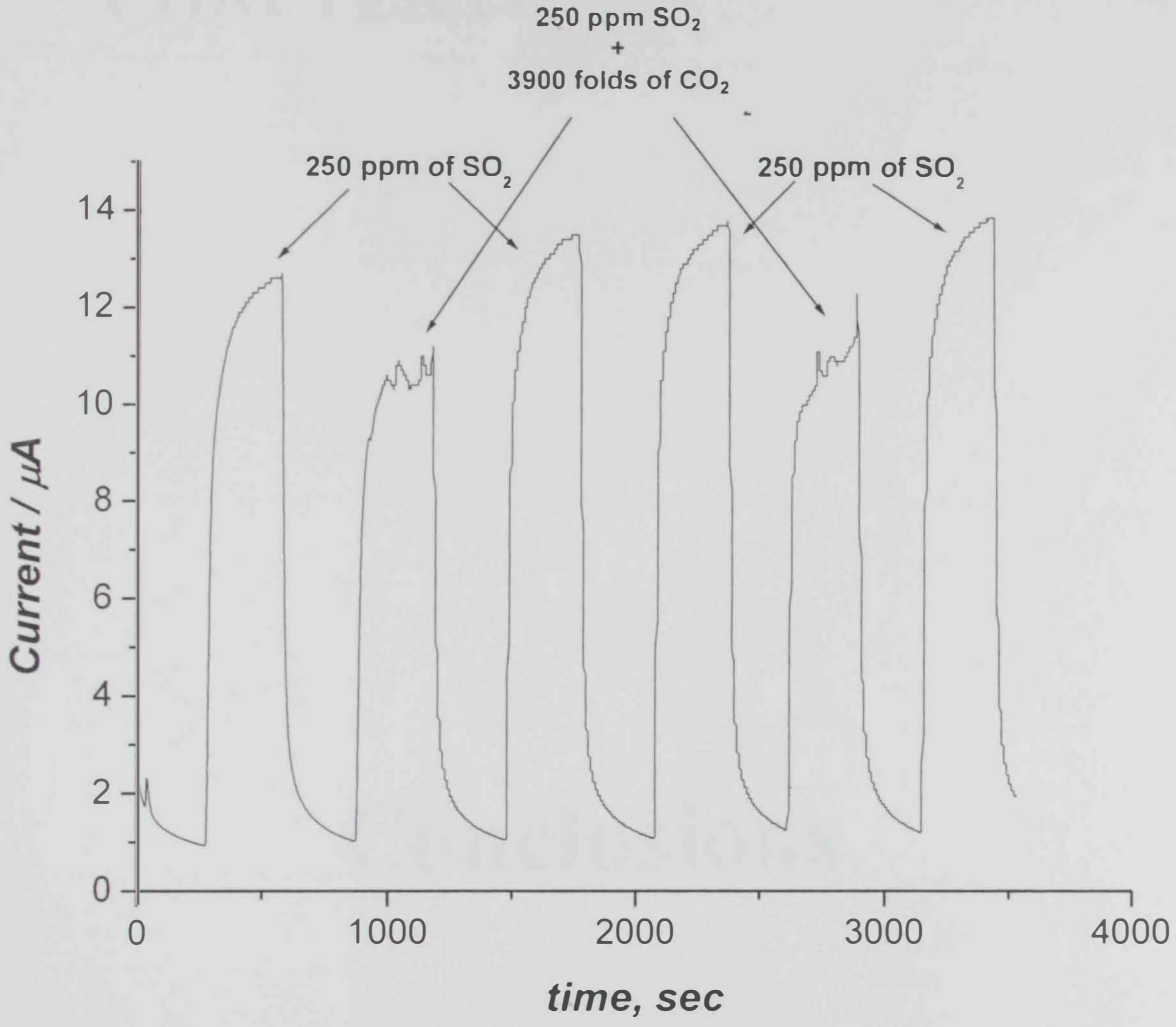

Figure 3.88: Tough selectivity test carried with 2 days old electrode in constant contact with buffer, using cross flow module, (TTF-TCNQ:Silicone oil = 1:1.25 – 12 mm dia.), 0.2 M K-phosphate buffer pH 6.5, carrier flow rate: 5 mL/min, applied potential 0.24 V (vs. SCE).

CHAPTER IV

Conclusions

4.1 Conclusions from the developed analyzer

i) The proposed analyzer setup was proved successfully for the continuous monitoring of SO_2 in gas streams.

ii) All the attempted detectors proved suitable and reliable for constructing SO_2 analyzer.

iii) The specifically developed and characterized TTF-TCNQ electrode provided the best amperometric response for sulfite determination.

iv) Comparison between the characteristics obtained with different detectors was given in Table 4.1.

v) The membrane modules based on PP were used extensively for at least 6 months without the need for either regeneration or replacement.

vi) - For industrial gas streams which contain particulates , an in line gas filter is recommended to avoid the possible fouling of the membrane module.

vii)- Since the analyzer response based on different detectors is sensitive to the gas flow rate, a mean for providing a fixed flow rate to the analyzer such as an in line flow restrictor or MFC is essential to obtain reliable quantitative measurements.

4.2 Environmental impact:

Several impacts can be drawn from the described SO_2 analyzer as follow:

i) The SO_2 analyzer can be used in monitoring of SO_2 removal in the industrial processes.

ii) The developed analyzer can be utilized in the determination of SO_2 preservative in food products using a setup similar to that shown in **Figure 4.1.**

iii) The advantages of the presented SO_2 analyzer suggest its further development into a portable analyzer used in the atmospheric monitoring of SO_2. The anticipated construction of the portable analyzer is shown in **Figure 4.2.**

Table 4.1: The optimum conditions and characteristics obtained by SO_2 analyzer based on different detectors.

	Potentiometric pH-detection	**Conductometric detection**	**Amperometric detection**
Carrier solution:	0.1 M potassium oxalate	1.0 mM hydrogen peroxide	0.2 M K-phosphate pH 6.5
Plot:	logarithmic	linear	linear
Detection limit:	<10 ppm	<16 ppm	<10 ppm
Linearity range:	Nernestian slope up to1000 ppm	Up to 2500 ppm	Up to 500 ppm
Selectivity:	CO_2: no interference up to 500 folds H_2S: no interference up to 5 folds	CO_2: no interference up to 100 folds H_2S: serious deleterious effect on the detector	CO_2: no interference up to 3900 folds H_2S: not measured
Major Advantages:	Very high linearity and sensitivity	Very high linearity and sensitivity	The ability to oxidize the SO_2 on the surface of TTF-TCNQ without modification. High selectivity to presence of CO_2. Long term stability. Easy to prepare the electrode. Novel detector.
Limitations:	Not suitable to work in high temperatures	Not suitable to work with stream gases that contain H_2S gas	Low linearity
Waste	Oxalate require simple treatment	No treatment required	No treatment required
Cost	low	low	low

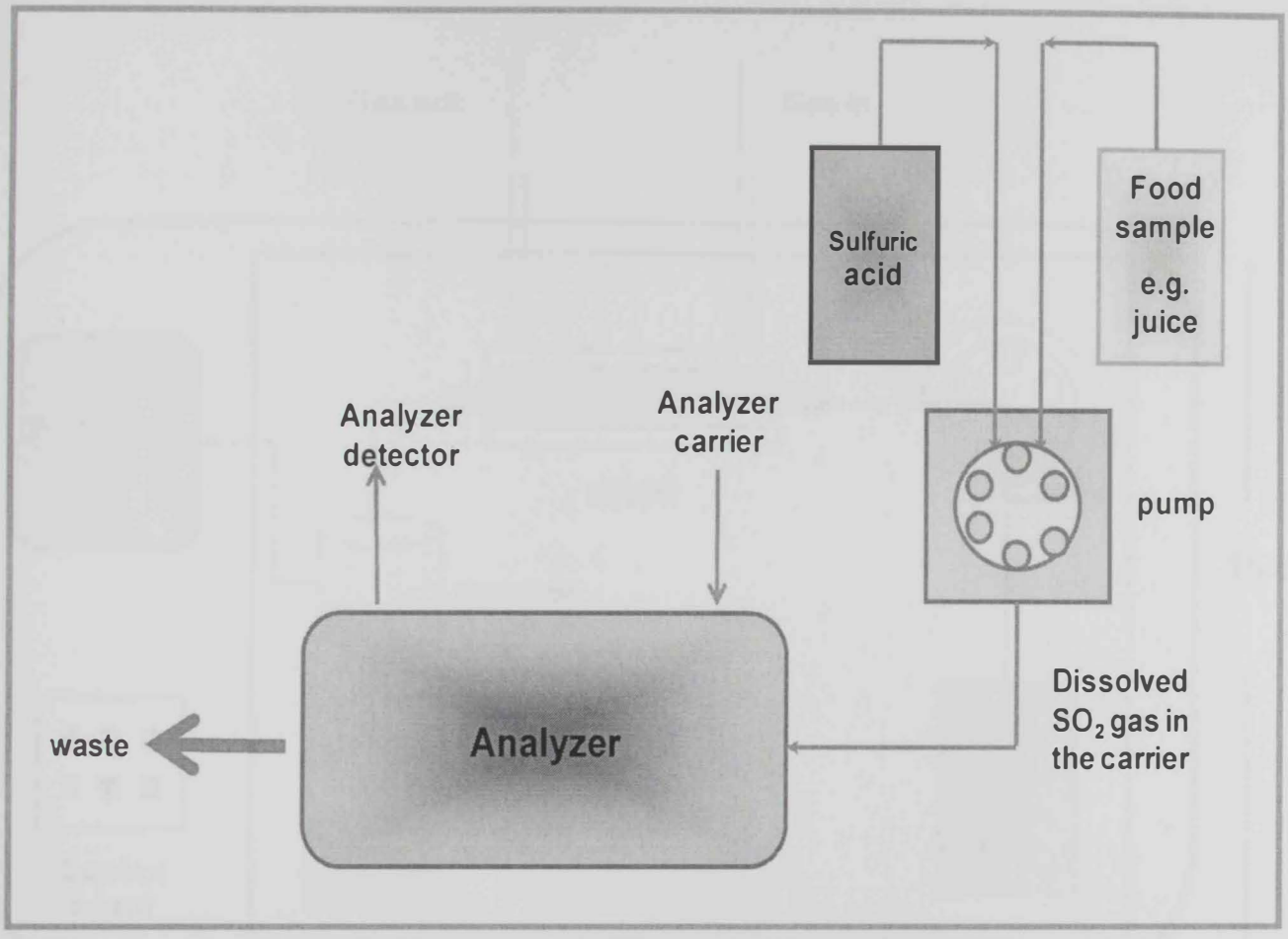

Figure 4.1: Analyzer setup used for determination of SO_2 preservatives in food.

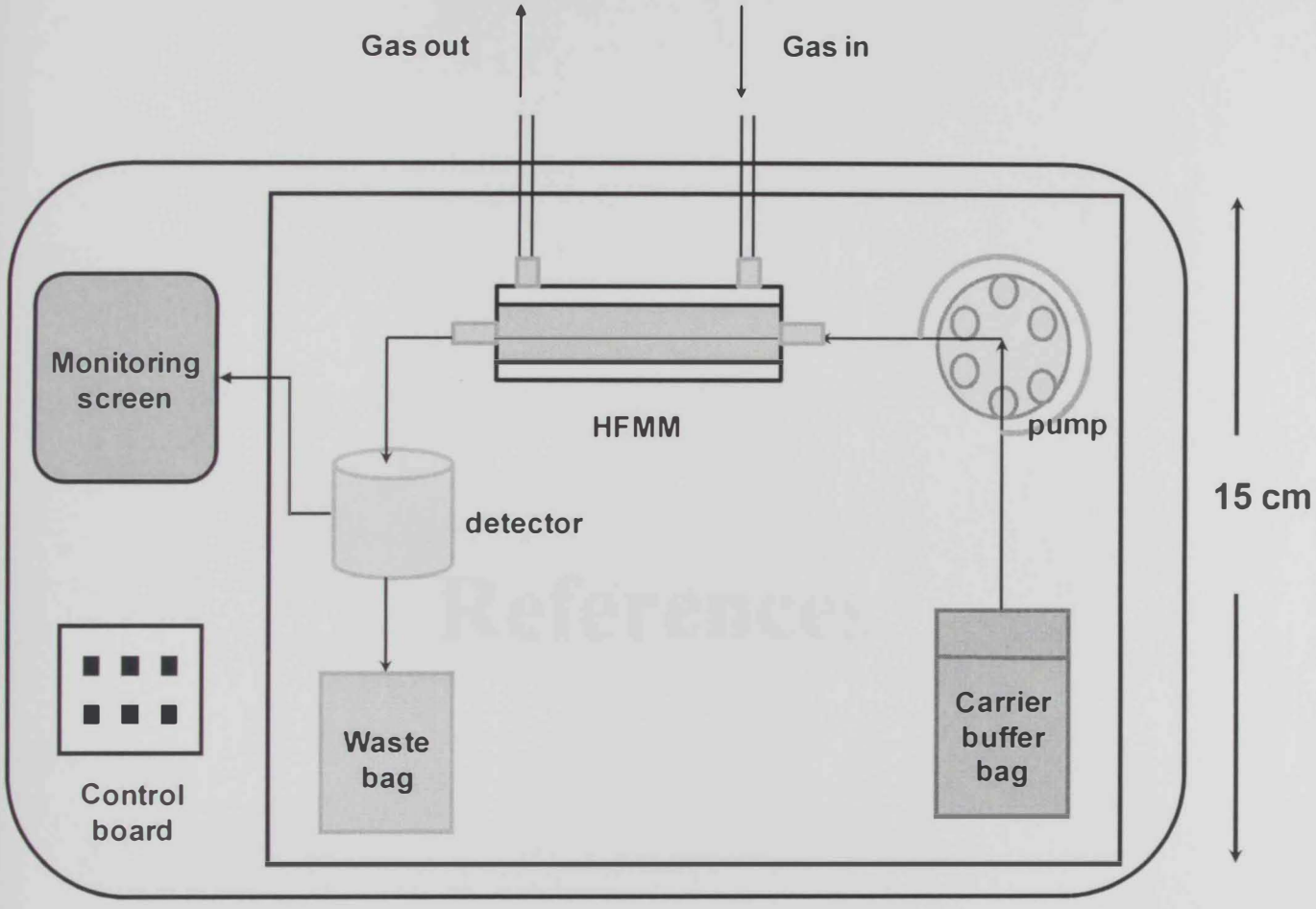

Figure 4.2: Construction of the portable analyzer.

CHAPTER V

References

References

[1]. Greenwood, Norman N.; Earnshaw, A. (1997), Chemistry of the Elements. 2nd ed. Oxford: Butterworth-Heinemann; 1997. p. 700.

[2]. Fl´avia L. Alves, Ivo M. Raimundo Jr., Iara F. Gimenez, Oswaldo L. Alves. An organopalladium-PVC membrane for sulfur dioxide optical sensing. *Sensors and Actuators B* 2005; 107: 47-52.

[3]. Hui Li, Qingjiang Wang, Jiming Xu, Wen Zhang, Litong Jin. A novel nano-Au-assembled amperometric SO_2 gas sensor: preparation, characterization and sensing behavior. *Sensors and Actuators B* 2002; 87: 18-24.

[4]. Wei Chang, Yasunari Ono, Momoko Kumemura, Takashi Korenaga. On-line determination of trace sulfur dioxide in air by integrated microchip coupled with fluorescence detection. *Talanta* 2005; 67: 646-650.

[5]. H. Vally, P.J. Thompson. Role of sulfite additives in wine induced asthma: single dose and accumulative dose studies. *Thorax* 2001; 56: 763-769.

[6]. M.R. Lester. Sulfite sensitivity: significance in human health. *Journal of the American College of Nutrition* 1995; 14: 229-232.

[7]. I. Beck-Speir, A.G. Lenz, J.J. Godleski, Response of human neutrophils to sulfite, *Journal of Toxicological and Environmental Health* 1994; 41: 285-297.

[8]. M. Pelletier, V. Lavastre, D. Girard. Activation of human epithelial lung A549 celss by the pollutant sodium sulfite: enhancement of neutrophil adhesion. *Toxicological Scences* 2002; 69: 210-216.

[9]. Anita Isaac, Callum Livingstone, Andrew J. Wain, Richard G. Compton, James Davis. Electroanalytical methods for the determination of sulfite in food and beverages. *Trends in Analytical Chemistry* 2006; 25: 589-599.

[10]. Guoyue Shi, Min Luo, Jian Xue, Yuezhong Xian, Litong Jin, Ji-Ye Jin. The study of PVP/Pd/IrO_2 modified sensor for amperometric determination of sulfur dioxide. *Talanta* 2001; 55: 241-247.

[11]. National Environment Protection Council (1998), National environment protection measure for the national pollutant inventory. December 1998 [cited 2009 Jan 8]. Available from: http://www.npi.gov.au/database/substance-info/profiles/77.html#common

[12]. C.F. Cullis, M.M. Hirschle. Atmospheric sulfur: Natural and man-made sources. *Atmospheric Environment* 1967; 14: 1263-1278.

[13]. M.M. Halmer, Geophysical research abstracts. 2006, Vol. 8, 03270.

[14]. Gregg Marland, Tom Boden, Bob Andres, University of North Dakota. SO_2 emissions per populated area (most recent) by country. Available from: http://www.nationmaster.com/graph/env_so2_emi_per_pop_are-so2-emissions-per-populated-area

[15]. B.R. Illery, E.R. Elkins, C.R. Warner, D. Daniels, T. Fazio, *Journal of AOAC International* 1989; 72: 470.

[16]. M. A. Joslyn. Sulfur dioxide content of wine I. Iodometric titration. *American Journal of Enology and Viticulture* 1955; 63: 1-10.

[17]. Z. Ning, Handbook for analysis of food ingredients, China Light Industry Press, Beijing (1998).

[18]. Amir Besada, Y. A. Gawargious, S. Y. Kareem. Micro and submicro iodometric determination of arsenite and sulphite ions by amplification reactions. *Talanta* 1976; 23: 392-394.

[19]. Bruce W. Zoecklein. Wine analysis and production, Germany: Springer Science & Business; 1994. Vol. 1. 189 p.

[20]. P. W. West, G. C. Gaeke. Fixation of sulfur dioxide as disulfitomercurate (ii) and subsequent colorimetric estimation. *Analytical Chemistry* 1956; 28: 1816-1819.

[21]. Yoshiko Arikawa, Takejiro Ozawa, Iwaji Iwasaki. An improved photometric method for the determination of sulfite with para-rosaniline and formaldehyde. 1968; 41: 1454-1456.

[22]. Purnendu K. Dasgupta, Kymron. DeCesare, James C. Ullrey. Determination of atmospheric sulfur dioxide without tetrachloromercurate(II) and the mechanism of the Schiff reaction. *Analytical Chemistry* 1980; 52: 1912-1922.

[23]. P. Richter, M. D. Luque de Castro, M. Valcárcel. Spectrophotometric flow-through sensor for the determination of sulfur dioxide. *Analytica Chimica Acta* 1993; 283: 408-413.

[24]. M. Kass, A. Ivaska. Spectrophotometric determination of sulfur dioxide and hydrogen sulfide in gas phase by sequential injection analysis technique. *Analytica Chimica Acta* 2001; 449: 189-197.

[25]. Yongjie Li, Meiping Zhao. Simple methods for rapid determination of sulfite in food products. *Food Control* 2006; 17: 975-980.

[26]. Ma´rcio Raimundo Milani, Jose´ Anchieta Gomes Neto, Arnaldo Alves Cardoso. Colorimetric determination of sulfur dioxide in air using a droplet collector of malachite green solution. *Microchemical Journal* 1999; 62: 273-281

[27]. K. Geetha, N. Balasubramanian. An indirect method for the determination of sulfur dioxide using Methyl Red. *Microchemical Journal* 2000; 65: 45-49.

[28]. Cameron Sadegh, Ronald P. Schreck. The spectroscopic determination of aqueous sulfite using ellman's reagent. *MIT Undergraduate Research Journal* 2003; 8: 39-43.

[29]. Parashar DC, Raman V, Singh M. Spectrophotometric determination of sulfur dioxide. *Environmental Pollution* 1987; 45: 125-132.

[30]. Ray E. Humphrey, George S. Ingram, Druce K. Crump. Spectrophotometric determination of sulfite with soluble mercury (II) compounds. *Microchemical Journal* 1982; 27: 351-356.

[31]. L.G. Decnop-Weever, J.C. Kraak. Determination of sulfite in wines by gas-diffusion flow injection analysis utilizing spectrophotometric pH-detection. *Analytica Chimica Acta* 1997; 337: 125-131.

[32]. A. Maquieira, F. Casamayor, R. Puchades. Determination of total and free sulfur dioxide in wine with a continuous-flow microdistillation system. *Analytica Chimica Acta* 1993; 283: 401-407.

[33]. E. Mataix, M. D. Luque de Castro. Sequential determination of total and volatile acidity in wines based on a flow injection-pervaporation approach. *Analytica Chimica Acta* 1999; 381: 23-28.

[34]. Purnendu K. Dasgupta, Vinay K. Gupta. Mambrane-based flow injection system for determination of sulfur (IV) in atmospheric water. *Environmental Science Technology* 1986; 20: 524-526.

[35]. A. Safavi, B. Haghighi. Flow injection analysis of sulphite by gas-phase molecular absorption UV/VIS spectrophotometry. *Talanta* 1997; 44: 1009- 1016.

[36]. Marcela A. Segundo, António O.S.S. Rangel. A gas diffusion sequential injection system for the determination of sulphur dioxide in wines. *Analytica Chimica Acta* 2001; 427: 279-286.

[37]. Taha M.A. Razek, Michael J. Miller, Saad S.M. Hassan, Mark A. Arnold. Optical sensor for sulfur dioxide based on fluorescence quenching. *Talanta* 1999; 50: 491-498.

[38]. Mana, H., Spohn, U. Sensitive and selective flow injection analysis of hydrogen sulfite/sulfur dioxide by fluorescence detection with and without membrane separation by gas diffusion. *Analytical Chemistry* 2001; 73: 3187-3192.

[39]. Dmitri Papkovsky, Marsha A. Uskova, Gelii V. Ponomarev, Timo Korpela, Sakari Kulmala, George G. Guilbault. Optical sensing of sulfite with a phosphorescent probe. *Analytica Chimica Acta* 1998; 374: 1-9.

[40]. Huang, Y. L., Kim, J. M., Schmid, R. D. Determination of sulfite in wine through flow-injection analysis based on the suppression of luminal chemiluminescence. *Analytica Chimica Acta* 1992; 266: 317-323.

[41]. Hui Meng, Fengwu Wu, Zhike He, Yun'e Zeng. Chemiluminescence determination of sulfite in sugar and sulfur dioxide in air using Tris(2,2%-bipyridyl)ruthenium(II)-permanganate system. *Talanta* 1999; 48: 571-577.

[42]. Innocenzo G. Casella, Rossella Marchese. Sulfite oxidation at a platinum glassy carbon electrode. Determination of sulfite by ion exclusion chromatography with amperometric detection. *Analytica Chimica Acta* 1995; 311: 199-210.

[43]. Makoto Nonomura, Toshiyuki Hobo. Simultaneous determination of sulfur oxides, nitrogen oxides and hydrogen chloride in flue gas by means of an automated ion chromatographic system. *Journal of Chromatography A* 1998; 804: 151-155.

[44]. Shin-Ichi Ohira, Kei Toda. Ion chromatographic measurement of sulfide, methanethiolate, sulfite and sulfate in aqueous and air samples. *Journal of Chromatography A* 2006; 1121: 280-284.

[45]. John Kenkel. Analytical Chemistry for Technicians: Second Edition. [monograph on the Internet]. CRC Press; 1994 [cited 2009 Mar 8] Available from: http://books.google.ae/books?id=sA_QpBimF7QC&printsec=frontcover#PPA429,M1

[46]. Benilda S. Ebarvia, Christina A. Binag, Fortunato Sevilla III. Surface and potentiometric properties of SO_2 sensor based on a hydrogel coated pH-FET. *Sensors and Actuators B* 2001; 76: 644-652.

[47]. Marshall G. B., Midgley D. Potentiometric determination of sulphite by use of mercury (I) chloride-mercury (II) sulphide electrodes in flow injection analysis and in air-gap electrodes. *Analyst* 1983; 108: 701-711.

[48]. R. S. Hutchins, P. Molina, M. Alajarín, A. Vidal , L. G. Bachas. Use of a Guanidinium Ionophore in a Hydrogen Sulfite-Selective Electrode. *Analytical Chemistry* 1994; 66: 3188-3192.

[49]. Ibrahim H. A. Badr, Mark E. Meyerhoff, Saad S. M. Hassan. Novel response mechanism and application of sulfite sensitive polymeric membrane electrode based on dithiocarbamate complexes of mercury (II). *Analytica Chimica Acta* 1995; 310: 211-221.

[50]. Saad S.M. Hassan, Sayed A. Marei, I.H. Badr, H.A. Arida. Flow injection analysis of sulfite ion with a potentiometric titanium phosphate–epoxy based membrane sensor. *Talanta* 2001; *54*: 773-782.

[51]. Hossam I. Al-Itawi, Hamdan Al-Ebaisat, Mazen Al-Garaleh. Simple method for simultaneous determination of carbonate, sulfite and hydroxide in solution. *Journal of Applied Sciences* 2007; 16: 2389-2392.

[52]. I. Gács, R. Ferraroli. Determination of nanomole amounts of sulphur dioxide in air by flow-injecton conductimetry with on-line preconcentration. *Analytica Chimica Acta* 1992; 269: 177-185.

[53]. Stan McLeod, David E. Davey. Rapid microstill determination of free and total sulfite in wine with conductimetric detection. *Analytica Chimica Acta* 2007; 600: 72-77.

[54]. Petr Kuban, Pavel Janos, Vlastimil Kuban. Gas diffusion-flow injection determination of free and total sulfur dioxide in wines by conductometry. *Collection of Czechoslovak Chemical Communications* 1998; 63: 770-782.

[55]. C.S. Tavares Arau´ jo, J. Lira de Carvalho, D. Ribeiro Mota, C.L. de Arau´ jo, N.M.M. Coelho. Determination of sulfite and acetic acid in foods by gas permeation flow injection analysis. *Food Chemistry* 2005; 92: 765-770.

[56]. H. Sid Kalal, M. Ghadiri, A.A. Miran Beigi, S.A. Seyed Sadjadi. Simultaneous determination of trace amounts of sulfite and thiosulfate in petroleum and its distillates by extraction and differential pulse polarography. *Analytica Chimica Acta* 2004; 502: 133-139.

[57]. Robert W. Garber, Claude E. Wilson. Determination of atmospheric sulfur dioxide by differential pulse polarography. *Analytical Chemistry* 1972; 44: 1357-1360.

[58]. Ümmihan T. Yilmaz, Güler Somer. Determination of trace sulfite by direct and indirect methods using differential pulse polarography. *Analytica Chimica Acta* 2007; 603: 30-35.

[59]. Guo Nan Chen, Jiang Sheng Liu, Jian Ping Duan, Hong Qing Chen. Coulometric detector based on porous carbon felt working electrode for flow injection analysis. *Talanta* 2000; 53: 651–660.

[60]. P. Westbroek, J. De Strycker, K. Van Uytfanghe, E. Temmerman. Electrochemical behaviour of sodium dithionite and sulfite at a gold electrode in alkaline solution. *Journal of electroanalyical chemistry* 2001; 516: 83-88.

[61]. Terence J. Cardwell, Melinda J. Christophersen. Determination of sulfur dioxide and ascorbic acid in beverages using a dual channel flow injection electrochemical detection system. *Analytica Chimica Acta* 2000; 416: 105-110.

[62]. E. Gasana, P. Westbroek, E. Temmerman, H. P Thun, P. Kiekens. A wall-jet disc electrode for simultaneous and continuous on-line measurement of sodium dithionite, sulfite and indigo concentrations by means of multistep chronoamperometry. *Analytica Chimica. Acta* 2003; 486: 73-83.

[63]. K. Scott, W.M. Taama. An investigation of anode materials in the anodic oxidation of sulfur dioxide in sulfuric acid solutions. *Electrochimica Acta* 1999; 44: 3421-3427.

[64]. Corbo, D., Bertotti, M. Use of a copper electrode in alkaline medium as an amperometric sensor for sulphite in a flow-through configuration. *Analytical and Bioanalytical Chemistry* 2002; 374: 416-420.

[65]. Arnold G. Fogg, Miguel A. Fernandez-Arciniega, Rosa M. Alonso. Oxidative amperometric flow injection determination of sulfite at an electrochemically pre-treated glassy carbon electrode. *Analyst* 1985; 110: 851-853.

[66]. Chakorn Chinvongamorn, Kulwadee Pinwattana, Narong Praphairaksit, Toshihiko Imato, Orawon Chailapakul. Amperometric determination of sulfite by gas diffusion- sequential injection with boron-doped diamond electrode. *Sensors* 2008; 8: 1846-1857.

[67]. M. B. Wygant, J.A. Statler, A. Henshall. Improvements in Amperometric Detection of Sulfite in Food Matrixes. *Journal of AOAC International* 1997; 80: 1374-1380.

[68]. R. A. Durst, A. J. Baumner, R. W. Murray, R. P. Buck, C. P. Andrieux. Chemically modified electrodes: recommended terminology and definitions. *Pure & Applied Chemistry* 1997; 69: 1317-1323.

[69]. Romina Carballo, Viviana Campo Dall'Orto, Alfredo Lo Balbo, Irene Rezzano. Determination of sulfite by flow injection analysis using a poly[Ni-(protoporphyrin IX)] chemically modified electrode. *Sensors and Actuators B* 2003; 88: 155-161.

[70]. M. H. Pournaghi-Azar, R. E. Sabzi. Electrocatalytic oxidation of sulfite on a cobalt pentacyanonitrosylferrate film modified glassy carbon electrode. *Electroanalysis* 2004; 16: 860-865.

[71]. M. Lucero, G. Ram´ırez, A. Riquelme, I. Azocar, M. Isaacs, F. Armijo, J.E. F¨orster, E. Trollund, M.J. Aguirre, D. Lexa. Electrocatalytic oxidation of sulfite at polymeric iron tetra (4-aminophenyl) porphyrin-modified electrode. *Journal of Molecular Catalysis A: Chemical* 2004; 221: 71-76.

[72]. M. H. Pournaghi-Azar, M. Hydarpour, H. Dastangoo. Voltammetric and amperometric determination of sulfite using an aluminum electrode modified by nickel pentacyanonitrosylferrate film Application to the analysis of some real samples. *Analytical Chimica Acta*, 2003; 497: 133-141.

[73]. Jahan Bakhsh Raoof, Reza Ojani, Hassan Karimi-Maleh. Electrocatalytic determination of sulfite at the surface of a new ferrocene derivative-modified carbon paste electrode. *International Journal of Electrochemical Science* 2007; 2: 257-269.

[74]. D. Ravi Shankaran, S. Sriman Narayanan. Chemically modified sensor for amperometric determination of sulfur dioxide. *Sensors and Actuators B* 1999; 55: 191-194.

[75]. R. Ojani, J.B. Raoof, A. Alinezhad. Catalytic Oxidation of Sulfite by Ferrocenemonocarboxylic Acid at the Glassy Carbon Electrode. Application to the Catalytic Determination of Sulfite in Real Sample. *Electroanalysis* 2002; 14: 1197-1202.

[76]. A. Salimi, S. Pourbeyrama, M.K. Amini. Renewable-surface sol-gel derived carbon ceramic electrode fabricated by [Ru(bpy)(tpy)Cl]PF6 and its application as an amperometric sensor for sulfide and sulfur oxoanions. *Analyst* 2002; 127: 1649-1656.

[77]. D.R. Shankaran, K.K. limura, T. Kato. Electrochemical sensor for sulfite and sulfur dioxide based on 3-aminopropyltrimethoxysilane derived sol-gel composite electrode. *Electroanalysis* 2004; 16: 556-562.

[78]. C.A. Groom, J.H.T. Luong, C. Masson. Development of a flow injection. analysis mediated biosensor for sulfite. *Journal of Biotechnology* 1993; 27; 117-127.

[79]. T. Yao, M. Satomura, T. Nakahara. Simultaneous determination of sulfite and phosphate in wine by means of immobilized enzyme reactions and amperometric detection in a flow-injection system. *Talanta* 1994; 41: 2113-2119.

[80]. Menzel C.; Lerch T.; Scheper T.; Schügerl K. Development of biosensors based on an electrolyte isolator semiconductor (EIS)-capacitor structure and their application for process monitoring. Part 1. Development of the biosensors and their characterisation. *Analytica Chimica Acta* 1995; 317: 259-264.

[81]. Manihar Situmorang, J. Justin Gooding, D. Brynn Hibbert. Immobilisation of enzyme throughout a polytyramine matrix: a versatile procedure for fabricating biosensors. *Analytica Chimica Acta* 1999; 394: 211-223.

[82]. A.K. Abass, J.P. Hart, D. Cowell. Development of an amperometric sulfite biosensor based on sulfite oxidase with cytochrome c, as electron acceptor, and a screen-printed transducer. *Sensors and Actuators B* 2000; 62: 148-153.

[83]. E. E. Ferapontova, T. Ruzgas, L. Gorton. Direct electron transfer of heme- and molybdopterin cofactor-containing chicken liver sulfite oxidase on alkanethiol-modified gold electrodes. *Analytical Chemistry* 2003; 75: 4841-4850.

[84]. Erhan Dinçkaya, Mustafa Kemal Sezgintürk, Erol Akyılmaz, F. Nil Ertaş. Sulfite determination using sulfite oxidase biosensor based glassy carbon electrode coated with thin mercury film. *Food Chemistry* 2007; 101: 1540-1544.

[85]. AF22M UV Fluorescent Sulfur Dioxide Analyzer. Environment S. A. http://www.environmental-expert.com/STSE_resulteach_product.aspx?cid=8255&idprofile=2734&idproduct=14354

[86]. Model 300 Single Gas Non-Dispersive Infrared NDIR Analyzer. VIG Industries - USA. http://www.vigindustries.com/m300.htm

[87]. Thermmo Scientific. Model 43C-TLE, SO_2 Analyzer http://www.thermo.com/com/cda/product/detail/1,1055,14396,00.html

[88]. Ling Wang, R.V. Kumar. A new SO_2 gas sensor based on an Mg^{2+} conducting solid electrolyte. *Journal of Electroanalytical Chemistry* 2003; 543: 109-114.

[89]. Beutler, H.O. A new enzymatic method for determination of sulfite in food. *Food Chemistry* 1984; 15: 157-164.

[90]. Karube, I., Sogabe, S., Matsunaga, T., Suzuki, S. Sulfite ion sensor with use of immobilized organelle. *European Journal of Applied Microbiology and Biotechnology* 1983; 17: 216-220.

[91]. Nakamura, K., Amano, Y., Nakayama, O. Determination of free sulfite in wine using a microbial sensor. *Appl. Microbiology and Biotechnology* 1989; 31: 351-354.

[92]. Douglas A. Skoog, F. James Holler, Timothy A. Nieman. Principles of instrumental analysis. 5th ed. USA: Thomson Learning Inc; 1998. 613p.

[93]. Frank A. Settle. Handbook of Instrumental Techniques for Analytical Chemistry. 1997. PrenticeHall, Inc. New Jersey.

[94]. William R. Lacourse. Pulsed electrochemical detection in high-performance liquid chromatography. John Wiley & Sons Inc. New York; 1997. 108 p.

[95]. Jing-Shan Do, Po-Jen Chen. Amperometric sensor array for NO_x, CO, O_2 and SO_2 detection. *Sensors and Actuators B* 2007; 122: 165-173.

[96]. Ren'e Knake, Patrick Jacquinot, Alexia W.E. Hodgson, Peter C. Hauser. Amperometric sensing in the gas-phase (review). *Analytica Chimica Acta* 2005; 549: 1-9.

[97]. Calvin D. Jaeger; Allen J. Bard. Electrochemical Behavior of Tetrathiafulvalene-Tetracyanoquinodimethane electrodes in aqueous media. *Journal of American chemical society* 1979; 101: 1691-1699.

[98]. Sayed A.M. Marzouk, Mohamed H. Al-Marzouqi. "Analyzer for CO_2 determination in gas streams", Japanese patent application number: 2007-299773.

[99]. Sayed A.M. Marzouk, Mohamed H. Al-Marzouqi. "Analyzer for H_2S determination in gas streams ", Unpublished work.

[100]. Olga V. Yagodina, Elena B. Nikolskaya. New potentiometric gas-gap sensor. *Analytica Chimica Acta* 1999; 385: 137-141.

[101].J.F. Currie, A. Essalik, J-C. Marusic. Micromachined thin film solid state electrochemical CO2, NO2 and SO_2 gas sensors. *Sensors and Actuators B* 1999; 59: 235-241.

[102].Saad S. M. Hassan; Mona A. Ahmed; Sayed A. M. Marzouk. Potentiometric Gas Sensor for the Selective Determination of Azides. *Analytical Chemistry* 1991; 63: 1547-1552.

[103].J.W.; Bradely, A.F. Severnghaus. *J. Appl. Physiol.* 1958; 13: 515.

[104].Marcel Mulder. Basic Principles of Membrane Technology, 2nd ed., Buston: Kluwer Academic Publsihers; 2003.

[105].Richard W. Baker. Membrane technology and Applications, 2nd ed., John Wiley & Sons (NJ); 2007.

[106].Pavel Kubáň and Peter C. Hauser. High-performance liquid chromatography with contactless conductivity detection for the determination of peptides and proteins using a monolithic capillary column. *Journal of Chromatography A* 2007; 1176: 185-191.

[107].L.R. Kuck, R.D. Godec, P. P. Kosenka, J.W. Birks, High-precision conductometric detector for the measurement for the measurement of atmospheric carbon dioxide, *Analytical Chemistry* 1998; 70: 4678-4682.

[108].Karl J. Umiker, Matthew J. Morra, I Francis Cheng. Aqueous sulfur species determination using differential pulse polarography. *Microchemical Journal* 2002; 73: 287-297.

[109].Guler Somer, Ali Kocak. Determination of Atmospheric Sulfur dioxide by Differential-Pulse polarography using Selenite. *Analyst* 1993; 118: 657-659.

[110].Jun Cheng, Petr Jandik, Xiaodong Liu, Christopher Pohl. Pulsed amperometric detection waveform with disposable thin-film platinum working electrodes in high performance liquid chromatography. *Journal of Electroanalytical Chemistry* 2007; 608: 117-124.

[111].M. Antonietta Baldo, Salvatore Daniele, Gian A. Mazzocchin. Voltammetry determination of free sulfur dioxide in wines, using platinum and gols disc microelectrodes. *Analyst* 1994; 119: 1239-1244.

[112].C. Quijada, A. Rodes, J. L. Vázquez, J. M. Pérez, A. Aldaz. Electrochemical behavior of aqueous SO_2 at Pt electrodes in acidic medium. A Voltammetric and in Situ Forier Transform IR Study. Part I Oxidation of SO_2 on Pt electrodes with sulfur-oxygen adsorbed species. *Journal of Electroanalytical Chemistry* 1995; 394: 217-227.

[113].T. Garcia, E. Casero, E. Lorenzo, F. Pariente. Electrochemical sensor for sulfite determination based on iron hexacyanoferrate film modified electrodes. *Sensors and Actuators B* 2005; 106: 803-809.

[114].C.M.N. Azevedo, K. Araki, H.E. Toma, L. Angnes. Determination of SO_2 in wines by gas diffusion FI analysis utilizing modified electrodes with electrostatically assembled films of tetraruthenated porphyrin, *Analytica Chimica Acta* 1999; 387: 175-180.

[115].Hong Zhou, WeiWei Yang, Changqing Sun. Amperometric sulfite sensor based on multiwalled carbon nanotubes/ferrocene-branched chitosan composite. *Talanta* 2008; 77: 366-371.

[116]. Abdollah Salimi, Mahmoud Roushani, Rahman Hallaj. Micromolar determination of sulfur oxoanions and sulfide at a renwable sol-gel carbon ceramic electrode modified with nickel powder. *Electrochimica Acta* 2006; 51: 1952-1959.

[117]. D. Ravi Shankaran, N. Uehera, T. Kato. Determination of sulfur dioxide based on a silver dispersed functional self-assembled electrochemical sensor. *Sensors and Actuators B* 2002; 87: 442--447

[118]. Tong Li, Zihua Yao, Liang Ding Development of an amperometric biosensor based on glucose oxidase immobilized through silica sol-gel film onto Prussian blue modified electrode. *Sensors and Actuators* 2004; 101: 155-160.

[119]. Maryann P. O'Halloran, Miloslav Pravda, George G. Guilbault. Prussian blue bulk modified screen printed electrodes for H_2O_2 detection and for biosensors. *Talanta* 2001; 55: 605-611.

[120]. Jian-Ding Qiu, Wen-Mei Zhou, Jin Guo, Rui Wang, Ru-Ping Liang. Amperometric sensor based on ferrocene-modified multiwalled carbon nanotube nanocomposites as electron mediator for the determination of glucose. *Analytical Biochemistry* 2009; 385: 264-269.

[121]. Gunasingham H.; Tan C-H, Aw T-C. Comparative study of first-, second- and third-generation amperometric glucose enzyme electrodes in continuous-flow analysis of undiluted whole blood. *Analytica Chimica Acta* 1990; 234: 321-330.

[122]. Almeida, Mulchandani, 1993. N.F. Almeida and A.K. Mulchandani, A mediated amperometric enzyme electrode using tetrathiafulvalene and L-glutamate oxidase for the determination of L-glutamic acid. *Analytica Chimica Acta* 1993; 282: 353-361.

[123].A. S. N. Murthy and Anita. Tetrathiafulvalene as a mediator for the electrocatalytic oxidation of L-ascorbic acid. *Biosensors & Bioekcrronics* 1996; 11: 191-193.

[124].Ashok Mulchandani, Amarjeet S. Bassi, Andrew Nguyen. Tetrathiafulvalene-mediated Biosensor for L-lactate in Dairy Products. *Journal of Food Science* 2006; 60: 74-78.

[125].P. Abu Nader, S. Sagrado Vives, Horacio A. Mottola. Studies with a sulfite oxidase-modified carbon paste electrode for detection/determination of sulfite ion and SO_2(g) in continuous –flow system. *Journal of Electroanalytical chemistry* 1990; 284: 323-333.

[126].J.P. Hart, A.K. Abass. A disposable amperometric gas sensor for sulfur-containing compounds based on a chemically modified screen printed carbon electrode coated with a hydrogel. *Analytica Chimica Acta* 1997; 342: 199-206.

[127].W. John Albery, Philip N. Bartlett, Derek H. Craston. Amperometric enzyme electrode. Part II: Conducting salts as electrode materials for oxidation of glucose oxidase. *Journal of Electroanalytical Chemistry* 1985; 194: 223-235.

[128].Martyn G. Boutelle, Clare Stanford, Marianne Fillenz, W. John Albery, Phillip N. Bartlett. An amperometric enzyme electrode for monitoring brain glucose in the freely moving rat. *Neuroscience Letters*; 1986; 72: 283-288.

[129].W. John Albery, Philip N. Bartlett; Mark Bycroft, Derek H. Craston. Amperometric enzyme electrode. Part III: A conducting salt electrode for the oxidation of four different flavoenzymes. *Journal of Electroanalytical Chemistry* 1987; 218: 119-126.

[130]. Ulrich Korell, Ursula E. Spichiger. Novel membraneless amperometric peroxide biosensor based on a tetrathiafulvalene–*p*-tetracyanoquinodimethane electrode. *Analytical Chemistry* 1994; 66: 510-515.

أكسيد الكبريت) وتأثير غاز كبريتيد الهيدروجين (٥ أضعاف غاز ثاني أكسيد الكبريت) فلوحظ أنه لا يوجد لهما تأثير على استجابة المجس الغازي لثاني أكسيد الكبريت.

النوع الثاني من الكواشف التي تم فحصها هو كاشف التوصيل الكهربائي الذي يعمل بأعلى كفاءة عند استخدام ١ميللي مول / لتر من محلول فوق أكسيد الهيدروجين بمعدل سريان يكافئ ٢،٠ مل / دقيقة، والسريان الغازي يساوي ٢٠٠ مل /دقيقة، وباستخدام وحدة ألياف بوليمرية مثقبة تحتوي على ألياف البولي بروبيلين وكاشف التوصيل الكهربائي التجاري.

وعليه فإن استجابة الكاشف تسلك سلوكا خطيا تبعاً لتغير نسبة غاز ثاني أكسيد الكبريت حتى ٢٥٠٠ (ج ف م)، وأصغر تركيز يمكن قياسه هو ١٦ (ج ف م) أو أقل من ثاني أكسيد الكبريت في النيتروجين، وقُدر زمن عودة الاستجابة من ١١٥-١٨٠ ثانية، كما أنه تم إثبات عدم تأثر استجابة المجس حتى ١٠٠ ضعف من ثاني أكسيد الكربون. ووفق هذه المعطيات تم استخدام هذا الكاشف بنجاح في إجراء تطبيق عملي لتتبع عملية نزع غاز ثاني أكسيد الكبريت من تيار غازي.

أما الكاشف الثالث الذي تم اختباره في هذا المشروع والذي يعتبر انجاز إضافي هام في هذا البحث، فهو كاشف التيار الكهربائي الذي يوظف أقطاب مصنوعة من الأملاح العضوية الموصلة للتيار الكهربائي مثل مركب تتراثيا فُلفالين-تتراسيانوكوينودايميثين (TTF-TCNQ complex) وتمت أكسدة أيونات الكبريتيت على سطح هذا القطب مباشرة دون الحاجة إلى تعديله باستخدام الوسائل البيولوجية مثل الأنزيمات ويمكن الحصول على أعلى كفاءة لهذا الكاشف في تقدير غاز ثاني أكسيد الكبريت عند استخدام ٠،٢ مول / لتر من محلول فوسفات البوتاسيوم و الرقم الهيدروجيني يساوي ٦،٥ كمحلول حامل بمعدل سريان ١،٠ مل / دقيقة وباستخدام وحدة الألياف البوليمرية التي تحتوي على ألياف البولي بروبيلين. بتطبيق فرق جهد قدره ٠،٢٤ فولت بالنسبة للقطب المرجعي SCE و قد كان قطر سطح القطب يساوي ١٢ مم ومصنوع من عجينة TTF-CNQ وزيت السيليكون بنسبة (١ : ١،٢٥). يعكس هذا الكاشف سلوكا خطيا لتغير تركيز غاز ثاني أكسيد الكبريت حتى ٥٠٠ (ج ف م) و أقل تركيز يمكن قياسه يساوي ١٠ (ج ف م) من ثاني أكسيد الكبريت في النيتروجين، و يمكنه مقاومة تأثير غاز ثاني أكسيد الكربون حتى ٥٠٠ ضعف من غاز ثاني أكسيد الكبريت.

و بالتالي فإن مزايا المجس الغازي الذي تم تطويره متعددة وتشمل: (١) إمكانية ضبط خصائص المحلل الغازي بحسب الحاجة لاستخدامه للحصول على أعلى حساسية أو أعلى سلوك خطي أو أعلى حساسية (٢)انخفاض تكلفة التصنيع و التشغيل، (٣) إمكانية التخلص من المخلفات الناتجة عنه بسهولة بدون الحاجة إلى معالجة، (٤) له خصائص وظيفية عالية مثل سرعة الاستجابة و ثبات الإشارة، (٥) إمكانية تصنيعه (بأحجام صغيرة و تكلفة منخفضة) و تسويقه لاستخدامه في الأغراض التحليلية في المجالات البيئية و الصناعية.

الملخص

غاز ثاني أكسيد الكبريت هو غاز شفاف ذو كثافة عالية وذوبانية مرتفعة في الماء ورائحته الخانقة. ينتج غاز ثاني أكسيد الكبريت عن النشاطات البركانية ويعتبر أحد الملوثات الرئيسية في الهواء الجوي التي تسبب ظاهرة الأمطار الحمضية. كما له تأثير ضار على صحة الإنسان في حال تعرضه لكميات كبيرة منه. ومن هنا تأتي أهمية استحداث طرق تحليلية لتقدير نسبة غاز ثاني أكسيد الكبريت في التيارات الغازية.

الهدف الرئيسي لهذا البحث العملي هو تطوير مجس غازي للتقدير الكمي لغاز ثاني أكسيد الكبريت في تيارات الغازات. ويعتمد عمل هذا المجس على وحدة لفصل الغاز بخاصية الانتشار (وحدة الألياف البوليمرية المثقبة، Hollow fiber membrane module) كمرحلة أولية لفصل الغاز من مجموعة من الغازات والذي يتم عن طريق الالتقاء بين غاز ثاني أكسيد الكبريت ومحلول سريان يتم اختياره، حيث يذوب الغاز بعد فصله في هذا المحلول محدثا تغيرات في طبيعة المحلول الحامل.

ويمكن قياس هذه التغيرات باستخدام كواشف متخصصة توضع في مسار تدفق المحلول الحامل فتنتج إشارة تحليلية تستخدم للتقدير الكمي لغاز ثاني أكسيد الكبريت في تيار الغاز، وتقتصر الكواشف المستخدمة في هذا البحث على الكواشف التي تعمل بالطرق الكهروكيميائية لأنها تتميز عن غيرها بالبساطة، عدم الحاجة إلى تعديل طبيعة العينة قبل تقديرها. ونظرا للخصائص الكيميائية لثاني أكسيد الكبريت فإنه تم استخدام كواشف ذات أهمية عالية مثل كشاف الأس الهيدروجيني، كشاف التوصيل الكهربائي، وكشاف التيار الكهربائي في تطوير المجس الغازي لتقدير نسبة ثاني أكسيد الكبريت.

أول الكواشف التي تم اختبارها في هذا البحث كان كاشف الأس الهيدروجيني والذي يعمل بأعلى كفاءة تحت الظروف المثالية الآتية: استخدام ٠،١ مول / لتر من محلول أوكسالات البوتاسيوم بمعدل سريان يعادل ١،٥ مل / دقيقة، ومعدل سريان الغاز يساوي ٢٥٠ مل / دقيقة بالإضافة إلى استخدام قطب قياس الأس الهيدروجيني ذو القاعدة المستوية ووحدة ألياف بوليمرية مثقبة تحتوي على ألياف البولي بروبيلين. وتحت هذه الظروف المثالية فإن الكاشف يسلك سلوكا خطيا بحسب معادلة نرنست حتى تركيز ١٠٠٠ (جزء في المليون) من ثاني أكسيد الكبريت.

أقل تركيز يمكن قياسه هو أقل من ١٠ (ج ف م)، وله زمن استجابه يقدر من ٢٠ إلى ٢٠٠ ثانية وزمن عودة الاستجابة يقدر بحوالي ٦٠٠ ثانية. وتمت دراسة تأثير غاز ثاني أكسيد الكربون (بمعدل ٥٠٠ ضعف بالنسبة لغاز ثاني

جامعة الإمارات العربية المتحدة
عمادة الدراسات العليا
برنامج ماجستير علوم البيئة

تطوير وتوصيف محلل غازي للتقدير الكمي لغاز ثاني أكسيد الكبريت

رسالة مقدمة من الطالبة

سميرة محمد سعيد محمد سعيد باعمران

إلى

جامعة الإمارات العربية المتحدة

أستكمالاً لمتطلبات الحصول على درجة الماجستير في علوم البيئة

٢٠٠٩